Review Article

Mohamed Abd Elkodous*#, Hussein M. El-Husseiny*#, Gharieb S. El-Sayyad*#, Amr Hosny Hashem*#, Ahmed S. Doghish*#, Dounia Elfadil, Yasmine Radwan, Hayam M. El-Zeiny, Heba Bedair, Osama A. Ikhdair, Hisham Hashim, Ahmed M. Salama, Heba Alshater, Ahmed Ali Ahmed, Mahmoud Gamal Elsayed, Maria Nagy, Nouran Y. Ali, Maryam Elahmady, Ahmed M. Kamel, Mahmoud Abd Elkodous, Imene Maallem, Maria B. Sh. Kaml, Nayera Nasser, Ahmed AlaaEldin Nouh, Fatma M. Safwat, Mai M. Alshal, Salma K. Ahmed, Taha Nagib, Fatma M. El-sayed, Manal Almahdi, Yahia Adla, Noha T. ElNashar, Aya Misbah Hussien, Alaa S. Salih, Somaya Abdulbaset Mahmoud, Shireen Magdy, Diana I. Ahmed, Fayrouz Mohamed Saeed Hassan, Nermin A. Edward, Kirolos Said Milad, Shereen R. Halasa, Mohamed M. Arafa, Abdullah Hegazy, Go Kawamura, Wai Kian Tan, and Atsunori Matsuda*

Recent advances in waste-recycled nanomaterials for biomedical applications: Waste-to-wealth

https://doi.org/10.1515/ntrev-2021-0099
received August 16, 2021; accepted September 27, 2021

Abstract: Global overpopulation, industrial expansion, and urbanization have generated massive amounts of

*** Corresponding author: Mohamed Abd Elkodous,** Department of Electrical and Electronic Information Engineering, Toyohashi University of Technology, 1-1 Hibarigaoka, Tempaku-Cho, Toyohashi, Aichi 441-8580, Japan, e-mail: mohamed.hamada.abdlekodous.xi@tut.jp
*** Corresponding author: Hussein M. El-Husseiny,** Department of Veterinary Medicine, Laboratory of Veterinary Surgery, Faculty of Agriculture, Tokyo University of Agriculture and Technology, 3-5-8 Saiwai Cho, Fuchu-shi, Tokyo 183-8509, Japan; Department of Surgery, Anesthesiology, and Radiology, Faculty of Veterinary Medicine, Benha University, Moshtohor, Toukh, Elqaliobiya, 13736, Egypt, e-mail: s195162s@st.go.tuat.ac.jp
*** Corresponding author: Gharieb S. El-Sayyad,** Drug Radiation Research Department, Drug Microbiology Lab, National Center for Radiation Research and Technology (NCRRT), Egyptian Atomic Energy Authority (EAEA), Cairo, Egypt; Chemical Engineering Department, Military Technical College (MTC), Egyptian Armed Forces, Cairo, Egypt, e-mail: Gharieb.S.Elsayyad@eaea.org.eg
*** Corresponding author: Amr Hosny Hashem,** Botany and Microbiology Department, Faculty of Science, Al-Azhar University, Cairo, 11884, Egypt, e-mail: amr.hosny86@azhar.edu.eg
*** Corresponding author: Ahmed S. Doghish,** Department of Biochemistry, Faculty of Pharmacy (Boys), Al-Azhar University, Nasr City, Cairo, Egypt; Department of Biochemistry, Faculty of Pharmacy, Badr University in Cairo (BUC), Badr City, Cairo, Egypt, e-mail: ahmed_doghish@azhar.edu.eg

# These authors contributed equally to this work.

*** Corresponding author: Atsunori Matsuda,** Department of Electrical and Electronic Information Engineering, Toyohashi University of Technology, 1-1 Hibarigaoka, Tempaku-Cho, Toyohashi, Aichi 441-8580, Japan, e-mail: matsuda@ee.tut.ac.jp, matsuda@ee.tut.ac.jp
Dounia Elfadil: Faculty of Sciences and Techniques, Hassan II University of Casablanca, Mohammedia, Morocco
Yasmine Radwan: Center for Materials Science, Zewail City of Science and Technology, Giza, 12578, Egypt; Nanoscale Science Program, Department of Chemistry, University of North Carolina, Charlotte, NC 28223, USA
Hayam M. El-Zeiny: Chemistry Department, Faculty of Science, Beni-Suef University, Beni Suef city, Egypt
Heba Bedair: Botany Department, Faculty of Science, Tanta University, 31527, Tanta, Egypt
Osama A. Ikhdair: Faculty of Medicine, Jordan University of Science and Technology, Ar-Ramtha, Jordan
Hisham Hashim: Department of Physics, Faculty of Science, Tanta University, Tanta, Elgharbiya, 31111, Egypt
Ahmed M. Salama: State Key Laboratory of Chemical Resource Engineering, Beijing University of Chemical Technology, P. O. Box 98, Beisanhuan East Road 15, Beijing, 100029, China
Heba Alshater: Forensic Medicine and Clinical Toxicology Department, Menoufia Hospital University, Shibin el Kom, Egypt
Ahmed Ali Ahmed: Faculty of Pharmacy, Alexandria University, Alexandria, Egypt
Mahmoud Gamal Elsayed: Faculty of Biotechnology, MSA University, Giza, Egypt
Maria Nagy: Biotechnology/Biomolecular Chemistry Program, Faculty of Science, Cairo University, 1 Gamaa Street, Giza, 12613, Egypt
Nouran Y. Ali: Faculty of Agriculture, Biotechnology Program, Ain Shames University, Cairo, Egypt
Maryam Elahmady: Faculty of Dentistry, New Giza University, Giza, Egypt

wastes. This is considered as a significant worldwide challenge that requires an urgent solution. Additionally, remarkable advances in the field of biomedicine have impacted the entire spectrum of healthcare and medicine. This has paved the way for further refining of the outcomes of biomedical strategies toward early detection and treatment of different diseases. Various nanomaterials (NMs) have been dedicated to different biomedical applications including drug delivery, vaccinations, imaging modalities, and biosensors. However, toxicity is still the main factor restricting their use. NMs recycled from different types of wastes present a pioneering approach to not only avoid hazardous effects on the environment, but to also implement circular economy practices, which are crucial to attain sustainable growth. Moreover, recycled NMs have been utilized as a safe, yet revolutionary alternative with outstanding potential for many biomedical applications. This review focuses on waste recycled NMs, their synthesis, properties, and their potential for multiple biomedical applications with special emphasis on their role in the early detection and control of multiple diseases. Their pivotal therapeutic actions as antimicrobial, anticancer, antioxidant nanodrugs, and vaccines will also be outlined. The ongoing advancements in the design of recycled NMs are expanding their diagnostic and therapeutic roles for diverse biomedical applications in the era of precision medicine.

Graphical abstract

Keywords: recycled nanomaterials, biomedical applications, antimicrobial activity, anticancer agents, biomass wastes

Ahmed M. Kamel: Biotechnology Program, Faculty of Agriculture, Ain Shams University, Cairo, Egypt
Mahmoud Abd Elkodous: Faculty of Veterinary Medicine, Kafr Elsheikh University, Kafr Al Sheikh, Egypt
Imene Maallem: Department of Pharmacy, Faculty of Medicine, Badji Mokhtar University, Zaafrania Road, Annaba, 23000, Algeria
Maria B. Sh. Kaml: Faculty of Medicine, Helwan university, Cairo, Egypt
Nayera Nasser: Department of Pharmaceutics and Industrial Pharmacy, Faculty of Pharmacy, Ain Shams University, Cairo, Egypt
Ahmed AlaaEldin Nouh: Department Zoology, Faculty of Science, Alexandria University, Alexandria, Egypt
Fatma M. Safwat: Faculty of Pharmacy, Deraya University, New Minya, Egypt
Mai M. Alshal: Faculty of Physical Therapy, October 6th University, 6 October City, Giza, 12585, Egypt
Salma K. Ahmed: Department of Biotechnology and Biomolecular Chemistry, Faculty of Science, Cairo University, Cairo, Egypt
Taha Nagib: Faculty of Medicine, University of Tripoli, Tripoli, Libya
Fatma M. El-sayed: Biotechnology Program, Faculty of Agriculture, Ain Shams University, Cairo, Egypt
Manal Almahdi: Al-Neelain University, Khartoum, Sudan
Yahia Adla: Department of Biology, College of Arts and Science, Stetson University, 421N. Woodland Blvd, Deland, Florida, 32723, United States of America
Noha T. ElNashar: Department of Pharmaceutical Technology, The German University in Cairo (GUC), Cairo, Egypt
Aya Misbah Hussien: Biotechnology Department, Institute of Graduate Studies and Research, Alexandria University, Alexandria, Egypt
Alaa S. Salih: Department of Human Medicine, Faculty of Medicine & Health Sciences, An-Najah National University, Nablus, Palestine
Somaya Abdulbaset Mahmoud: Faculty of Pharmacy, October 6th University, Giza, Egypt
Shireen Magdy: Biomedical Sciences Program, University of Science and Technology, Zewail City of Science and Technology, Giza, 12578, Egypt
Diana I. Ahmed: Department of Microbiology and Chemistry, Faculty of Science, Aswan University, Aswan, Egypt
Fayrouz Mohamed Saeed Hassan: Information Technology and Computer Science, Nile University, Giza, Egypt
Nermin A. Edward: Department of Biochemistry, Faculty of Science, Ain Shams University, Cairo, Egypt
Kirolos Said Milad: Department of NanoScience, Faculty of Science, Zewail City of Science and Technology, Giza, 12578, Egypt
Shereen R. Halasa: Faculty of Nursing, Al-Quds University, Al-Quds, Palestine
Mohamed M. Arafa: Department of Chemistry, Faculty of Science, Tanta University, Tanta, Egypt
Abdullah Hegazy: Faculty of Science, University of Science and Technology, Zewail City, Cairo, Egypt
Go Kawamura: Department of Electrical and Electronic Information Engineering, Toyohashi University of Technology, 1-1 Hibarigaoka, Tempaku-Cho, Toyohashi, Aichi 441-8580, Japan
Wai Kian Tan: Institute of Liberal Arts and Sciences, Toyohashi University of Technology, 1-1 Hibarigaoka, Tempaku-Cho, Toyohashi, Aichi, 441-8580, Japan

Abbreviations

AC	activated carbon
Anti-EGFR	anti-epidermal growth factor receptor
BBB	blood–brain barrier
CT	computed tomography
CAs	contrast agents
CDs	carbon dots
CG	chitosan-doped graphene
CNCs	cellulose nanocrystals
CNFs	carbon nanofibers
CQDs	carbon quantum dots
CNMs	carbon nanomaterials
CNTs	carbon nanotubes
DCs	dendritic cells
Au NPs	gold nanoparticles
GO	graphene oxide
GQDs	graphene quantum dots
IO-CDs	iron oxide nanoparticle-doped carbon dots
IQDs	inorganic quantum dots
IO NPs	iron oxide nanoparticles
MOs	metal oxides
MNPs	magnetic nanoparticles
MPI	magnetic particle imaging
MRI	magnetic resonance imaging
MWCNTs	multi-walled carbon nanotubes
MIC	minimum inhibitory concentration
NMs	nanomaterials
NGO	nanographene oxide
PEG	polyethylene glycol
PEG-AuIONPs	PEG-coated iron-oxide–gold core–shell nanoparticles
QDs	quantum dots
ROS	reactive oxygen species
RNMs	recycled nanomaterials
rGO	reduced graphene oxide
SPIO NPs	superparamagnetic iron oxide nanoparticles
SWCNTs	single-walled carbon nanotubes
WCO	waste cooking oil
ZnO NPs	zinc oxide nanoparticles

1 Introduction

Since the emergence of the term nanotechnology, much effort has been dedicated to the investigation of the outstanding properties of nanomaterials (NMs) and their potential applications [1]. Materials having at least one dimension on the nanoscale (<100 nm) are identified as NMs [2]. NMs are quite fascinating and have wide applications in different fields such as biology, medicine, industry, energy, and so on [3–7].

Among all the possible applications of NMs, their biomedical applications are of particular interest and have led to the maturation of nanomedicine [8–21]. Various kinds of NMs have been prepared and their applicability has been extensively studied. NMs have shown the potential to overcome many severe drawbacks compared to other pharmacologically active agents and chemicals, including biological instability, lack of water solubility, and ineffectiveness *in vivo* [22]. Nowadays, NMs are used in many biomedical applications, such as drug delivery systems, treatment of diseases, early disease diagnosis, vaccines, biosensors, and bioimaging [23,24]. For the preparation of NMs, many methods have been developed, as shown in Figure 1.

However, there are concerns about the toxicity of NMs [25,26]. Thus, other more benign routes for the preparation of biocompatible NMs are important due to their interaction with the biological environment. Sustainability, referring to the production of NMs from everyday domestic and industrial wastes, can be a revolutionary solution and a route to achieve waste-to-wealth and zero-waste initiatives.

Many valuable NMs, such as carbon NMs (CNMs), gold nanoparticles (Au NPs), inorganic quantum dots (IQDs), and metal oxides (MOs) can be extracted from waste materials that include cooking oil, biomass, and industrial wastes. Interestingly, agricultural biomass wastes can be a valuable source for the green synthesis of NMs possessing many attractive properties such as lower toxicity, cost-effectiveness, tiny size, and higher stability [27]. These NMs have found many uses in biomedical applications [28–34].

More than 6 million tons of agricultural biomass is produced worldwide every year. Of this, 10% is produced in Europe (600,000 tons per year) [35]. Every year, huge amounts of waste cooking oils (WCOs) are produced worldwide, especially in developed countries [36]. In the USA, the daily estimation of WCO by the Energy Information Administration is 100 million gallons and the average per capita amount of WCO is reported to be nine pounds. The total WCO produced yearly in Canada is reaching approximately 135,000 tons [37]. In European Union countries, the amount of yearly WCO ranges from 750,000 to one million tons [38] and 200,000 tons are produced annually in the United Kingdom. Moreover, electronic

waste (e-waste) has become a rapidly growing global concern. In European countries, 17 kg of e-waste per capita is produced yearly. In China and India, 1 kg of e-waste per capita is generated annually and includes Cu, Al, and iron metals [39]. According to the US Environmental Protection Agency, 4.6 million tons of e-waste entered US landfills in 2000 and that amount is rapidly increasing and expected to grow four-fold in coming years [40].

Within the past few years, a circular economy has become an important academic research domain. A significant increase in the number of articles addressing this topic has been published, as shown in Figure 2.

Further investigation on the progress of recycled NMs (RNMs) from wastes and their biomedical applications are of significant importance. In this study, various types of RNMs from three different sources (cooking oil, biomass, and industrial waste) are summarized. In addition, their synthesis, properties, and vital biomedical applications are presented. Our review offers a comprehensive, critical, and accessible overview of this innovative and sustainable trending topic.

2 NMs recycled from cooking oil, biomass, and industrial wastes for biomedical applications

2.1 Carbon-based NMs

2.1.1 Activated carbon (AC)

The AC available in the market is usually made from coal, lignite, peat, petroleum residue, and wood, which are known to be very expensive and exhaustible [41]. Chemical methods, such as chemical vapor deposition (CVD) and laser ablation, are the dominant fabrication methods for AC NPs, but these methods are toxic and highly expensive. Therefore, cooking oil waste, agricultural wastes, fruit peels, and industrial wastes, which cause many problems in the environment, have been used for CNM synthesis by green methods. Arie *et al.* [42] used WCO for CNM synthesis through nebulized spray pyrolysis while varying the processing temperature from 650 to 750°C.

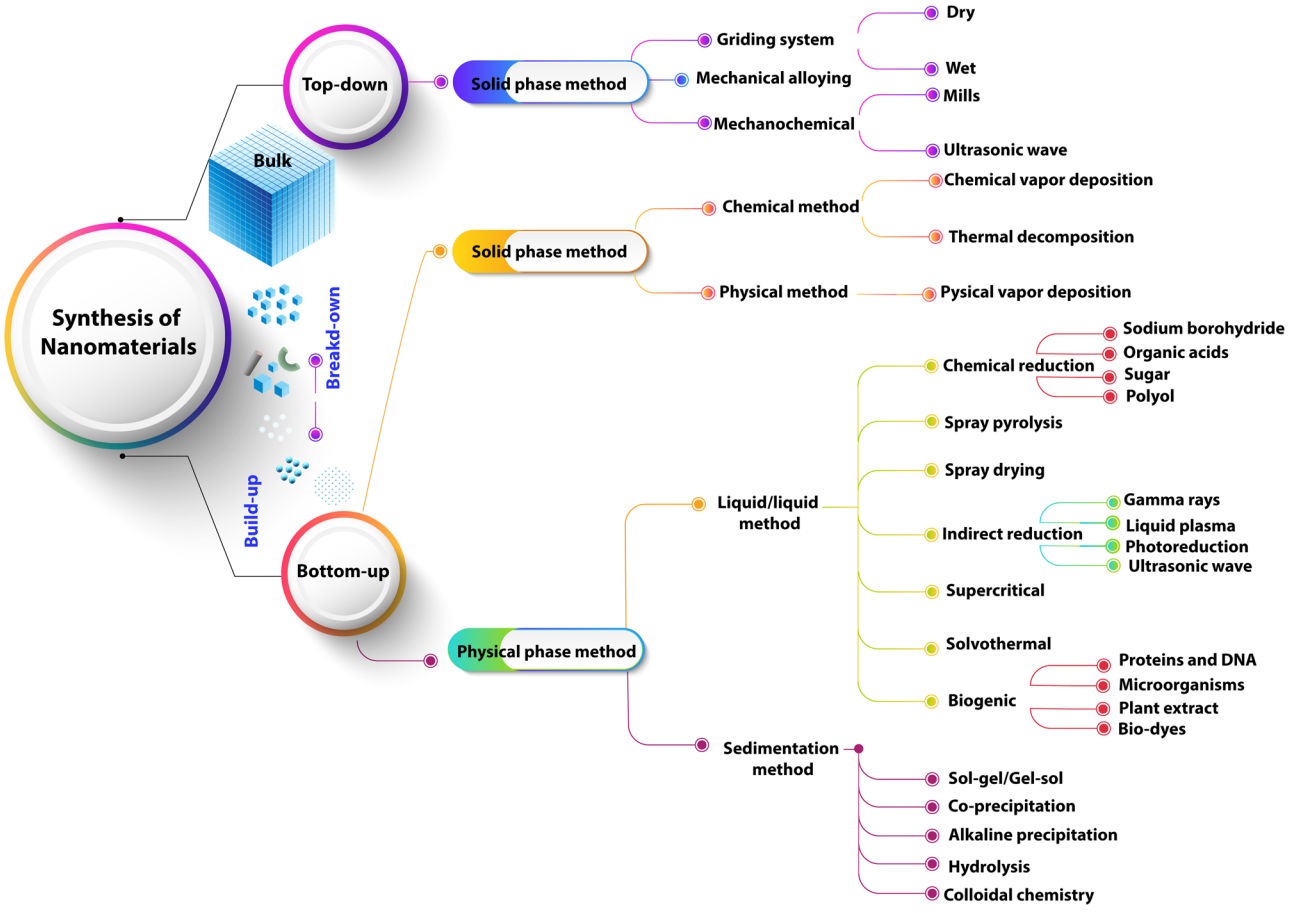

Figure 1: Synthesis routes for NMs.

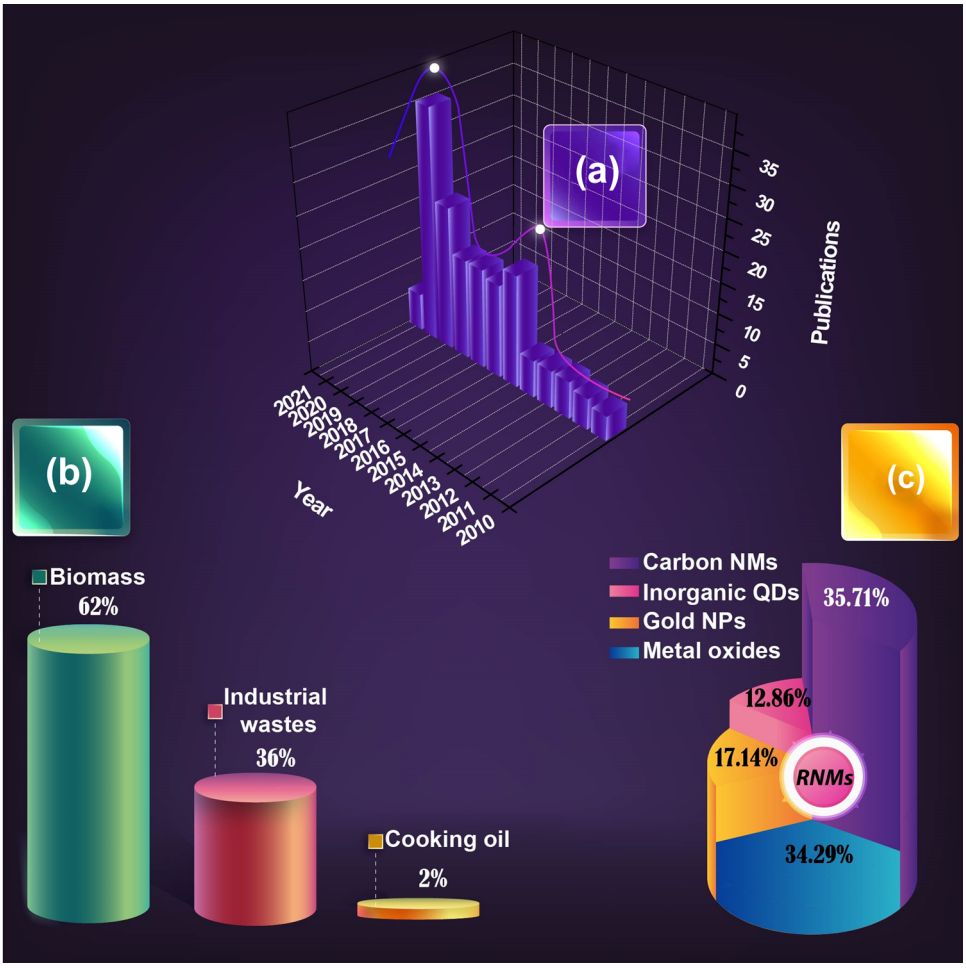

Figure 2: (a) Number of publications in the past ten years that address NMs (CNMs, IQDs, and MOs) recycled from biomass, cooking oil, and industrial wastes; (b) percentage according to waste type; and (c) percentage of each group of NMs.

Many researchers have used agricultural wastes as precursors for the production of AC for four primary reasons: renewable sources, cheap, readily available, and ecofriendly [43,44]. Agricultural wastes are widely used for the biosynthesis of AC [45,46]. Many studies have used olive stones for AC biosynthesis through ecofriendly methods [47,48], as well as walnut shells [49]. Yang *et al.* [50] used coconut shells *via* microwave heating for the production of AC. Another study biosynthesized AC from desiccated coconut waste [51] while AC was produced from *Nicotiana tabacum* stems using the carbonization process and KOH [52]. Gao *et al.* [53] synthesized AC from activated rice straw (RS), and AC particles were also produced from RS waste, which was applied in adsorption processes [54].

Fruit peels are considered one of the most important agricultural wastes. Fruit peels, such as banana peels [45], watermelon peels [55], bitter orange peels [56], cucumis melo peels [57], and durian peels [58], have been widely used for AC biosynthesis. Therefore, the utilization of the inedible parts of fruits (peels) may prove profitable for farmers in the near future since certain fruit peels are of great value as a source of bioactive compounds [59,60]. Potato peel from domestic and industrial waste was used for AC fabrication [61,62], and date seeds were used for the green biosynthesis of AC [63]. Likewise, *Polyalthia longifolia* seeds [64], African star apple seed husks, oil seeds, and whole seed [65] were validated. Additionally, stalks, such as arhar stalks [66] and grape stalks [67], were used to produce AC *via* the chemical activation method. Therefore, the use of these agricultural materials for the production of ACs makes them inexpensive and more efficient. Most agricultural wastes and fruit peel wastes used for AC biosynthesis are summarized in Table 1.

Table 1: Different types of recycled wastes used for the biosynthesis of NMs

NMs	Wastes	References
AC	WCO	[42]
	Olive stone	[47–49]
	Walnut shell	[49]
	Coconut shell	[230]
	Nicotiana tabacum stem	[52]
	RS	[53,54]
	Banana peel	[45]
	Watermelon peel	[55]
	Orange peel	[56]
	Cucumis melo peel	[57]
	Durian peel	[58]
	Potato peel	[106,288]
	Date seed	[288]
	Polyalthia longifolia seed	[64]
	Star apple seed husk	[65]
	Arhar stalk	[336]
	Grape stalk	[67]
CNFs	Palm kernel shell	[74]
	Pine nut shell	[75]
	Walnut shell	[78]
	Sugarcane bagasse	[73]
	Palm fruit stalk	[80]
	Oil palm empty fruit and oil palm trunk	[81]
	Rice stems	[82]
	Banana peel	[84]
	Pine fruit wastes	[85]
	Liquid organic waste	[86]
	Shrimp shell	[87]
	Coal fly ash	[88]
	Waste tire	[88]
CNTs	Wheat straw	[102,104]
	Oat hull	[102]
	Rapeseed cake	[102]
	Hazelnut hull	[102]
	Sugarcane bagasse	[103]
	Potato peel	[106]
	Chickpea peel	[107]
	Banana peel	[105]
G	Waste cooking palm oil	[108]
	Chicken frying oil	[32]
	Oil palm fiber	[127]
	Peanut shell	[110]
	Tea tree plant extract	[112]
	Wheat straw	[113]
	Soybean shell	[114]
	Coconut shell	[115]
	Sugarcane bagasse	[117,122,123]
	Camphor leaf	[116]
	Alfalfa plant shoot	[118]
	Coir pith	[119]
	Rice husk	[120]
	Wild carrot root	[121]
	Bougainvillea glabra flower	[124]
	Mango peel	[125]
	Banana peel	[126]
CQDs	Frying oil waste	[131]
	Egg white and yolk	[132]
	Eggshell	[133]
	Sugarcane bagasse	[122,142–144]
	Peanut shell	[145]
	Coconut husk	[146]
	Tofu waste	[147]
	Beet	[148]
	Walnut shell	[149]
	Corn stalk shell	[150]
	Corncob residue	[151]
	Date kernel	[152]
	Mangosteen pulp	[153]
	Coconut shell	[154]
	Papaya waste pulp	[337]
	Rice residue	[156]
	Platanus waste	[157]
	Wheat straw	[158,159]
	Bamboo residue	[159]
	Banana pseudo-stem	[160]
	Onion peel	[161]
	Prawn shell	[162]
	Corn bran	[163]
	Tea stalk	[164]
	Coriander leaf	[165]
	Purslane leaf	[166]
	Azadirachta indica leaf	[167]
	Catharanthus roseus leaf	[168]
	Prosopis juliflora leaf	[169]
	Tea leaves	[170]
	Orange peel	[174–177]
	Watermelon peel	[178]
	Lemon peel	[179]
	Mango peel	[181,182]
	Pomegranate peel	[179]
GQDs	Cooking palm oil	[186]
	Rice husk	[187,188,190,191,338]
	Coconut husk	[192]
	Coffee grounds	[190]
	Sugarcane bagasse	[193,194]
	Bamboo timber waste	[195]
	Neem leaf	[190,196,197]
	Mango leaf	[198,199]
	Guava leaf	[200]
	Fenugreek leaf	[197]
IO NPs	Sugarcane bagasse	[205]
	Sorghum bran	[206]
	Eucalyptus leaf	[207]
	Carob leaf	[208]
	Ruellia tuberosa leaf	[155]
	Platanus orientalis leaf	[209]
	Green tea leaf	[210]
	Mango leaf	[210]
	Rose leaf	[210]

(*Continued*)

Table 1: *Continued*

NMs	Wastes	References
	Oregano leaf	[210]
	Curry leaf	[210]
	Oak leaf	[211]
	Pomegranate leaf	[211]
	Green tea leaf	[211]
	Grape leaf	[212]
	Garlic vine leaf	[213]
	Oolong tea leaf	[214]
	Salvia officinalis leaf	[215]
	Syzygium cumini seed	[216]
	Watermelon peel	[217]
	Orange peel	[219,220]
	Pomegranate peel	[218]
	Tangerine peel	[221]
	Aloe vera peel extract	[222]
TiO_2 NPs	*Calotropis gigantea* (L.) Dryand leaf	[231]
	S. cumini leaf	[232]
	Psidium guajava leaf	[233]
	Orange peel	[234,293]
	Plum peel	[228]
	Peach peel	[228]
	Kiwi peel	[228]
	Tangerine peel	[236]
	Annona squamosa peel	[227]
	Watermelon peel	[237]
ZnO NPs	Rice husk	[242]
	Sugarcane bagasse	[243]
	Albizia lebbeck stem bark	[244]
	Potato peel	[245]
	Sheep and goat fecal matter	[246,247]
	Coriandrum sativum leaf	[250]
	Calotropis gigantea leaf	[250]
	Acalypha leaf	[250]
	Moringa oleifera	[251]
	Saffron leaf	[252]
	C. sativum leaf	[253]
	Aloe vera leaf	[254]
	Water hyacinth leaf	[255]
	Black nightshade leaf	[256]
	Santa maria leaf	[257]
	Banana peel	[259–262]
	Orange peel	[263–267]
	Pomegranate peel	[268–271]
	Rambutan peel	[272]
	Pineapple peel	[273]
CuO NPs	Cooking oil waste	[281]
	Sugarcane bagasse	[282]
	Walnut shell	[284–286]
	Zea mays L. dry husk	[287]
	Date stone	[288]
	Pomegranate leaf	[289]
	Andean sacha inchi leaf	[290]
	Brassica oleracea subsp. botrytis	[291]

Table 1: *Continued*

NMs	Wastes	References
	Eupatorium odoratum leaf	[339]
	Acanthospermum hispidum leaf	[339]
	Hylotelephium telephium flower	[340]
	Kalopanax pictus leaf	[341]
	Pterolobium hexapetalum leaf	[342]
	Juglans regia leaf	[293]
	Adhatoda vasica Nees leaf	[294]
	Blumea balsamifera leaf	[295]
	Ailanthus altissima leaf	[296]
	Orange peel	[298,299]
	Papaya peel	[280]
	Garcinia mangostana fruit pericarp	[300]
	Pomegranate peel	[301,302]
	Banana peel	[303]
	Lemon peel	[299]
Au NPs	Coconut oil	[308]
	Palm oil	[309]
	De-oiled jatropha waste	[311]
	Nepenthes khasiana leaf	[312]
	Crinum latifolium leaf	[315]
	Azadirachta indica leaf	[316]
	Coleus aromaticus leaf	[317]
	Elettaria cardamomum seed	[318]
	Abelmoschus esculentus seed	[319]
	Crocus sativus extract	[316]
	Cassava starch	[313]
	Nut shells	[314]
	Orange peel	[324,332,333]
	Pomegranate peel	[325–327]
	Banana peel	[328,329]
	Avocado peel	[330]
	Garcinia mangostana peel	[331]
	Watermelon peel	[334]

2.1.2 Carbon nanofibers (CNFs)

CNFs belong to a new category of outstanding nanostructured materials due to their extraordinary mechanical and electrical properties [68]. In previous years, CNFs were manufactured using a variety of techniques such as laser ablation, arc discharge, sonochemical/hydrothermal methods, electrospinning, dry autoclaving, CVD, and the plasma-enhanced CVD process [69,70]. As these methods are toxic and expensive, wastes are now being used for CNF biosynthesis. WCO becomes an issue when solid waste laws prohibit liquids from being disposed of in landfills [71]. Utilizing WCO as a carbon precursor for the

production of CNFs is a low-cost ecofriendly emerging technology. Indeed, mustard, turpentine, *Eucalyptus*, camphor, sunflower, palm, castor, and sesame oils have been proved to contain high carbon compositions [72]. The production of CNFs is fueled by the decomposition of hydrocarbon chains in oil [69].

Agricultural wastes, including plant shooting systems and wood, contain lignocellulosic materials such as lignin, cellulose, and hemicellulose [73]. In recent years, researchers have succeeded in the fabrication of CNFs from several different agricultural precursors. CNFs have been derived from palm kernel shell [74], and Zhang *et al.* [75] manufactured CNFs from pine nut shells by microwave pyrolysis. Furthermore, Wang *et al.* [76] reported that CNFs can be produced by the pyrolysis method using fir sawdust, bamboo, palm kernel shell, and pine nut shell. Likewise, loofah sponge was used to produce porous AC for use as a supercapacitor [77]. Porous CNFs produced from walnut shells were utilized as anodes in lithium-ion batteries [78]. In the same context, Chen *et al.* [73] produced highly effective CNFs from sugarcane bagasse and activated CNFs were also derived from hemp straw through carbonization and KOH [79]. In addition, CNFs can be fabricated from palm fruit stalks [80], oil palm trunk, and fruit bunches [81], which can be widely adopted for water purification. Furthermore, stems of rice plants were used as raw materials for CNF synthesis by the thermal decomposition method [82].

Industrial byproducts, that is, fruit peels, petrochemical wastes, or organic liquid wastes, could be used for CNF manufacturing. The fruit juice industry consumes fruits as juice and the peels are detached from the fleshy part of the fruit. These peels can be used as a carbon precursor for CNF production, thus reducing the environmental pollution resulting from the disposal of these wastes. Yadav and Sharma [83] prepared an extract from orange peels and utilized it as a precursor for CNF preparation by pyrolysis and chemical activation (using KOH). Likewise, banana peels were utilized for CNF biosynthesis [84]. Pine fruit wastes were also used as precursors for CNF synthesis by Shahba and Sabet [85]. Liquid organic wastes generated by petrochemical and chemical industries have been used to produce gas by electro-cracking; the gas acts as a carbon source for CNF manufacturing [86]. Moreover, shrimp shell wastes were used as a precursor of chitin nanofibers under acidic conditions utilizing a simple blending treatment [87], while coal fly ash and waste tires were utilized as precursors in CNF synthesis by pyrolysis [88]. Most of the agricultural and fruit peel wastes used for CNF biosynthesis are summarized in Table 1.

2.1.3 Carbon nanotubes (CNTs)

Nanocarbon material is a carbon-based material with a specified size and particle structure [42]. Numerous precursors of carbon, such as methane, acetylene, and benzene, have been used as carbon source material to synthesize CNTs [89–91]. In 1991, CNTs were discovered by Iijima as a cylindrical carbon nanostructure [92]. CNTs have been notable for many applications including energy storage electrodes in supercapacitors, polymers, gas storage materials, sensors, electronics, catalysts, and separation [34,93,94]. After the increase of environmental concerns and the growing demand for CNTs, many researchers have tried to increase CNT production while developing green technology [34]. CNT production is costly using traditional sources. So there is a need to find renewable resources for their production. Innovative research efforts that focus on the use of cost-effective and readily available renewable materials, like biomass, are required [95]. Therefore, the use of WCO is necessary, as it is generated from natural vegetable oils and animal fats that lose their nutritional value during the cooking process or deep processing [96]. The average amount of WCOs is remarkable worldwide and it may cause severe environmental, economic, and social problems [97]. The estimated worldwide annual production of waste vegetable oils is over 15 million tons, with around 1 million tons per year by the European Union [97–99]. WCO can be used as a starting material in the industrial-scale production of CNTs, which makes it both economical and environmentally beneficial [100].

Agricultural wastes have a high carbon content, with cellulose, hemicellulose, and lignin used extensively as carbon precursors [34]. Besides increasing its value, the use of cellulose-rich biomass (agricultural waste) would also help resolve environmental problems [101]. Therefore, renewable precursors should be widely used in future as they can be replenished fairly rapidly [95]. Hidalgo *et al.* [102] used wheat straw, oat hulls, rape seed cake, and hazelnut hulls as biomass waste for CNT production using a novel method of solvent self-ignition. Likewise, Mugadza *et al.* [103] produced nitrogen-doped multi-walled CNTs from sugarcane bagasse using the floating catalyst CVD method at 850°C. CNTs were synthesized from pretreated RS through the CVD of camphor [104]. Fruit peels were one of the agricultural wastes used for CNT synthesis. Mopoung [105] reported that banana peel mixed with mineral oil is the main precursor for the synthesis of CNTs. Another waste, potato peel, was used for the synthesis of CNTs for bio removal of heavy metals [106]. Moreover, chickpea peel waste was used for the synthesis of CNTs for bioimaging applications [107].

Most of the agricultural and fruit peel wastes used for CNT biosynthesis are summarized in Table 1.

2.1.4 Graphene (G)

G consists of pure carbon, wherein carbon atoms are arranged in a single layer to create a honeycomb pattern. It should be stressed that this layer of carbon is only one atom thick, although some authors consider up to ten layers of carbon to be G [108]. G is one of the most attractive CNMs due to its extraordinary electronic, optical, magnetic, thermal, and mechanical properties and wide applications [108,109]. There are many methods used in G synthesis, such as chemical synthesis, chemical exfoliation, mechanical exfoliation, and pyrolysis [109]. However, while these methods are very effective for G synthesis they are highly expensive and not ecofriendly. Therefore, there is a new direction in G synthesis by green methods using wastes, such as cooking oil, agricultural wastes, and industrial wastes. Robaiah *et al.* [108] verified waste cooking palm oil for G synthesis at different temperatures. In addition, Azam *et al.* [32] used palm-based waste chicken frying oil for G nanotablet synthesis.

Recently, scientists have been working on the large scale manufacture of G from biological sources like waste plant shells, plant aerial parts, plant seeds, biochar, eggshell, microorganisms, and even human hair [110]. Lignocellulosic agricultural wastes essentially consist of proteins, lignin, carbohydrates, cellulose, and hemicelluloses; their use for the production of adsorbents has piqued interest [110,111]. In this context, Jacob *et al.* [112] synthesized G from the tea tree plant (*Melaleuca alternifolia*) while Chen *et al.* [113] prepared value-added G from wheat chaff (*Triticum* sp.) by graphitization and hydrothermal methods, which were then applied in lithium-ion batteries. Furthermore, soybean shell (*Glycine max*) was used as a carbon precursor for G production by KOH followed by thermal treatment; it proved its efficiency in oxygen reduction reactions [114]. Likewise, Sun *et al.* [115] prepared G from the shell of coconut (*Cocos nucifera*) using $ZnCl_2$ and $FeCl_3$, and then used the resultant G as a supercapacitor. Additionally, ref. [110] used KOH for activation and then exfoliation to render G from peanut shells. Sugarcane bagasse and dried camphor leaves (*Cinnamomum camphora*) have also been validated in the biosynthesis of G [116,117]. G was produced from the aerial parts of alfalfa plants (*Medicago sativa* L.) with the oxidative action of HNO_3 under a feasible process [118] and coir pith was used for G biosynthesis by a ball milling activation method [119]. Furthermore, G was synthesized using rice husk activated by KOH at 900°C for use in energy storage applications [120]. Kuila *et al.* [121] utilized wild carrot roots for the green biosynthesis of G oxide (GO) where the roots contain endophytic microorganisms responsible for the reduction process through an environmentally safe method. Baweja and Jeet [122] reported that sugarcane bagasse is an effective, economical, and suitable source for G biosynthesis. Likewise, Somanathan *et al.* [123] validated sugarcane bagasse for the biosynthesis of GO. Moreover, the flower extract of *Bougainvillea glabra* was used as a reducing agent for the biosynthesis of GO used in sensing applications [124].

Many fruits have been used for producing juice, syrup, nectar, sugar, or in the flavor industry. Consequently, large quantities of their waste products can be harmful to the environment. These byproducts are abundant in pectin, lipids, cellulose, proteins, hemicellulose, and enzymes, which can be exploited as raw material for G manufacturing [125]. Multi G layers were produced from mango peels on copper sheets using plasma [125]. Furthermore, highly effective antibacterial GO was produced from banana peel waste [126]. Tahir *et al.* [127] grew pure G on copper sheets by CVD using oil palm fiber and fruit trash. Ruan *et al.* [128] synthesized high-quality single-layered G from food wastes, for example, chocolate and cookie wastes, and solid wastes, for example, blades of grass, dog feces, and bulk polystyrene plastic, by CVD using hydrogen gas. Dung and the bones of cows, newspapers, and soot powders in diesel vehicle exhausts were used as precursors for G synthesis *via* the chemical exfoliation method [129]. Most of the agricultural and fruit peel wastes used for G biosynthesis are summarized in Table 1.

2.2 IQDs

2.2.1 Carbon quantum dots (CQDs)

CQDs are carbon NPs with a size less than 10 nm and have acted as surface passivation for inorganic materials. Moreover, they have good solubility, high stability, and are easily controllable by size and functional groups [130]. There is a need for clean materials in the synthesis of CQDs in the modern era of nanoscale materials. Previous studies have validated the use of agri-based wastes, such as frying oil waste [131], egg whites and yolks [132], and eggshells [133], for the synthesis of CQDs. Muthoni *et al.* [131] used frying oil waste as a precursor for the one-step synthesis of sulfur-doped carbon dots (CDs) with pH-sensitive photoluminescence. Egg yolk oil is known in traditional medicine in China and can be obtained by refining cooked egg yolks of *Gallus domesticus* Brisson [134]. Nowadays, focus has been on the preparation of CQDs from "green" materials with no chemicals included

in the CQD synthesis and waste management utilized to create cheap and renewable materials with potential for commercial scale-up [135].

Agriculture wastes are considered a big threat to our environment as it is found within the soil as a byproduct from agriculture, industry, and domestic activities use [136]. However, most of these wastes are discarded, which cause environmental problems that threaten human health.

These wastes are known as renewable, naturally inviting, liberally accessible, and harmless carbon sources for carbon dot (C-dot) generation [137,138]. There are many types of these wastes such as sugar cane bagasse, coir, banana, and pineapple leaf, which cause pollution [139]. Sugarcane bagasse is one of the most abundant wastes, hence, efforts have been made to use it as a bio-fuel, in food products, and in carbon production [140,141]. Sugarcane bagasse was used for CQD biosynthesis *via* hydrothermal [142] and carbonization methods [143]. Sugarcane bagasse has also been used in CQD biosynthesis through a simple, efficient, economic, and sustainable approach [122,144]. Large amounts of peanut shells are dumped as waste every year. The quantity of waste peanut shells is huge and it is difficult to recycle [145]. Zhu *et al.* [145] used a novel method for synthesis of CQDs using peanut shells. Their generated CQDs were soluble in water. Chunduri *et al.* [146] reported that coconut husk can be used as a carbon source for the green synthesis of CQDs. Zhang *et al.* [147] synthesized two types of CQDs with tofu waste. Wang *et al.* [148] reported a strategy to prepare CQDs utilizing beet as the carbon source, as beets are rich in sucrose and other carbohydrates and are utilized to manufacture granulated sugar. Walnut shells were also used for the preparation of green photoluminescent CQDs, which are used in intracellular bioimaging [149]. Likewise, corn stalk shell [150], corncob residues [151], date kernel [152], mangosteen pulp [153], coconut shell [154], papaya waste pulp [155], rice residue [156], platanus waste [157], wheat straw [158,159], banana pseudo-stem [160], onion peels [161], prawn shells [162], corn bran [163], and tea stalks [164] were used for CQD biosynthesis by hydrothermal and carbonization methods. Additionally, plant leaf extracts, such as coriander [165], purslane [166], *Azadirachta indica* [167], *Catharanthus roseus* [168], *Prosopis juliflora* [169], and tea [170], were used for the green biosynthesis of CQDs. Fruit peel wastes have also been used for the green biosynthesis of CQDs. Banana peel is an agricultural solid waste that was used in the green hydrothermal synthesis of CQDs without the addition of any supplements [171–173]. Furthermore, orange peel [174–177], watermelon peel [178,179], lemon peel [180], mango peel [181,182], and pomegranate peel wastes [179] were used for the green and ecofriendly biosynthesis of CQDs. Most of the agricultural and fruit peel wastes used for CQDs biosynthesis are summarized in Table 1.

2.2.2 G quantum dots (GQDs)

GQDs are a new kind of quantum dot (QD) that have an intrinsic inert carbon property, which explains their chemical and physical stability [183]. Recently GQDs have received a lot of attention due to their unique properties, which include being environmentally friendly, non-toxic, biologically inert, biocompatible, and having high conductivity, broad surface area, low toxicity, and long lifetimes [184]. As a result of the high market cost of inorganic QDs, their industrial use has been limited. In addition, application development has been interrupted by the high toxicity of inorganic QDs. Therefore, the synthesis of GQDs from biowaste is considered a cost-effective alternative [185]. Cooking palm oil has been used for GQDs biosynthesis [186] and biomass, such as plant leaves, grass, coffee grounds, rice husks, and wood charcoal, stand out as a green, natural, cheap, sustainable, and renewable carbon source for the scalable production of GQDs [184]. Agricultural wastes, such as rice husk [187–191], coconut husk [192], coffee grounds [188,190], sugarcane bagasse [193,194], and bamboo timber waste [195], are widely used for the green biosynthesis of GQDs through ecofriendly methods. Moreover, plant leaf extracts, such as neem [190,196,197], mango [198,199], guava [200], fenugreek [197], and dried pine leaves have been used to synthesize GQDs [201]. Most of the agricultural and fruit peel wastes used for GQD biosynthesis are summarized in Table 1.

2.3 MO-based NMs

2.3.1 Iron oxide NPs (IO NPs)

IO NPs have shown many advantages for use in medicine and pharmaceutical applications. IO NPs are characterized by their low toxicity, high biocompatibility, and injectability; their magnetic and semiconductor properties have made them perfect candidates for drug delivery, magnetic resonance imaging, and cancer treatment and diagnosis [202]. Essential oils can be used to increase the stabilization of IO NPs as they have shown antimicrobial activity and can prevent pathogens from forming biofilms. These oils can be obtained from aromatic plants by steam distillation or mechanically from the pericarp [203].

Researchers continue efforts to develop facile, effective, and reliable green chemistry processes for the

production of NMs. Recent studies have used agricultural wastes for IO NP synthesis [155,204]. Sugarcane bagasse was used to create magnetic IO NP for the removal of chromium ions from tannery effluent [205]. Njagi *et al.* [206] used waste sorghum bran to synthesize IO NPs using green technology. Leaf extracts, such as *Eucalyptus* [207] and carob [208], are widely used for IO NPs. Vasantharaj *et al.* [155] used the leaf extract of *Ruellia tuberosa* for IO NP biosynthesis through a green method that targeted photocatalytic degradation. Similarly, Devi *et al.* [209] synthesized ecofriendly IO NPs using the leaf extract of *Platanus orientalis*. IO NPs have been synthesized using green tea, mango, rose, oregano, and curry leaves [210]. Another study utilized oak, pomegranate, and green tea leaves and produced the richest extracts for green biosynthesis of IO NPs [211]. Similar studies also utilized grape leaf extract [212] and garlic vine leaf extract [213] for IO NPs through green and ecofriendly methods. Furthermore, Oolong tea and *Salvia officinalis* leaves were used in IO NP biosynthesis [214,215]. Venkateswarlu *et al.* [216] used the seed extract of *Syzygium cumini* for green biosynthesis of IO NPs.

Recent studies used fruit peel extract, such as watermelon rinds [217] and pomegranate peel [218], to create IO NPs through green and ecofriendly methods. Moreover, orange peel extract was used for IO NP biosynthesis [219,220] and IO NPs were synthesized in an ecofriendly manner from other peels such as tangerine [221] and *Aloe vera* extract [222]. Bishnoi *et al.* [223] validated *Cynometra ramiflora* fruit extract waste for the synthesis of magnetic IO NPs. Most of the agricultural and fruit peel wastes used for IO NP biosynthesis are summarized in Table 1.

2.3.2 TiO_2 NPs

TiO_2 NPs have been extensively studied because they have high quantum efficiency, application-appropriate electronic band structure, high specific surface area, chemical innerness, and stability [224]. TiO_2 NPs are widely used in cosmetics and pharmaceuticals [225] and are also used as antibacterial agents [226]. Agricultural wastes, WCO, and fruit peel wastes are used in TiO_2 NP biosynthesis through a green strategy [227–229].

Recently developed technologies have the potential to convert agricultural wastes into functional NPs. One important agricultural waste that may act as a promising biotemplate for the synthesis of TiO_2 NPs is RS. It was demonstrated that mesoporous silica (MCM-41) obtained from rice husks enhanced the performance of TiO_2-based photocatalyst for the degradation of trimethyl ammonium [230]. Another biomass waste of interest is the leaves of plants, which are incredibly useful for the production of MO NPs. Marimuthu *et al.* [231] reported that the leaf extract of *Calotropis gigantea* (L.) Dryand is promising for TiO_2 NP fabrication. After 6 h, the extract contains primary amines that have an important role in the bioreduction of TiO_2 to TiO_2 NPs. Furthermore, Sethy *et al.* [232] used the leaves of *S. cumini* for producing TiO_2 NPs through a non-toxic, simple, cost-effective, and ecofriendly fabrication method. Kalyanasundaram *et al.* synthesized TiO_2 NPs from the aqueous leaf extract of *Pithecellobium dulce* and *Lagenaria siceraria* in 2018. Moreover, the aqueous leaf extract of *Psidium guajava* was used in TiO_2 NP biosynthesis [233].

Orange peel extract from sweet orange (*Citrus sinensis* (L.)) was used in a green method for the synthesis of TiO_2 NPs [234]. Additionally, Amanulla and Sundaram [235] synthesized TiO_2 NPs from titanium tetra chloride using orange peel extract (*C. sinensis*), showing that the green biological synthesis methods used in preparing NPs exhibit better results compared to TiO_2 NPs obtained chemically. Moreover, TiO_2 NPs were synthesized by revalorization of agri-waste material such as peels of the rosaceous fruits *Prunus domestica* L. (plum), *Prunus persica* L. (peach), and *Actinidia deliciosa* (Kiwi), where the peel extract acts as reducing and capping agents [228]. Ajmal *et al.* [228] reported the ease, cost-effectiveness, economic viability, and useful biomedical property of the green chemistry approach for the biosynthesis of TiO_2 NPs. Nanocrystals (NCs) produced with alternative synthesis methods transform the TiO_2 precursor in TiO_2 NCs using two volumetric ratios of tangerine peels (*Citrus reticulata*), an organic waste, as bio-mediator of chemical reactions [236]. The peel extract of *Annona squamosa* was utilized as a precursor for TiO_2 NPs biosynthesis [227] and TiO_2 NPs loaded onto AC prepared from watermelon peel waste were used for dye removal [237]. On the other hand, nanowaste management needs further study to determine their environmental impact, as it was reported that TiO_2 NPs and ZnO NPs from sunscreen could have a role in the formation of free radicals in skin cells, which further damage to DNA and favor tumorigenesis and cancer development [238]. Most of the agricultural and fruit peel wastes used for TiO_2 NPs biosynthesis are summarized in Table 1.

2.3.3 ZnO NPs

There is extensive research underway to commercialize NPs due to their remarkable features. There have also been huge efforts to synthesize different types of NPs from unconventional sources, like cooking oil. ZnO NPs are one of the MO NPs that can be used as an

antimicrobial and antioxidant agent [239,240]. Agricultural biomass waste is considered one of the most common organic and nontoxic materials that could be used in several industrial domains. These agricultural biomasses mainly contain lignin, which is a byproduct from paper and pulp industries. Annually, tons of lignin are produced and more than 95% are dumped in rivers, which is a loss as it is an environmentally friendly product not being properly utilized [241]. The usage of lignin, which is cheap biomass, could serve two important purposes: reducing wastes and transforming them into valuable materials, instead of dumping in rivers and causing major pollution. This transformation could be done through ZnO NP production from safe sources.

Agricultural wastes, such as rice husk [242], sugarcane bagasse [243], and *Albizia lebbeck* stem bark [244], are widely used for the green biosynthesis of ZnO NPs. Moreover, potato peels have been used for the biosynthesis of ZnO NPs, which were in turn used to target photocatalytic activity against methylene blue [245]. Other wastes can also be used in the biosynthesis process, such as sheep and goat fecal matter [246,247]. Chikkanna *et al.* [248] used sheep and goat fecal matter as a reducing agent for the production of ZnO NPs.

Ali *et al.* [249] explained the importance of utilizing green sources, such as leaves, roots, or shoot powders and flowers, in a form of solvent-based extract as stabilizing or capping agents to synthesize pure ZnO NPs. Leaf extracts from sources such as *Coriandrum sativum* plant leaves, *C. gigantea* leaves, and *Acalypha* leaves [250] have also been used for the biosynthesis of ZnO NPs. Surendra *et al.* [251] used *Moringa oleifera* for the biosynthesis of ZnO NPs and applied them for their antimicrobial activity. Rahaiee *et al.* [252] used the leaf extract of saffron as a reducing and stabilizing agent for ZnO NP production through a facile green approach. Furthermore, the leaf extract of *C. sativum* was also used for ZnO NP production [253]. Other leaf extracts, such as *Aloe vera* [254], water hyacinth [255], black nightshade [256], and Santa maria [257] have been used in the ecofriendly biosynthesis of ZnO NPs.

Fruit peel wastes are an ecofriendly and economic source for ZnO NP production. Peels of tomato, orange, grapefruit, and lemon were used for green biosynthesis of ZnO NPs [258]. More recent studies used banana peel extract for ZnO NP synthesis. The synthesized ZnO NPs were used in different applications due to their antimicrobial, antioxidant, and anticancer actions, and in photocatalytic degradation [259–262]. Furthermore, orange peel extract was used for the green synthesis of ZnO NPs that were applied in antibacterial activity, strawberry preservation, and photocatalytic degradation [263–267]. Other fruit peel wastes, such as pomegranate [268–271], rambutan [272], and pineapple peels [273], have also been used in the synthesis of ZnO NPs. Most of the agricultural and fruit peel wastes used for ZnO NP biosynthesis are summarized in Table 1.

2.3.4 CuO NPs

Copper is considered an important trace element in humans, animals, and plants [274]. CuO NPs have received much attention in recent years due to their wide application in many fields [275]. General applications of CuO NPs concern antimicrobial, antioxidant, and anticancer materials, gas sensors, conducting materials, magneto resistant materials, remediation, and biological removal of dyes and heavy metals [276–278]. In the last two decades, wastes, such as frying oil, agricultural, and industrial wastes, have been widely used for the synthesis of CuO NPs [279,280]. CuO NPs were synthesized *in situ* within ionic liquid-in-vegetable oil micro-emulsions [279]. Sarno *et al.* [281] prepared Cu NPs directly from WCO through a green strategy.

There have been various challenges in the production of biomass-assisted MO NPs, like CuO NPs, from agricultural wastes. Kumar *et al.* [282] reported that the biosynthesis of MO NPs using agricultural wastes is essential as these wastes are renewable sources, cheap, safe, and environmentally friendly. Agricultural wastes, specifically the lignocellulosic wastes such as rice husk, straws, and walnut shells, are very well known for their availability and low cost. Sugarcane bagasse [282,283], walnut shells [284–286], *Zea mays* L. dry husk [287], and date stones [288] have been used for green biosynthesis of CuO NPs.

Leaf extracts, such as those from pomegranate [289], Andean sacha inchi [290], *Brassica oleracea* subsp. botrytis (L.) [291], *Eupatorium odoratum*, *Acanthospermum hispidum*, *Hylotelephium telephium*, *Kalopanax pictus*, and *Pterolobium hexapetalum* [292], *Juglans regia* [293], *Adhatoda vasica* Nees [294], *Blumea balsamifera* [295], *Ailanthus altissima* [296], and *Drypetes sepiaria* [297], have also been used to create CuO NPs. Furthermore, fruit peels, such as orange peel [298,299], papaya extract (*Carica papaya* L.) peel waste [280], *Garcinia mangostana* fruit pericarp [300], pomegranate peel extract [301,302], banana peel [303], and lemon peel [299], were used for the green and ecofriendly biosynthesis of CuO NPs. Most of the agricultural and fruit peel wastes used for CuO NP biosynthesis are summarized in Table 1.

2.4 Au NPs

There are various techniques for Au NP synthesis, such as chemical reduction, microwave, ultraviolet radiation, photochemical, and sonochemical methods [304,305]. While these methods are effective for the biosynthesis of Au NPs, they are toxic and expensive. Therefore, green methods using WCO, biomass, and agricultural wastes are an optimistic approach toward NP synthesis in a clean, simple, safe, and environment friendly manner [306,307]. Au NPs are a bio-based product that can be synthesized using WCO, which is a cheap and renewable stock for biomedical products when efficiently collected and recycled. Otherwise, if WCO is illegally disposed of many environmental problems may occur [71]. Coconut oil has been used as a reducing and stabilizing agent for the synthesis of Au NPs, which were spherical with varied particle sizes [308]. Likewise, Sadrolhosseini *et al.* [309] reported the synthesis of Au NPs dispersed in palm oil (as a stabilizing agent) at different temperatures using the laser ablation technique. Palm oil is characterized by long hydrocarbon chains, which prevent NP agglomeration, and polar ester bonds, which can cap the NPs.

Agricultural wastes used for Au NP biosynthesis depend on upcoming methods that reduce the target biomass by converting Au(III) to Au(0), forming Au NPs. Armendariz *et al.* [310] utilized wheat and oat (*Avena sativa*) biomass and successfully confirmed Au NPs with different morphologies, including face-centered cubic (FCC) tetrahedral, decahedral, hexagonal, *etc*. Moreover, fungal biomass can be used as it too has reducing capability. Kanchi *et al.* [311] used de-oiled jatropha waste for Au NP synthesis. Recent research projects synthesized Au NPs from the leaf extract of *Nepenthes khasiana* [312], liquefied mash of cassava starch [313], macadamia nut shell waste [314], and *Crinum latifolium* leaf [315]. Additionally, *Crocus sativus* liquid extract, *A. indica* leaves [316], and the leaf extract of *Coleus aromaticus* [317] were used for Au NP biosynthesis through green and ecofriendly methods. Seeds of an herbaceous plant called *Elettaria cardamomum* (of the ginger family whose seeds contain many phytochemicals) are capable of reducing gold ions and stabilizing formed NPs [318]. Also, the seed aqueous extract of *Abelmoschus esculentus* was utilized for the biosynthesis of Au NPs and their fungal activity was evaluated [319].

Fruit peel wastes are a promising source for the synthesis of metallic NPs, such as Au NPs, where their extracts act as a reducing agent in the synthesis [320,321]. The recycling of these biomass wastes makes it an environment-friendly method due to efficient management and usage [322]. Different fruit wastes, such as grape, jatropha, mango peel, banana peel, and watermelon rind wastes, were successfully used for Au NP synthesis [323]. Castro *et al.* [324] reported the use of orange peel for the synthesis of Au NPs wherein the initial pH was adjusted to control their size, shape, and structure. Furthermore, pomegranate peel waste is widely used for the conversion of $HAuCl_4$ to Au NPs for biomedical applications [325–327]. In the same context, banana peel waste was used for Au NP biosynthesis [328,329] while Adebayo *et al.* [330] used an aqueous extract of avocado (*Persea americana*) fruit peel to synthesize spherical and FCC Au NPs. In addition, *G. mangostana* fruit, sweet orange (*C. sinensis*), and *Citrus maxima* peel extracts have all been approved for Au NP synthesis, confirming that fruit wastes are a promising resource for Au NP stability and synthesis [331–333]. Chums-ard *et al.* [334] synthesized Au NPs using the red and green parts of watermelon waste. The red part extract formed spherical and hexagonal plates of Au NPs while the green part waste formed triangular NPs. Likewise, watermelon peel waste has been confirmed useful for the biosynthesis process [335]. Most of the agricultural and fruit peel wastes used for Au NP biosynthesis are summarized in Table 1.

3 Synthesis and properties of RNMs

3.1 Carbon-based NMs

3.1.1 AC

The use of fruits and vegetable peels as an activator for carbon has prevailed for the purification of aqueous environments. In 2009, orange peels were used for waste water purification and the orange peels were then used with lemon peels to produce AC [343]. Many other agricultural wastes and biomass seeds have been used to produce AC, such as potato peels, which were used in the treatment of pharmaceutical effluents [344,345] and to absorb heavy metals from aqueous media [61].

Torres *et al.* extracted soybean peroxidase (SP), a residue with large carbon and moderate ash content [345]. This residue was applied as a carbonaceous precursor to provide AC with a high surface area (1,603 $m^2 g^{-1}$), as shown in Figure 3. The waste originating from SP was washed with distilled water, dried at 60°C for 24 h, then treated with zinc chloride, and pyrolyzed in a tubular oven under an N_2 flow at 550°C for 3 h. The produced AC was used as support for

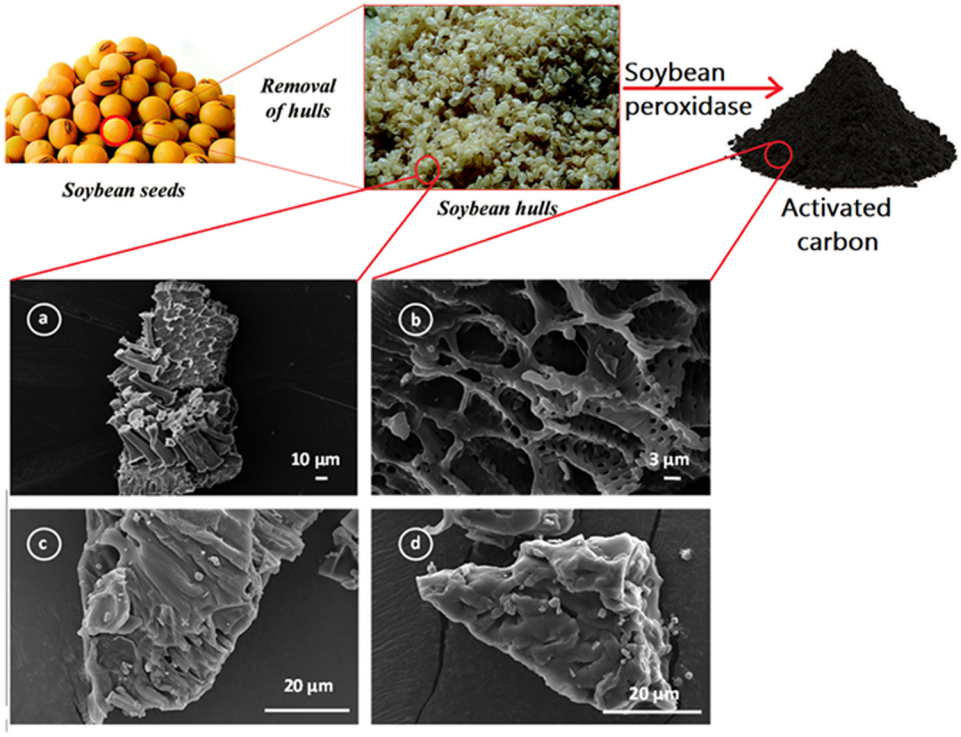

Figure 3: Removal of soybean hulls to produce AC and scanning electron microscopy (SEM) images of precursor (soybean hulls) for AC (a) after activation with $ZnCl_2$ and (b) after immobilization at different magnifications (c) and (d). Copyright © 2017, Royal Society Publishing Group [345].

SP immobilization for different biomedical and pharmaceutical applications.

With industrial and technological development and the emergence of the plastic waste crisis, many researchers have used polyethylene terephthalate (PET) to produce AC. PET was used for the first time in 1999 by Marzec *et al.*, who investigated the effect of the adsorption capacity of carbon [346]. The preparation of AC from a precursor rich in carbon content has received attention. The AC can be produced in two ways: physical and chemical activation [347]. Two steps are required in the physical activation method: first is the carbonization of the precursor material, which takes place at a temperature that ranges from 400 to 800°C, and the second is activation, which takes place at a very high temperature, beginning from 800°C and reaching 1,000°C in the presence of the oxidizing agent (CO_2 or air). A complete list of the methods are noted in Tables 2 and 3 [347].

Additionally, chemical activation can be done in one step and at a low temperature. Therefore, many researchers prefer to use this method to save time and money. The chemical agent represents the oxidant and dehydrating agent added to the precursor and mixed at a temperature less than 800°C, as noted in Tables 4 and 5 [347]. No result

Table 2: Different physical methods for AC production from biomass with corresponding properties

Material	Activating agent	Temperature (°C)	Surface area ($m^2\ g^{-1}$)
Coconut shell [347]	CO_2	—	—
Corncob [347,348]	CO_2	800	919–986
Rice husk [347]	CO_2	700 and 750	—
Rice husk [349]	Hydrothermal carbonization	—	243
Almond tree pruning (non-catalytic gasification) [347,350]	Air	190	116–469
Almond tree pruning (catalytic gasification) [347]	Air	190–260	959
Olive tree wood [347,351]	Air	400	413
Corn Stover [351]	Microwave pyrolysis	—	1671.4

Table 3: Different physical methods for AC production from industrial wastes with corresponding properties

Material	Carbonization	Carbonization temperature (°C)	Activating agent	Activating temperature (°C)	Surface area ($m^2 g^{-1}$)
PET [352]	Under N_2	800	N_2 and CO_2	975	790
Polyvinyl chloride(PVC) [353]	Air	900	Steam	900	1,000–2,000
Refuse paper and plastic fuel [353]	–	–	Wet N_2 (20% steam)	–	500
Sawdust [354]	Under N_2	–	CO_2	700, 720, 740, and 760	302–405
Sawdust [355]	N_2 isotherms	–	CO_2 flow and by pyrolysis	200–900	–
Paper mill waste [356]	–	300	Steam	850	135.49

was found regarding the use of WCOs to prepare AC. The use of AC for filtration of cooking oil meant for use as pet food [357] and as a homogenous catalyst to prepare biodiesel from WCO [358] has been reported.

3.1.2 CNFs

CNFs have been in history for over a century. In an 1889 patent, carbon filaments were reported to be made from carbon-containing gases using a metal crusher as a catalyst [360]. Ghosh *et al.* was considered the first to describe the interaction between methane, metal surfaces, and graphical carbon at relatively low temperatures [361]. In 2019, catalytic decomposition of biogas over a Ni: Co/Al_2O_3 catalyst was generated in a rotator bed reactor by fishbone-type CNFs.

Agricultural waste (nutshell and wheat straw) has been used to manufacture AC. The applied method was respectful of the environment and the total cost of production was reduced. Fe and Ca in biomass derived ACs have a total content of less than 3%. The main steps involved to form CNFs on AC are the decrease in iron particles with H_2, the dissociated ethylene chemical adsorption of some faces in iron particle antipersonnel, a dispersal of carbon species created during decomposition by the catalyst particle, and solid carbon precipitation on other metal faces to form a fibrous structure. Suriani *et al.* [362] validated chicken fat waste for CNF production. The ecofriendly consequences of their contribution are shown in Figure 4. The waste commodity of the poultry industry has significantly interfered with the field. The main fatty acids recently reported in chicken fat are oleic, palmitic, and linoleic acids. This initial study resulted in the synthesis of CNFs using an easy and viable CVD process with chicken waste fat and skin [363]. A dry rendering process was used to extract chicken oil from the chicken fat and skin. The fat and skin were heated to 200°C to isolate the liquid oil from the solids. The oil was filtered and then blended directly with ferrocene at 5.33 wt%. The oil-purified mixture was thoroughly stirred for 30 min and 6 mL was cross sprayed in a vaporization furnace at 470°C, followed by 60 min of synthesis performed at 750°C. Brief descriptions of the synthesized CNFs and their significant characteristics were provided. The CNFs were described as urchin-like (urchin being a marine creature). The clusters were composed of a multi-needle-like nucleus, with a diameter of 146 nm, and radially developed from the heart, as presented in Figure 4 [364].

Sami *et al.* [86], showed that CNFs developed with different morphology and graphitization degrees through

Table 4: Different chemical methods for AC production from biomass with corresponding properties

Material	Activating agent	Temperature (°C)	Surface area ($m^2 g^{-1}$)
Potato peel [143]	H_3PO_4, KOH, and $ZnCl_2$	400, 600, and/or 800	—
Rice husk [351]	KOH	750	2,696
Rice husk [351]	H_3PO_4	500	1,741
Rice husk [351]	$ZnCl_2$	500	2,434
Peanut shell [351]	KOH	—	706.1
Coconut shell [351]	$ZnCl_2$	900	332.4
Coconut shell [351]	KOH	900	682.0
Banana peel [351]	KOH	800	217.3
Soybean [351]	KOH	—	2690.3
Wheat straw [351]	KOH	—	1,066
Pomelo peel [351]	KOH	—	1,533
Pomelo peel[351]	H_3PO_4	—	1,272
Citrus peel [351]	KOH	—	1,167
Olive stone [351]	KOH	—	587

decomposition of the electrical cracking gas on Fe_2O_3. Compared to conventional physical methods, such as laser ablation and CVD, the benefits of this process are CNFs with high performance, high selectiveness, and low cost. The use of electric cracking gas to synthesize CNFs is promising [86]. It enables organic liquid waste from the chemical industry to be used while carbon and hydrogen are obtained at moderate temperatures. The synthesis of CNFs was done using an integrated reactor based on a fluid laboratory design. The electrical cracking gas was removed from the electrical gas storage using a valve, regulated by a valve, and operated by a water U-tube manometer at atmospheric pressure. Physical, morphological, chemical, and environmental features of produced nanofibers were studied by scanning electron microscopy (SEM). Many advanced properties were exhibited wherein the catalytic decomposition was shown to be the main pathway for CNF growth [365].

3.1.3 CNTs

Suriani *et al.* [100] produced CNTs from refined domestic cooking palm oil that was used to fry three loads of fish. The synthesis process was carried out in a floating-catalyst thermal CVD reactor. Alves *et al.* [366] synthesized CNTs from sugarcane bagasse supplied from the ethanol industry. In that study, pyrolysis was used in which the materials were decomposed by a thermal treatment in the absence of oxygen. Qu *et al.* [367] synthesized CNTs by heating leaves of poplar to 450°C in air and Suriani *et al.* [368] succeeded in the production of vertically aligned CNTs by catalytic thermal CVD using waste chicken fat and skin collected from a wet market and then converted into carbon precursor through a rendering process.

Bernd *et al.* [371] produced CNTs through pyrolysis of wood sawdust in a tubular reactor and Lotfy *et al.* [369] applied a novel pyrolysis system to prepare CNTs from RS, which is considered an undesirable biomass in Egypt. Singh *et al.* [370] succeeded in the synthesis of CNTs from polyvinyl alcohol (PVA) using fly ash, red mud, and rock samples *via* an alkali treatment followed by the fabrication of thin films and pyrolysis of composite films. Finally, Bernd *et al.* [371] synthesized carbon nanostructures by the pyrolysis of wood sawdust in a tubular reactor, as shown in Figure 5. Table 6 summarizes the different methods used for the production of CNTs and their corresponding properties.

3.1.4 G

Renewable biomass resources are essential for G precursors such as glucose, rice husk, hemp, and disposable paper cups. Recently, glucose was used as a preparatory material for G with the aid of $FeCl_3$. The obtained G had effective electrical conductivity [374]. Researchers also synthesized "patched graphene," G produced using glucose with the aid of dicyandiamide (DCDA). The author of this study claimed the resulting G to be highly crystalline and clean. Luyi *et al.* succeeded in the production of biocompatible G from rice husk [375–377]. The obtained G could be used for bioimaging and bioprobing [188]. Fibrous hemp waste was successfully converted to G by Wang *et al.* [378] while Zhao obtained high quality and high yield G using disposable paper cups as a precursor [379]. Industrial

Table 5: Different chemical methods for AC production from industrial wastes with corresponding properties

Material	Carbonization	Carbonization temperature (°C)	Activating agent	Activating temperature (°C)	Surface area
PET [346]	N_2 for AC-a				402 $m^2 g^{-1}$ for AC-a
	$N_2 + H_2O$ for AC-b				359 $m^2 g^{-1}$ for AC-b
	CO_2 for AC-c	50	$FeCl_3$	500	123 $m^2 g^{-1}$ for AC-c
PET [353]	N_2	600	KOH in a nitrogen stream	850	2,831 and 2,666 $m^2 g^{-1}$
PVC [353]	Air	300	KOH in the presence of nitrogen	750	–
Refuse paper and plastic fuel [353]	–	–	K_2CO_3	–	1,330 $m^2 g^{-1}$
Sawdust [359]	–	–	KOH	500,	1876.16 $m^2 g^{-1}$

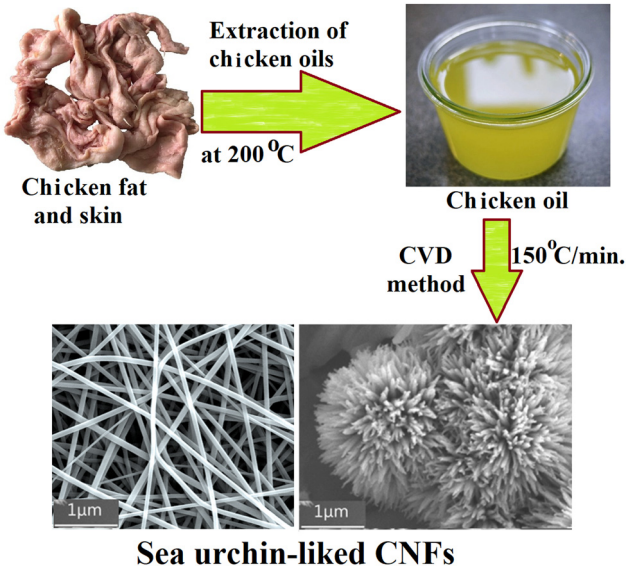

Figure 4: (Bottom) SEM images of CNFs synthesized using waste chicken fat. Copyright © 2015, Elsevier Publishing Group [362].

wastes, such as plastic, can be used as precursors for G production. A group of researchers developed an approach to produce G from various wastes and food using CVD. This new approach is sensible, however, its yield is a matter of concern [374]. The production of G from WCO is a very interesting topic to many researchers. Recently, a group of researchers developed a method to produce G from waste cooking palm oil due to the presence of palmitic acid, $CH_3(CH_2)_{14}COOH$, which is the source of carbon. Consequently, this method indicates the possibility of using waste cooking palm oil to obtain G at a low cost and without consumption of fossil fuels [380].

Graphite and organic materials are fundamental sources for the preparation of G. The approach of each method to prepare G, CVD on metallic films [381], liquid exfoliation of graphite crystal [382], mechanical cleavage [383], growth on silicon carbide [384], and chemical reduction of GO [385], has been illustrated by Ren and Cheng [386].

Glucose extracted from vegetable waste (as biomass) was first used to produce G in the presence of $FeCl_3$ [387]. Initially, the glucose and $FeCl_3$ were dissolved in water at 80°C to form carbonized glucose and $FeCl_2$ (H_2O_2). The production of G was obtained at 700°C. DCDA was added to glucose in the presence of nitrogen to form graphite carbon nitride (g-C_3N_4) [388]. At a temperature higher than 750°C, G sheets were obtained, as shown in Figure 6.

Biomass material, like hemp, can be converted to G by the hydrothermal method [378]. In this technique, fibrous hemp is heated around 180°C for an entire day. Then, KOH is added to produce porous G. Disposable

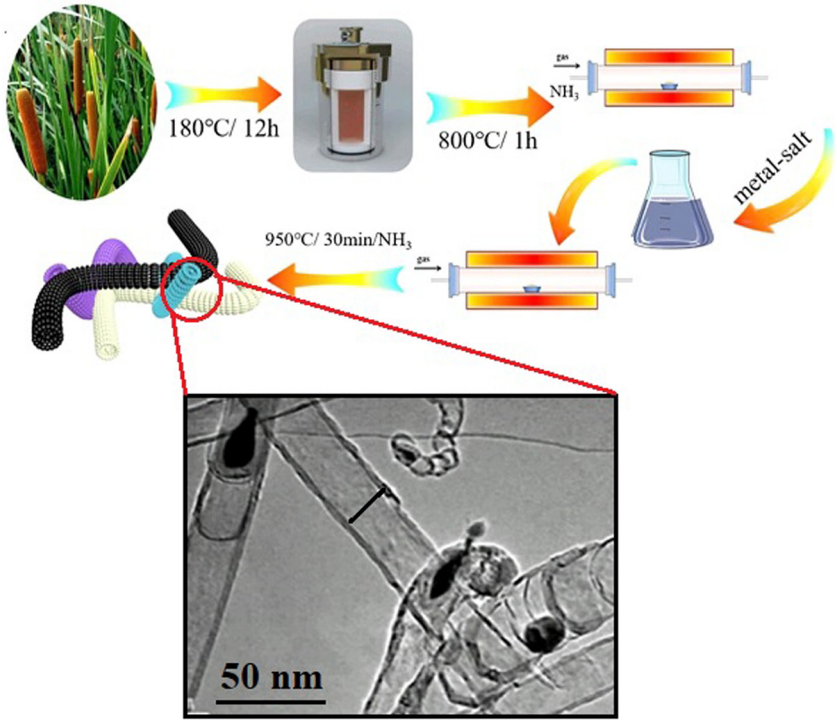

Figure 5: Schematic of the preparation of CNTs with corresponding particle size determination using high resolution transmission electron microscopy (HRTEM) imaging [371].

paper cups can be used as a precursor for G production. In this approach, iron has been used as a catalyst to form Fe_3C layers by heating the activated paper cup at high temperatures [379]. Industrial waste, such as plastic, is also a good source of carbon for G production. CVD is the most common approach to produce G from industrial waste [128]. Finally, cooking palm oil is an organic molecule that has been used as a precursor for G production *via* double thermal CVD using nickel as the deposition surface with variable temperature (850–1,100°C in 50°C increments) [389].

3.2 IQDs

3.2.1 CQDs

Biomass has a high carbon and oxygen content and is a non-toxic and widely available feedstock, making it a fascinating CQD source. Currently, several agricultural, forestry, and food waste types, such as rice husk, wheat straw, sugar cane bagasse, soya, onion, peanut cotton shell, potato, durian, and fruit/vegetable peel (orange, banana, pineapple, onion, seaweed, watermelon peel, *etc.*), have been utilized to manufacture low-cost CQDs [390,391]. Several precursors have been used for the preparation of CQDs, including banana peel waste, while using easy and green hydrothermal methods without passivates or additives [392].

By using red cabbage (RC) and a one-step hydrothermal method, Sharma *et al.* [393] evaluated a green method for the creation of CQDs. Yang *et al.* [394] studied expired fruits as carbon sources for the preparation of CQDs and Luo *et al.* [395] prepared CQDs using loofah sponge-based AC fiber as the raw material. Zhang *et al.* [396] used black soya beans (BS) as a cheap source of carbon for the green synthesis of BS-CQDs. Such high-value CNMs, such as the CQDs, can be synthesized using other abundant waste, such as low-cost petroleum coke byproducts and humic acid. Tajik *et al.* [397] also described the graphitic framework of petroleum coke with benzene or aromatic fields, which permits a chemical oxidation process for the synthesis of CQDs.

Compounds such as chitosan, citric acid, urea, and ascorbic acid, as well as a variety of foods, plants, waxes, and wastes, such as peels (mango, orange, banana, pineapple, onion, seaweed, *etc.*), egg yolk oil, meat, grains, nuts, or vegetable byproducts, have been used in the synthesis of CQDs. These compounds are low cost starting material for the creation of carbon materials [398]. Due to their green chemistry, hydrothermal and solvothermal methods are ecofriendly, mass-producible,

Table 6: Different synthesis methods and corresponding properties of CNTs

Method of preparation	Carbon source	Type and shape of CNTs	Catalyst and temperature	Diameter	Surface area	Notes	References
WCO							
Catalytic cracking	WCO model compound	Few multi-walled CNTs and some CNTs with an open-top structure	Catalyst: Ni-Co/SBA-15 catalysts Temperature: 750°C	50–100 nm	—	—	[96]
Waste biomass							
Pyrolysis	Wood sawdust	Single and double-walled CNTs	Catalyst: Ferrocene or Fe/Mo/MgO Temperature: 750°C for 3 h	25 nm	—	Wood sawdust was mixed with reducing agents (commercial zinc), calcite (bed material), and catalyst and arranged in the column reactor, as shown in Figure 5	[371]
Pyrolysis	Hydrocarbons of:	Type of CNTs depends on the type of RS precursor	Catalyst: Fe-Ni oxides supported on Al_2O_3	The diameter of CNTs differ according to the type of RS precursor	The surface area of CNTs from raw RS is 188 $m^2 g^{-1}$	Hydrothermal treatment was carried out to produce hydrocarbons as an intermediate carbon source	[369]
	Raw RS	Multi-walled CNTs (from raw RS and RS-neutral)		Raw RS (from 15 to 40 nm)			
	RS-neutral pulp	Needle-shaped CNTs (from RS-AP and RS-SP)	Temperature: 750°C for 120 min	RS-NP (from 14.7 to 47.9 nm)			
	RS-alkaline pulp (AP)			RS-AP (from 2.5 to 6.8 nm)			
	RS-sulfite pulp (SP)			RS-SP (from 4 to 8 nm)			
Hydrothermal + temperature calcination approach	Recyclable plant *Typha orientalis*	Nitrogen-doped CNTs	Catalyst: – Temperature: 180°C for 12 h, washed, freeze dried, and annealed at 800°C for 1 h in NH_3 atmosphere	CNTs: 150 nm Pore diameter: 4 nm	281.3 $m^2 g^{-1}$	—	[372]
Industrial wastes							
Pyrolysis	Fly ash, red mud, and rock sample	Different types of CNTs	Catalyst: – Temperature: 500°C for 20 min	20–30 nm	CNTs from: fly ash (42.3 $m^2 g^{-1}$), red mud (38.8 $m^2 g^{-1}$), and rock sample (19.7 $m^2 g^{-1}$)	—	[373]

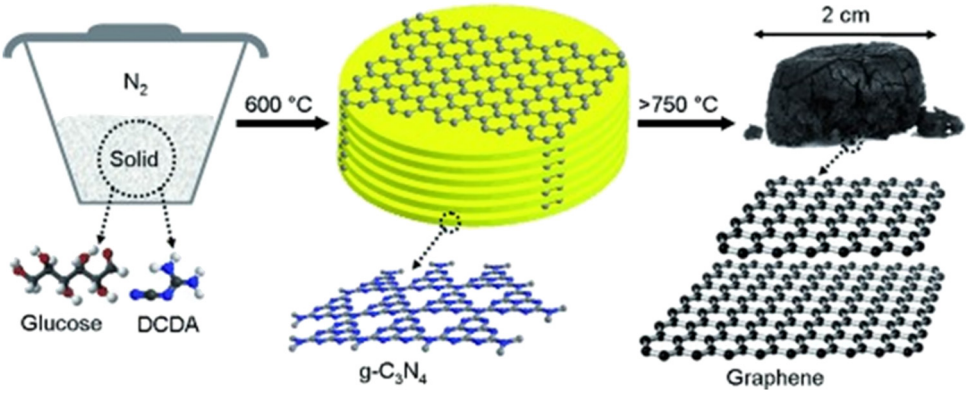

Figure 6: Proposed synthesis method for free-standing G. Bottom: repetition motifs of an ideal $g\text{-}C_3N_4$ plane (middle) and of G (right); C is indicated by black or gray, N is indicated by blue. Copyright © 2012, Wiley Publishing Group [387].

cost effective, clear, and applicable for the synthesis of CQDs using various organic sources [393]. Başoğlu *et al.* [399] studied a simple CQD green synthesis method that used rusty chickpea as the single-stage carbon source, with no chemical additives. In another example, expired passion fruit shell (EPFS) and pulp were separated physically and the EPFS was cleaned using pure water. Then, the EPFS was placed into a furnace at 120°C for 28 h. After drying, the EPFS was crushed into a fine powder and placed into a 60-mesh sieve. Next, 2 g of EPFS powder with 40 mL of ultra-pure water was added to a polytetrafluoroethylene lined reactor and heated for 3 h at 175°C. Then, the received brown solution was filtered by a polyether sulfone membrane and centrifuged for 20 min at 15,000 rpm. After centrifugation, the product was dialyzed using a 2,000 days dialysis bag for two days. After the dialysis, the solution was freeze-dried to achieve the desired solid CQDs. The obtained CQDs were uniformly dispersed and spherical, with a size below 5 nm, indicating good dispersion (Figure 7).

3.2.2 GQDs

High-quality GQDs with a yield of ~15 wt% were prepared from rice husk biomass by Wang *et al.* [188]. Also, GQDs were produced utilizing a low-cost, green, and renewable biomass resource *via* microwave treatment by Abbas *et al.* [400]. Recently, scientists have targeted the transference of 2D G into 0D GQDs and studied the impact of edge

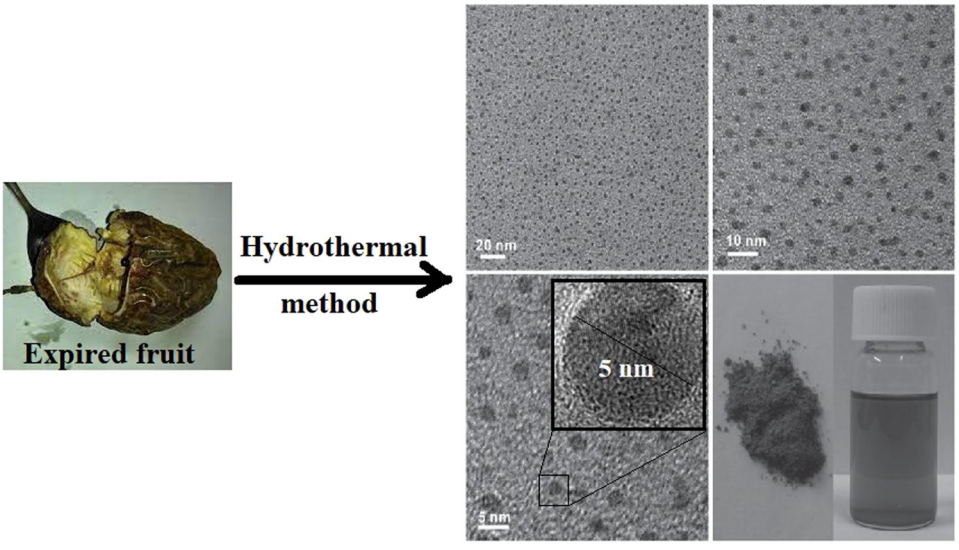

Figure 7: Proposed synthesis technique for powder CQDs by the hydrothermal method and corresponding transmission electron microscopy (TEM) images at different magnifications. Copyright © 2021, Springer Publishing Group [399].

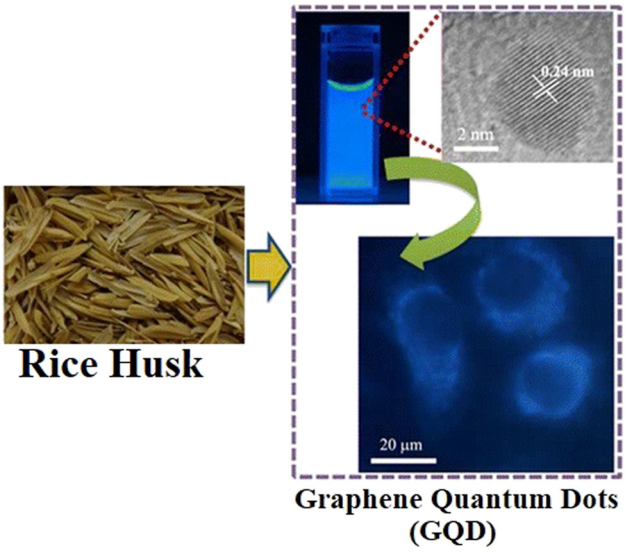

Figure 8: Proposed synthesis for powder GQDs by the hydrolysis method and corresponding TEM imaging. Copyright © 2016, ACS Publishing Group [188].

effects and quantum confinement on the properties of the new material [401]. GQDs are synthesized from molecules with aromatic structures (biomass and cooking oils) where the formation of GQD moieties can undergo a step-by-step chemical reaction by molecular precursors. These approaches allow for excellent control of the properties of the final product [401,402].

The synthesis of GQDs from a low cost, green, and renewable biomass resource, rich in carbon, was achieved using microwave treatment of carbon biochar through the pyrolysis of biomass waste. Increasing the reaction time or microwave power resulted in an increase in the product yield (~84% yield was achieved) [400]. Wang *et al.* [188] synthesized high-quality GDQs from rice husk biomass and it was found to be a useful source that produced a yield of ~15 wt%. HRTEM, atomic force microscopy, and Raman spectroscopy were used to determine the size, structure, and morphology of the rice husk, as shown in Figure 8.

3.3 MO-based NMs

3.3.1 Iron oxide

Bishnoi *et al.* [223] used the extract of *C. ramiflora*, an inedible fruit waste, for the synthesis of magnetic IO NPs. *C. ramiflora* belongs to the leguminosae family. It is largely found in Africa, as shown in Figure 9, and is used for biomedical and environmental applications.

Additionally, IO NPs have been synthesized using tangerine peel extract and used as an adsorbent for cadmium ion removal from contaminated solutions. Ehrampoush *et al.* [221] prepared IO NPs by the co-precipitation method in the presence of tangerine peel extract, which prevented accumulation and reduced the diameter of the synthesized IO NPs. Sundaram *et al.* [403] isolated the *Bacillus subtillis* bacterial strain from rhizosphere soil to produce IO NPs through the fermentation process. Khan *et al.* [404] described the synthesis of superparamagnetic IO NPs in bio char from the condensed tannin extract of *Acacia mearnsii*. They utilized a single-step process compliant with the principles of green chemistry. By the warm deterioration of iron oleate within sight of sodium oleate (from biomass waste), Xie *et al.* [405]

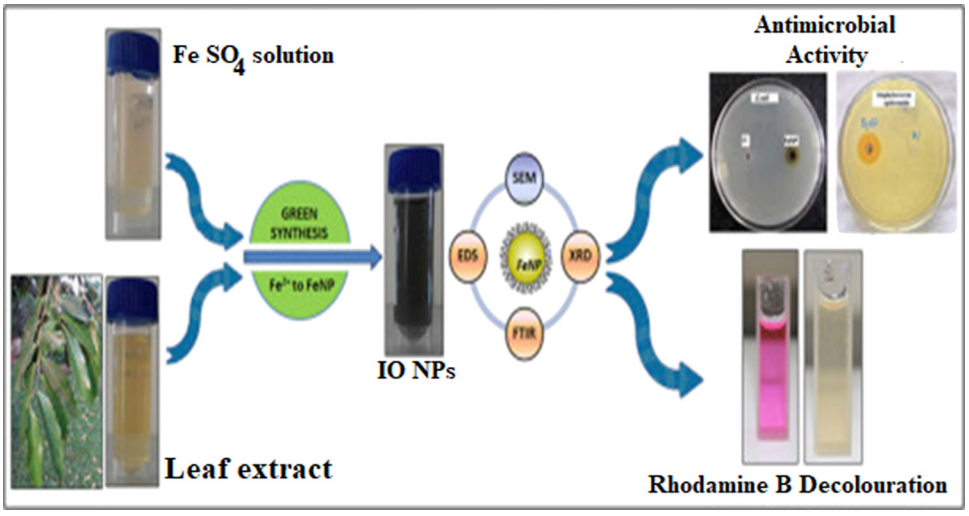

Figure 9: Biosynthesis of IO NPs using *Cynometra ramiflora* leaf extract for biomedical and environmental applications.

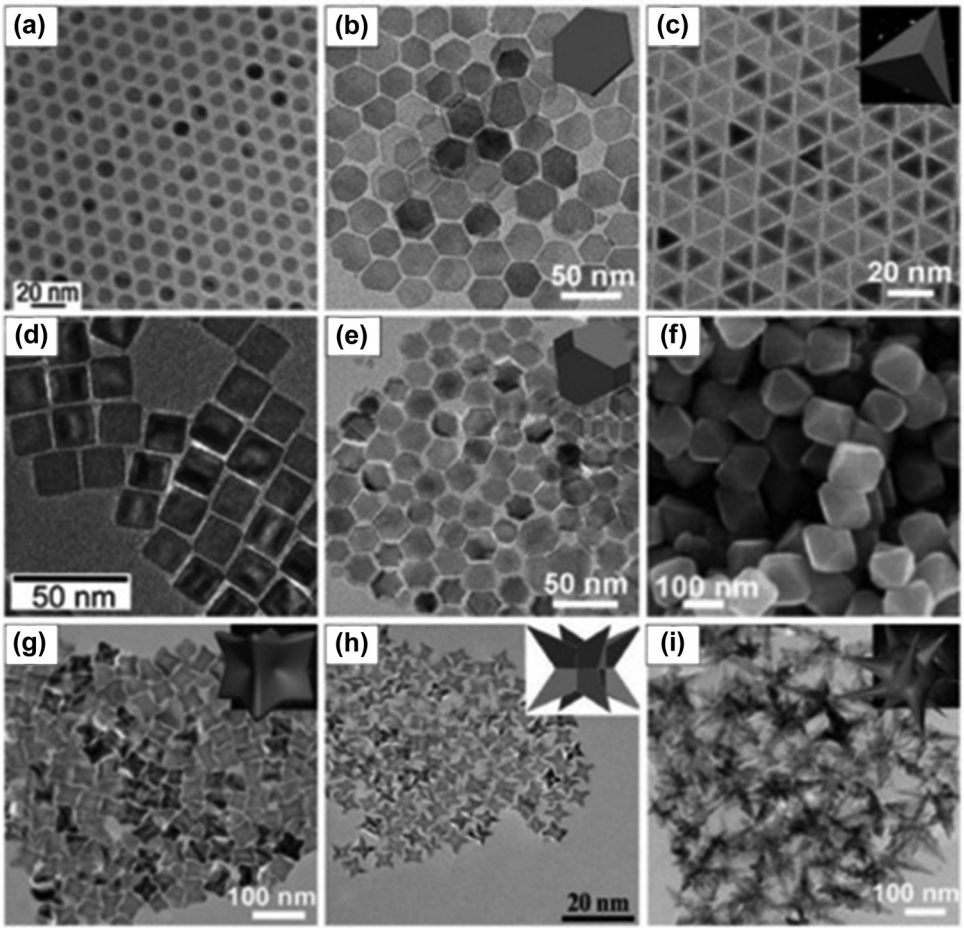

Figure 10: Example morphologies of 0D IO NPs synthesized from iron oleate and sodium oleate (biomass wastes): (a) nanospheres, (b) plates, (c) tetrahedrons, (d) cubes, (e) truncated octahedrons, (f) octahedrons, (g) concaves, (h) octapods, and (i) multi branches [405].

integrated IO NPs with different shapes. By tuning the molar proportion of sodium/iron oleate or the response temperature, plates, tetrahedrons, octahedrons, curves, multi-branches, or self-gathered designs could be achieved (Figure 10).

Another study [155] synthesized IO NPs utilizing *R. tuberosa* leaf fluid concentrate and their ultraviolet-visible spectroscopy investigation showed obvious tops at 405 nm. Dynamic light dissipation determined the normal size of IO NPs to be around 52.78 nm and differential scanning colorimetry demonstrated the strength of IO NPs until reaching the high temperature of 165.52°C.

Promptly after adding iron sulfate to the leaf extract, IO NPs were shaped and in this manner, the technique is straightforward and quick [406]. In this investigation, a basic, fast, and eco-accommodating green technique was used to create magnetite IO NPs utilizing the fluid concentrates of two food-handling wastes, in particular the velvety hairs of corn (*Zea mays* L.) and external leaves of Chinese cabbage (*Brassica rapa* L. subsp. pekinensis). The bubbled arrangements of satiny hairs (MH) and external leaves of Chinese cabbage (CCP) were utilized to blend IO NPs under photograph uncovered conditions [407]. Another study revealed that *C. maxima* peel extract yielded IO NPs with a diameter of 10–100 nm and high stability [408].

3.3.2 TiO_2

TiO_2 NPs have been prepared from biomass, cooking oils, and industrial waste through chemical, physical, and biological approaches. There are also different chemical methods to create TiO_2 NPs, such as sol–gel, solvo-thermal, hydrothermal, and co-precipitation methods [409]. Table 7 summarizes the different chemical methods used to fabricate TiO_2 NPs from biomass and their corresponding properties.

On the other hand, physical methods, such as electrophoretic, thermal plasma, spray pyrolysis, and microwave-assisted techniques, have been applied for TiO_2 NP

Table 7: Different chemical methods for the synthesis of TiO_2 NPs and their corresponding properties

Material	Method	Initial temperature (°C)	Final temperature (°C)	Pressure (bar)	Surface area ($m^2 g^{-1}$)	Size (nm)
RS [229]	Sol–gel	80	500	—	97	13.0 ± 3.3
Eggshell [410]	Solvothermal	—	454	227	—	78.73

synthesis from different biomass wastes [409]. Biological synthesis methods (also called green synthesis methods), use plants and fruit extracts, in addition to their waste materials and microorganisms (*via* fermentation methods), for the synthesis of NMs, to reduce the use of costly, toxic chemicals. Thus, they are considered as cost-effective and ecofriendly methods [409]. Table 8 summarizes the different biological methods used for the synthesis of TiO_2 NPs from microorganisms and fruit peel extracts with their corresponding properties.

3.3.3 ZnO

Ramimoghdam *et al.* [412] suggested a method for recycling waste oil for the synthesis of ZnO NPs. The group used palm olein, the liquid fraction of palm oil, as a biotemplate to synthesize NPs with different morphologies. Bio-templating is the use of a biological structure that serves as a template, guiding the assembly of inorganic materials into NPs of the desired morphology.

Industrial waste first supplied a pure zinc source in 2011 when Deep *et al.* [413] dismantled spent Zn–MnO_2 batteries, separated their metal components, and used the purified zinc for NP synthesis. In a later study, Deep *et al.* (2016) [414] also used spent Zn–MnO_2 batteries to propose a simpler, more efficient synthesis method: a one-pot solvothermal process. This method resulted in the isolation of highly pure ZnO NPs at a recovery percentage ≥95%. Farzana *et al.* [415] similarly synthesized ZnO NPs from Zn–C spent batteries.

The use of microbial biomass (nanofactories), acting as reducing and capping agents through the fermentation process, was first investigated by Jayaseelan *et al.* [424] for the preparation of ZnO NPs by adding ZnO to a suspension of *Aeromonas hydrophila* bacteria. More recent studies have reported the use of C-phycocyanin pigment from cyanobacteria in the synthesis of phycocyanin–ZnO nanorods [417] with the use of zinc-tolerant *Lactobacillus plantarum* [425].

Agricultural waste and inedible plant leaves and peels are also being used as bio-reductants for green ZnO NP synthesis, mainly due to their polyphenolic content. Different wastes have been used for the biosynthesis of TiO_2 NPs, such as rambutan peel [272], *M. oleifera* peel [251], and agricultural waste [426], which contains bioreductant and secondary metabolites such as terpenoids, alkaloids, and flavonoids. In 2020, ZnO NPs were synthesized using orange peel [427], non-edible cauliflower leaves [291], garlic skin extract [428], and banana peel [429]. In 2021, Rambabu *et al.* [423] used date pulp waste to synthesize ZnO NPs. Table 9 includes all the methods applied for ZnO NP synthesis from industrial waste, biomass, and cooking oils.

Table 8: Different synthetic biological methods, and corresponding properties of TiO_2 NPs

Material	Initial temperature (°C)	Final temperature (°C)	Size (nm)
Orange peel extract [235]	100	500	21.61 and 17.30
Plum peel extract [228]	70–80	400–500	47.1 and 63.21
Peach peel extract [228]	70–80	400–500	200
Kiwi peel extract [228]	70–80	400–500	54.17 and 85.13
Sugar-apple [411]	—	—	23
Aeromonas hydrophila [411]	—	—	40.50
Bacillus amyloliquefaciens [411]	—	—	22.1–97.2
Bacillus mycoides [411]	—	—	40–60
Bacillus subtilis [411]	—	—	30–40
Lactobacillus sp. [411]	—	—	24.63
Planomicrobium sp [411]	—	—	100
Aspergillus niger [411]	—	—	73.58

Table 9: Different waste materials and synthesis methods used to create ZnO NPs with different sizes and morphologies

Source of waste material	Type of waste material	Zinc source	Type of synthesis	Name of synthesis method	Reaction temp. (°C)	Calcination temp. (°C)	Size (nm)	Morphology	Ref.
Industrial waste	Spent Zn–MnO_2 batteries	Zinc extracted from waste electrode material	Chemical	Solvothermal synthesis	250	NA	5	Spherical	[414]
Industrial waste	Spent Zn–C batteries	Zinc from waste electrode material	Chemical	Thermal nanosizing	900	NA	50	Spherical	[416]
WCO	Palm oil	Zinc acetate	Chemical	Hydrothermal method using palm olein as a bio-template	120	NA	Micro- and nano-sized particles, depending on the volume of palm olein added and reaction time	Different morphologies, depending on the volume of palm olein added and reaction time	[412]
Microbial biomass	Phycocyanin extract from *Cyanobacterium Limnothrix* sp. K005	Zinc acetate	Biological (fermentation)	NA	30	NA	33–35	Nanorods	[417]
Microbial biomass	*Serratia nematodiphila*	Zinc sulfate	Biological (fermentation)	NA	NA	NA	15–30	Spherical	[418]
Plant biomass	*Moringa oleifera* peel extract	Zinc acetate	Biological + physical	Microwave-assisted synthesis	Microwave power of 300 W	400 and 600	40–45	Spherical	[419]
Plant biomass	Sheep and goat fecal matter (agri waste)	Zinc sulfate	Biological	NA	Room temperature	350–400	24.4–28.5	Spongy and flower shaped	[248]
Plant biomass	Orange peel extract	Zinc nitrate	Biological	NA	60	400	Different sizes depending on reaction temperature and pH	Different morphologies depending on reaction temperature and pH	[263]
Plant biomass	Cauliflower leaf extract	Zinc nitrate	Biological	NA	Sonication at 30	NA	100	Spherical	[419]
Plant biomass	Pectin from durian rind	Zinc acetate	Biological	NA	Room temp.	NA	280–456	Spherical	[420]
Plant biomass	Pectin from banana peel	Zinc acetate	Biological + chemical	Co-precipitation	Room temp.	NA	20–40	Thin flakes, nanocones, flower-shaped, and cubic-shaped	[421]
Plant biomass	Banana peel extract	Zinc acetate	Biological	NA	NA	NA	20–90	Spherical, triangular	[422]
Plant biomass	Garlic skin extract	Zinc chloride	Biological	NA	NA	NA	7.77	Rod shaped, hexagonal	[428]
Plant biomass	Date pulp waste	Zinc nitrate	Biological	NA	Room temp.	400	30	Spherical	[423]

3.3.4 CuO

The green biosynthesis of CuO NPs from different waste materials, such as cooking oil, biomass (including plants and microorganisms), and industrial wastes, is common, as shown in Figure 11. Javed *et al.* used waste palm oil as a base solvent for the synthesis of ecofriendly, highly stable, and bio-renewable CuO NPs [430]. The synthesis of CuO NPs using bio-waste plant peels, lignocellulosic biomass-rich materials, and seed extract, such as citrus peel (orange, lemon, and tangerine) [430,431], banana peel (*Musa acuminate*) [303,432], pomegranate peel (*Punica granatum*) [302,433,434], pomegranate seeds [435], papaya peel (*C. papaya*) [280], date stone [434], *Zea mays* husk [435–437], onion peel (*Allium cepa*) [438], fava bean seed peel [439], cauliflower (*B. oleracea*), potato (*Solanum tuberosum*) and pea (*Pisum sativum*) peels [440], and *Colocasia esculenta* leaf waste has been reported (Table 10) [441]. Recycling a variety of industrial wastes is a low-cost and safe method for CuO NP production. CuO NPs have been recovered from Cu-rich industrial waste, such as e-waste that includes SIM cards [442] and printed circuit boards (PCBs) [443–446], batteries, including LIBs and NiMH batteries [447], waste sludge [448,449], and wastewater (Table 11) [450].

3.4 Au NPs

The synthesis of NPs using chemical methods is usually associated with the formation of toxic byproducts. Therefore, the use of biosurfactants/biological materials (biomasses like microbes and plants) for the synthesis and stabilization of Au NPs is gaining importance since a decade [458]. The microbial route for the synthesis of Au NPs is a very exciting process, as several factors including microbial cultivation methods on organic and/or inorganic wastes and extraction techniques can be optimized for the fast synthesis of monodispersed NPs by the fermentation process. Many biological systems such as those of fungi [459] and algae [460] have been studied for the biosynthesis of Au NPs.

A newer Au NP synthesis technique includes materials such as oat and wheat biomasses, which have been shown to reduce aqueous gold ions to gold zero-valent forming Au NPs [310]. Recently, a method was developed for the preparation of Au NPs that involves application of an alternating current voltage to metal electrodes in an electrolyte solution containing a water-soluble polymer dispersant and a reducing agent [461]. A method for the extraction of gold from waste electrical and electronic equipment as NPs stabilized with phospholipids was suggested using 1,2-dioleoylsn-glycero-3-phosphocholine [461].

WCO contains long hydrocarbon chains and polar ester bonds that make it a good choice for stabilizing Au NPs. In this preparation method, Au NPs are synthesized in WCO using the laser ablation technique at different temperatures. A gold plate (high impurity 99.99%) was immersed in 10 mL of pure palm oil, which was extracted from WCO. A laser beam of 532 nm wavelength, with a period and energy of 10 ns and 1,200 MJ, respectively, was used to ablate the gold plate at different temperatures for 5–60 min with a 30–60 Hz repetition rate.

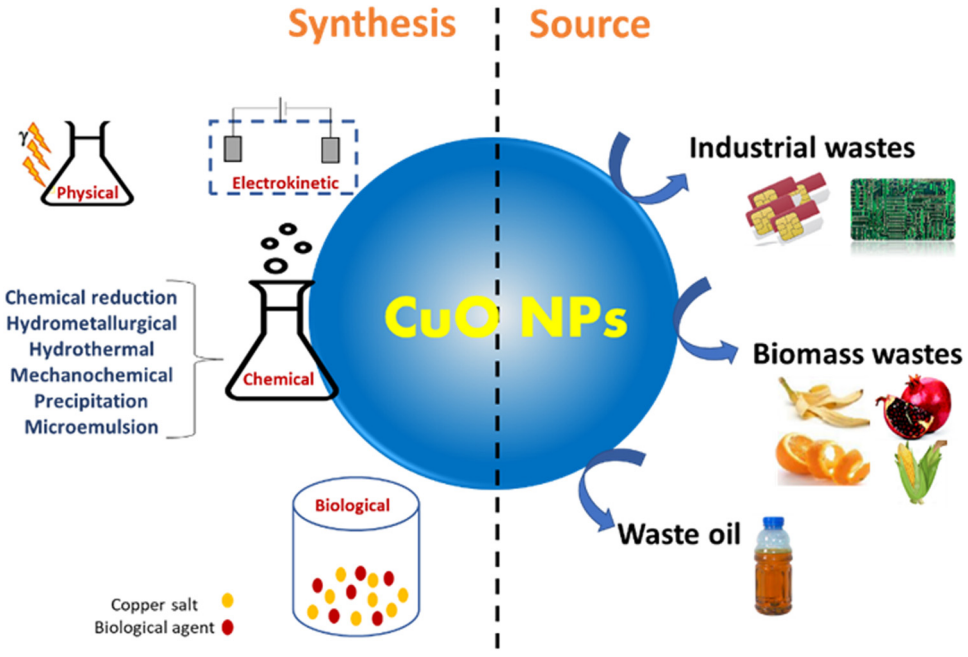

Figure 11: An illustration of the green synthesis of CuO NPs from waste materials by different physical, chemical, and biological methods.

Table 10: Green synthesis methods for producing CuO NPs from waste materials and their properties

Method	Waste material	Cu precursor	Size	Shape	Yield	Process	Advantages	Ref.
Industrial wastes								
Physical	Waste PCBs (WPCBs)	PCBs of old telephones and PCs	5–40 nm	Spherical	90%	Electro-kinetic (EK) method	Simple, ecofriendly, and cost effective	[444]
Chemical	Waste SIM cards	Waste mobile SIM cards	2–50 nm	Cauliflower like	95.3%	Wet chemical method	Simple and ecofriendly	[442]
	WPCBs	WPCBs	Different sizes	Irregular sheet	98%	Mechanochemical method	Simple and ecofriendly	[445]
	WPCBs	Old computer WPCBs	15–16 nm	Spherical	Over 90%	Chemical reduction "hydrometallurgical approach"	Cost effective/ecofriendly, high pure particles.	[451]
	WPCBs	Copper-containing waste etchants and $CuCl_2$	2–50 nm	Spherical	>99.90%	Microemulsion	Simple, economical, and safe, with low energy consumption, high production yield with high purity (>99.0%)	[443]
	WPCBs	WPCBs and $CuSO_4$	—	Spherical	96.9%	Chemical reduction	Simple, ecofriendly, cost effective, high production yield	[452]
	Wastewater	Wastewater from electroplating industry and $CuSO_4$	20–80 nm	Crystalline	99.98–99.99%	Precipitation method	Economic and safe process, with high production yield	[450]
	Wastewater sludge	Industrial wastewater	200–400 nm	Feather like	90%	Hydrometallurgical method by acid leaching	Simple, cost effective, and high production yieldwith high purity 98.26%	[449]
Waste oil								
Biological and chemical	Palm oil	Copper nitrate	25 nm	Spherical	—	Precipitation method	Simple, cost effective, and economic process	[430]
Plant wastes								
Biological and chemical	Lemon pulp	$CuCl_2$	20–40 nm	Irregular	103 mg/g	Hydrothermal method	Simple, rapid, ecofriendly, and cost effective with high yields	[453]
	Waste bamboo leaf	Copper acetate	70–80 nm	Hierarchical	—	Hydrothermal method	Simple, rapid, ecofriendly, cost effective, high production yield	[454]
	Onion peel	Copper chloride	11.7–45.5 nm	Berry-like	—	Microwave-assisted	Simple, rapid, ecofriendly, cost effective	[438]
Biological and physical	Fava bean seed peel	Copper sulfate	29.82 nm	Spherical	—	Gamma radiation	Simple, rapid, ecofriendly, cost effective	[439]
Biological method	Banana pulp waste	Copper acetate	1–4 µm	Octahedral	—	Banana pulp waste extract as a reductant	Simple, green, ecofriendly	[455]
	Banana peel	Copper sulfate	50–60 nm	Spherical	—	Banana peel extract as a reductant	Simple, green, ecofriendly	[432]
	Pomegranate peel and date stone	Copper sulfate	6–20 nm	Crystalline	—	Pomegranate peel and date stone extract as a reductant	Simple, green, ecofriendly	[434]

(*Continued*)

Table 10: *Continued*

Method	Waste material	Cu precursor	Size	Shape	Yield	Process	Advantages	Ref.
	Pomegranate peel	Copper chloride	5–25 nm	Rod and spherical	—	Pomegranate peel extract as a reductant	Simple, rapid, safe, with low energy consumption	[433]
	Pomegranate seeds	Copper nitrate	—	Broccoli	—	Pomegranate seeds extract as a reductant	Simple, green, ecofriendly	[435]
	Citrus peel	Copper nitrate	22.4–94.8 nm	Spherical	—	Citrus peel extract as a reductant	Simple, green, ecofriendly	[431]
	Papaya peel	Copper nitrate	85–140 nm	Crystalline	—	Papaya peel extract as a reductant	Simple, rapid, cost effective	[280]
	Zea mays husk	Copper acetate	20–70 nm	Spherical		Waste maize extract as a reductant	Simple, green, eco- and economically friendly	[437]
	Brown algae *Macrocystis pyrifera*	Copper sulfate	2–50 nm	Spherical	—	Brown algae extract as a reductant	Simple, ecofriendly	[456]

The solution temperature was raised using a hot plate. Au NPs formed during the laser ablation with an ablation time of 25 min. This experiment was conducted at different temperatures (40, 64, 75, 83, and 92°C). The solution was stirred during the ablation and the solution container was moved horizontally to obtain a fresh surface area for the Au NPs to guarantee that the Au NPs were dispersed equally in the WCO [309].

Velmurugan *et al.* [462] synthesized Au NPs from ginger waste, which includes the aqueous extract of waste ginger. Ginger waste acts as both a reducing and stabilizing agent. For a typical synthesis, 5 mL of the extract is added to 3 mL of freshly prepared 1 mM solution of $HAuCl_4$. The mixture was allowed to boil by rapid microwave heating. The appearance of the red color in the reaction mixture indicated the formation of Au NPs. The colored solution of Au NPs was then centrifuged, and the Au NPs were redisposed to remove any unreacted ions and molecules from the product. The produced Au NPs were highly stable and spherical, with diameters of 15.5 nm.

Liu *et al.* [463] synthesized Au NPs from banana peel by the hydrothermal process. After mixing with $HAuCl_4$ as the precursor, the banana peel was heated with water and acetone at 98°C. No extra chemical protectant or reductant was added. Finally, Au NPs with four leaf clover (dendrite) morphology were obtained, which were named Au dendrites, as indicated in Figure 12.

4 Biomedical applications of RNMs: Role of RNMs in the early detection of diseases

4.1 Fluorescence imaging

Biological components are too small to be observed by traditional microscopy, which lacks the accuracy and high-resolution localization to image the biological processes inside these components. A fluorescent dye fixes this problem by providing several optimal approaches to track cells and evaluate their functionality. Fluorescence imaging is a common tool used to visualize precious molecular mechanisms [464,465], gene and protein expressions [466–468], and interactions between cellular components, providing a deeper understanding of the biological process.

The advantages of fluorescence imaging over other imaging techniques are high selectivity of the desired

Table 11: : Various waste materials for CuO NP synthesis and their corresponding properties

Waste material	Cu precursor	Size (nm)	Shape	Ref.
Plant wastes				
Citrus peel (orange, lemon, and tangerine)	Copper nitrate	22.4–94.8 and	Spherical and	[430]
		8–8.9	irregular	[431]
Banana peel	Copper acetate	7.33	Spherical	[457]
		60		[303]
Pomegranate peel	Copper acetate and	10–100	Spherical	[302]
	Copper sulfate	6	Crystalline	[434]
Pomegranate seeds	Copper nitrate	—	Broccoli	[435]
Papaya peel	Copper nitrate	85–140	Crystalline	[280]
Date stone	Copper sulfate	20	Crystalline	[434]
Zea mays husk	Copper acetate	36–73	Spherical	[436]
		20–70	Spherical	[437]
Onion peel	Copper chloride	—	Berry like	[438]
Cauliflower peels, potato peels, and pea peels	Copper chloride	<100	Irregular	[440]
Colocasia esculenta leaf	Copper nitrate	<100	—	[441]
Industrial wastes				
e-waste	Waste mobile SIM cards	2–50	Cauliflower like and spherical	[442]
SIM cards	Waste telephones, PCBs	11, 25, and 40		[444]
PCBs	PCBs and chloride ($CuCl_2$)	20–50		[443]
Wastewater	Copper sulfate	20–80	Crystalline	[450]

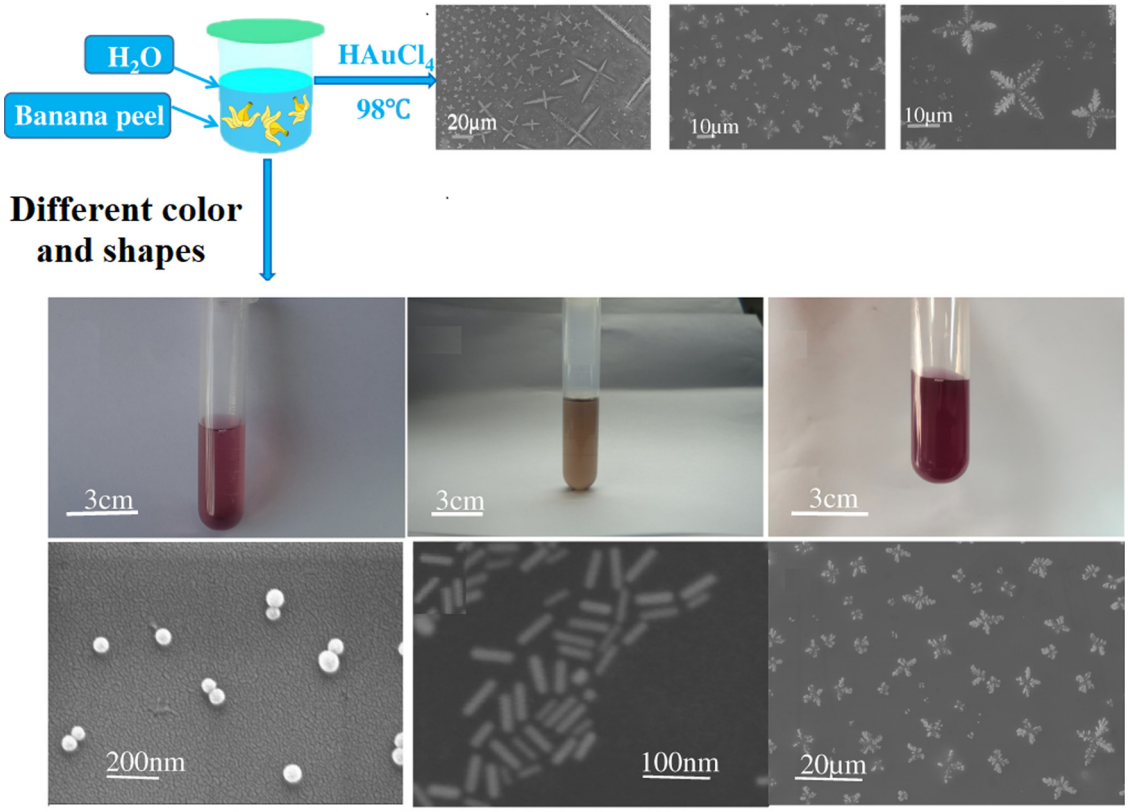

Figure 12: Simplified diagram of the synthesis process of Au dendrites and the different shapes with their corresponding colors. Copyright © 2020, Dove press Publishing Group [463].

area, high-resolution power, identification of microelements inside the cellular component, and production of high-contrast images [469]. Fluorescent NPs have promising qualifications for fitting the small size of the cellular components while providing more abilities compared to other fluorescent techniques, such as a low cytotoxicity level, better selectivity, smooth entrance, the ability to target a large number of cells at the same time, low chemical structure changes, and high-throughput screening [470,471].

Long-period cellular tracking *in vivo* provides valuable information regarding the biological process and biomedical therapeutics. Several biological imaging modalities have been developed for those applications, including magnetic resonance imaging (MRI), magnetic particle imaging (MPI), and fluorescence imaging. Merging nanotechnology with these methods has improved the safety of cellular tracking *in vivo* and has overcome some challenges of traditional imaging methods. Compared to conventional fluorescent methods, fluorescent NPs support the unique advantages of photofading resistance, higher brightness, and better size control [472]. Cellular tracking fluorescent NPs are inorganic QDs [473,474], nanodiamonds [475], fluorescent latex/silica nanobeads [476], and organic NPs [477].

The early detection of diseases is currently a critical point of focus in clinical practices. One of the most prominent examples is the early detection of cancer. It was reported that patients who were diagnosed early with gastrointestinal cancer had a higher survival rate than those who did not benefit from early detection (92.3% *versus* 33.3%) [478]. One of the key players in the early detection of diseases is biomedical imaging, which includes MRI, positron emission tomography, ultrasound, X-ray radiography, single-photon emission computed tomography, computed tomography (CT), and fluorescence imaging [479]. However, structural imaging modalities, such as CT, ultrasound, and MRI, are not useful in the detection of some tumors due to their detection limitations (0.5 cm) and spatial resolution. Imaging modalities can be combined to improve the efficiency of tumor detection [480]. Contrast agents (CAs) are used to provide accurate functional and anatomical information. Medical imaging CAs usually used are small molecules that have low undesirable toxicity, non-specific distribution, and fast metabolism. However, nanoimaging CAs are currently being studied extensively due to their outstanding properties compared to traditional CAs. Nanoimaging CAs exhibit a high surface-area-to-volume ratio, leading to enhanced surface functionalization and lower toxicity profiles [481]. Additionally, nanoimaging CAs exhibit a longer plasma circulation time and better biodistribution and bioavailability, thus enhancing the tumor-to-background contrast signal. Furthermore, the manipulation of NP properties allows optimized loading of imaging compounds [482,483].

4.2 Role of NPs in fluorescence imaging

Fluorescence imaging technology is currently widely used for disease diagnosis as it provides the highest spatial resolution compared to other imaging technologies [484]. However, fluorescence imaging in clinical settings is hindered by some limitations, including non-specific tissue auto-fluorescence, and limited penetration depth. Also, photobleaching effects and limited fluorescence in the target site decrease the sensitivity of the technology for disease detection [483,485–487].

NMs play a key role in the enhancement of fluorescence imaging to overcome limitations. Near infrared (NIR) fluorescence quenching could be avoided by using modified NPs [488]. NPs could also reduce photobleaching effects by converting low-energy photons into high-energy photons [489]. In addition, NPs allow the loading of more dye molecules, thus providing higher signals [490]. NPs could also be targeted to tumors or target sites through passive or active targeting, allowing accumulation in desired sites and increasing the fluorescent dye concentrations and thus the signal. Hence, fluorescent NPs are being extensively developed and investigated for biomedical applications [483]. For example, NP fluorescence imaging is currently used in several biomedical applications, such as enzyme activity evaluation, gene detection, cell tracking, protein analysis, real-time monitoring of therapeutic effects, and early detection of diseases [490–493]. For cancer diagnoses, fluorescent NPs play a crucial role as they provide high-resolution images at the cellular level. Examples of promising fluorescent NPs include QDs, organic dye-doped NPs, upconversion NPs, and Au NPs [494]. The different examples of NPs used in fluorescence imaging for early detection of different diseases are provided in Table 12.

4.3 CQDs for early disease detection *via* fluorescence imaging

Fluorescence imaging has gained increasing attention recently due to its high sensitivity, selectivity, and high-throughput ability. Developing optimum fluorescent probes has always been a challenge. QDs are inorganic

Table 12: Selected examples of NPs recycled from different wastes and employed in fluorescence imaging for early detection of different diseases

Authors	NPs	Waste source	Disease diagnosed/cells imaged	Ref.
Zhou *et al.* (2012)	CQDs	Waste watermelon peel	HeLa cells	[178]
Hu *et al.* (2014)	CQDs doped with sulfur	Waste frying oil	HeLa cells	[513]
Park *et al.* (2014)	CQDs	Food waste	HepG2 cells/Liver Carcinoma	[514]
Xue *et al.* (2105)	CQDs	Lychee seed	HepG2 cells	[515]
Xue *et al.* (2016)	CQDs	Peanut shell waste	Multicolor imaging of HepG2 live cells	[516]
Yao *et al.* (2017)	Gd@CQDs	Crab shell waste	HeLa and HepG2 cells	[517]
Bankoti *et al.* (2017)	CQDs co-doped with nitrogen, sulfur, and phosphorous	Culinary onion peel waste	MG63 and HFFs cells	[518]
Manaf *et al.* (2017)	CQDs	Sago bark industrial biowaste	N2a and melanoma A-375 cells	[519]
Cheng *et al.* (2017)	CQDs	Walnut shell biowaste	MC_3T_3 cells	[520]
Cheng *et al.* (2019)	N/S-CQDs	Cellulose-based biowaste from willow catkin	HeLa cells	[505]
Anthony *et al.* (2020)	Recycled CQDs	Rice waste	A549 cells	[551]
Ding *et al.* (2018)	GQDs	Lignin biowaste	RAW 264.7 cells, monocytes/macrophage-like cells	[552]
Zhang *et al.* (2019)	N-GQDs	Marigold plant	Detecting of Fe^{3+} ions as a target for bioimaging inside the living cells	[553]

semiconductor NCs that possess exceptional photophysical characteristics. Based on their quantum properties, QDs can emit a wide and broad spectrum of different fluorescent wavelengths that give them preference for use in biomedical applications, particularly in the tracking of circulating tumor cells and early diagnosis of abnormal tumor masses [495–497]. Briefly, QDs are made from a metallic-semiconductor core that includes elements of both II–VI (*e.g.*, ZnSe, CdTe, CdS, and CDSe) and III–V (*e.g.*, InAs and InP) groups of the periodic table, which are coated with a shell of biomolecules, like polysaccharides, peptides, or proteins, to prevent the leakage of toxic heavy metals and to provide good stability for the NP in a biological environment.

Although QDs have shown highly promising results among traditional fluorescent probes, it has been found that QDs exhibit some toxic effects, which limit the applications of heavy metal QDs. Alternatively, using safe, cost-effective, and ecofriendly materials that have been recycled from biological wastes has become a trend since they are readily available and less toxic. For example, CQDs produced from recycled biomass waste have been applied in fluorescent imaging.

CQDs are small nanostructures with carbon as the core element. Currently, this type of QD has received much interest due to its unique properties, including its size (below 10 nm), chemical stability, wide range of fluorescence emission, high availability, easy synthesis, and water solubility. The fluorescence of CQD emission ranges in the NIR spectrum and, in addition, CQDs have low physiological toxicity compared to semiconductor QDs, making them a superior choice for biomedical applications. The biomedical applications of CQDs are *in vitro* and *in vivo* bioimaging, drug delivery [498,499], tumor mass detection [500], and cancer therapy [501–503].

One of the main properties of CQDs is their fluorescence, which promotes their application in fluorescence imaging. Narrow emission spectrum, wide excitation spectrum, high fluorescence stability, and resilient resistance to photobleaching are all outstanding fluorescence properties of CQDs [137]. However, these excellent CQD properties are affected by the CQD source, such as CQDs biomass wastes. A study by Zhang *et al.* reported that the organic solvent used for CQDs affected the fluorescence emission peak position and fluorescence emission intensities of CQDs synthesized from polystyrene foam waste [504]. Another study by Cheng *et al.* stated that CQDs co-doped with nitrogen or sulfur and prepared from cellulose-based biowaste showed low cytotoxicity, good biocompatibility, and high fluorescence quantum yield and, thus, could be used in intracellular imaging applications [137,505].

The potential applications of CQDs in bioimaging have got much attention, particularly in cellular imaging. This application was first applied in 2006 to stain human colorectal adenocarcinoma cells (Caco-2 cell line) *in vitro* [398]. Additionally, several attempts have been made on different cell lines *in vitro*, such as HeLa [506,507], HepG2 [507], and A549 cells [508], for internal imaging. Also, bioimaging *in vivo* has been reported since researchers have managed to track murine alveolar macrophage *in vivo* [509], human neural stem cells [510], cardiac and pancreatic progenitors [511], as well as imaging ClO-ions inside nude mice [512].

Zhou *et al.* used waste watermelon peel for large-scale synthesis of CQDs. The produced CQDs exhibited high stability in a high salinity solution and a wide range of pH values with exceptional water solubility. The system was effectively used in fluorescence imaging of HeLa cells. Thus, the produced CQDs could be used as optical imaging probes in biomedical applications [178]. Moreover, Hu *et al.* demonstrated the synthesis of pH sensitive fluorescent CQDs doped with sulfur from waste frying oil for imaging and sensing of pH changes in HeLa living cells. The obtained CQDs exhibited high photostability, good fluorescence quantum yield, and low cytotoxicity, making them biolabeling probe candidates for imaging living cells [513].

Park *et al.* used ultrasonic treatment for the large-scale production of CQDs from food waste. The produced CQDs exhibited high photostability, good fluorescence, low toxicity, and high water solubility. The CQDs were used for the fluorescence imaging of human hepatocellular liver carcinoma (HepG2) cells and the nuclei of the cells produced a strong, red-colored fluorescence, indicating the ability of the CQDs to penetrate the cells while maintaining their properties intracellularly [137,514].

Xue *et al.* produced CQDs from lychee seeds by one-step pyrolysis. The CQDs exhibited low cytotoxicity, excellent biocompatibility, and could be used as an eco-friendly material for *in vitro* and *in vivo* bioimaging applications in cell biology and other sensing applications. Moreover, these CQDs were used for the fluorescence imaging of HepG2 live cells [515].

Another study conducted by Xue *et al.* used peanut shell waste to produce CQDs *via* the pyrolysis technique. The produced CQDs exhibited excellent photostability, high stability for a wide range of pH values, low photobleaching, outstanding biocompatibility, and low cytotoxicity. The CQDs were used as a fluorescent probe for multicolor imaging of HepG2 live cells. Bright blue, green, and red fluorescence were observed in the cytoplasm upon excitation at 405, 488, and 514 nm, respectively [516].

Yao *et al.* demonstrated the synthesis of magneto fluorescent CQDs through a one-pot microwave-assisted hydrothermal method using the transition metal ions Gd^{3+}, Mn^{2+}, and Eu^{3+} and crab shell waste. The formed Gd@CQDs were conjugated to folic acid (FA) and doxorubicin (DOX). The conjugated Gd@CQDs allowed specific targeting and fluorescence imaging of HeLa and HepG2 cells and displayed high cytotoxic effects on HeLa cells. Also, this prepared nanocomposite system showed high biocompatibility and low cytotoxic effects *in vitro* and *in vivo* (zebrafish embryos model). Hence, the nanocomposite could be used as theranostic agents or cancer diagnostic probes [137,517].

A study conducted by Bankoti *et al.* used onion peel from cooking waste to synthesize CQDs co-doped with nitrogen, sulfur, and phosphorous. The co-doped CQDs showed stable strong green fluorescence when used for imaging live MG63 and HFFs cells, with maximum emission at a pH of 7–8, indicating its potential for use in biomedical imaging applications. The reported system also exhibited good cytocompatibility, high blood compatibility, high stability against pH, and considerable wound healing activity [137,518].

Manaf *et al.* used sago bark industrial biowaste to synthesize CQDs *via* the pyrolysis method. The cell viability results indicated the produced CQDs had low cytotoxicity. Thus, they were used for fluorescence imaging of N2a and melanoma A-375 cells. Due to its safety, it is proposed that a higher concentration of the produced CQD fluorescence probes could be used to image samples that cannot be imaged using low probe concentrations [519].

A study conducted by Cheng *et al.* reported the synthesis of CQDs from walnut shell biowaste *via* the chemical cutting method. The obtained CQDs exhibited high photostability, outstanding cytocompatibility, and high ionic strength resistance. The CQDs emitted green fluorescence when used to image MC_3T_3 live cells. A high ability for intracellular trafficking by only staining the cytoplasm and not the nucleus was also demonstrated [520].

Another study by Cheng *et al.* demonstrated the use of cellulose-based biowaste, obtained from willow catkin, to synthesize CQDs doped with nitrogen or sulfur. The doped N/S-CQDs showed resistance to high ionic strength, outstanding photostability, excellent fluorescence quantum yield, good biocompatibility, and low cytotoxicity. They also exhibited the ability to detect intracellular Fe^{3+} ions, leading to quenching of their fluorescence. HeLa cells were used to demonstrate the detectability of the intracellular Fe^{3+} ions by N/S-CQDS through fluorescence imaging. Upon increasing the Fe^{3+} ion concentration, the blue fluorescence

intensity diminished due to significant quenching. Hence, the obtained N/S-CQDs could be used for labeling intracellular Fe^{3+} ions in living cells and aid in the detection of any imbalance in intracellular Fe^{3+}, which leads to several diseases [505].

4.4 Au NPs for early disease detection *via* fluorescence imaging

Due to the increased commercial demand for Au NPs in various applications, more green and sustainable methods have been attempted for their synthesis. One of the prominent approaches to restore this resource-limited material is the recycling of nanowaste and, also, development of nanoparticles synthesis methods depending on the recovered materials. Pati *et al.* (2016) developed a method to recover gold from nanowaste using α-cyclodextrin. This laboratory-scale strategy successfully recovered gold that was used for the production of Au NPs [521]. A study by Oestreicher *et al.* recycled aqueous laboratory nanowaste into aqueous $HAuCl_4$. The recovery rate was more than 99% and the recovered gold solution was used in the synthesis of Au NPs through the seed-mediated growth method. This work highlights the completion of a recycling cycle following green chemistry guidelines and considering ecological and economical aspects to achieve sustainability and follow the circular economy approach [522].

Au NPs have great potential in the early detection and diagnosis of diseases, especially cancer. This is due to their outstanding properties. For example, the high fluorescence quenching efficiency of Au NPs is used in fluorescence imaging for switching from on to off states of fluorescence [523–525]. In addition, Au NPs are very biocompatible and highly photostable. Au NPs range from single to hundreds of nanometers in size and can be easily functionalized and modified [526]. When excited with a wavelength equivalent to their surface plasmon resonance frequency, Au NPs scatter light resonantly, showing a distinctive optical response [527]. Moreover, Au NPs have outstanding anti-photobleaching behavior when excited by strong light. Although Au NPs have low quantum yields, they strongly display native fluorescence when excited with high energy light [528]. Based on this, fluorescence imaging using Au NPs was developed for cell imaging; the procedures include staining the cells with Au NPs then emitting high energy light, followed by collecting the native fluorescence of Au NPs from cells to develop a cell image [529]. Therefore, Au NPs are a good candidate for the early detection of diseases [483].

A study conducted by He *et al.* assessed the use of Au NPs as targeted probes for the detection of cancer cells by fluorescence imaging. First, the autofluorescence of HeLa cells was photobleached by strong excitation with light and then Au NP fluorescence was observed. Au NPs were taken in the cells *via* endocytosis in the differentiation and proliferation phases of the cells. The Au NPs were conjugated to anti-epidermal growth factor receptor antibodies to function as targeted probes for cancer cells, allowing their fluorescence imaging. The fluorescence imaging exhibited high selectivity when compared to other imaging techniques, including dark field imaging. While comparing the Au NPs as a fluorescent probe with other probes, such as QDs and fluorescent dyes, the Au NPs have better potential as a fluorescent probe due to their good photostability, high biocompatibility, ease of synthesis, and ease of functionalization. Hence, as fluorescent probes Au NPs have high potential in targeted drug delivery, cell imaging, and early cancer detection [529].

Au NPs are used extensively in tumor detection. Ultra-small Au NPs are reported to have an enhanced permeability and retention (EPR) effect in tumor sites; they could escape kidney filtration and have a longer half-life in the plasma [530]. A study conducted by Zheng *et al.* used ultrasmall Au NPs (2.5 nm) functionalized by glutathione (GSH) for fluorescent imaging of mice bearing MCF-7 tumors. The functionalized Au NPs were compared to IRDye 800CW (a small dye molecule) and the results revealed that the Au NP functionalized system had better fluorescence. Moreover, the system showed an enhanced EPR effect and was rapidly cleared from normal tissue after imaging. It has also been reported that the application of GSH–AuNPs is very promising in fluorescent imaging for cancer diagnosis [531,532].

Intracellular pH variations could be used for disease diagnosis. For example, cancer cells deregulate pH intracellularly as they flourish only in an acidic environment [533]. Yu *et al.* (2016) investigated cellular pH variations through fluorescence imaging. The group developed "submarines" formed from Au NPs that were pH sensitive and functionalized with fluorescent dyes that responded to basic and acidic pH. The submarines showed a great ability to map intracellular pH variations and to pass the blood–brain barrier (BBB). The BBB permeable submarines could be exploited in imaging and treating central nervous system (CNS) diseases, such as adult CNS tumors [534].

Another study conducted by Yu *et al.* investigated pH-responsive MRI and fluorescence imaging dual-modal Au NPs for tumor diagnosis and imaging. These nanovehicles have the ability for intercellular pH sensing, MRI, and fluorescence imaging of *in vivo* tumors, and cancer detection due to their modification by the tumor-targeting peptide cyclic arginine–glycine–aspartate (cRGD). Also, it has been reported that these modified nanovehicles could pass the BBB; thus, they could potentially be used in the detection of CNS diseases. To conclude, the developed Au NP based imaging agent, based on sensing pH changes in living cells and determining the size and location of tumors *via* fluorescence imaging, is a very promising tool for early detection of cancer [535].

4.5 GQDs for early disease detection *via* fluorescence imaging

GQDs are 0D NPs derived from carbon and consist of at least one G sheet in the nanoscale. Similar to CQDs, GQDs provided high-quality imaging, low toxicity, water solubility, and safe renal clearance with fluorescence emission at the NIR spectral region. Several applications regarding cell motion tracking and tumor imaging with GQDs have been tested. Chen *et al.* successfully synthesized GQDs to interact with cell surface carbohydrates for tracking cell receptor monosaccharides [536]. After one year, the same group managed to image the hydrogen sulfide level in living cells [537]. Due to the ultra-small size of the GQDs, they can penetrate cell nuclease and have been used for tumor cell detection *in vitro*. It was reported that GQDs can emit multifluorescent colors, which help detect more than one component within the cell-like emission of red, yellow, and blue fluorescence, allowing multicolor imaging of a glioblastoma U78 tumor cell line *in vitro* [538]. Similarly, coating GQDs with photoluminescence material has supported multicolor imaging inside the HeLa cell line *in vitro* [539,540]. Additionally, GQDs showed high selectivity and specificity for detecting more cell lines *in vitro*, including the Schwan cell line rsc96 [541] and murine alveolar macrophage cells (MH-S) [509].

In cancer detection applications, GQDs have been combined with well-known biological NPs, like IO NPs, to enhance the detection of carcinogenic HeLa and MCF-7 cell lines *in vitro* [542]. Similarly, GQDs were combined with fluorine for detecting HepG2 cells within a 3D model structure, mimicking the tumor microenvironment of these cells [543]. From this point, bioimaging *in vivo* has begun. Initially, GQDs were injected intravenously, subcutaneously, and intramuscularly in nude mice to evaluate the bioimaging of biological components *in vivo* as well as the biosafety of GQDs [509,540,541]. Furthermore, GQDs have been reported to have the potential for targeting tumor cells inside mice models. Nurunnabi *et al.* evaluated carboxylated GQDs cytotoxicity in addition to detecting the KB tumor of mice models [544]. Also, the targeting of reactive oxygen species (ROS), as a tumor biomarker of a pancreatic cancer cell line (PANC-1) injected inside a nude mice model, by synthesized cyclotriphosphazene-doped GQDs (C-GQDs) has been reported [545]. These results gave hope for treating cancer cells with more accurate drug delivery by targeting only tumor cells rather than normal cells [499,546]. Huang *et al.* managed to introduce folate–GQDs as an anti-cancer treatment for human liver carcinoma (HepG2) and human cervical (HeLa) cancer cell lines *in vitro* by injecting folate–GQDs inside zebrafish embryos to assess cytotoxicity [547]. Yao *et al.* used a combination of mesoporous silica NP GQDs (GQD–MSNs) using DOX as chemical – a photothermal drug for targeting the 4T1 breast cancer cell line [548]. Joshi *et al.* introduced sliver–GQDs loaded with inulin as a cancer therapy into pancreatic cancer cells *in vitro* and *in vivo* [549].

Biomass wastes originate from living organisms that contain carbon atoms as their major chemical element. For example, fossils, coal, petroleum, and natural gases release CO_2 when burned. Interestingly, CQDs successfully synthesized from biological wastes have been used in several bioimaging applications. For example, Atchudan *et al.* created recycled CQDs from banana peel waste and used them for bioimaging in nematodes [550]. Anthony *et al.* recycled CQDs from rice wastes and imaged A549 cells *in vitro* and *in vivo* (injected inside rat models) [551]. Although the synthesis of GQDs from biological wastes is rarely reported, some successful attempts have been established [184]. In 2018, Ding *et al.* synthesized GQDs from lignin biowaste and introduced them to RAW 264.7 cells (monocytes/macrophage-like cells) for bioimaging [552]. Likewise, Zhang *et al.* synthesized nitrogen-doped GQDs (N-GQDs) from the marigold plant for detecting Fe^{3+} ions as a target for bioimaging inside living cells [553].

4.6 Magnetic imaging

The application of novel diagnostic tools in biomedical sciences enables early diagnosis of many diseases, such as cancers [554] and Alzheimer's disease, which may help

to ensure appropriate therapy, delay disease progression [555], and limit complications [556]. This would imply intensive development of different molecular imaging techniques [557] and medical diagnosis, including medical imaging [483], which allows identification of anatomical structures, as well as molecular and cellular imaging [558]. These techniques are classified as low and high magnetic field techniques, including MRI [559], which represents one of the medical imaging modalities widely used in detecting many diseases, like rheumatoid arthritis while differentiating it from other inflammatory arthropathies [560].

MRI is one of the most powerful diagnostic methods for *in vivo* molecular imaging through non-invasive prediction of diseases at the molecular level. This allows visualization of the molecular characteristics of physiological or pathological processes, without invasive procedures, in living organisms before they manifest in the form of anatomic changes [561]. MRI is based on the features of hydrogen nuclei preceding an applied magnetic field. The relaxation processes, through which the nuclei return to their original aligned condition, can be taken advantage of with the application of a radiofrequency pulse and magnetic field gradients [562–564]. Nevertheless, the resolution and imaging sensitivity of MRI relies heavily on the use and performance of metallic CAs [563]. Three categories of MRI CAs have been distinguished. The first is T1-weighted CAs, wherein most medical agents belong and confer a positive contrast (*i.e.*, paramagnetic materials) [565]. T2-weighted CAs, which shorten the T2 relaxation time and confer a dark contrast (*i.e.*, superparamagnetic iron oxide) [566], have been widely used as MRI CAs to detect cancer [567]. Dual-weighted contrast, the third category, shortens both T1 and T2 relaxation times [568]. MRI presents advantages over the other medical imaging techniques thanks to its high resolution, deep penetration [569], efficient intrinsic contrast [570], and its ability to image soft tissues [571].

Although its applications are vast, magnetic imaging modality lacks specificity, which may leads to false-positive results [572]. It also presents technological, physical, financial, and safety limitations [573 as well as bulky instruments [574] and inhomogeneity of the magnetic field, which may result in non-homogeneity in image signals [575]. To overcome some of these disadvantages, the application of NMs in medical imaging can help minimize detection limits [576] and increase sensitivity through the generation of efficient interaction of molecules with signal generating particles [577]. Compared to bulk materials, NMs provide more advantages due to their magnetic susceptibility [578], finite sizes, and the magnetic behaviors of particles. Magnetic NPs (MNPs) have demonstrated wide applications as CAs that enhance the MRI signal and image quality and present different characteristics, like superparamagnetism [557], that provide more magnetization [558]. Depending on their medical applications, MNPs are divided into paramagnetic, ferromagnetic, and superparamagnetic particles, which impact MRI contrast differently and have different core sizes and shapes that define their magnetic properties [579].

Recently, more attention has been given to the development of new NMs, such as QDs and MOs, for the diagnosis and/or treatment of various diseases [580]. Here, we cite some of the NMs, as shown in Figure 13, used with MRI for the early detection of diseases.

4.7 Magnetic iron oxide

Magnetic iron oxide has unparalleled properties, such as its interaction with magnetic fields and field gradients. These properties enable magnetic separation, improvement, and recycling of MNPs, as well as the tracking and visualization of the local MNP environment and labeling of cells through MRI. Yan *et al.* found that iron oxide (Fe_3O_4) MNPs exhibited an intrinsic peroxidase mimicking activity. Moreover, the enzyme sensitivity of Fe_3O_4 measures the enzyme activity of proteases, methylases, and restriction endonucleases [561,581]. For *in vivo* tumor imaging, MNP probes could be delivered to tumors by either a passive or active targeting mechanism. In the passive mode, macromolecules and nanometer-sized particles have been accumulated preferentially at tumor sites through EPR effects. This effect is believed to arise from two factors. The first factor is antigenic tumors, which produce vascular endothelial growth factors that hyper permeabilize tumor-associated neo-vasculatures and cause leakage of circulating macromolecules and small particles. The second factor is that tumors decrease the effective lymphatic drainage system, which leads to a subsequent macromolecule or NP accumulation. Passive tumor targeting requires MNP probes to have long plasma circulation times, which are typically achieved by shielding the MNPs with polymers, such as polyethylene glycol (PEG) and dextran. PEG and dextran are hydrophilic polymers with low immunogenicity and can help NPs escape uptake by the reticuloendothelial system (RES) [561,582–584]. Radionuclides, such as 18F or 64 Cu, have been loaded to surface-limited organic ligands on MNPs for tumor diagnosis [580]. Lai *et al.* covered MNPs with an iridium complex that reacted with silane and

combined them with tetraethyl orthosilicate. The final mixture was hydrolyzed over the NP surface. This multimodal system was used for phosphorous labeling and, at the same time, for apoptosis of cancer cells induction by synthesis of O_2 [580,585].

4.8 Superparamagnetic IO NPs (SPIONs)

SPIONs are the most widely used NMs in clinical MRI [586], where they have shown remarkable enhancement in sensitivity [587]. These NPs can be functionalized and adapted to different soft tissues for paramagnetic agents [588]. SPIONs have presented the unique biological property of uptake by macrophages during the inflammatory response. This property could present advantages for visualizing several afflictions indirectly using MRI [589], such as atherosclerosis [590], myocarditis, and several kinds of infections [591]. SPIONs were effective as negative CAs due to their ability to decrease the transverse relaxation of tissue water protons and enhance the relaxivity (r^2) value. Different T2 CAs (*i.e.*, magnetic ferrites $CoFe_2O_4$ and $MnFe_2O_4$) have been used as a T2 due to their superior properties in enhancing the distinction between healthy and infected tissues [592–594].

SPIONs are characterized by low toxicity, but they present difficulty in being distinguished from other iron-rich tissue [595,596] that would interfere with the biological iron metabolism [597,598]. On the other hand, these MNPs present an instability problem. This could be remediated by the application of surface coating, which could decrease their potential toxicity, increase their efficiency, as well as control their size and limit their accumulation [599]. Feridex®, an example illustrating this procedure, is a commercialized medical product used for the detection of liver lesions and identifying abnormal hepatic cells. The principle of this product is based on the uptake of the SPIONs [595] and biocompatible NPs that can be recycled using simple magnets [600] with phagocytic kupffer cells located in the RES. These cells are absent within malignant liver cells. This would create a signal intensity difference between normal and abnormal cells, hence generating a difference in contrast when visualizing using MRI [595].

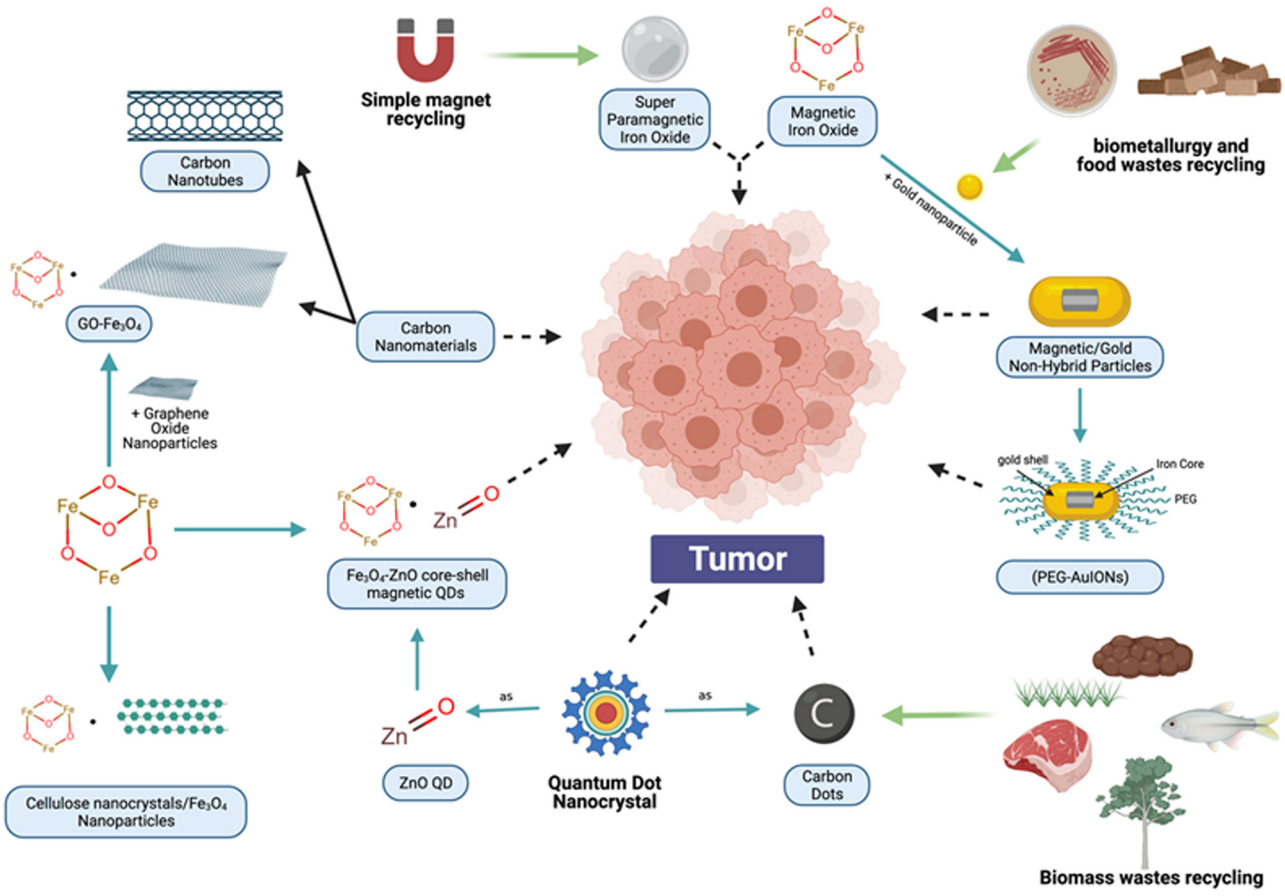

Figure 13: Schematic representation of some NPs recycled from wastes and used in MRI for the diagnosis of diseases, especially tumors.

Another study realized by Lindemann *et al.* presented dextran-coated SPIONs as innovative tracer material for tumor cell analysis in MPI [601]. This MPI presented better sensitivity than MRI and used an oscillating magnetic field that served to generate the signal derived from MNPs [602].

The use of intraprostatic injections of SPIONs by MRI is safe and efficient in the identification of sentinel lymph nodes for prostate cancer detection [568]. The conjugation of the chitosan-coated MNPs and of surviving antisense oligonucleotides to formulate survivin-targeted NPs could be used with MRI for pancreatic tumor detection [572].

4.9 Cellulose nanocrystals (CNCs)/ Fe_3O_4 NPs

The use of CNCs/Fe_3O_4 nanocomposites has attracted great attention because of their current and potential ability as dual T1–T2 CAs for MRI [603]. CNCs are a type of cellulose NM that act as dual CAs because of their advantages, such as nontoxicity, large surface area, low price, high mechanical strength, and stiffness [604,605]. Moreover, they have been used in biomedicine, tissue engineering, and biosensors [606]. CNC/Fe_3O_4 nanocomposite for Pickering emulsions based on ultra-small Fe_3O_4 NPs and CNC–poly citric acid (CNC–PCA) nanoplatforms have been investigated as dual magnetic CAs [603]. The results of *in vitro* cytotoxicity tests on HeLa cell lines at 24 and 48 h revealed compatibility and low cytotoxicity (up to 200 μg mL^{-1} Fe). *In vitro*, the MR relaxivity ratio (r^2/r^1) of CNC–PCA/Fe_3O_4 nanocomposites was calculated to be 7.0. Consequently, these novel composites have potential for MRI applications as dual CAs for the early detection of disease.

4.10 Au NPs (magnetic/gold non-hybrid particles)

Au NPs are an exciting class of NMs that can be recycled from various types of wastes, such as wastes using microorganisms (biometallurgy) [607] and food wastes [329,334]. Au NPs could be used for various biomedical uses, including bioimaging, because of their bioinertness, surface chemistry controllability, X-ray opacity, and optical features [608,609].

A green chemistry process using grape seed proanthocyanidin as a reducing agent has been used to produce crystalline magnetite/gold nanohybrid particles (~35 nm in size) from a single iron precursor ($FeCl_3$) [608,610]. The hybrid Fe_3O_4 compound showed superparamagnetization with dark T2 contrast ($124.2 \pm 3.02\ mM^{-1}\ s^{-1}$) from MRI and magnetization analysis. Moreover, phantom CT imaging showed sufficient X-ray contrast due to the presence of nanogold in the hybrid component. Given its possible use for stem cell monitoring and imaging, compatibility assessment was carried out on human mesenchymal stem cells. The serial optical parts of the cells incubated with NPs showed that the particles were distributed after they were taken up. Moreover, even at a high concentration of 500 μg mL^{-1} and incubation up to 48 h with no apoptotic signals or ROS formation, strong biocompatibility was observed. This is in line with the outcomes of cytotoxicity experiments and can be considered strong evidence that the biocompatibility of the diagnostic nanoprobe is valid [608]. Considering the described properties of Fe_3O_4 and Au NPs, it seems that mixing both NPs in a single nanocomplex may have potential in the fields of cancer diagnosis and therapy [611].

4.11 PEGylated iron-oxide–gold core–shell NPs

PEG-coated Fe_3O_4 NPs produced to date are too large to enter pancreatic tumors as they have insufficient circulation in the blood compartment [612,613]. Recently, superparamagnetic gold-coated core–shell NPs have been considered very important in biomedical applications [613–618]. NPs with Au and iron oxides are considered biocompatible and have been widely used in both optical and magnetic applications. In addition, a gold layer on NPs was found to be stable under biological conditions [611,613,619].

Kumagai *et al.* worked on developing PEG-coated iron-oxide–gold core–shell NPs (PEG–AuIONPs) for use as a T2-weighted MRI CA for pancreatic tumor model imaging. Their findings showed that PEG–AuIONPs have extended circulation in blood and improved the MRI of models of subcutaneous colon and pancreatic tumors. These results indicate that PEG–AuIONPs are a successful way to develop MRI CAs for the diagnosis of many tumor groups, for example, pancreatic cancer. By using their method, precise control of hydrodynamic size and efficient PEG density on the AuIONPs was achieved [613].

4.12 Carbon NPs

CNMs have shown wide applications in biomedical tumor imaging due to their optical and magnetic properties.

CNTs and G are some of the CNMs used due to their structural and physicochemical properties [620] as well as for their ability to be functionalized [621]. These two agents could be used in biomedicine as nanocarriers [622] for cancer theranostics, which combine both diagnosis and therapy [623,624]. A research study has been carried out to develop a GO and gadolinium (Gd^{3+}) complex for use as a theranostic agent. This was achieved through the conjugation of diethylene-triamine-penta-acetic acid with GO and complexing it with Gd^{3+} followed by loading the surface of the GO with DOX, an anti-cancer drug. The formed complex showed better contrast imaging ability than Gd^{3+}, abased T1 CA, and DOX was released successfully during the chemotherapy [625].

The conjugation of GO–Fe_3O_4 could be utilized as a CA for magnetic imaging [626]. Another study referred to the conjugation of amino dextran coated Fe_3O_4 NPs to GO. This hybridization showed an enhancement in the MRI detection of human cervical cancer compared to Fe_3O_4 NPs alone [627]. From another context, a research study succeeded in covering magnetic single-walled carbon nanotubes (SWCNTs) with magnetic Fe_3O_4 NPs and coating them with multilayer polyelectrolytes, which were then linked covalently to FA as a targeting agent. The *in vitro* results showed an enhancement in the MRI for human cervical cancer HeLa cells [628]. Another *in vitro* study related to the enhancement of single-walled carbon-NPs magnetic targeting properties through MRI used Fe_3O_4 tagged SWCNTs to enhance its sensitivity for the detection of 4T1 induced breast cancer in murine. The results showed efficient and safe employment of the MRI signals for cancer cell detection, which encourages further studies utilizing this nanocarrier for other biomedical applications, including diagnosis and drug delivery [629].

4.13 GO NPs

GO has huge potential for integration in biomedical applications as it is a most promising NM among the carbon family for efficient multifunctional theranostic agents. GO has high bioavailability and biocompatible properties in biological systems. Also, it is photothermal, magnetically thermal, paramagnetic, hydrophobic, and has low cytotoxicity. To enhance the biocompatibility of CAs and improve the MRI capabilities of Fe_3O_4, GO–Fe_3O_4 has been synthesized in conjunction with SPIONs and GO. This succeeded in improving physiological stability, cellular MRI, and decreased cytotoxicity [517,630–632]. Moreover, GO–Fe_3O_4 with SPIONs helped overcome side effects, such as heart failure, aggregation in the skin, kidneys, and brain, which may lead to kidney disease and nephrotic system fibrosis, common in other MRI CAs, such as Gd^{3+} or Mn^{2+} [633,634].

4.14 CDs

CDs include carbon nanodots, CQDs, quantum graph dots, and carbonized polymer dots [635]. Biomass is a good source for the production of CDs due to its abundance, availability, environmentally friendly nature, and being a source of low-cost renewable raw substances [137]. Biomass is an abundant, complex, heterogeneous, biodegradable, and bioorganic material that can be collected from various sources including perennial grass, organic domestic waste, agricultural residues, poultry, fishery, forestry, and related industries. Natural organic biomass waste is primarily made up of cellulose, hemicellulose, lignin, proteins, ash, and some other ingredients [137,636,637]. Xu *et al.* synthesized CQDs from apple juice [638,639]. CDs from *Trapa bispinosa* peel were prepared by Mewada *et al.* and showed low cytotoxicity and good biocompatibility in Madin–Derby canine kidney cells. Hence, they are promising for use in biomedical applications [137,640].

There are two methods for adapting CDs for the improvement of MRI CAs: (1) incorporate Gd^{3+} or Mn^{2+} in CDs for T1 contrast enhancement [517,641] and (2) hybridize CDs with IO NPs for T2/T2* contrast enhancement [641–643]. Using natural chemical exchange saturation transfer (CEST), the MRI contrast properties of metal-free CDs could be utilized to create contrast without (super)paramagnetic labels. This is in contrast to paramagnetic metals that might present toxicity problems or the CD/iron oxide combination, which could present undesirable outcomes. CDs, with their favorable size and biocompatibility properties, are appealing diamagnetic CEST CAs. These agents have been used for a wide range of biomedical applications, such as tumor screening and cancer cell theragnostics [639,644,645], or are used as specific markers for tumor vasculature [641,646]. Besides iron oxides, both fluorescence and ferromagnetic properties were shown in the transition metal ion doped CDs. Ji *et al.* have synthesized Mn-doped CDs (Mn-CDs) that presented clear MR imaging abilities of the brain glioma area after 30 min and 2 h [645]. Moreover, Pakkath *et al.* produced TM^{2+} doped CDs (Mn^{2+}, Fe^{2+}, Co^{2+}, and Ni^{2+}) and applied them as T1-weighted contrasts. Upon injection of 10 mL TM^{2+} doped CDs into zebrafish, *in vivo* fluorescence and magnetic imaging showed that the TM-doped CDs were suitable agents for T1-

weighted contrast with bright green emission at administrable amounts [646]. Although these magnetic characteristics are too poor to apply to MRI, this indicates a new path for the combination of optical and magnetic properties. A composite of IO NP doped CDs (IO-CDs) provides both fluorescent and magnetic capabilities. These properties could be used for MRI/fluorescence multimodal bioimaging. IO-CDs are characterized by low cytotoxicity and good fluorescence imaging ability and could be potential T1/T2 CAs and efficient fluorescent biomarkers for *in vivo* magnetic fluorescence/resonance imaging [635,647].

4.15 ZnO NPs

Due to their biodegradable properties in biological media, both ZnO NPs and aluminum-doped ZnO (AZO) NPs have been used for biomedical applications such as monitoring tumor progression by MRI, delivering substances through the gut barrier, and surgery. On the other hand, AZO NPs can be a non-degradable matrix and, therefore, might be used for their biostability properties in fluorescence-directed biopsy [648]. A ZnO matrix doped with foreign ions has luminescence properties. These nanocomposites could be used in biomedical applications thanks to their phonons, efficient excitation, and emission properties in the visible region [649]. Gd-doped ZnO QDs, a ZnO nanocomposite containing Gd^{3+} ions, can decrease the time of longitudinal (T1) relaxation of water protons with bright contrast at its location. These QDs and ZnO have weak toxicity, and the nanocomposites were effective in biomedical imaging for *in vitro* MRI [650]. In a study related to the functionalization of NMs, Gd-doped ZnO QDs nanocomposites were formulated (with sizes <6 nm) for both optical and MRI owing to the direct relationship between the emission intensity of the Gd-doped ZnO QDs and the concentration of Gd^{3+}. Remarkable maximum emission intensity was observed at 550 nm. Surface coating of Gd-doped ZnO QDs with *N*-(2-aminoethyl)aminopropyltrimethoxysilane showed low toxicity to HeLa cells and the ability to enhance imaging quality for *in vitro* visualization of HeLa cells with both confocal microscopy and MRI [651].

4.16 Biosensors

There are biological markers that need frequent and continuous measurement. Traditional methods for biomarker detection are costly, time consuming, and need complex devices and experts to work devices. The use of biosensors with nanotechnology has been one of the best biomedical applications for the rapid and accurate diagnosis of disease as appropriate treatment can be given at an early stage reducing the mortality rate [652].

Biosensors are high-sensitivity analytical devices that have become an essential part of our modern life because they provide precise monitoring of our bodies and the surrounding environment. Biosensors, a hybrid of biological elements and physicochemical components used to detect particular biological molecules or biomarkers of a medium and generate a measurable signal (usually a voltage), analyze the biological response of living organisms [653,654].

The first biosensor was designed by the biochemist Leland Clark, who is called the father of biosensors, in 1950 [655]. The term "biosensor" was coined in 1977 by Karl Cammann [656] and consists of two terms: the term "bio" is short for "biological response" and the term "sensor" originates from the Latin word "sentire," which means "to feel or to identify" something [657]. Biosensors are characterized as highly sensitive, highly specific, and easy to use analytical devices. In principle, the biosensing technique consists of three fundamental components: receptor, transducer, and reader device. These components measure the physical or chemical changes in the element or biological marker to be measured. A receptor, which is a biological element, senses the physical or chemical stimuli and transforms them into electrical energy, wherein the generated electrical energy depends on the type of biological element. The transducer performs the function of converting this energy into an analytical signal, which can be analyzed and presented in an electronic form that is transmitted to the reader device. The reader device consists of an amplifier, conditional filter circuits, and a display unit, which further implement the detection response and represent it as a numerical value [652,658].

Biosensors are classified according to the parameter that is measured by the physicochemical transducer of the biological biomarkers, such as optical, electrochemical, acoustic, and thermal [659]. In the last few decades, biosensors have been widely used for the detection of several components including gases, metabolites, pollutants, microbial load, and other organic compounds, and in a wide range of biological applications such as food analysis, detection of biomolecules that are either an indicator of a disease or target of a drug, as clinical tools to detect diabetes, and to monitor protein fragments that are basic cancer biomarkers. Scientists anticipate that, in the near future, we could detect several diseases,

such as diabetes, airborne diseases, and cancer, at a very early stage to provide a good chance of treatment [660,661].

4.17 Early detection of diabetes

Diabetes is a common disease that strikes different age groups, the young, the elderly, and even children, and requires periodic, rapid, and accurate analysis of glucose level to keep it at normal levels [662]. Electrochemical biosensors have contributed to the rapid evolution of glucose level monitoring in blood. Enzymatic biosensors are traditional electrochemical glucose biosensors that use glucose oxidase enzyme (GOx) as a catalyst to oxidize the glucose at the electrode, producing gluconolactone, H_2O_2, and electrons [663,664]. The generated H_2O_2 and electrons are related to the glucose concentration in the sample. Limitations of this technique include some difficulties in handling, short storage life, and being easily affected by temperature and chemicals, which prevent accurate early detection of high blood glucose levels.

Nanostructured materials have been utilized to produce electrochemical non-enzymatic biosensors to overcome the above-mentioned challenges, receive an accurate record of glucose levels, obtain stability and reproducibility, and form nanozymes on the surface of the electrode that offer several advantages in the detection of glucose, such as simplicity, low cost, long storage life, and high selectivity/sensitivity [664,665].

In enzyme-free glucose biosensing, CuO and CD nanocomposites have been used as nanozymes with unique properties, such as enhanced surface area and improved electrode sensitivity. CuO NPs have been used as a catalyst because of their low cost, facile preparation, low toxicity, and notable electrochemical catalytic properties [666]. Moreover, CDs composed of CNPs with diameters of less than 10 nm, high surface area, and chemical stability could improve sensing sensitivity due to the enhanced electron transfer characteristics associated with CuO NPs and increased electrode surface area. This makes non-enzymatic electrochemical biosensors effective in the early detection of diabetes [667,668]. Mehrab *et al.* proved that recycled CuO could be used effectively and repeatedly as nanocatalysts with notable electrochemical catalytic properties, low cost, facile, and non-toxic preparation [667]. Nanocomposites of recycled CuO nanocatalysts and CDs merge the advantages of both recycled NPs and could be used effectively for the detection of diabetes at early stages [669,670].

Ahmad *et al.* (2017) fabricated non-enzymatic glucose detecting electrodes using ZnO nanorods (NRs) grown vertically on fluorine-doped tin oxide (FTO) electrodes. The electrodes were then decorated by CuO NPs to enhance the stability and efficiency of the CuO–ZnO NR/FTO electrode. In addition to improved reproducibility and anti-interference, the electrodes were able to be reused more than five times. The response of the sensor was found to range from 93 to 97% of the original response [671].

Several NPs recycled from different sources of waste have been utilized as biosensors for the early detection of different diseases, as illustrated in Table 13. Recycled Fe_3O_4 MNPs were utilized in electrochemical biosensors owing to their low biotoxic effect, biocompatibility, and strong superparamagnetic properties [672]. Li *et al.* revealed that recycled Fe_3O_4 NPs could be used as a NP-based catalyst qualified for recycling more than eight times while maintaining a high level of operation without any significant losses in activity [673]. Zhang *et al.* incorporated Fe_3O_4 NPs with synthesized nitrogen-containing chitosan-doped G (CG), wherein chitosan improved the biocompatibility of the electrode and provided a suitable environment for enzyme immobilization. This combination increased catalytic activity, provided a larger active surface area, and enhanced the transportation of electrons, which enabled Fe_3O_4/CG to exhibit high-performance catalytic activity as electrochemical biosensors for the detection of glucose in blood [674–676].

4.18 Early detection of cancer

Cancer is the second leading cause of death in the world [677]. Early diagnosis of cancer is crucial to increase the chances of survival and provide more affordable treatment [678]. Recycled NP biosensors have shown high efficiency in the early detection of different cancers where current diagnostic methods failed [679]. Biosensors manufactured from RNMs are designed with many binding sites that capture various tumor biomarkers. Various CNMs have been used in the development of biosensors as they offer biocompatibility, high specific area, and excellent optical, electrical, and mechanical properties [680].

Two-dimensional nano-GO (NGO) conjugated with an aptamer biosensor showed high sensitivity and selectivity in the early stage detection of the main types of cancer biomarkers [681]. NGO chemical properties allow the formation of many covalent and non-covalent bonds with other NP, polymer, and biological entities [682]. From an industrial approach, NGO has low cost, high production yield, and distinctive physicochemical properties that

Table 13: NPs recycled from different sources of waste and utilized as biosensors for the early detection of different diseases

NP	Usage	Advantage	Signal transduction	Limitation	Source	Ref.
CuO	Detection of glucose in the blood	Recyclability Selectivity Low cost Chemical stability	Electrochemical	—	Vegetable waste	[666]
ZnO	Detection of glucose in the blood	Reproducibility Anti-interference Recyclability	Electrochemical	Complex fabrication process	Zn–C and Zn–MnO_2 batteries	[671,701]
Fe_3O_4	Detection of glucose in the blood	Recyclability Low toxic effect Biocompatibility Strong superparamagnetic property	Electrochemical	Easy aggregate High oxidization probability	Steel industry waste	[672,702]
NGO	Aptamers, DNA or RNA biosensors	Low cost High yield production Distinctive physicochemical properties	Electrochemical	Hard to dissolve in water	Agricultural waste	[683]
CNTs	Early cancer diagnosis	High conductivity Large surface area Fast electron transfer High mechanical strength	Electrochemical, optical	Need to functionalize the surface Irreversible agglomerates in aqueous solution	Polymer waste	[683]

present great potential in biology [683], as shown in Table 13. Aptamers, single-stranded nucleic acid particles, DNA or RNA, attach to NGO instead of antibodies because of their easy synthesis, low cost, low immunogenicity, and low variability empower. Upon conjugation to the NGO, aptamers act as exchangeable building blocks for functionalizing CNMs, which facilitates their clinical application [681]. Tan *et al.* designed a probe using NGO and carboxyfluorescein-labeled Sgc8 aptamer (FAM-apt) to detect CCRF-CEM cells (human acute leukemic lymphoblast cell lines) based on the fluorescent quenching property of NGO [684]. Their probe can isolate CCRF-CEM cells from a peripheral blood sample that contains target and non-target cells suffering from acute lymphocytic leukemia. When the aptamers are adsorbed to the NGO surface by π–π stacking, the fluorescence of the FAM-apt is quenched when there are no target cells as the NGO and the fluorophore are too close to transfer energy. In case CCRF-CEM cells are detected, the weak binding force of the NGO–aptamer allows the aptamer to fall off the NGO surface and bind to the cells, causing fluorescence. In the absence of the cells, the aptamer is still connected to the NGO with no fluorescence to restore. The more CCRF-CEM cells found, the higher the fluorescence intensity. In addition to CCRF-CEM cells, NGO–aptamer has the potential to detect early other cancer cells, such as Ramos cells, H22 cells, and 293T.

Multi-walled carbon nanotubes (MWCNTs) have also been used to develop biosensors. Berkmans *et al.* have developed the rotating cathode arc discharge technique to create MWCNTs from PET waste [685]. This method recycles PET mineral water bottles and creates MWCNTs in the cathode, paving the way for the manufacture of biosensors. Moreover, Singh *et al.* have developed MWCNT biosensors that detect aflatoxins in the body related to the early diagnosis of cancer [686]. The International Agency for Research on Cancer has categorized B_1 aflatoxins as a group one carcinogen, while G_1, G_2, and B_2 aflatoxins are group two carcinogens [687]. These materials are found in many agricultural products and have mutagenic and carcinogenic effects [688]. Liver cancer is most prevalent in people affected by aflatoxins, even in small concentrations [689]. Hence, the early detection of aflatoxins in the body helps either prevent the primary occurrence or avoid the reoccurrence of cancer. The MWCNT electrochemical-based biosensor will help in detecting aflatoxins because of its captivating properties such as high conductivity, large surface area, fast electron transfer properties, biocompatibility, and high mechanical strength. MWCNTs have been treated using nitric/sulfuric acid solutions to form carboxylated MWCNTs (c-MWCNTs) that form covalent bonds with anti-aflatoxin B1 antibodies (anti-AFB_1). Then, the c-MWCNTs are deposited onto an indium tin oxide substrate using the electrophoretic

deposition technique to give it electrochemical sensation. The anti-AFB1/MWCNT/ITO bioelectrode showed sensitive detection of aflatoxin B_1; the electrode current increased when the concentration of aflatoxin B_1 antigen increased [686].

Au NPs have played an important role in the evolution of biosensors. Their electronic, magnetic, optical, physical, and chemical properties make them great sensing material. They are noble, biocompatible, their shape and size can be easily tuned, and their surfaces can be easily functionalized [690]. However, the production methods of Au NPs are based on the use of reducing agents, which are toxic and considered a human health threat in addition to their environmental pollution burden. Another traditional method depends on the breakdown of Au NPs, which requires a lot of energy and negatively affects the environment. A green method was developed to biosynthesize Au NPs from plant tissue extract and different plant parts, including leaf, bark, stem, and root [691]. This extract was simply treated with auric salt solutions, which helped to separate the Au from the extract and change it to NPs. Then, the Au NPs could be obtained by centrifugation for use in many biomedical applications, including biosensors [692].

4.19 Early detection of Parkinson's disease (PD)

Recycled waste materials, such as Au NPs and SWCNTs, have been involved in the manufacture of biosensors for the early detection of PD [693]. PD is a neurodegenerative disorder where brain neurons die, especially in the *Substantia nigra* area, with a high incidence in elderly people [694]. Following the death of nerve cells, Lewy bodies are the surviving lesions found in PD-affected persons. The early diagnosis of PD is important for prompt and effective treatment using neuroprotective therapeutics to avoid complete loss of the *substantia nigra* of dopaminergic neurons [695].

In a study conducted by Zhang *et al.*, SWCNTs seeded with Au NP–urchin conjugated antibodies on an interdigitated electrode (IDE) was developed and had high performance in detecting α-synuclein [693]. SWCNTs were used to act as an attractive NM due to its high-affinity molecular recognition, biocompatibility, and higher level of fluorescence quantum efficiency [696]. SWCNTs are mainly used in electrically based applications as their electrical signals reflect the movement of biomolecules and their interactions with the biosensor [697]. Au NPs have easy functionalization and excellent optical properties, in addition to their good conductivity, biocompatibility, and catalytic properties [698]. Sea urchin-shaped Au NPs were used either on the surface to conjugate the capture molecule or to immobilize the target [699]. An IDE has been fabricated with nanocomposite on silica. This IDE sensor was designed with a dielectrode, uniformly arranged fingers, and gaps that cannot be modified and where molecules can be assembled to transduce current [700].

5 Role of RNMs in the treatment of diseases

5.1 Antimicrobial activity

A key biomedical application of NPs is their use as innovative antimicrobial agents, as shown in Table 14, which overcomes the drawbacks of conventional antimicrobial drugs [703]. NPs have diverse mechanisms of action to kill pathogenic microorganisms, such as oxidative stress and metal ion release [704]. It has been proven that the smaller the particle size, the better the antimicrobial activity [705].

CNMs, such as CNFs, G, AC, and CNTs, can cause membrane damage in bacteria owing to oxidative stress and other modes of action [706]. CNMs synthesized from rapeseed oil cake, which is an industrial bulk waste byproduct produced during the oil extraction process, can prevent the growth of *Staphylococcus aureus, Pseudomonas diminuta, Yersinia enterocolitica, Salmonella enterica* Typhimurium, *Candida albicans,* and *Escherichia coli* [707].

CNFs killed methicillin-resistant *Staphylococcus epidermidis* after 2 h of direct contact [708]. The antibacterial effect of CNFs from electrospun biomass using biomass tar and silver NPs has been confirmed [709]. This result can be explained by the disruption of the bacteria membrane or the oxidative stress process [708], as shown in Figure 14. Moreover, GO, especially rGO synthesized from biomass sources, has shown superior antibacterial activity [710]. Furthermore, biomass-synthesized G from the leaf extract of *Tridax procumbens* has shown antibacterial potential against both gram-positive and gram-negative bacteria through the interaction of G with the microbial cell; they connect to the cell surface, causing cell membrane disruption and oxidative stress [711].

rGO using *Chenopodium album* demonstrated efficacy against *S. aureus* and *E. coli* [710]. The minimum inhibitory

Table 14: Application of recycled NPs as therapeutic antimicrobial agents

NM	Biomass sources	Applications	Ref.
Au NPs	Watermelon rind	Antibacterial activity against *Escherichia coli*, *Bacillus cereus*, and *Listeria monocytogenes*	[335]
Au NPs	*Citrus maxima* peel	Antibacterial activity against *E. coli* and *Staphylococcus aureus*	[333]
Au NPs	*Allium noeanum* leaf	Antibacterial activity against *E. coli*, *Streptococcus pneumoniae*, *Bacillus subtilis*, *S. aureus*, *Staphylococcus saprophyticus*, *Salmonella typhimurium*, *Pseudomonas aeruginosa*, and *Shigella flexneri*	[731]
rGOX	*Chenopodium album*	Antibacterial activity against *S. aureus* and *E. coli*	[710]
AC	Bamboo charcoal	Antibacterial activity against coliform bacteria and *Salmonella*	[712]
AC	Kitchen soot	Antibacterial activity	[713]
CNMs	Rapeseed oil cake	Antibacterial activity against *S. aureus*, *Pseudomonas diminuta*, *Yersinia enterocolitica*, *Salmonella enterica* Typhimurium, *Candida albicans*, and *E. coli*	[707]
CNFs	Electrospun biomass using biomass tar and silver NPs	Antibacterial activity against *E. coli* and *S. aureus*	[709]
G	*Tridax procumbens* leaf	Antibacterial activity against *E. coli* and *S. aureus*	[711]
CuO NPs	*Aspergillus niger*	Antibacterial activity against *E. coli*, *S. aureus*, *Klebsiella pneumoniae*, *Micrococcus luteus*, and *B. subtilis*	[715]
Cu NPs	*Cissus arnotiana* biomass	Antibacterial activity against *E. coli*	[716]
CuO NPs	*Camellia sinensis* leaf biomass	Antibacterial activity against *K. pneumoniae* and *S. aureus*	[717]
ZnO NPs	*Punica granatum* fruit peel biomass	Antibacterial activity against *E. coli* and *Enterococcus faecalis*	[718]
ZnO NPs	*Tabernaemontana divaricata* leaf	Antibacterial activity against *E. coli* and *S. aureus*	[719]
Iron NPs	*Citrullus colocynthis* pulp and seed biomass	Antibacterial activity against *B. subtillis*, *S. aureus*, *E. coli*, and *P. aeruginosa* pathogenic bacterial strains, and moderately inhibited *C. albicans*	[721]
Iron NPs	*Azadirachta indica* (neem) leaf	Antibacterial activity	[724]
Iron NPs	*T. procumbens* leaf	Antibacterial activity against *P. aeruginosa*	[725]
Iron NPs	*Kappaphycus alvarezii*	Antibacterial activity against *E. coli* and *S. aureus*	[726]
Iron NPs	*Mimosa pudica* root	Antibacterial activity	[722]
Iron NPs	*Dodonaea viscosa* leaf	Antibacterial activity against *E. coli*, *B. cereus*, *S. aureus*, *K. pneumoniae*, *P. fluorescens*, *B. subtilis*, and *L. monocytogenes*	[723]
Iron NPs	*Eucalyptus robusta* leaf	Antibacterial activity against *S. aureus*, *P. aeruginosa*, and *B. subtilis*	[727]
TiO_2 NPs	Plum, peach, and kiwi fruits	Antibacterial activity against *E. coli* and *B. substilis*	[228]
TiO_2 NPs	*Artemisia haussknechtii* leaf biomass	Antibacterial activity against *E. coli*	[730]
TiO_2 NPs	*Morinda citrifolia* leaf biomass	Antibacterial activity against *E. coli*	[728]
CQDs	*Lactobacillus plantarum* biomass	Antibacterial activity against *E. coli*	[733]

concentration (MIC) of rGO against both bacteria strains was 125 μg/mL, unlike conventional GO, which had a MIC value of 250 μg/mL [710]. This reflects the benefits of the biomass-derived reduction method *versus* other synthesis methods. The suggested rGO mechanism of action is disruption of the bacteria cell wall or cytotoxicity through oxidative stress formation [710]. Another antimicrobial agent from biomass-synthesized CNMs is AC. Charcoal from bamboo sources significantly reduced the counts of coliform bacteria and *Salmonella* while increasing the level of beneficial fecal anaerobic bacteria [712]. Furthermore, AC NPs produced from kitchen soot, which is a carbon-rich byproduct of the combustion process, are antimicrobial as well [713]. AC can penetrate the bacteria cell membrane and then interact with intracellular sites, which leads to cell division inhibition and, consequently, cell death [713].

CNTs are considered ideal antimicrobial agents due to their small diameter and higher surface area [714]. CNTs begin their effect by first connecting to the microorganisms and then disrupting their cellular membrane and morphology [714]. They also prevent DNA replication and generate ROS [714]. CNTs showed antibacterial efficacy toward *E. coli* and *S. enterica* [714].

MO NPs encompass many elements that have demonstrated powerful antimicrobial properties. CuO NPs synthesized from fungi biomass showed antimicrobial effects against *E. coli*, *S. aureus*, *Klebsiella pneumoniae, Micrococcus luteus*, and *B. subtilis* [715]. Cu NPs biosynthesized from *Aspergillus niger* biomass were highly metal resistant and simple to treat [715]. After adsorption of these NPs into the bacterial cell membrane, they disrupt the membrane and cause damage to the bacteria [715]. Another study confirmed the antimicrobial

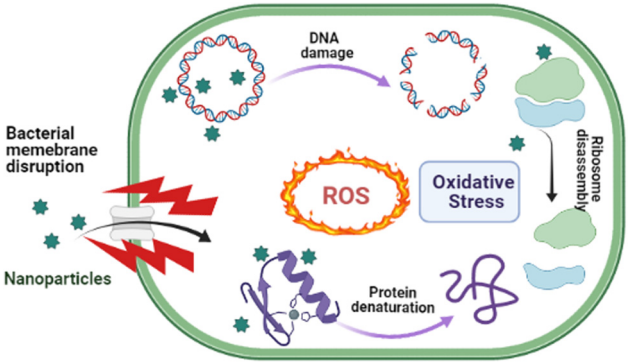

Figure 14: General mechanisms for antimicrobial action of NPs.

potency of biosynthesized Cu NPs [716]. A medicinal plant, *Cissus arnotiana*, was used to synthesize Cu NPs and they exhibited promising antibacterial activity against *E. coli*, with an inhibition zone of 22.20 mm at a concentration of 75 µg/mL [716]. The authors explained this activity through two mechanisms: (1) damaging of the cell membrane and the cellular genetic materials and (2) initiation of oxidative stress [716]. CuO NPs from *Camellia sinensis* leaf biomass is active against *S. aureus* (as a gram-positive bacteria) and *K. pneumoniae* (as a gram-negative bacteria) [717].

ZnO NPs synthesized from biological agents are less toxic, affordable, and ecofriendly compared to traditional chemical and physical synthesis methods [718]. As an antibacterial agent, ZnO NPs from *P. granatum* fruit peel extract induces oxidative stress that leads to permanent damage to the cell membrane and DNA. Consequently, the ZNO NPs lead to apoptosis of the bacteria. Thus, *P. granatum*/ZnO-NPs killed both *E. coli* and *Enterococcus faecalis* [718]. ZnO NPs from *Tabernaemontana divaricata* leaf extract exhibited high antibacterial activity against *E. coli* and *S. aureus* [719]. Recently, substrates from plants and microorganisms have been used to fabricate magnetic IO NPs that exhibit antimicrobial potency [720]. For example, IO NPs produced from pulp and seed aqueous extract of *Citrullus colocynthis*, a wild medicinal plant, effectively inhibited the growth of *B. subtillis*, *S. aureus, E. coli,* and *Pseudomonas aeruginosa* pathogenic bacterial strains, and moderately inhibited *C. albicans* [721]. The iron NPs synthesized from the aqueous extract of *Mimosa pudica* root, *Dodonaea viscosa, A. indica* (neem), *Kappaphycus alvarezii*, and *T. procumbens* leaf biomass have antibacterial activity [722–726]. Moreover, iron NPs from *Eucalyptus robusta* leaves significantly inhibited *S. aureus, P. aeruginosa,* and *B. subtilis* [727]. An inverse relationship between NP size and inhibitory efficacy was observed, which highlights the benefits of iron NPs fabricated from plant aqueous extract [727]. These IO NPs produce ROS, such as hydroxyl radicals, which lead to oxidative stress and bacteria apoptosis [727]. TiO_2 is another effective antimicrobial agent in the MO NP group. After activation of TiO_2 by the photocatalysis process, it produces ROS, which causes damage to the protein, lipids, mitochondria, and DNA of the bacteria [228]. TiO_2 produced from the extract of three rosaceous fruits (plum, peach, and kiwi) peel agriwaste, *Artemisia haussknechtii*, and *Morinda citrifolia* leaf biomass exhibited dose-dependent antibacterial activities against *E. coli* [228,728–730]. TiO_2 produced from peel agriwaste also inhibited the growth of *B. substilis*, a gram-positive bacteria, with a zone of inhibition of 17–19 mm at 100 µg/mL concentration [228].

Au NPs have exhibited antimicrobial potency and when these NPs are produced from plant biomass, their solubility becomes better and presents a better antimicrobial effect [731]. According to a recent study, Au NPs synthesized from the fresh leaves of *Allium noeanum* worked as a strong antibacterial agent against a wide spectrum of bacterium: *Streptococcus pneumoniae, B. subtilis, S. aureus, Staphylococcus saprophyticus, Salmonella typhimurium, P. aeruginosa, Shigella flexneri,* and *E. coli* [731]. Also, Au NPs from an aqueous extract of watermelon rind waste was active against *E. coli*, *Bacillus cereus*, and *Listeria monocytogenes* [335]. Another biomass waste used for the biosynthesis of Au NPs was *C. maxima* peel extract. *C. maxima*–Au NPs exhibited a strong antibacterial effect against *S. aureus* and *E. coli* [333]. In addition, the inhibitory effect slightly increased with the increasing Au NP concentration and, therefore, this biosynthesized Au NP can be used as an effective disinfectant with good antibacterial activity [333].

IQDs, such as CQDs and GQDs, have been used in biomedicine as antimicrobial agents [732]. CDs from the biomass of *L. plantarum* prevented *E. coli* biofilm formation, did not interfere with the growth of *E. coli* and mammalian cells, and had high biocompatibility and low cytotoxicity [733].

5.2 Anticancer activity

Recently, cancer has motivated researchers to seek out more advanced treatments than chemo and radiative therapy. High toxicity and deficient specificity are the major concerns of these traditional therapies [734]. The optimal cancer drug should have a specific targeted delivery system, in addition to appropriate drug-release. Therefore, a variety of nanoscale-based drug carriers have recently been developed and investigated [735]. The typical approach of cancer treatment

with NMs is based on the transportation of the chemotherapeutic agent, which has a narrow therapeutic index, reduced cellular penetration, and highly toxic effects [736].

Biomass-based CNMs have shown promise as they have excellent chemical and physical properties, making them excellent nanocarriers with a large efficacy and low systemic toxicity for targeted drug transportation [737].

Biomass-synthesized CNFs have demonstrated anticancer activity based on the drug type. For example, a previous study showed Cu NP dispersed CNFs encapsulated in PVA and cellulose acetate phthalate composite material for drug delivery. The CNFs were capable of lifting the Cu NPs to their surface in the composite, allowing them to control metal ion release into the required cancer sites [738]. Additionally, Wang *et al.* provided another example of CNF's anticancer activity through the synthesis of CNF-coated Ni metal, which worked as a drug transporter and favorably delivered the anticancer drug DOX to the targeted cancer cells [739].

Biomass-based CNTs have revealed ecofriendly anticancer activity when they were functionalized with chitosan and thereafter coated by DOX to target MDA-MB-231-TXSA breast cancer cells. The CNTs overexpressed CD44, resulting in decreased cell metastasis, inhibition of proliferation, and the beginning of apoptosis. In addition, photothermal therapy has been used for targeting both bladder and prostate cancer [735,736].

G particles originating from *C. album* and *T. procumbens* have anti-cancer activity against breast, lung, and colon cancers. The particles produce mitochondrial disruption and DNA damage. Moreover, *Lantana camara* and *T. procumbens* precursors of G have shown a cytotoxic effect against A549 cell lines [710,740].

AC originating from biomass materials, such as wood, coal, bamboo, and coconut shells, has shown excellent photothermal properties against human H-1299 lung cancer cells. The AC converts light energy into heat exceeding 42.5°C, which eventually kills cancerous cells [740]. Additionally, AC has shown long-term photothermal therapy as no antibodies or peptides conjugate onto AC particles when they migrate to cancerous cells, thus they are taken up by endocytosis, which consequently prevents NPs from escaping cells once they have penetrated [741].

Inorganic QDs, specifically CQDs, have been proven to possess excellent anti-cancer activity. Interestingly, CQDs from an *Andrographis paniculata* were applied to both malignant human umbilical vein endothelial cells (HUVECs) and mesothelioma cell lines (H2452). It accumulated in their nucleus or cytoplasm and inhibited their growth in a time and dose-dependent fashion [742]. Furthermore, CQDs originating from *Allium fistulosum* exhibited high viability against myelogenous leukemia cells (K562, suspension cells) and a breast cancer cell line (MCF-7, adherent cells) through the penetration of cell membranes and distribution over the cytoplasm [742,743]. In addition, CQDs made from *Nerium oleander* leaf biomass have an anti-proliferative effect *in vitro* against breast cancer MCF7 cells [742]. *Hypocrella bambusae* CQDs have shown an efficient capability for the generation of O_2 and heat for synergistic photodynamic and photothermal therapy, which exhibits significant anticancer efficacy [744].

Similarly, biomass-synthesized GQDs have shown excellent anti-cancer activity. For example, *Ficus racemose*-derived GQDs showed excellent photodynamic and photothermal properties, which make them a potent anticancer agent in the targeting of breast cancer cells [744]. Furthermore, a previous study demonstrated that biomass-synthesized GQDs with Cys–berberine hydrochloride (BHC) composite can be used for the delivery of BHC (anticancer agent). The GQDs with the Cys–BHC system were also investigated for their antiproliferative activity against HeLa cells and MDA-MB-231 cells [746].

Recent research has also demonstrated the anticancer activity of Au NPs [747]. For example, the anticancer properties of Au NPs synthesized from *Anacardium occidentale* leaves were studied. These Au NPs showed 23.56% availability on MCF-7 cell lines at a maximum concentration of 100 mg/mL [748]. The apoptosis produced by *Curcuma wenyujin*–AuNPs was investigated by ROS. The caspases levels in a *C. wenyujin*–AuNP-treated MDA-MB231/HER2 cell line are shown in Figure 15. Additionally, stable Au NPs made from *Taxus baccata* extracts have demonstrated potent, selective, dose, and time-dependent anticancer activity on breast (MCF-7), cervical (HeLa), and

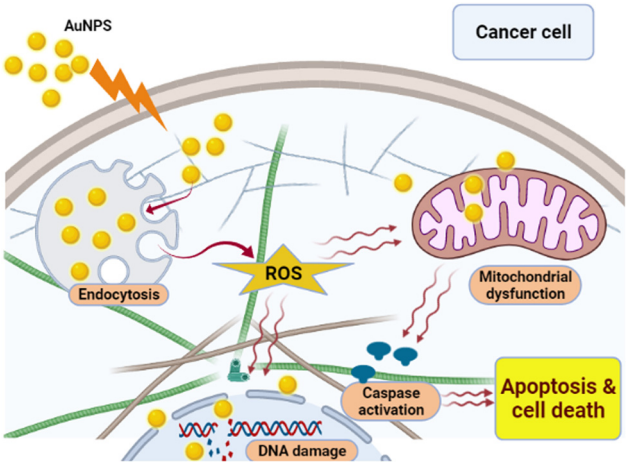

Figure 15: Mechanisms of anticancer activity for Au NPs.

ovarian (Caov-4) cancer cells [749]. Researchers have used flow cytometry and reverse transcription polymerase chain reaction to conduct *in vitro* studies, wherein cells were exposed to synthesized Au NPs, and have claimed that the caspase-independent death program was the most viable anti-cancer mechanism of action [749]. The leaf biomass of *Mappia foetida* was used to efficiently deliver DOX to cancer cells in humans in conjugation with FA [750].

MO NPs have piqued the interest of biomedical researchers due to their structural, physical, and chemical features [751]. The anticancer activity of MO NPs has been demonstrated through binding to cell surfaces or by cellular internalization. Therefore, because of their low stability, some NPs dissociate into their ionic states in body fluid after being administered while other stable NPs directly enter the cancer cells. The formation of ROS by NPs is the main mechanism of action by which cancerous cells are inhibited. [752].

CuO NPs have shown anticancer activity by enhancing the intensity of apoptosis (programmed cell death) in cancer cells [752]. CuO NPs from *Ficus religiosa* leaf extract instigate anticancer activity in A549 lung cancer through the inhibition of histone deacetylase [753,754]. In addition, CuO NPs reduced the expression of oncogenes while increasing the expression of tumor suppressor proteins in A549 cells [754]. MCF-7 cell viability was reduced by 50% when CuO NPs from *C. sinensis* leaf biomass were used at a concentration of 50 g/mL. The imaging-based quantification of cellular CuO NP uptake showed a clear dependent toxic activity [717].

In SKOV3 and AMJ13 cancer cells, Cu NPs made from *Olea europaea* leaf biomass inhibited cell growth and induced apoptosis [755]. CuO/Zn NP hybrids made from *Duchesnea indica* leaf biomass were used to improve kidney cancer therapy [756].

ZnO NPs have a distinct electrostatic property that aids in the selective targeting of cancer cells. Anionic phospholipids are abundant on the surface of cancer cells, resulting in electrostatic attraction with ZnO NPs. Small ZnO NPs increase the permeation and retention of NPs within tumor cells and thus help the NPs act upon them, while large ZnO NPs promote cellular uptake of ZnO NPs by cancer cells and ultimately leads to cytotoxicity [757]. When compared to normal cells, ZnO NPs produce a large amount of ROS in cancer cells, resulting in a large amount of oxidative stress from which the cancer cells die [758]. Furthermore, the synthesis of ZnO NPs from *Laurusobilis* leaves has shown anticancer activity in A549 lung cancer. Normal murine macrophage RAW264.7 cells were found to be unaffected by ZnO NPs, but the NPs were effective in inhibiting the viability of human A549 lung cancer cells at greater concentrations of 80 g/mL [759]. Additionally, the ZnO NPs synthesised from *Eclipta-prostrata* leaves have been tested on the human liver carcinoma line (HeO-G2) [760] while ZnO NPs synthesised from *Ziziphus nummularia* leaves have shown anticancer activity against the HeLa cancer cell line [761].

Primary solid–solution NPs, or ions, have potential applications in drug and gene delivery, in specific medical specialties and as theranostic NPs [754]. In essence, two distinct approaches for treating tumors with SPIONs are frequently used. Magnetically evoked hyperthermia, drug targeting, and selective neoplasm growth suppression are implemented. Researchers have shown that cancer cells become more aggressive when exposed to iron compound NPs. Consequently, it was concluded that these NPs could be used to treat tumors safely, without harming healthy cells. In addition, researchers have observed how much ROS was produced when A549 cancer cells were treated with ions, which accordingly induced autophagy [754]. SPIONs successfully synthesized from fruit peel biomass had anticancer activity against HeLa [762] and iron NPs synthesized from brown seaweed biomass had anticancer activity [763].

TiO_2 NPs from *Vigna radiata* legume extract effectively killed HeLa cells through photocatalysis, which suggests that TiO_2 NPs could be used to decrease the recurrence of osteosarcoma and chondrosarcoma by inducing cytotoxicity in bone tumor cells [764,765]. This can be achieved by increasing ROS levels. Interestingly, these findings suggested that TiO_2 NPs could be used to reduce or prevent osteosarcoma and chondrosarcoma recurrence [764]. Table 15 shows the anticancer activity of recycled NPs.

5.3 Antioxidant activity

An antioxidant is a material that prevents molecules within a cell from oxidizing. During the biological oxidation reaction, free radicals are produced, and a chain reaction is started concurrently because the radicals are reactive. A cell may be damaged or may die as a result of this [767]. Antioxidants bind to free radicals, stopping harmful chain reactions and converting them to harmless byproducts. Antioxidants thus reduce oxidative stress and are important in the treatment of diseases caused by free radicals, such as heart disease, neurodegenerative disorders, cancer, and the aging process.

However, the efficiency of natural and synthetic antioxidants is limited due to poor absorption, difficulty

Table 15: Application of recycled NPs as therapeutic anti-cancer agents

NM	Biomass sources	Applications	Ref.
GNPs	*Chenopodium album*	Anti-cancer activity against breast, lung, and colon cancers	[710]
GNPs	*Tridax procumbens*	Anti-cancer activity against breast, lung, and colon cancers	[766]
GNPs	*Lantana camara* leaves	Cytotoxic effect against A549 cell lines	[711]
AC	Wood biomass	Anti-cancer activity against human H-1299 lung cancer cells	[741]
AC	Coal biomass	Anti-cancer activity against human H-1299 lung cancer cells	[741]
AC	Bamboo biomass	Anti-cancer activity against human H-1299 lung cancer cells	[741]
AC	Coconut biomass	Anti-cancer activity against human H-1299 lung cancer cells	[741]
CQDs	*Andrographis paniculata*	Anti-cancer activity against malignant HUVECs and mesothelioma cell lines (H2452)	[742]
CQDs	*Allium fistulosum*	Anti-cancer activity against myelogenous leukemia cells (K562, suspension cells) and breast cancer cell line (MCF-7)	[743]
CQDs	*Nerium oleander* leaves	Anti-cancer activity against breast cancer MCF7 cells	[743]
CQDs	*Hypocrella bambusae* trees	Anti-cancer activity	[744]
GQDs	*Ficus racemose* leaves	Anti-cancer activity against breast cancer cell	[745]
Au NPs	*Anacardium occidentale* leaves	Anti-cancer activity against human cell lines for breast cancer (MCF-7 cell lines)	[748]
Au NPs	*Taxus baccata* extract	Anti-cancer activity against human cell lines for breast (MCF-7), cervical (HeLa), and ovarian (Caov-4) cancer cells	[749]
Au NPs	*Mappia foetida* leaf	Deliver DOX to cancer cells	[750]
		Toxic to many human cancer cells, such as HeLa, SiHa, MDA-MB-231, and Hep-G2	[750]
CuO NPs	*Ficus religiosa* leaves	Anti-cancer activity against A549 lung cancer	[757,759]
CuO NPs	*Camellia sinensis* leaves	Anti-cancer activity against MCF-7 (breast cancer cells)	[717]
CuO/Zn NPs	*Duchesnea indica* leaves	Improve kidney cancer therapy	[756]
ZnO NPs	*Laurus nobilis* leaves	Anti-cancer activity against A549 lung cancer	[759]
ZnO NPs	*Ecliptaprostrata* leaves	Anti-cancer activity against human liver carcinoma line (HeO-G2)	[760]
ZnO NPs	*Ziziphus nummularia* leaves	Anti-cancer activity against human cervical epithelial cancer cells (HeLa)	[761]
SPIONs	Fruit peel biomass	Anti-cancer activity against human cervical epithelial cancer cells (HeLa)	[762]
Iron NPs	Brown seaweed biomass	Anti-cancer activity against human cell lines for breast cancer, leukemia, liver cancer, and cervical cancer	[763]
TiO_2 NPs	*Vigna radiata* legume	Anti-cancer activity against Mg 63 osteosarcoma and chondrosarcoma cancer cell lines	[764,765]

crossing cell membranes, and degradation during delivery, all of which contribute to their low bioavailability [768]. Antioxidants have been covalently connected to NPs to provide improved stability, sustained release, compatibility, and targeted delivery of antioxidants [768]. Therefore, we now discuss some examples of NPs used as antioxidants and their biomass waste-derived origins, as shown in Table 16.

CQDs were made using a carbonization technique that used waste green tea leaves as a carbon source. 2,2-diphenyl-1-picrylhydrazyl (DPPH) quenching by hydrogen atom transfer from the carboxyl, hydroxyl, and/or amino groups for CQDs is a potential mechanism for DPPH reduction by CQDs [769]. Au NPs created as a waste product from an aqueous extract of *A. noeanum* leaves, *Abroma augusta* L. bark, or watermelon rind have exhibited antioxidant properties [335,731,770]. This may be due to the ability of Au NPs to neutralize and scavenge DPPH free radicals by donating hydrogen ions or electrons [335,731,770]. The antioxidant activity of iron NPs

Table 16: Application of recycled NPs as antioxidants

NM	Biomass sources	Ref.
CQDs	Green tea waste	[769]
Au NPs	*Allium noeanum* leaves	[731]
Au NPs	*Abroma augusta* L. bark	[770]
Au NPs	Watermelon rind	[335]
ZnO NPs	*Punica granatum* peel	[718]
Iron NPs	*Camellia sinensis* (green tea) leaves	[772]
Iron NPs	*Murraya koenigii* leaves	[773]
Iron NPs	*Phoenix dactylifera*	[771]
TiO_2 NPs	Kola seed	[774]
TiO_2 NPs	*Artemisia haussknechtii*	[730]
TiO_2 NPs	*Psidium guajava*	[233]
TiO_2 NPs	*Morinda citrifolia* leaves	[728]

synthesized from *Phoenix dactylifera*, which contain a high amount of polyphenols, has been well established. Their antioxidant potential was carried out by determining the products from oxidation or by assessing the ability to retain the radicals of the reaction patterns [771]. Antioxidant properties have also been demonstrated in iron NPs derived from *C. sinensis* (green tea) and *Murraya koenigii* leaves [772,773].

After incubation, biosynthesized TiO_2 NPs were capable of causing DPPH decolorization, indicating that they are antioxidants in nature. DPPH was scavenged in a dose-dependent manner at tested concentrations of 10–80 g/mL, yielding responses of 32.61–62.06% [772,773]. Kola seed-mediated particles have been the most intense among photosynthesized TiO_2 NPs, with the least activities obtained for KS–TiO_2 NPs, which had the highest performance of 52.37% [774]. Antioxidant activities have been also reported for TiO_2 NPs made from fruit peel agriwaste, *L. siceraria*, *P. dulce*, *P. guajava*, *Allium eriophyllum*, *A. haussknechtii*, and the leaf biomass of *M. citrifolia* [228,233,728,730]. Furthermore, plant aqueous extract and synthesized TiO_2 NPs were found to possess maximum antioxidant activity compared to ascorbic acid [233].

5.4 Nanodrugs and nanovaccines

Nanopharmaceuticals combine nanotechnology with biomedical and pharmaceutical sciences. Nanomedicine is a new and rapidly growing field. NPs can be used in drug formulations due to their pharmacokinetics, safety, efficacy, and targeting ability [775]. Many drug-based NPs have enrolled in clinical trials, however, drug-based NPs face a lot of challenges because of their toxicity issues, need for better characterization, and the absence of regulatory guidelines [775].

IO NPs have been used in many drugs as iron replacement therapy. These include Ferrlecit (sodium ferric gluconate complex in sucrose injection, Sanofi-Aventis, US), Venofer (iron sucrose injection, American Regent, Inc.), Dexferrum (iron dextran injection, American Regent, Inc.), and Infed (iron dextran injection, Actavis Pharma), which are all used in the treatment of anemia associated with chronic kidney disease [775,776]. These nano-formulations contain an iron oxide core covered with hydrophilic polymers, such as dextran or sucrose that allow the iron to be dissolved slowly after injection. These formulations permit fast administration of large doses without increased iron-free blood levels, preventing toxicity [777]. SPIONs are biodegradable, have low toxicity, and remain in blood circulation for a long time. SPIONs made from fruit peel biomass respond strongly when exposed to magnetic fields, releasing energy that can be used in targeting specific tumors [762]. Nanotherm, for example, is a drug that treats glioblastoma tumors. A different magnetic field is applied to selectively heat particles after injection of Nanotherm directly into the tumor [778]. This leads to local heating of the tumor to 40–45°C, resulting in programmed and non-programmed cell death. Nanotherm is now awaiting Food and Drug Administration (FDA) approval.

The negative nature of functional groups loaded on CNFs made from chitin biowaste has enabled their electrostatic binding to the protonated drug R-NH3+, as in the DOX anticancer drug [779]. In the last decade, CNTs made from agricultural biomass sources have received more interest in research applications in the field of drug delivery [34]. Various strategies for binding different CNT drugs were established through either covalent binding or non-covalent adsorption [780]. Functionalization of CNTs is therefore required for benign compatibility and good solubility. Additionally, GO has the benefits of low cost, two external surfaces, simple manufacturing, and alteration, and lack of toxic metal particles. GO also has an ultrahigh surface area for effective drug binding for all sp^2 carbon atoms exposed on its surface. In addition, planar GO sheets for future multi-modal imaging and treatment applications can easily be complexed with functional NPs [780]. G made from biomass is also gaining popularity in research applications in the field of drug delivery [781,782].

Due to the large surface area of Au NPs, they are useful in the delivery of drugs. Drug molecules can bind to the conjugate Au NPs by physical absorption or by a covalent or ionic bond. DOX is an anticancer drug that can attach to Au NPs *via* a pH-sensitive linker. This DOX–Au NP attachment allows the intracellular release of DOX from Au NPs inside acidic organelles. This release allows a rapid increase in the concentration of intracellular DOX, enhancing therapeutic efficacy in tumor cells [783]. *M. foetida* leaf biomass and onion peel extract were used as a bioreductant in the synthesis of Au NPs, which were then used to efficiently deliver DOX to cancer cells [750,784].

The presence of efficient fluorescent labels makes QDs suitable for drug delivery systems as these labels track the metabolism process of the drug in the body. QDs are also able to cross cell membranes and their large surface area provides several drug targeting attachment sites. GQDs can load drugs on their surface hydrophobically or through noncovalent π–π interactions [785]. GQDs are also biocompatible and the small size of CQDs

make them ideal for drug delivery. CQDs made from crab shell have enabled specific targeting to cancer cells [517] while those made from bamboo-leaf cellulose have been used to deliver DOX to cancer cells [786]. Sugarcane bagasse CQDs have exhibited a greater drug loading capacity [787].

In summary, NPs have several characteristics that are useful in drug manufacturing. Their biocompatibility and small size makes them useful for the delivery of drugs and carrying the drug into the cell while their fluorescence or photoluminescence can be used to track the metabolism of the drugs *in vivo*. Additionally, the magnetic and thermal energy of NPs kills tumor cells when exposed to light or a magnetic field.

Nanotechnology has merged with vaccine development in the fight against diseases caused by bacterial or viral infections, as well as malignant tumors, resulting in nanovaccines, which are crucial [788]. Nanovaccines have many advantages over conventional vaccines as antigens can be encapsulated in nanocarriers to avoid antigenic degradation. Also, antigen-presenting cells (APCs) can quickly process and phagocytize nanovaccines [789].

NMs have provided one-of-a-kind opportunities to increase the therapeutic efficacy of cancer vaccines' antigens while molecular or nanoadjuvants, and nanocarriers are commonly used in nanovaccines [790]. In melanoma, colon cancer, and human papillomavirus E6/E7, nanovaccines have triggered significant immune responses that inhibited tumor growth [791]. Tumor-specific immune responses can be induced by cancer vaccines and T cells that are specific to tumors and ensure that they are activated and expanded. Recent progress in NP-based nanovaccines has focused on the co-delivery of tumor-specific antigens and adjuvants to APCs, such as dendritic cells (DCs) [789].

Immunization with colloidal gold conjugated to haptens (small molecules that can only induce an immune response when attached to a carrier) and antigens resulted in higher antibody levels than immunization with complete Freund's adjuvant. Furthermore, when compared to complete Freund's adjuvant immunization, the amount of antigen required with colloidal gold is lower [792]. In addition, Au NPs are appealing nanocarriers because they are non-toxic, inert, and easily endocytosed by DCs. DCs can filter vaccine peptides on the particles to activate cytotoxic T lymphocytes (CTLs) and uptake Au nanovaccines with minimal toxicity. Au nanovaccines with high peptide density stimulate CTLs better than free peptides and have a lot of potential as vaccine carriers [793].

SPIONs are the NPs used for vaccine delivery [794]. SPIONs provide a novel way to activate the humoral and cellular immune systems in the fight against cancer. SPIONs coated with recombinant heat shock protein 70 (Hsp70), which is known to chaperone antigenic peptides, had increased immunostimulatory ability. Hsp70–SPIONs bind to tumor lysates and deliver immunogenic peptides to DCs, triggering a tumor-specific CD8+ cytotoxic T cell response [795]. The use of DCs pulsed with Hsp70–SPIONs and tumor lysates to immunize C6 glioma-bearing rats resulted in a delay in tumor development (as measured by MRI) and an improvement in overall survival. Parallel to this, increased interferon secretion was found in the serum of these animals and immunohistological examination of subsequent glioma cryosections showed increased infiltration of memory CD45RO+ and cytotoxic CD8+ T cells. The results demonstrate that magnetic nanocarriers, such as SPIONs coated with Hsp70, can be used as a medium for enhancing anti-cancer immune responses [795]. Many basic objectives in this field include magnetic properties of IO NPs, complete control over particle size distribution, ability to carry different types of biomolecules with respect to surface functional groups, low-cost development, and good immune status [794].

DC vaccines have a lot of promise in cancer immunotherapy but their anti-tumor effectiveness is hampered by their poor design and the immunosuppressive tumor microenvironment. Semiconductor QDs have been designed to serve as fluorescence nanoprobes, immunomodulatory adjuvants, and nanocarriers for tumor antigens and Toll-like receptor 9 agonists, among other applications [796]. QD-pulsed DC vaccines allow for spatiotemporal lymphatic drainage monitoring and DC immunotherapy efficacy evaluation, as well as potent immune activation. Designer DC vaccines combined with macrophage polarization elicits a powerful immune response that stimulates both innate and adaptive antitumor immunity while improving the immunosuppressive tumor microenvironment. As a unique combination treatment, this approach significantly increases antigen-specific T-cell immunity, inhibiting local tumor growth and metastasis *in vivo*. This research could lead to a new cancer immunotherapy treatment [797]. Table 17 shows the application of recycled NPs in nanodrugs and nanovaccines.

6 Cytotoxicity of NMs

6.1 CNMs

The CNMs' complexity and variety in size, chemical compositions, shape, charge, manufacturing methods, and surface functionalization are all important variables in

Table 17: Application of recycled NPs as nanodrugs and nanovaccines

NM	Biomass source	Applications	Ref.
Au NPs	*Mappia foetida* leaf biomass	DOX delivery to cancer cells	[750]
Au NPs	Onion peel extract	Targeted drug delivery for treatment of cancer	[784]
Au NPs	*M. foetida* leaves	Nanovaccine	[750]
Ag/Au	*Parkia roxburghii*	Nanovaccine	[306]
CQDs	Sugarcane bagasse	Provides the NM with greater drug loading capacity	[787]
CQDs	Crab shell	Enables specific targeting to cancer cells	[517]
CQDs	Bamboo-leaf cellulose	DOX delivery to cancer cells	[786]
CQDs	*Nerium oleander* leaf	Nanovaccine	[743]
SPIONs	Fruit peel biomass	Drug delivery	[762]
Iron oxide	Fruit peel biomass	Nanovaccine	[762]
G/GO NPs	Biomass-synthesized G	Drug delivery	[782]
CNTs NPs	Agricultural biomass sources	Drug delivery	[34]
CNFs NPs	Chitin biowaste	Drug delivery	[779]
CNMs	Plastic bags	Nanovaccine	[797]

their cytotoxicity [798]. CNMs can enter the body by a variety of methods including inhalation, oral administration, and injection. They can easily move throughout organs to the circulatory system [799]. When CNMs are injected intravenously or taken orally, they might cause inflammation in vulnerable organs such as the liver, kidneys, and lungs [800].

The cytotoxicity of CNTs in healthy tissues is a serious challenge in biomedical applications. As a result of the various techniques of synthesis, CNTs vary in size, shape, structure, and purity [801]. CNTs cytotoxicity is related to their synthesis process, length, functional group(s), structure, surface-to-volume ratio, concentration, composition, amount of oxidation, and the extent of aggregation [802].

Furthermore, insufficient removal of metal catalysts utilized during CNTs preparation has been linked to their increased cytotoxicity [803]. The CNTs' limited biocompatibility, on the other hand, is a major barrier to their usage in biomedical applications due to their poor solubility. The hydrophobic surface of CNTs as well as their tendency to aggregate are thought to be contributing factors in their toxicity *in vitro* [804]. However, by coating the surface of CNTs with biocompatible surfactants or polymers, these adverse effects can be reduced [805]. Oxidative stress, cell membrane injury, DNA damage, and death are all potential pathways for CNTs cytotoxicity [806].

Structure, surface chemistry, number of layers, functional groups, and the employment of reducing agents for functionalization, all play a role in G and its derivatives' cytotoxicity [807]. The principle mechanism of cytotoxicity of G-based NMs is the generation of ROS [808].

Normal cells may be harmed by G-based NMs, because they disrupt the physiological conditions. When G-based NMs are used, a lot of ROS is produced. Increased levels of ROS can cause diseases such as diabetes [809], Alzheimer's disease [810], atherosclerosis [811], and carcinogenesis [812]. Polysaccharide modification of G NMs is a promising method for lowering their toxicity and improving their targeting ability, which improves biotherapeutic efficacy [813].

6.2 IQDs

In 2011, the US FDA approved the first human clinical trial of QD technology. Most chemotherapeutics and cytotoxic medicines are now given as QDs for an improved pharmacological action [814]. The major concern for the use of QDs in biomedical application is their toxicity. QDs toxicity is determined by their size, dose, delivery method, and the capping material [814]. Although the regulatory status of QDs is unclear, they are nevertheless considered safe to use. However, the development of harmless QDs such as CQDs and GQDs could help to overcome this to some extent [814].

The main way of reducing the toxicity of QDs is using metal-free materials for QDs preparation [815]. In addition, biocompatible functionalization was also used to reduce the toxicity of QDs. QDs can be enclosed in phospholipid micelles for biological applications, resulting in no surface modifications and the retention of optical properties [816]. The other approach is antibody conjugation [814].

6.3 MO-based NMs

MOs are likely to accumulate in the environment after their use, generating adverse effects on the environment and human health, due to their higher chemical reactivity

resulting in an increased generation of ROS [817]. Indeed, the surface of MOs is a major factor in their toxicity as a result of the interaction of their surfaces with the biological system [818]. Different MOs can be found in nature, however, some of them have a wide range of biomedical applications, including IO NPs, TiO_2 NPs, ZnO NPs, and CuO NPs [819].

The cytotoxicity of IO NPs is one of the major challenges to their translation into biomedical applications. Generation of ROS, including hydroxyl radicals, superoxide anion, and nonradical H_2O_2, is responsible for the majority of IO NPs intracellular cytotoxicity [820]. The generation of ROS from the NP surface, ROS creation by leaching of iron molecules, modifying mitochondrial functions, and stimulation of signaling pathways are the four primary sources of oxidative damage in response to IO NPs [821]. Surface coating is one method for making IO NPs non-toxic and biocompatible [822].

With rapid nanotechnology development, TiO_2 NPs and ZnO NPs are widely used in various fields. People working in such environments, as well as researchers in laboratories, are more likely to be exposed to TiO_2 NPs and ZnO NPs [823,824]. Furthermore, increasing data suggest that TiO_2 NPs concentrations are elevated in animal organs following systematic exposure, and that these accumulated NPs may cause organ damage. Oxidative stress, autophagy, apoptosis, inflammatory response, genotoxic effects, and signaling pathways all contribute to TiO_2 NPs toxicity [823]. Cell membrane damage, cytotoxicity, and increased oxidative stress have been described in diverse mammalian cell lines as the most common harmful effect of ZnO NPs [825]. ZnO NPs have been shown to have genotoxic potential in both *in vivo* and *in vitro* experiments, in addition to cytotoxicity [826].

CuO NPs have been shown to cause harmful effects on the liver and kidneys in many experiments [827]. In experimental animals, CuO NPs have caused severe damage in the liver, spleen, and kidneys. Highly reactive ionic copper is generated after oral administration and interaction with gastric fluid, which is then deposited in the kidneys of exposed animals [828].

6.4 Au NPs

Au NPs have received a lot of interest in the biomedicine field because of its electrical, chemical, thermal, mechanical, and optical properties, With the high potentials, the high risk of toxicity came, as a result of their interaction with biological tissues and biomolecules [829]. *In vivo* and *in vitro* experiments on Au NPs were carried out. Both showed some oxidative damage to organs and cell lines *in vivo* and *in vitro* respectively, with the liver, kidney, and spleen being the most impacted [829].

The size and shape of Au NPs are the most essential factors that contribute to their cytotoxicity, because they are directly associated to the process of cellular internalization [830]. The cytotoxicity of Au NPs is size dependent, with smaller (1.4 nm) Au NPs being more cytotoxic than larger (15 nm) ones [831]. In HeLa cells, SK-Mel-28 melanoma cells, L929 animal fibroblasts, and mouse monocytic/macrophage cells, Pan *et al.* found that 1.4 nm Au NPs caused rapid cell death through necrosis, whereas 1.2 nm Au NPs caused cell death through apoptosis [831]. The large surface areas of these extremely small particles can contribute to the production of ROS. ROS injure cells by destroying proteins, membranes, DNA, and other organelles like the mitochondria, cytoplasm, and nucleus [829].

Vales *et al.* found that, in addition to size and shape, surface functionalization of Au NPs has a role in their cytotoxicity. Three functionalization were used in this study: negative (carboxylate), positive (ammonium), and neutral (PEG). In comparison to anionic and neutral Au NPs, cationic Au NPs were more cytotoxic. A positive surface charge appears to exacerbate the cytotoxicity of Au NPs [832].

7 Conclusion and future prospects

To summarize, the authors have shed light on valuable NMs that can be extracted from waste sources originating from everyday life, including biomass wastes, cooking oil, and industrial wastes, to achieve “waste-to-wealth” and meet the “zero-waste” challenge. Different CNMs, including inorganic QDs, various MOs, and Au NPs, can be easily extracted from the above-mentioned sources. Then the different synthesis approaches used to synthesize these NMs, which could be classified into top-down and bottom-up routes, were presented. Additionally, their potential roles in the early detection of serious diseases, with a special focus on their roles in fluorescent imaging, magnetic imaging, and when acting as biosensors, were summarized. Moreover, the promising therapeutic modalities of NMs as antimicrobial, anticancer, antioxidant agents, and as nanodrugs and vaccines were analyzed in detail.

Many other recyclable NMs are valuable for biomedical applications. Recently, palladium and platinum NPs were introduced as potential and novel mineral derived NPs synthesized from different sources of waste

via diverse green synthesis strategies [833–837]. They are amongst the widely used NPs for applications in biomedicine like drug delivery, biosensors, imaging, photothermal therapy, cosmetics, antimicrobials, and therapeutics for many afflictions (AIDS, cancer, and malaria), and implants [838–842]. Furthermore, they have unique anticancer [843], antioxidant, and antibacterial capabilities [844]. However, further research is needed to highlight their role in the early detection of different diseases. Although RNMs have shown many outstanding characteristics such as cost-effectiveness, ease of manipulation, and good physiological properties, many investigations are still required for their further isolation and purification. In addition, the use of RNMs for other biomedical applications, such as bio-scaffolds in tissue engineering and regenerative medicine and wound-healing applications, has not yet been addressed.

Acknowlegement: A. Matsuda and G. Kawamura acknowledge Japan Society for Promotion of Science (JSPS) KAKENHI Grant No. 18H03841 and No. 21K18823, for partially funding this study.

Funding information: Japan Society for Promotion of Science (JSPS) KAKENHI Grant No. 18H03841 and No. 21K18823.

Author contributions: All authors have accepted responsibility for the entire content of this manuscript and approved its submission.

Conflict of interest: The authors state no conflict of interest.

References

[1] Aflori M. Smart nanomaterials for biomedical applications – a review. Nanomaterials. 2021;11(2):396.

[2] Jeevanandam J, Barhoum A, Chan YS, Dufresne A, Danquah MK. Review on nanoparticles and nanostructured materials: history, sources, toxicity and regulations. Beilstein J Nanotechnol. 2018;9(1):1050–74.

[3] Lyu Q, Peng L, Hong X, Fan T, Li J, Cui Y, et al. Smart nano-micro platforms for ophthalmological applications: the state-of-the-art and future perspectives. Biomaterials. 2021;270:120682.

[4] Lan L, Yao Y, Ping J, Ying Y. Recent advances in nanomaterial-based biosensors for antibiotics detection. Biosens Bioelectron. 2017;91:504–14.

[5] Colino CI, Lanao JM, Gutiérrez-Millán C. Recent advances in functionalized nanomaterials for the diagnosis and treatment of bacterial infections. Mater Sci Eng: C. 2021;121:111843.

[6] Nejati K, Dadashpour M, Gharibi T, Mellatyar H, Akbarzadeh A. Biomedical applications of functionalized gold nanoparticles: a review. J Clust Sci. 2021;1–16 doi: 10.1007/s10876-020-01955-9.

[7] Jadoun S, Arif R, Jangid NK, Meena RK. Green synthesis of nanoparticles using plant extracts: a review. Environ Chem Lett. 2020;19:1–20.

[8] Abd Elkodous M, El-Sayyad GS, Abdelrahman IY, El-Bastawisy HS, Mohamed AE, Mosallam FM, et al. Therapeutic and diagnostic potential of nanomaterials for enhanced biomedical applications. Colloids Surf B: Biointerfaces. 2019;180:411–28.

[9] Abd Elkodous M, El-Sayyad GS, Youssry SM, Nada HG, Gobara M, Elsayed MA, et al. Carbon-dot-loaded $CoxNi_{1-x}Fe_2O_4$; $x = 0.9/SiO_2/TiO_2$ nanocomposite with enhanced photocatalytic and antimicrobial potential: an engineered nanocomposite for wastewater treatment. Sci Rep. 2020;10(1):11534.

[10] El-Sayyad GS, Abd Elkodous M, El-Khawaga AM, Elsayed MA, El-Batal AI, Gobara M. Merits of photocatalytic and antimicrobial applications of gamma-irradiated $CoxNi_{1-x}Fe_2O_4$/SiO_2/TiO_2; $x = 0.9$ nanocomposite for pyridine removal and pathogenic bacteria/fungi disinfection: implication for wastewater treatment. RSC Adv. 2020;10(9):5241–59.

[11] Wong CW, Chan YS, Jeevanandam J, Pal K, Bechelany M, Abd Elkodous M, et al. Response surface methodology optimization of mono-dispersed MgO nanoparticles fabricated by ultrasonic-assisted sol–gel method for outstanding antimicrobial and antibiofilm activities. J Clust Sci. 2020;31(2):367–89.

[12] Abd Elkodous M, El-Sayyad GS, Nasser HA, Elshamy AA, Morsi M, Abdelrahman IY, et al. Engineered nanomaterials as potential candidates for HIV treatment: between opportunities and challenges. J Clust Sci. 2019;30(3):531–40.

[13] Abd Elkodous M, El-Sayyad GS, Abdel Maksoud MIA, Abdelrahman IY, Mosallam FM, Gobara M, et al. Fabrication of ultra-pure anisotropic zinc oxide nanoparticles *via* simple and cost-effective route: implications for UTI and EAC medications. Biol Trace Elem Res. 2020;196(1):297–317.

[14] El-Batal AI, Mosallam FM, Ghorab MM, Hanora A, Gobara M, Baraka A, et al. Factorial design-optimized and gamma irradiation-assisted fabrication of selenium nanoparticles by chitosan and Pleurotus ostreatus fermented fenugreek for a vigorous *in vitro* effect against carcinoma cells. Int J Biol Macromol. 2020;156:1584–99.

[15] Elkhenany H, Abd Elkodous M, Ghoneim NI, Ahmed TA, Ahmed SM, Mohamed IK, et al. Comparison of different uncoated and starch-coated superparamagnetic iron oxide nanoparticles: implications for stem cell tracking. Int J Biol Macromol. 2020;143:763–74.

[16] El-Batal AI, Abd Elkodous M, El-Sayyad GS, Al-Hazmi NE, Gobara M, Baraka A. Gum Arabic polymer-stabilized and Gamma rays-assisted synthesis of bimetallic silver-gold nanoparticles: powerful antimicrobial and antibiofilm activities against pathogenic microbes isolated from diabetic foot patients. Int J Biol Macromol. 2020;165:169–86.

[17] Abd Elkodous M, El-Sayyad GS, Abdel-Daim MM. Engineered nanomaterials as fighters against SARS-CoV-2: the way to control and treat pandemics. Environ Sci Pollut Res. 2020;28:40409–15.

[18] Eldebany N, Abd Elkodous M, Tohamy H, Abdelwahed R, El-kammar M, Abou-Ahmed H, et al. Gelatin loaded titanium dioxide and silver oxide nanoparticles: implication for skin tissue regeneration. Biol Trace Elem Res. 2020;199:3688–99.
[19] Elkhenany H, Elkodous MA, Newby SD, El-Derby AM, Dhar M, El-Badri N. Tissue Engineering Modalities and Nanotechnology. In: El-Badri N, editor. Regenerative medicine and stem cell biology. Cham: Springer International Publishing; 2020. p. 289–322.
[20] Attia MS, El-Sayyad GS, Abd Elkodous M, Khalil WF, Nofel MM, Abdelaziz AM, et al. Chitosan and EDTA conjugated graphene oxide antinematodes in Eggplant: toward improving plant immune response. Int J Biol Macromol. 2021;179:333–44.
[21] Attia MS, Balabel NM, Ababutain IM, Osman MS, Nofel MM, Abd Elkodous M, et al. Protective role of copper oxide-streptomycin nano-drug against potato brown rot disease caused by ralstonia solanacearum. J Clust Sci. 2021;28:27577–92.
[22] Jung Y, Huh Y, Kim D. Recent advances in surface engineering of porous silicon nanomaterials for biomedical applications. Microporous Mesoporous Mater. 2020;310:110673.
[23] Tang H, Zhao X, Jiang X. Synthetic multi-layer nanoparticles for CRISPR-Cas9 genome editing. Adv drug Delivery Rev. 2021;168:55–78.
[24] Zaheer T, Pal K, Zaheer I. Topical review on nano-vaccinology: biochemical promises and key challenges. Process Biochem. 2020;100:237–44.
[25] Lubick N. Nanosilver toxicity: ions, nanoparticles or both? ACS Publications; 2008.
[26] Zoroddu MA, Medici S, Ledda A, Nurchi VM, Lachowicz JI, Peana M. Toxicity of nanoparticles. Curr Med Chem. 2014;21(33):3837–53.
[27] Al-Tamimi SA. Biogenic green synthesis of metal oxide nanoparticles using oat biomass for ultrasensitive modified polymeric sensors. Green Chem Lett Rev. 2021;14(2):166–79.
[28] Nasrollahzadeh M, Sajjadi M, Iravani S, Varma RS. Carbon-based sustainable nanomaterials for water treatment: state-of-art and future perspectives. Chemosphere. 2020;263:128005.
[29] Goldoni R, Farronato M, Connelly ST, Tartaglia GM, Yeo W-H. Recent advances in graphene-based nanobiosensors for salivary biomarker detection. Biosens Bioelectron. 2020;171:112723.
[30] Omoriyekomwan JE, Tahmasebi A, Dou J, Wang R, Yu J. A review on the recent advances in the production of carbon nanotubes and carbon nanofibers *via* microwave-assisted pyrolysis of biomass. Fuel Process Technol. 2020;214:106686.
[31] Esposito Corcione C, Ferrari F, Striani R, Greco A. Transport properties of natural and artificial smart fabrics impregnated by graphite nanomaterial stacks. Nanomaterials. 2021;11(4):1018.
[32] Azam MA, Abd Mudtalib NESA, Seman RNAR. Synthesis of graphene nanoplatelets from palm-based waste chicken frying oil carbon feedstock by using catalytic chemical vapour deposition. Mater Today Commun. 2018;15:81–7.
[33] Asiya S, Pal K, Kralj S, El-Sayyad G, de Souza F, Narayanan T. Sustainable preparation of gold nanoparticles *via* green chemistry approach for biogenic applications. Mater Today Chem. 2020;17:100327.
[34] Fathy NA, Basta AH, Lotfy VF. Novel trends for synthesis of carbon nanostructures from agricultural wastes, carbon nanomaterials for agri-food and environmental applications. Elsevier; 2020. p. 59–74
[35] de Diego-Díaz B, Cerdán JMA, Peñas FJ, Fernández-Rodríguez J. Impact of supplementary nutrients on codigestion of agricultural waste: study of temperatures. Food Bioprod Process. 2018;110:120–5.
[36] Radich A. Biodiesel performance, costs, and use. US Energy Information Administration; 2006.
[37] Kulkarni MG, Dalai AK. Waste cooking oil an economical source for biodiesel: a review. Ind Eng Chem Res. 2006;45(9):2901–13.
[38] Carter D. How to make biodiesel, low-impact living initiative; 2005.
[39] Stewart E, Lemieux P. Emissions from the incineration of electronics industry waste. IEEE International Symposium on Electronics and the Environment. IEEE; 2003. p. 271–5.
[40] Huo X, Peng L, Xu X, Zheng L, Qiu B, Qi Z, et al. Elevated blood lead levels of children in Guiyu, an electronic waste recycling town in China. Environ Health Perspect. 2007;115(7):1113–7.
[41] Ozdemir I, Şahin M, Orhan R, Erdem M. Preparation and characterization of activated carbon from grape stalk by zinc chloride activation. Fuel Process Technol. 2014;125:200–6.
[42] Arie AA, Hadisaputra L, Susanti RF, Devianto H, Halim M, Enggar R, et al. Synthesis of carbon nano materials originated from waste cooking oil using a nebulized spray pyrolysis. J Phys Conf Ser. IOP Publishing; 2017. p. 012020.
[43] Nazem MA, Zare MH, Shirazian S. Preparation and optimization of activated nano-carbon production using physical activation by water steam from agricultural wastes. RSC Adv. 2020;10(3):1463–75.
[44] Sivaprakash S, Kumar PS, Krishna S. Synthesis & characteristic study of agricultural waste activated carbon/Fe_3O_4–Nano particles. Int J Mater Sci. 2017;12(1):97–105.
[45] Sinto J, Nugroho YW, Naf'an HI. Preparation of activated carbon from banana peel waste as adsorbent for motor vehicle exhaust emissions, E3S web of conferences. EDP Sci. 2018;03020.
[46] Afdhol M, Amiliana R, Hanafi A, Rachmanda B. Preparation of activated carbon from palm shells using KOH and $ZnCl_2$ as the activating agent. IOP Conf Ser Mater Sci Eng. IOP Publishing; 2017. p. 012282
[47] Román S, González J, González-García C, Zamora F. Control of pore development during CO_2 and steam activation of olive stones. Fuel Process Technol. 2008;89(8):715–20.
[48] Kula I, Uğurlu M, Karaoğlu H, Celik A. Adsorption of Cd (II) ions from aqueous solutions using activated carbon prepared from olive stone by $ZnCl_2$ activation. Bioresour Technol. 2008;99(3):492–501.
[49] Martinez ML, Torres MM, Guzman CA, Maestri D. Preparation and characteristics of activated carbon from olive stones and walnut shells. Ind Crop Products. 2006;23(1):23–8.
[50] Yang K, Peng J, Srinivasakannan C, Zhang L, Xia H, Duan X. Preparation of high surface area activated carbon from

coconut shells using microwave heating. Bioresour Technol. 2010;101(15):6163–9.
[51] Yahya MA, Al-Qodah Z, Ngah CZ. Agricultural bio-waste materials as potential sustainable precursors used for activated carbon production: a review. Renew Sustain Energy Rev. 2015;46:218–35.
[52] Musuna-Garwe CC, Mukaratirwa-Muchanyereyi N, Mupa M, Mahamadi C, Mujuru M. Preparation and characterization of nanocarbons from Nicotiana tabacum stems. 2018
[53] Gao P, Liu Z-h, Xue G, Han B, Zhou M-h. Preparation and characterization of activated carbon produced from rice straw by (NH) 2HPO4 activation. Bioresour Technol. 2011;102(3):3645–8.
[54] Nandiyanto ABD, Putra ZA, Andika R, Bilad MR, Kurniawan T, Zulhijah R, et al. Porous activated carbon particles from rice straw waste and their adsorption properties. J Eng Sci Technol. 2017;12(8):1–11.
[55] Gin W, Jimoh A, Abdulkareem A, Giwa A. Production of activated carbon from watermelon peel. Int J Sci Eng Res. 2014;5:66–71.
[56] Roopa D. Preparation of activated carbon from bitter orange peel (citrus aurantium) and preliminary studies on its characteristics. J Clin Diag Res: JCDR. 2016;10:6–11.
[57] Elaiyappillai E, Srinivasan R, Johnbosco Y, Devakumar P, Murugesan K, Kesavan K, et al. Low cost activated carbon derived from Cucumis melo fruit peel for electrochemical supercapacitor application. Appl Surf Sci. 2019;486:527–38.
[58] Yuliusman MPAyu, Hanafi A, Nafisah AR. Activated carbon preparation from durian peel wastes using chemical and physical activation. AIP Conf Proc. AIP Publishing LLC; 2020. p. 030020
[59] Murugesan K, Tareke K, Gezehegn M, Kebede M, Yazie A, Diyana G. Rapid development of activated carbon and ZnO nanoparticles *via* green waste conversion using avocado fruit peel powder and its high performance efficiency in aqueous dye removal application. J Inorg Organomet Polym Mater. 2019;29(4):1368–74.
[60] Vinha AF, Moreira J, Barreira SV. Physicochemical parameters, phytochemical composition and antioxidant activity of the algarvian avocado (Persea americana Mill.). J Agric Sci. 2013;5(12):100.
[61] Osman AI, Blewitt J, Abu-Dahrieh JK, Farrell C, Ala'a H, Harrison J, et al. Production and characterisation of activated carbon and carbon nanotubes from potato peel waste and their application in heavy metal removal. Environ Sci Pollut Res. 2019;26(36):37228–41.
[62] Moreno-Piraján J, Giraldo L. Activated carbon obtained by pyrolysis of potato peel for the removal of heavy metal copper (II) from aqueous solutions. J Anal Appl Pyrolysis. 2011;90(1):42–7.
[63] Ogungbenro AE, Quang DV, Al-Ali KA, Vega LF, Abu-Zahra MR. Synthesis and characterization of activated carbon from biomass date seeds for carbon dioxide adsorption. J Environ Chem Eng. 2020;8(5):104257.
[64] Srinivasan R, Elaiyappillai E, Pandian HP, Vengudusamy R, Johnson PM, Chen S-M, et al. Sustainable porous activated carbon from Polyalthia longifolia seeds as electrode material for supercapacitor application. J Electroanalytical Chem. 2019;849:113382.
[65] Abatan OG, Oni BA, Agboola O, Efevbokhan V, Abiodun OO. Production of activated carbon from African star apple seed husks, oil seed and whole seed for wastewater treatment. J Clean Prod. 2019;232:441–50.
[66] Prakash MO, Raghavendra G, Ojha S, Panchal M. Characterization of porous activated carbon prepared from arhar stalks by single step chemical activation method. Mater Today: Proc. 2020;39:1476–81.
[67] Shahraki ZH, Sharififard H, Lashanizadegan A. Grape stalks biomass as raw material for activated carbon production: synthesis, characterization and adsorption ability. Mater Res express. 2018;5(5):055603.
[68] Khanna V, Bakshi BR, Lee LJ. Carbon nanofiber production: life cycle energy consumption and environmental impact. J Ind Ecol. 2008;12(3):394–410.
[69] Alfarisa S, Abu Bakar S, Mohamed A, Hashim N, Kamari A, Md Isa I, et al. Carbon nanostructures production from waste materials: a review. Advanced Materials Research. Trans Tech Publ; 2015. p. 50–4.
[70] Hussain CM. Handbook of nanomaterials for industrial applications. Elsevier; 2018.
[71] Tsai W-T. Mandatory recycling of waste cooking oil from residential and commercial sectors in Taiwan. Resources. 2019;8(1):38.
[72] Janas D. From bio to nano: a review of sustainable methods of synthesis of carbon nanotubes. Sustainability. 2020;12(10):4115.
[73] Chen W, Meng X-T, Wang H-H, Zhang X-Q, Wei Y, Li Z-Y, et al. Way to produce carbon nanofiber by electrospinning from sugarcane Bagasse. Polymers. 2019;11(12):1968.
[74] Chen X-W, Timpe O, Hamid SB, Schlögl R, Su DS. Direct synthesis of carbon nanofibers on modified biomass-derived activated carbon. Carbon. 2009;47(1):340–3.
[75] Zhang J, Tahmasebi A, Omoriyekomwan JE, Yu J. Direct synthesis of hollow carbon nanofibers on bio-char during microwave pyrolysis of pine nut shell. J Anal Appl Pyrolysis. 2018;130:142–8.
[76] Wang Z, Shen D, Wu C, Gu S. State-of-the-art on the production and application of carbon nanomaterials from biomass. Green Chem. 2018;20(22):5031–57.
[77] Su X-L, Chen J-R, Zheng G-P, Yang J-H, Guan X-X, Liu P, et al. Three-dimensional porous activated carbon derived from loofah sponge biomass for supercapacitor applications. Appl Surf Sci. 2018;436:327–36.
[78] Tao L, Huang Y, Zheng Y, Yang X, Liu C, Di M, et al. Porous carbon nanofiber derived from a waste biomass as anode material in lithium-ion batteries. J Taiwan Inst Chem Eng. 2019;95:217–26.
[79] Shi G, Liu C, Wang G, Chen X, Li L, Jiang X, et al. Preparation and electrochemical performance of electrospun biomass-based activated carbon nanofibers. Ionics. 2019;25(4):1805–12.
[80] Hassan M, Abou-Zeid R, Hassan E, Berglund L, Aitomäki Y, Oksman K. Membranes based on cellulose nanofibers and activated carbon for removal of escherichia coli bacteria from water. Polymers. 2017;9(8):335.
[81] Fadillah A, Hartoyo A, Solikhin A. Business model development of oil palm empty fruit bunch and trunk carbon nanofibers–based water purifier. IOP Conf Ser Earth Environ Sci. IOP Publishing; 2020. p. 012018.

[82] Gaud B, Singh A, Jaybhaye S, Narayan H. Synthesis of carbon nano fiber from organic waste and activation of its surface area. Int J. 2019;2766:2748.
[83] Yadav S, Sharma CS. Novel and green processes for citrus peel extract: a natural solvent to source of carbon. Polym Bull. 2018;75(11):5133–42.
[84] Sari SN, Melati A. Facile preparation of carbon nanofiber from banana peel waste. Mater Today: Proc. 2019;13:165–8.
[85] Shahba H, Sabet M. Two-step and green synthesis of highly fluorescent carbon quantum dots and carbon nanofibers from pine fruit. J Fluorescence. 2020;30(4):927–38.
[86] Sami A, Mohammed M, Dhary A. Synthesis of carbon nanofibers from decomposition of liquid organic waste from chemical and petrochemical industries. Energy Proc. 2015;74:4–14.
[87] Biswas SK, Das AK, Yano H, Shams M. Development of high performance transparent nanocomposites reinforced with nanofibrillated chitin extracted from shrimp wastes. J Chitin Chitosan Sci. 2013;1(2):138–43.
[88] Rambau KM, Musyoka NM, Manyala N, Ren J, Langmi HW, Mathe MK. Preparation of carbon nanofibers/tubes using waste tyres pyrolysis oil and coal fly ash derived catalyst. J Environ Sci Health, Part A. 2018;53(12):1115–22.
[89] Widiatmoko P, Nugraha N, Devianto H, Nurdin I, Prakoso T. Upscaled synthesis of carbon nanotube from palm oil mill effluent using pyrolysis for supercapacitor application. IOP Conf Ser Mater Sci Eng. IOP Publishing; 2020. p. 012040
[90] Vinayan B, Nagar R, Raman V, Rajalakshmi N, Dhathathreyan K, Ramaprabhu S. Synthesis of graphene-multiwalled carbon nanotubes hybrid nanostructure by strengthened electrostatic interaction and its lithium ion battery application. J Mater Chem. 2012;22(19):9949–56.
[91] Robati D. Pseudo-second-order kinetic equations for modeling adsorption systems for removal of lead ions using multi-walled carbon nanotube. J Nanostruct Chem. 2013;3(1):1–6.
[92] Iijima S. Helical microtubules of graphitic carbon. Nature. 1991;354(6348):56–8.
[93] Yan Y, Miao J, Yang Z, Xiao F-X, Yang HB, Liu B, et al. Carbon nanotube catalysts: recent advances in synthesis, characterization and applications. Chem Soc Rev. 2015;44(10):3295–3346.
[94] De Volder MF, Tawfick SH, Baughman RH, Hart AJ. Carbon nanotubes: present and future commercial applications. Science. 2013;339(6119):535–9.
[95] Mugadza K, Stark A, Ndungu PG, Nyamori VO. Synthesis of carbon nanomaterials from biomass utilizing ionic liquids for potential application in solar energy conversion and storage. Materials. 2020;13(18):3945.
[96] Liu W, Yuan H. Simultaneous production of hydrogen and carbon nanotubes from cracking of a waste cooking oil model compound over Ni-Co/SBA-15 catalysts. Int J Energy Res. 2020;44(14):11564–82.
[97] Mannu A, Ferro M, Pietro MED, Mele A. Innovative applications of waste cooking oil as raw material. Sci Prog. 2019;102(2):153–60.
[98] Gui MM, Lee K, Bhatia S. Feasibility of edible oil vs. non-edible oil vs. waste edible oil as biodiesel feedstock. Energy. 2008;33(11):1646–53.
[99] Lin CSK, Pfaltzgraff LA, Herrero-Davila L, Mubofu EB, Abderrahim S, Clark JH, et al. Food waste as a valuable resource for the production of chemicals, materials and fuels. Current situation and global perspective. Energy Environ Sci. 2013;6(2):426–64.
[100] Suriani A, Nor RM, Rusop M. Vertically aligned carbon nanotubes synthesized from waste cooking palm oil. J Ceram Soc Jpn. 2010;118(1382):963–8.
[101] Sangeetha J, Thangadurai D, Hospet R, Purushotham P, Manowade KR, Mujeeb MA, et al. Production of bionanomaterials from agricultural wastes. Nanotechnology. Springer; 2017. p. 33–58
[102] Hidalgo P, Coronado G, Sánchez A, Hunter R. Agro-industrial waste as precursor source for carbon nanotubes (cnts) synthesis using a new technical of solvent autoignition. IOP Conf Ser Earth Environ Sci. 2020;503:012025.
[103] Mugadza K, Ndungu PG, Stark A, Nyamori VO. Conversion of residue biomass into value added carbon materials: utilisation of sugarcane bagasse and ionic liquids. J Mater Sci. 2019;54(19):12476–87.
[104] Fathy NA. Carbon nanotubes synthesis using carbonization of pretreated rice straw through chemical vapor deposition of camphor. RSC Adv. 2017;7(45):28535–41.
[105] Mopoung S. Occurrence of carbon nanotube from banana peel activated carbon mixed with mineral oil. Int J Phys Sci. 2011;6(7):1789–92.
[106] Osman AI, Blewitt J, Abu-Dahrieh JK, Farrell C, Al-Muhtaseb AAH, Harrison J, et al. Production and characterisation of activated carbon and carbon nanotubes from potato peel waste and their application in heavy metal removal. Environ Sci Pollut Res. 2019;26(36):37228–41.
[107] Singh V, Chatterjee S, Palecha M, Sen P, Ateeq B, Verma V. Chickpea peel waste as sustainable precursor for synthesis of fluorescent carbon nanotubes for bioimaging application. Carbon Lett. 2020;31:1–7.
[108] Robaiah M, Rusop M, Abdullah S, Khusaimi Z, Azhan H, Asli N. Synthesis graphene layer at different waste cooking palm oil temperatures. AIP Conf Proc. AIP Publishing LLC; 2017. p. 030008
[109] Bhuyan MSA, Uddin MN, Islam MM, Bipasha FA, Hossain SS. Synthesis of graphene. Int Nano Lett. 2016;6(2):65–83.
[110] Purkait T, Singh G, Singh M, Kumar D, Dey RS. Large area few-layer graphene with scalable preparation from waste biomass for high-performance supercapacitor. Sci Rep. 2017;7(1):1–14.
[111] Gupta K, Gupta D, Khatri OP. Graphene-like porous carbon nanostructure from Bengal gram bean husk and its application for fast and efficient adsorption of organic dyes. Appl Surf Sci. 2019;476:647–57.
[112] Jacob MV, Rawat RS, Ouyang B, Bazaka K, Kumar DS, Taguchi D, et al. Catalyst-free plasma enhanced growth of graphene from sustainable sources. Nano Lett. 2015;15(9):5702–8.
[113] Chen F, Yang J, Bai T, Long B, Zhou X. Facile synthesis of few-layer graphene from biomass waste and its application in lithium ion batteries. J Electroanal Chem. 2016;768:18–26.
[114] Zhou H, Zhang J, Amiinu IS, Zhang C, Liu X, Tu W, et al. Transforming waste biomass with an intrinsically porous network structure into porous nitrogen-doped graphene for highly efficient oxygen reduction. Phys Chem Chem Phys. 2016;18(15):10392–99.

[115] Sun L, Tian C, Li M, Meng X, Wang L, Wang R, et al. From coconut shell to porous graphene-like nanosheets for high-power supercapacitors. J Mater Chem A. 2013;1(21):6462–70.
[116] Shams SS, Zhang LS, Hu R, Zhang R, Zhu J. Synthesis of graphene from biomass: a green chemistry approach. Mater Lett. 2015;161:476–9.
[117] Long S-Y, Du Q-S, Wang S-Q, Tang P-D, Li D-P, Huang R-B. Graphene two-dimensional crystal prepared from cellulose two-dimensional crystal hydrolysed from sustainable biomass sugarcane bagasse. J Clean Prod. 2019;241:118209.
[118] Qu J, Luo C, Zhang Q, Cong Q, Yuan X. Easy synthesis of graphene sheets from alfalfa plants by treatment of nitric acid. Mater Sci Eng: B. 2013;178(6):380–2.
[119] Karuppannan M, Kim Y, Sung Y-E, Kwon OJ. Nitrogen and sulfur co-doped graphene-like carbon sheets derived from coir pith bio-waste for symmetric supercapacitor applications. J Appl Electrochem. 2019;49(1):57–66.
[120] Singh P, Bahadur J, Pal K. One-step one chemical synthesis process of graphene from rice husk for energy storage applications. Graphene. 2017;6(3):61–71.
[121] Kuila T, Bose S, Khanra P, Mishra AK, Kim NH, Lee JH. A green approach for the reduction of graphene oxide by wild carrot root. Carbon. 2012;50(3):914–21.
[122] Baweja H, Jeet K. Economical and green synthesis of graphene and carbon quantum dots from agricultural waste. Mater Res Exp. 2019;6(8):0850g8.
[123] Somanathan T, Prasad K, Ostrikov KK, Saravanan A, Krishna VM. Graphene oxide synthesis from agro waste. Nanomaterials. 2015;5(2):826–34.
[124] Mahendran GB, Ramalingam SJ, Rayappan JBB, Kesavan S, Periathambi T, Nesakumar N. Green preparation of reduced graphene oxide by Bougainvillea glabra flower extract and sensing application. J Mater Sci: Mater Electron. 2020;31(17):14345–56.
[125] Shah J, Lopez-Mercado J, Carreon MG, Lopez-Miranda A, Carreon ML. Plasma synthesis of graphene from mango peel. ACS Omega. 2018;3(1):455–63.
[126] Subramaniyan R, Kiruthika N, Somanathan T, Sriraman V, Shanmugam M. High performance of graphene oxide from banana peel against Pseudomonas aeruginosa and Escherichia coli. Res J Pharm Technol. 2018;11(7):2932–4.
[127] Tahir NAM, Abdollah MFB, Tamaldin N, Zin MRBM, Amiruddin H. Optimisation of graphene grown from solid waste using CVD method. Int J Adv Manuf Technol. 2020;106(1):211–8.
[128] Ruan G, Sun Z, Peng Z, Tour JM. Growth of graphene from food, insects, and waste. ACS Nano. 2011;5(9):7601–7.
[129] Akhavan O, Bijanzad K, Mirsepah A. Synthesis of graphene from natural and industrial carbonaceous wastes. RSC Adv. 2014;4(39):20441–48.
[130] Chandrasekar S, Viswanathan PK, Uthirakumar P, Montanari GC. Investigations on novel carbon quantum dots covered nanofluid insulation for medium voltage applications. J Electr Eng Technol. 2020;15(1):269–78.
[131] Muthoni J, Shimelis H, Melis R, Kinyua Z. Response of potato genotypes to bacterial wilt caused by Ralstonia solanacearum (Smith)(Yabuuchi et al.) in the tropical highlands. Am J Potato Res. 2014;91(2):215–32.
[132] Wang J, Wang CF, Chen S. Amphiphilic egg-derived carbon dots: rapid plasma fabrication, pyrolysis process, and multicolor printing patterns. Angew Chem Int Ed. 2012;51(37):9297–9301.
[133] Ke Y, Garg B, Ling Y-C. Waste chicken eggshell as low-cost precursor for efficient synthesis of nitrogen-doped fluorescent carbon nanodots and their multi-functional applications. RSC Adv. 2014;4(102):58329–36.
[134] Zhao Y, Zhang Y, Liu X, Kong H, Wang Y, Qin G, et al. Novel carbon quantum dots from egg yolk oil and their haemostatic effects. Sci Rep. 2017;7(1):1–8.
[135] Thangaraj B, Solomon PR, Ranganathan S. Synthesis of carbon quantum dots with special reference to biomass as a source-a review. Curr Pharm Des. 2019;25(13):1455–76.
[136] Thambiraj S, Shankaran R. Green synthesis of highly fluorescent carbon quantum dots from sugarcane bagasse pulp. Appl Surf Sci. 2016;390:435–43.
[137] Kang C, Huang Y, Yang H, Yan XF, Chen ZP. A review of carbon dots produced from biomass wastes. Nanomaterials. 2020;10(11):2316.
[138] Babbar N, Oberoi HS. Enzymes in value-addition of agricultural and agro-industrial residues. In: Brar SK, Verma M, editors. Enzymes in value-addition of wastes; 2014. p. 29–50.
[139] Zhuo C, Alves JO, Tenorio JA, Levendis YA. Synthesis of carbon nanomaterials through up-cycling agricultural and municipal solid wastes. Ind Eng Chem Res. 2012;51(7):2922–30.
[140] Jaguaribe EF, Medeiros LDL, Barreto MDCS, Araujo LPD. The performance of activated carbons from sugarcane bagasse, babassu, and coconut shells in removing residual chlorine. Braz J Chem Eng. 2005;22(1):41–7.
[141] Lakshmidevi R, Muthukumar K. Enzymatic saccharification and fermentation of paper and pulp industry effluent for biohydrogen production. Int J Hydrog Energy. 2010;35(8):3389–400.
[142] Du F, Zhang M, Li X, Li J, Jiang X, Li Z, et al. Economical and green synthesis of bagasse-derived fluorescent carbon dots for biomedical applications. Nanotechnology. 2014;25(31):315702.
[143] Arampatzidou AC, Deliyanni EA. Comparison of activation media and pyrolysis temperature for activated carbons development by pyrolysis of potato peels for effective adsorption of endocrine disruptor bisphenol-A. J Colloid Interface Sci. 2016;466:101–12.
[144] Xu-Cheng F, Xuan-Hua L, Jin J-Z, Zhang J, Wei G. Facile synthesis of bagasse waste derived carbon dots for trace mercury detection. Mater Res Exp. 2018;5(6):065044.
[145] Zhu J, Zhu F, Yue X, Chen P, Sun Y, Zhang L, et al. Waste utilization of synthetic carbon quantum dots based on tea and peanut shell. J Nanomater. 2019;2019(2019):1–7.
[146] Chunduri L, Kurdekar A, Patnaik S, Dev BV, Rattan TM, Kamisetti V. Carbon quantum dots from coconut husk: evaluation for antioxidant and cytotoxic activity. Mater Focus. 2016;5(1):55–61.
[147] Zhang J, Wang H, Xiao Y, Tang J, Liang C, Li F, et al. A simple approach for synthesizing of fluorescent carbon quantum dots from tofu wastewater. Nanoscale Res Lett. 2017;12(1):611.
[148] Wang K, Ji Q, Xu J, Li H, Zhang D, Liu X, et al. Highly sensitive and selective detection of amoxicillin using carbon quantum dots derived from beet. J Fluorescence. 2018;28(3):759–65.

[149] Cheng C, Shi Y, Li M, Xing M, Wu Q. Carbon quantum dots from carbonized walnut shells: structural evolution, fluorescence characteristics, and intracellular bioimaging. Mater Sci Eng: C. 2017;79:473–80.
[150] Li Z, Wang Q, Zhou Z, Zhao S, Zhong S, Xu L, et al. Green synthesis of carbon quantum dots from cQuantum Yield Measurements.orn stalk shell by hydrothermal approach in near-critical water and applications in detecting and bioimaging. Microchem J. 2021;166:106250.
[151] Zhang L, Wang Y, Liu W, Ni Y, Hou Q. Corncob residues as carbon quantum dots sources and their application in detection of metal ions. Ind Crop Products. 2019;133:18–25.
[152] Amin N, Afkhami A, Hosseinzadeh L, Madrakian T. Green and cost-effective synthesis of carbon dots from date kernel and their application as a novel switchable fluorescence probe for sensitive assay of Zoledronic acid drug in human serum and cellular imaging. Anal Chim Acta. 2018;1030:183–93.
[153] Yang R, Guo X, Jia L, Zhang Y, Zhao Z, Lonshakov F. Green preparation of carbon dots with mangosteen pulp for the selective detection of Fe^{3+} ions and cell imaging. Appl Surf Sci. 2017;423:426–32.
[154] Narayanan DP, Cherikallinmel SK, Sankaran S, Narayanan BN. Functionalized carbon dot adorned coconut shell char derived green catalysts for the rapid synthesis of amidoalkyl naphthols. J Colloid Interface Sci. 2018;520:70–80.
[155] Vasantharaj S, Sathiyavimal S, Senthilkumar P, LewisOscar F, Pugazhendhi A. Biosynthesis of iron oxide nanoparticles using leaf extract of Ruellia tuberosa: antimicrobial properties and their applications in photocatalytic degradation. J Photochem Photobiol B: Biol. 2019;192:74–82.
[156] Qi H, Teng M, Liu M, Liu S, Li J, Yu H, et al. Biomass-derived nitrogen-doped carbon quantum dots: highly selective fluorescent probe for detecting Fe^{3+} ions and tetracyclines. J Colloid Interface Sci. 2019;539:332–41.
[157] Ren X, Zhang F, Guo B, Gao N, Zhang X. Synthesis of N-doped micropore carbon quantum dots with high quantum yield and dual-wavelength photoluminescence emission from biomass for cellular imaging. Nanomaterials (Basel, Switz). 2019;9(4):495–508.
[158] Yuan M, Zhong R, Gao H, Li W, Yun X, Liu J, et al. One-step, green, and economic synthesis of water-soluble photoluminescent carbon dots by hydrothermal treatment of wheat straw, and their bio-applications in labeling, imaging, and sensing. Appl Surf Sci. 2015;355:1136–44.
[159] Huang C, Dong H, Su Y, Wu Y, Narron R, Yong Q. Synthesis of carbon quantum dot nanoparticles derived from byproducts in bio-refinery process for cell imaging and *in vivo* bioimaging. Nanomaterials (Basel). 2019;9(3):387.
[160] Vandarkuzhali SAA, Jeyalakshmi V, Sivaraman G, Singaravadivel S, Krishnamurthy KR, Viswanathan B. Highly fluorescent carbon dots from Pseudo-stem of banana plant: applications as nanosensor and bio-imaging agents. Sens Actuators B: Chem. 2017;252:894–900.
[161] Bandi R, Gangapuram BR, Dadigala R, Eslavath R, Singh SS, Guttena V. Facile and green synthesis of fluorescent carbon dots from onion waste and their potential applications as sensor and multicolour imaging agents. RSC Adv. 2016;6(34):28633–9.
[162] Gedda G, Lee C-Y, Lin Y-C, Wu H-F. Green synthesis of carbon dots from prawn shells for highly selective and sensitive detection of copper ions. Sens Actuators B: Chem. 2016;224:396–403.
[163] Zheng M, Li Y, Liu S, Wang W, Xie Z, Jing X. One-pot to synthesize multifunctional carbon dots for near infrared fluorescence imaging and photothermal cancer therapy. ACS Appl Mater Interfaces. 2016;8(36):23533–41.
[164] Chen K, Qing W, Hu W, Lu M, Wang Y, Liu X. On-off-on fluorescent carbon dots from waste tea: their properties, antioxidant and selective detection of CrO42–, Fe3+, ascorbic acid and L-cysteine in real samples. Spectrochim Acta Part A: Mol Biomole Spectrosc. 2019;213:228–34.
[165] Sachdev A, Gopinath P. Green synthesis of multifunctional carbon dots from coriander leaves and their potential application as antioxidants, sensors and bioimaging agents. Analyst. 2015;140(12):4260–9.
[166] Amer WA, Rehab AF, Abdelghafar ME, Torad NL, Atlam AS, Ayad MM. Green synthesis of carbon quantum dots from purslane leaves for the detection of formaldehyde using quartz crystal microbalance. Carbon. 2021;179:159–71.
[167] Yadav PK, Singh VK, Chandra S, Bano D, Kumar V, Talat M, et al. Green synthesis of fluorescent carbon quantum dots from azadirachta indica leaves and their peroxidase-mimetic activity for the detection of H2O2 and ascorbic acid in common fresh fruits. ACS Biomater Sci Eng. 2019;5(2):623–32.
[168] Arumugham T, Alagumuthu M, Amimodu RG, Munusamy S, Iyer SK. A sustainable synthesis of green carbon quantum dot (CQD) from Catharanthus roseus (white flowering plant) leaves and investigation of its dual fluorescence responsive behavior in multi-ion detection and biological applications. Sustain Mater Technol. 2020;23:e00138.
[169] Pourreza N, Ghomi M. Green synthesized carbon quantum dots from Prosopis juliflora leaves as a dual off-on fluorescence probe for sensing mercury (II) and chemet drug. Mater Sci Eng: C. 2019;98:887–96.
[170] Shivaji K, Mani S, Ponmurugan P, De Castro CS, Lloyd Davies M, Balasubramanian MG, et al. Green-synthesis-derived CdS quantum dots using tea leaf extract: antimicrobial, bioimaging, and therapeutic applications in lung cancer cells, cancer cells. ACS Appl Nano Mater. 2018;1(4):1683–93.
[171] Atchudan R, Jebakumar Immanuel Edison TN, Shanmugam M, Perumal S, Somanathan T, Lee YR. Sustainable synthesis of carbon quantum dots from banana peel waste using hydrothermal process for *in vivo* bioimaging. Phys E: Low-dimensional Syst Nanostruct. 2021;126:114417.
[172] Nguyen TN, Le PA, Phung VBT. Facile green synthesis of carbon quantum dots and biomass-derived activated carbon from banana peels: synthesis and investigation. Biomass Convers Biorefinery. 2020;1–10 doi: 10.1007/s13399-020-00839-2.
[173] Atchudan R, Edison TNJI, Perumal S, Muthuchamy N, Lee YR. Hydrophilic nitrogen-doped carbon dots from biowaste using dwarf banana peel for environmental and biological applications. Fuel. 2020;275:117821.
[174] Surendran P, Lakshmanan A, Vinitha G, Ramalingam G, Rameshkumar P. Facile preparation of high fluorescent carbon quantum dots from orange waste peels for nonlinear optical applications. Luminescence. 2020;35(2):196–202.

[175] Prasannan A, Imae T. One-pot synthesis of fluorescent carbon dots from orange waste peels. Ind Eng Chem Res. 2013;52(44):15673–78.
[176] Wang C, Shi H, Yang M, Yan Y, Liu E, Ji Z, et al. Facile synthesis of novel carbon quantum dots from biomass waste for highly sensitive detection of iron ions. Mater Res Bull. 2020;124:110730.
[177] Hu X, Li Y, Xu Y, Gan Z, Zou X, Shi J, et al. Green one-step synthesis of carbon quantum dots from orange peel for fluorescent detection of Escherichia coli in milk. Food Chem. 2021;339:127775.
[178] Zhou J, Sheng Z, Han H, Zou M, Li C. Facile synthesis of fluorescent carbon dots using watermelon peel as a carbon source. Mater Lett. 2012;66(1):222–4.
[179] Muktha H, Sharath R, Kottam N, Smrithi SP, Samrat K, Ankitha P. Green synthesis of carbon dots and evaluation of its pharmacological activities. BioNanoScience. 2020;10(3):731–44.
[180] Tyagi A, Tripathi KM, Singh N, Choudhary S, Gupta RK. Green synthesis of carbon quantum dots from lemon peel waste: applications in sensing and photocatalysis. RSC Adv. 2016;6(76):72423–32.
[181] Sun X, Liu Y, Niu N, Chen L. Synthesis of molecularly imprinted fluorescent probe based on biomass-derived carbon quantum dots for detection of mesotrione. Anal Bioanal Chem. 2019;411(21):5519–30.
[182] Jiao X-Y, Li L-S, Qin S, Zhang Y, Huang K, Xu L. The synthesis of fluorescent carbon dots from mango peel and their multiple applications. Colloids Surf A: Physicochem Eng Asp. 2019;577:306–14.
[183] Tian P, Tang L, Teng K, Lau S. Graphene quantum dots from chemistry to applications. Mater Today Chem. 2018;10:221–58.
[184] Abbas A, Mariana LT, Phan AN. Biomass-waste derived graphene quantum dots and their applications. Carbon. 2018;140:77–99.
[185] Iravani S, Varma RS. Green synthesis, biomedical and biotechnological applications of carbon and graphene quantum dots. A review. Environ Chem Lett. 2020;18(3):703–27.
[186] Robaiah M, Mahmud M, Salifairus M, Khusaimi Z, Azhan H, Abdullah S, et al. Synthesis and characterization of graphene from waste cooking palm oil at different deposition temperatures. AIP Conf Proc. AIP Publishing LLC; 2019. p. 020026
[187] Berktas I, Hezarkhani M, Haghighi Poudeh L, Saner Okan B. Recent developments in the synthesis of graphene and graphene-like structures from waste sources by recycling and upcycling technologies: a review. Graphene Technol. 2020;5(3):59–73.
[188] Wang Z, Yu J, Zhang X, Li N, Liu B, Li Y, et al. Large-scale and controllable synthesis of graphene quantum dots from rice husk biomass: a comprehensive utilization strategy. ACS Appl Mater Interfaces. 2016;8(2):1434–9.
[189] Li Y, Yu H, Han F, Wang M, Luo Y, Guo X. Biochanin A induces S phase arrest and apoptosis in lung cancer cells. BioMed Res Int. 2018;2018:1–12.
[190] Mahesh S, Lekshmi CL, Renuka KD. New paradigms for the synthesis of graphene quantum dots from sustainable bioresources. N J Chem. 2017;41(17):8706–10.
[191] Mahmoud ME, Fekry NA, Abdelfattah AM. A novel nanobiosorbent of functionalized graphene quantum dots from rice husk with barium hydroxide for microwave enhanced removal of lead (II) and lanthanum (III). Bioresour Technol. 2020;298:122514.
[192] Kumar YR, Deshmukh K, Sadasivuni KK, Pasha SKK. Graphene quantum dot based materials for sensing, bioimaging and energy storage applications: a review. RSC Adv. 2020;10(40):23861–98.
[193] Fathima N, Pradeep N, Balakrishnan J. Green synthesis of graphene quantum dots and the dual application of graphene quantum dots-decorated flexible MSM p-type ZnO device as UV photodetector and piezotronic generator. Bull Mater Sci. 2021;44(1):33.
[194] Chai X, He H, Fan H, Kang X, Song X. A hydrothermal-carbonization process for simultaneously production of sugars, graphene quantum dots, and porous carbon from sugarcane bagasse. Bioresour Technol. 2019;282:142–7.
[195] Tade RS, Patil PO. Green synthesis of fluorescent graphene quantum dots and its application in selective curcumin detection. Curr Appl Phys. 2020;20(11):1226–36.
[196] Suryawanshi A, Biswal M, Mhamane D, Gokhale R, Patil S, Guin D, et al. Large scale synthesis of graphene quantum dots (GQDs) from waste biomass and their use as an efficient and selective photoluminescence on–off–on probe for Ag+ ions. Nanoscale. 2014;6(20):11664–70.
[197] Roy P, Periasamy AP, Chuang C, Liou Y-R, Chen Y-F, Joly J, et al. Plant leaf-derived graphene quantum dots and applications for white LEDs. N J Chem. 2014;38(10):4946–51.
[198] Singh J, Kaur S, Lee J, Mehta A, Kumar S, Kim K-H, et al. Highly fluorescent carbon dots derived from Mangifera indica leaves for selective detection of metal ions. Sci Total Environ. 2020;720:137604.
[199] Kumawat MK, Thakur M, Gurung RB, Srivastava R. Graphene quantum dots from mangifera indica: application in near-infrared bioimaging and intracellular nanothermometry. ACS Sustain Chem Eng. 2017;5(2):1382–91.
[200] Khose RV, Chakraborty G, Bondarde MP, Wadekar PH, Ray AK, Some S. Red-fluorescent graphene quantum dots from guava leaf as a turn-off probe for sensing aqueous Hg (ii). N J Chem. 2021;45(10):4617–25.
[201] Yunus Ö, Şifa K, İ, Dehri, Ramazan E. Synthesis and characterization of graphene quantum dots from dried pine leaves. J Turkish Chem Soc Sect B: Chem Eng. 2019;2(2):109–20.
[202] Siddique S, Chow JC. Application of nanomaterials in biomedical imaging and cancer therapy. Nanomaterials. 2020;10(9):1700.
[203] Miguel MG, Lourenço JP, Faleiro ML. Superparamagnetic iron oxide nanoparticles and essential oils: a new tool for biological applications. Int J Mol Sci. 2020;21(18):6633.
[204] Khandanlou R, Bin Ahmad M, Shameli K, Kalantari K. Synthesis and characterization of rice straw/Fe_3O_4 nanocomposites by a quick precipitation method. Molecules. 2013;18(6):6597–607.
[205] Jabasingh SA, Belachew H, Yimam A. Iron oxide induced bagasse nanoparticles for the sequestration of Cr6+ ions from tannery effluent using a modified batch reactor. J Appl Polym Sci. 2018;135(36):46683.
[206] Njagi EC, Huang H, Stafford L, Genuino H, Galindo HM, Collins JB, et al. Biosynthesis of iron and silver nanoparticles at room temperature using aqueous sorghum bran extracts. Langmuir. 2011;27(1):264–71.

[207] Wang Z. Iron complex nanoparticles synthesized by Eucalyptus leaves. ACS Sustain Chem Eng. 2013;1(12):1551–4.
[208] Awwad AM, Salem NM. A green and facile approach for synthesis of magnetite nanoparticles. Nanosci Nanotechnol. 2012;2(6):208–13.
[209] Devi HS, Boda MA, Shah MA, Parveen S, Wani AH. Green synthesis of iron oxide nanoparticles using Platanus orientalis leaf extract for antifungal activity. Green Process Synth. 2019;8(1):38–45.
[210] Monalisa P, Nayak P. Ecofriendly green synthesis of iron nanoparticles from various plants and spices extract. Int J Plant, Anim Environ Sci. 2013;3(1):68–78.
[211] Machado S, Pinto SL, Grosso JP, Nouws HPA, Albergaria JT, Delerue-Matos C. Green production of zero-valent iron nanoparticles using tree leaf extracts. Sci Total Environ. 2013;445–446:1–8.
[212] Luo F, Chen Z, Megharaj M, Naidu R. Biomolecules in grape leaf extract involved in one-step synthesis of iron-based nanoparticles. RSC Adv. 2014;4(96):53467–74.
[213] Prasad AS. Iron oxide nanoparticles synthesized by controlled bio-precipitation using leaf extract of Garlic Vine (Mansoa alliacea). Mater Sci Semicond Process. 2016;53:79–83.
[214] Huang L, Weng X, Chen Z, Megharaj M, Naidu R. Synthesis of iron-based nanoparticles using oolong tea extract for the degradation of malachite green. Spectrochim Acta Part A: Mol Biomole Spectrosc. 2014;117:801–4.
[215] Wang Z, Fang C, Mallavarapu M. Characterization of iron–polyphenol complex nanoparticles synthesized by Sage (Salvia officinalis) leaves. Environ Technol Innov. 2015;4:92–7.
[216] Venkateswarlu S, Natesh Kumar B, Prasad CH, Venkateswarlu P, Jyothi NVV. Bio-inspired green synthesis of Fe_3O_4 spherical magnetic nanoparticles using Syzygium cumini seed extract. Phys B: Condens Matter. 2014;449:67–71.
[217] Prasad C, Gangadhara S, Venkateswarlu P. Bio-inspired green synthesis of Fe_3O_4 magnetic nanoparticles using watermelon rinds and their catalytic activity. Appl Nanosci. 2016;6(6):797–802.
[218] Yusefi M, Shameli K, Ali RR, Pang S-W, Teow S-Y. Evaluating anticancer activity of plant-mediated synthesized iron oxide nanoparticles using punica granatum fruit peel extract. J Mol Struct. 2020;1204:127539.
[219] Lopez-Tellez G, Balderas-Hernández P, Barrera-Díaz C, Vilchis-Nestor A, Roa-Morales G, Bilyeu B. Green method to form iron oxide nanorods in orange peels for chromium (VI) reduction. J Nanosci Nanotechnol. 2013;13(3):2354–61.
[220] Kumar B, Smita K, Galeas S, Sharma V, Guerrero VH, Debut A, et al. Characterization and application of biosynthesized iron oxide nanoparticles using Citrus paradisi peel: a sustainable approach. Inorg Chem Commun. 2020;119:108116.
[221] Ehrampoush MH, Miria M, Salmani MH, Mahvi AH. Cadmium removal from aqueous solution by green synthesis iron oxide nanoparticles with tangerine peel extract. J Environ Health Sci Eng. 2015;13(1):84.
[222] Chaudhary A, Kumar N, Kumar R, Salar RK. Antimicrobial activity of zinc oxide nanoparticles synthesized from Aloe vera peel extract. SN Appl Sci. 2019;1(1):136.
[223] Bishnoi S, Kumar A, Selvaraj R. Facile synthesis of magnetic iron oxide nanoparticles using inedible Cynometra ramiflora fruit extract waste and their photocatalytic degradation of methylene blue dye. Mater Res Bull. 2018;97:121–7.
[224] Lai Y, Wang L, Liu D, Chen Z, Lin C. TiO_2-based nanomaterials: design, synthesis, and applications. Hindawi: 2015.
[225] Sinha A, Khare SK. Mercury bioaccumulation and simultaneous nanoparticle synthesis by Enterobacter sp. cells. Bioresour Technol. 2011;102(5):4281–4.
[226] Allahverdiyev AM, Abamor ES, Bagirova M, Rafailovich M. Antimicrobial effects of TiO_2 and Ag_2O nanoparticles against drug-resistant bacteria and leishmania parasites. Future Microbiol. 2011;6(8):933–40.
[227] Roopan SM, Bharathi A, Prabhakarn A, Rahuman AA, Velayutham K, Rajakumar G, et al. Efficient phyto-synthesis and structural characterization of rutile TiO_2 nanoparticles using Annona squamosa peel extract. Spectrochim Acta Part A: Mol Biomole Spectrosc. 2012;98:86–90.
[228] Ajmal N, Saraswat K, Bakht MA, Riadi Y, Ahsan MJ, Noushad M. Cost-effective and eco-friendly synthesis of titanium dioxide (TiO_2) nanoparticles using fruit's peel agro-waste extracts: characterization, *in vitro* antibacterial, antioxidant activities. Green Chem Lett Rev. 2019;12(3):244–54.
[229] Ramimoghadam D, Bagheri S, Abd Hamid SB. Biotemplated synthesis of anatase titanium dioxide nanoparticles *via* lignocellulosic waste material. BioMed Res Int. 2014;2014:205636.
[230] Yang X, Ikehata K, Lerner R, Hu Y, Josyula K, Chang SX, et al. Agricultural wastes. Water Environ Res. 2010;82(10):1396–425.
[231] Marimuthu S, Rahuman AA, Jayaseelan C, Kirthi AV, Santhoshkumar T, Velayutham K, et al. Acaricidal activity of synthesized titanium dioxide nanoparticles using Calotropis gigantea against Rhipicephalus microplus and Haemaphysalis bispinosa. Asian Pac J Tropical Med. 2013;6(9):682–8.
[232] Sethy NK, Arif Z, Mishra PK, Kumar P. Green synthesis of TiO_2 nanoparticles from Syzygium cumini extract for photo-catalytic removal of lead (Pb) in explosive industrial wastewater. Green Process Synth. 2020;9(1):171–81.
[233] Kalyanasundaram S, Prakash MJ. Biosynthesis and characterization of titanium dioxide nanoparticles using pithecellobium dulce and lagenaria siceraria aqueous leaf extract and screening their free radical scavenging and antibacterial properties. ILCPA. 2015;50:80–95.
[234] Rao KG, Ashok C, Rao KV, Chakra CS, Rajendar V. Synthesis of TiO_2 nanoparticles from orange fruit waste. Synthesis. 2015;2(1):1.
[235] Amanulla AM, Sundaram R. Green synthesis of TiO_2 nanoparticles using orange peel extract for antibacterial, cytotoxicity and humidity sensor applications. Mater Today: Proc. 2019;8:323–31.
[236] Rueda D, Arias V, Zhang Y, Cabot A, Agudelo AC, Cadavid D. Low-cost tangerine peel waste mediated production of titanium dioxide nanocrystals: synthesis and characterization. Environ Nanotechnol, Monit Manag. 2020;13:100285.
[237] Masoudian N, Rajabi M, Ghaedi M. Titanium oxide nanoparticles loaded onto activated carbon prepared from bio-waste watermelon rind for the efficient ultrasonic-assisted

adsorption of congo red and phenol red dyes from wastewaters. Polyhedron. 2019;173:114105.
[238] Samaddar P, Ok YS, Kim K-H, Kwon EE, Tsang DCW. Synthesis of nanomaterials from various wastes and their new age applications. J Clean Prod. 2018;197:1190–209.
[239] Baum MK, Shor-Posner G, Campa A. Zinc status in human immunodeficiency virus infection. J Nutr. 2000;130(5):1421S–3S.
[240] Siddiqi KS, Ur Rahman A, Husen A. Properties of zinc oxide nanoparticles and their activity against microbes. Nanoscale Res Lett. 2018;13(1):1–13.
[241] Tribot A, Amer G, Abdou Alio M, de Baynast H, Delattre C, Pons A, et al. Wood-lignin: supply, extraction processes and use as bio-based material. Eur Polym J. 2019;112:228–40.
[242] Alomair NA, Mohamed HH. Green synthesis of ZnO hollow microspheres and ZnO/rGO nanocomposite using red rice husk extract and their photocatalytic performance. Mater Res Exp. 2018;5(9):095012.
[243] Kumar H, Gehlaut AK, Gaur A, Park J-W, Maken S. Development of zinc-loaded nanoparticle hydrogel made from sugarcane bagasse for special medical application. J Mater Cycles Waste Manag. 2020;22(6):1723–33.
[244] Umar H, Kavaz D, Rizaner N. Biosynthesis of zinc oxide nanoparticles using Albizia lebbeck stem bark, and evaluation of its antimicrobial, antioxidant, and cytotoxic activities on human breast cancer cell lines. Int J Nanomed. 2019;14:87–100.
[245] Alharthi FA, Al-Zaqri N, El Marghany A, Alghamdi AA, Alorabi AQ, Baghdadi N, et al. Synthesis of nanocauliflower ZnO photocatalyst by potato waste and its photocatalytic efficiency against dye. J Mater Sci: Mater Electron. 2020;31(14):11538–47.
[246] Jha AK, Prasad K. Synthesis of ZnO nanoparticles from goat slaughter waste for environmental protection. Int J Curr Eng Technol. 2016;6(1):147–51.
[247] Agarwal H, Venkat Kumar S, Rajeshkumar S. A review on green synthesis of zinc oxide nanoparticles – An eco-friendly approach. Res-Effic Technol. 2017;3(4):406–13.
[248] Chikkanna MM, Neelagund SE, Rajashekarappa KK. Green synthesis of zinc oxide nanoparticles (ZnO NPs) and their biological activity. SN Appl Sci. 2019;1(1):1–10.
[249] Ali A, Phull A-R, Zia M. Elemental zinc to zinc nanoparticles: is ZnO NPs crucial for life? Synthesis, toxicological, and environmental concerns. Nanotechnol Rev. 2018;7(5):413–41.
[250] Sabir S, Arshad M, Chaudhari SK. Zinc oxide nanoparticles for revolutionizing agriculture: synthesis and applications. Sci World J. 2014;2014:925494.
[251] Surendra TV, Roopan SM, Al-Dhabi NA, Arasu MV, Sarkar G, Suthindhiran K. Vegetable peel waste for the production of ZnO nanoparticles and its toxicological efficiency, antifungal, hemolytic, and antibacterial activities. Nanoscale Res Lett. 2016;11(1):546.
[252] Rahaiee S, Ranjbar M, Azizi H, Govahi M, Zare M. Green synthesis, characterization, and biological activities of saffron leaf extract-mediated zinc oxide nanoparticles: a sustainable approach to reuse an agricultural waste. Appl Organomet Chem. 2020;34(8):e5705.
[253] Hassan SS, El Azab WI, Ali HR, Mansour MS. Green synthesis and characterization of ZnO nanoparticles for photocatalytic degradation of anthracene. Adv Nat Sci: Nanosci Nanotechnol. 2015;6(4):045012.
[254] Ali K, Dwivedi S, Azam A, Saquib Q, Al-Said MS, Alkhedhairy AA, et al. Aloe vera extract functionalized zinc oxide nanoparticles as nanoantibiotics against multi-drug resistant clinical bacterial isolates. J Colloid Interface Sci. 2016;472:145–56.
[255] Vanathi P, Rajiv P, Narendhran S, Rajeshwari S, Rahman PKSM, Venckatesh R. Biosynthesis and characterization of phyto mediated zinc oxide nanoparticles: a green chemistry approach. Mater Lett. 2014;134:13–5.
[256] Ramesh M, Anbuvannan M, Viruthagiri G. Green synthesis of ZnO nanoparticles using Solanum nigrum leaf extract and their antibacterial activity. Spectrochim Acta Part A, Mol Biomol Spectrosc. 2015;136(Pt B):864–70.
[257] Raliya R, Tarafdar JC. ZnO nanoparticle biosynthesis and its effect on phosphorous-mobilizing enzyme secretion and gum contents in clusterbean (Cyamopsis tetragonoloba L.). Agric Res. 2013;2(1):48–57.
[258] Nava OJ, Soto-Robles CA, Gómez-Gutiérrez CM, Vilchis-Nestor AR, Castro-Beltrán A, Olivas A, et al. Fruit peel extract mediated green synthesis of zinc oxide nanoparticles. J Mol Struct. 2017;1147:1–6.
[259] Hamed O. Fabrication of zinc oxide nanoparticles and films by banana peel extract food waste and investigation on their antioxidant and antibacterial activities. American University in Cairo Scholarly Communications; 2018. http://dar.aucegypt.edu/handle/10526/5314.
[260] Ruangtong J, T-Thienprasert J, T-Thienprasert NP. Green synthesized ZnO nanosheets from banana peel extract possess anti-bacterial activity and anti-cancer activity. Mater Today Commun. 2020;24:101224.
[261] Abdol Aziz R, Abd Karim SF, Rosli NA. The effect of ph on zinc oxide nanoparticles characteristics synthesized from banana peel extract. Key Eng Mater, Trans Tech Publ. 2019;797:271–9.
[262] Abdullah FH, Abu Bakar NHH, Abu Bakar M. Low temperature biosynthesis of crystalline zinc oxide nanoparticles from Musa acuminata peel extract for visible-light degradation of methylene blue. Optik. 2020;206:164279.
[263] Thi TUD, Nguyen TT, Thi YD, Thi KHT, Phan BT, Pham KN. Green synthesis of ZnO nanoparticles using orange fruit peel extract for antibacterial activities. RSC Adv. 2020;10(40):23899–907.
[264] Luque PA, Soto-Robles CA, Nava O, Gomez-Gutierrez CM, Castro-Beltran A, Garrafa-Galvez HE, et al. Green synthesis of zinc oxide nanoparticles using Citrus sinensis extract. J Mater Sci: Mater Electron. 2018;29(12):9764–70.
[265] Krishnan RA, Mhatre O, Sheth J, Prabhu S, Jain R, Dandekar P. Synthesis of zinc oxide nanostructures using orange peel oil for fabricating chitosan-zinc oxide composite films and their antibacterial activity. J Polym Res. 2020;27(8):206.
[266] Gao Y, Xu D, Ren D, Zeng K, Wu X. Green synthesis of zinc oxide nanoparticles using Citrus sinensis peel extract and application to strawberry preservation: a comparison study. LWT. 2020;126:109297.
[267] Ibrahim TA, Salman TA, Abbas SA-R. Biosynthesis of zinc oxide nanoparticles using orange peels extract for biological applications. Plant Arch. 2021;21(1):329–32.

[268] Mohamad Sukri SNA, Shameli K, Mei-Theng Wong M, Teow S-Y, Chew J, Ismail NA. Cytotoxicity and antibacterial activities of plant-mediated synthesized zinc oxide (ZnO) nanoparticles using Punica granatum (pomegranate) fruit peels extract. J Mol Struct. 2019;1189:57–65.
[269] Husain WM, Araak JK, Ibrahim OM. Green synthesis of zinc oxide nanoparticles from (Punica granatum L) pomegranate aqueous peel extract. Iraqi J Veter Med. 2019;43(2):6–14.
[270] Kokabi M, Ebrahimi SN. Polyphenol enriched extract of pomegranate peel; a novel precursor for the biosynthesis of zinc oxide nanoparticles and application in sunscreens. Pharm Sci. 2020;27(1):102–10.
[271] Rashtbari Y, Hazrati S, Azari A, Afshin S, Fazlzadeh M, Vosoughi M. A novel, eco-friendly and green synthesis of PPAC-ZnO and PPAC-nZVI nanocomposite using pomegranate peel: cephalexin adsorption experiments, mechanisms, isotherms and kinetics. Adv Powder Technol. 2020;31(4):1612–23.
[272] Yuvakkumar R, Suresh J, Nathanael AJ, Sundrarajan M, Hong SI. Novel green synthetic strategy to prepare ZnO nanocrystals using rambutan (Nephelium lappaceum L.) peel extract and its antibacterial applications. Mater Sci Eng C, Mater Biol Appl. 2014;41:17–27.
[273] Hassan Basri H, Talib RA, Sukor R, Othman SH, Ariffin H. Effect of synthesis temperature on the size of ZnO nanoparticles derived from pineapple peel extract and antibacterial activity of ZnO–starch nanocomposite films. Nanomaterials. 2020;10(6):1061.
[274] Raha S, Mallick R, Basak S, Duttaroy AK. Is copper beneficial for COVID-19 patients? Med Hypoth. 2020;142:109814.
[275] Krishnan B, Mahalingam S. Improved surface morphology of silver/copper oxide/bentonite nanocomposite using aliphatic ammonium based ionic liquid for enhanced biological activities. J Mol Liq. 2017;241:1044–58.
[276] Verma N, Kumar N. Synthesis and biomedical applications of copper oxide nanoparticles: an expanding horizon. ACS Biomater Sci Eng. 2019;5(3):1170–88.
[277] Chang M-H, Liu H-S, Tai CY. Preparation of copper oxide nanoparticles and its application in nanofluid. Powder Technol. 2011;207(1–3):378–86.
[278] Devi HS, Singh TD. Synthesis of copper oxide nanoparticles by a novel method and its application in the degradation of methyl orange. Adv Electron Electr Eng. 2014;4(1):83–8.
[279] Wang A, Chen L, Xu F, Yan Z. In situ synthesis of copper nanoparticles within ionic liquid-in-vegetable oil microemulsions and their direct use as high efficient nanolubricants. RSC Adv. 2014;4(85):45251–7.
[280] Phang Y-K, Aminuzzaman M, Akhtaruzzaman M, Muhammad G, Ogawa S, Watanabe A, et al. Green synthesis and characterization of cuo nanoparticles derived from papaya peel extract for the photocatalytic degradation of palm oil mill effluent (POME). Sustainability. 2021;13(2):796.
[281] Sarno M, Spina D, Senatore A. One-step nanohybrid synthesis in waste cooking oil, for direct lower environmental impact and stable lubricant formulation. Tribol Int. 2019;135:355–67.
[282] Kumar H, Gehlaut AK, Gupta H, Gaur A, Park JW. Development of copper loaded nanoparticles hydrogel made from waste biomass (Sugarcane Bagasse) for special medical application. Key Eng Mater, Trans Tech Publ. 2020;847:102–7.
[283] Yadav S, Chauhan M, Mathur D, Jain A, Malhotra P. Sugarcane bagasse-facilitated benign synthesis of Cu2O nanoparticles and its role in photocatalytic degradation of toxic dyes: a trash to treasure approach. Environ, Develop Sustain. 2021;23(2):2071–91.
[284] Abtahi Froushani SM, Zamani A, Abbasi A. Cytotoxic effects of combined walnut shell-extracted copper oxide: nanoparticles and hydroalcoholic extracts of aloe vera against human leukemic cell line. Zahedan J Res Med Sci. 2021;23(1):e94572.
[285] Mehdizadeh T, Zamani A, Abtahi Froushani SM. Preparation of Cu nanoparticles fixed on cellulosic walnut shell material and investigation of its antibacterial, antioxidant and anticancer effects. Heliyon. 2020;6(3):e03528.
[286] Mohammadi SZ, Lashkari B, Khosravan A. Green synthesis of Co_3O_4 nanoparticles by using walnut green skin extract as a reducing agent by using response surface methodology. Surf Interfaces. 2021;23:100970.
[287] Nwanya AC, Razanamahandry LC, Bashir AKH, Ikpo CO, Nwanya SC, Botha S, et al. Industrial textile effluent treatment and antibacterial effectiveness of Zea mays L. Dry husk mediated bio-synthesized copper oxide nanoparticles. J Hazard Mater. 2019;375:281–9.
[288] Mahmoud NMR, Mohamed HI, Ahmed SB, Akhtar S. Efficient biosynthesis of CuO nanoparticles with potential cytotoxic activity. Chem Pap. 2020;74(9):2825–35.
[289] Vidovix TB, Quesada HB, Bergamasco R, Vieira MF, Vieira AMS. Adsorption of Safranin-O dye by copper oxide nanoparticles synthesized from Punica granatum leaf extract. Environ Technol. 2021;1–40. doi: 10.1080/09593330.2021.1914180.
[290] Kumar B, Smita K, Debut A, Cumbal L. Andean Sacha Inchi (Plukenetia Volubilis L.) leaf-mediated synthesis of Cu_2O nanoparticles: a low-cost approach. BioEng. 2020;7(2):54.
[291] Gupta V, Chandra N. Biosynthesis and antibacterial activity of metal oxide nanoparticles using Brassica oleracea subsp. botrytis (L.) leaves, an agricultural waste. Proc Natl Acad Sci, India Sect B: Biol Sci. 2020;90(5):1093–100.
[292] Akintelu SA, Folorunso AS, Folorunso FA, Oyebamiji AK. Green synthesis of copper oxide nanoparticles for biomedical application and environmental remediation. Heliyon. 2020;6(7):e04508.
[293] Asemani M, Anarjan N. Green synthesis of copper oxide nanoparticles using Juglans regia leaf extract and assessment of their physico-chemical and biological properties. Green Process Synth. 2019;8(1):557–67.
[294] Bhavyasree PG, Xavier TS. Green synthesis of copper oxide/carbon nanocomposites using the leaf extract of Adhatoda vasica Nees, their characterization and antimicrobial activity. Heliyon. 2020;6(2):e03323.
[295] Ginting B, Maulana I, Karnila I. Biosynthesis copper nanoparticles using blumea balsamifera leaf extracts: characterization of its antioxidant and cytotoxicity activities. Surf Interfaces. 2020;21:100799.
[296] Awwad A, Amer M. Biosynthesis of copper oxide nanoparticles using Ailanthus altissima leaf extract and antibacterial activity. Chem Int. 2020;6:210–17.

[297] Narasaiah P, Mandal BK, Sarada N. Biosynthesis of copper oxide nanoparticles from Drypetes sepiaria leaf extract and their catalytic activity to dye degradation. IOP Conf Ser Mater Sci Eng. IOP Publishing; 2017. p. 022012
[298] EL-Moslamy H, Shokry H, Rezk H, Abdel-Fattah R. Bioprocess strategies and characterization of anti-multidrug resistant human pathogens copper/copper oxide nanoparticles from citrus peel waste extracts. J Nanomater Mol Nanotechnol. 2017;13:21–3.
[299] Tshireletso P, Ateba CN. Spectroscopic and antibacterial properties of CuONPs from orange, lemon and tangerine peel extracts: potential for combating bacterial resistance. Molecules. 2021;26(3):586.
[300] Aminuzzaman M, Ying LP, Goh W-S, Watanabe A. Green synthesis of zinc oxide nanoparticles using aqueous extract of Garcinia mangostana fruit pericarp and their photocatalytic activity. Bull Mater Sci. 2018;41(2):1–10.
[301] Siddiqui VU, Ansari A, Chauhan R, Siddiqi WA. Green synthesis of copper oxide (CuO) nanoparticles by Punica granatum peel extract. Mater Today: Proc. 2021;36:751–5.
[302] Ghidan AY, Al-Antary TM, Awwad AM. Green synthesis of copper oxide nanoparticles using Punica granatum peels extract: effect on green peach Aphid. Environ Nanotechnol, Monit Manag. 2016;6:95–8.
[303] Aminuzzaman M, Kei LM, Liang WH. Green synthesis of copper oxide (CuO) nanoparticles using banana peel extract and their photocatalytic activities. AIP Conf Proc. AIP Publishing LLC; 2017. p. 020016
[304] Dong S-A, Zhou S-P. Photochemical synthesis of colloidal gold nanoparticles. Mater Sci Eng: B. 2007;140(3):153–9.
[305] Shang Y, Min C, Hu J, Wang T, Liu H, Hu Y. Synthesis of gold nanoparticles by reduction of HAuCl4 under UV irradiation. Solid State Sci. 2013;15:17–23.
[306] Paul B, Bhuyan B, Purkayastha DD, Dhar SS. Photocatalytic and antibacterial activities of gold and silver nanoparticles synthesized using biomass of Parkia roxburghii leaf. J Photochem Photobiol B: Biol. 2016;154:1–7.
[307] Ahmed S, Ikram S. Biosynthesis of gold nanoparticles: a green approach. J Photochem Photobiol B: Biol. 2016;161:141–53.
[308] Kumari MM, Philip D. Facile one-pot synthesis of gold and silver nanocatalysts using edible coconut oil. Spectrochim Acta Part A: Mol Biomole Spectrosc. 2013;111:154–60.
[309] Sadrolhosseini AR, Abdul Rashid S, Zakaria A. Synthesis of gold nanoparticles dispersed in palm oil using laser ablation technique. J Nanomater. 2017;2017:1–5.
[310] Armendariz V, Herrera I, Jose-yacaman M, Troiani H, Santiago P, Gardea-Torresdey JL. Size controlled gold nanoparticle formation by Avena sativa biomass: use of plants in nanobiotechnology. J Nanopart Res. 2004;6(4):377–82.
[311] Kanchi S, Kumar G, Lo A-Y, Tseng C-M, Chen S-K, Lin C-Y, et al. Exploitation of de-oiled jatropha waste for gold nanoparticles synthesis: a green approach. Arab J Chem. 2018;11(2):247–55.
[312] Bhau B, Ghosh S, Puri S, Borah B, Sarmah D, Khan R. Green synthesis of gold nanoparticles from the leaf extract of Nepenthes khasiana and antimicrobial assay. Adv Mater Lett. 2015;6(1):55–8.
[313] Zeng S, Du L, Huang M, Feng J-X. Biological synthesis of Au nanoparticles using liquefied mash of cassava starch and their functionalization for enhanced hydrolysis of xylan by recombinant xylanase. Bioprocess Biosyst Eng. 2016;39(5):785–92.
[314] Dang H, Fawcett D, Poinern GEJ. Green synthesis of gold nanoparticles from waste macadamia nut shells and their antimicrobial activity against Escherichia coli and Staphylococcus epidermis. Int J Res Med Sci. 2019;7(4):1171.
[315] Vo T-T, Nguyen TT-N, Huynh TT-T, Vo TT-T, Nguyen TT-N, Nguyen D-T, et al. Biosynthesis of silver and gold nanoparticles using aqueous extract from Crinum latifolium leaf and their applications forward antibacterial effect and wastewater treatment. J Nanomater. 2019;140:420–33.
[316] Castillo-Henríquez L, Alfaro-Aguilar K, Ugalde-Álvarez J, Vega-Fernández L, Montes de Oca-Vásquez G, Vega-Baudrit JR. Green synthesis of gold and silver nanoparticles from plant extracts and their possible applications as antimicrobial agents in the agricultural area. Nanomaterials. 2020;10(9):1763.
[317] Boomi P, Ganesan R, Poorani G, Prabu HG, Ravikumar S, Jeyakanthan J. Biological synergy of greener gold nanoparticles by using Coleus aromaticus leaf extract. Mater Sci Eng: C. 2019;99:202–10.
[318] Rajan A, Rajan AR, Philip D. Elettaria cardamomum seed mediated rapid synthesis of gold nanoparticles and its biological activities. OpenNano. 2017;2:1–8.
[319] Jayaseelan C, Ramkumar R, Rahuman AA, Perumal P. Green synthesis of gold nanoparticles using seed aqueous extract of Abelmoschus esculentus and its antifungal activity. Ind Crop Products. 2013;45:423–9.
[320] Vijayakumar S. Eco-friendly synthesis of gold nanoparticles using fruit extracts and *in vitro* anticancer studies. J Saudi Chem Soc. 2019;23(6):753–61.
[321] Kumar H, Bhardwaj K, Dhanjal DS, Nepovimova E, Şen F, Regassa H, et al. Fruit extract mediated green synthesis of metallic nanoparticles: a new avenue in pomology applications. Int J Mol Sci. 2020;21(22):8458.
[322] Devadiga A, Shetty KV, Saidutta MB. Timber industry waste-teak (Tectona grandis Linn.) leaf extract mediated synthesis of antibacterial silver nanoparticles. Int Nano Lett. 2015;5(4):205–14.
[323] Adelere IA, Lateef A. A novel approach to the green synthesis of metallic nanoparticles: the use of agro-wastes, enzymes, and pigments. Nanotechnol Rev. 2016;5(6):567–87.
[324] Castro L, Blázquez ML, González F, Muñoz JA, Ballester A. Gold, silver and platinum nanoparticles biosynthesized using orange peel extract. Adv Mater Res. 2013;825:556–9.
[325] Ahmad N, Sharma S, Rai R. Rapid green synthesis of silver and gold nanoparticles using peels of Punica granatum. Adv Mater Lett. 2012;3(5):376–80.
[326] Patel M, Siddiqi NJ, Sharma P, Alhomida AS, Khan HA. Reproductive toxicity of pomegranate peel extract synthesized gold nanoparticles: a multigeneration study in C. elegans. J Nanomater. 2019;2019:1–7.
[327] Manna K, Mishra S, Saha M, Mahapatra S, Saha C, Yenge G, et al. Amelioration of diabetic nephropathy using pomegranate peel extract-stabilized gold nanoparticles: assessment of NF-κB and Nrf2 signaling system. Int J Nanomed. 2019;14:1753–77.

[328] Bankar A, Joshi B, Ravi Kumar A, Zinjarde S. Banana peel extract mediated synthesis of gold nanoparticles. Colloids Surf B: Biointerfaces. 2010;80(1):45–50.
[329] Deokar GK, Ingale AG. Green synthesis of gold nanoparticles (Elixir of Life) from banana fruit waste extract – an efficient multifunctional agent. RSC Adv. 2016;6(78):74620–9.
[330] Adebayo AE, Oke AM, Lateef A, Oyatokun AA, Abisoye OD, Adiji IP, et al. Biosynthesis of silver, gold and silver–gold alloy nanoparticles using Persea americana fruit peel aqueous extract for their biomedical properties. Nanotechnol Environ Eng. 2019;4(1):13.
[331] Xin Lee K, Shameli K, Miyake M, Kuwano N, Bt Ahmad Khairudin NB, Bt Mohamad SE, et al. Green synthesis of gold nanoparticles using aqueous extract of garcinia mangostana fruit peels. J Nanomater. 2016;2016:8489094.
[332] Yang B, Qi F, Tan J, Yu T, Qu C. Study of green synthesis of ultrasmall gold nanoparticles using citrus sinensis peel. Appl Sci. 2019;9(12):2423.
[333] Yuan CG, Huo C, Gui B, Cao WP. Green synthesis of gold nanoparticles using Citrus maxima peel extract and their catalytic/antibacterial activities. IET Nanobiotechnol. 2017;11(5):523–30.
[334] Chums-ard W, Fawcett D, Fung CC, Poinern GEJ. Biogenic synthesis of gold nanoparticles from waste watermelon and their antibacterial activity against Escherichia coli and Staphylococcus epidermidis. Int J Res Med Sci. 2019;7(7):2499–505.
[335] Patra JK, Baek K-H. Novel green synthesis of gold nanoparticles using Citrullus lanatus rind and investigation of proteasome inhibitory activity, antibacterial, and antioxidant potential. Int J Nanomed. 2015;10:7253.
[336] Om Prakash M, Raghavendra G, Ojha S, Panchal M. Characterization of porous activated carbon prepared from arhar stalks by single step chemical activation method. Mater Today: Proc. 2021;39:1476–81.
[337] Pooja D, Singh L, Thakur A, Kumar P. Green synthesis of glowing carbon dots from Carica papaya waste pulp and their application as a label-freechemo probe for chromium detection in water. Sens Actuators B: Chem. 2019;283:363–72.
[338] Wang W, Wang Z, Liu J, Peng Y, Yu X, Wang W, et al. One-pot facile synthesis of graphene quantum dots from rice husks for Fe^{3+} sensing. Ind Eng Chem Res. 2018;57(28):9144–50.
[339] Gowri M, Latha N, Rajan M. Copper oxide nanoparticles synthesized using eupatorium odoratum, acanthospermum hispidum leaf extracts, and its antibacterial effects against pathogens: a comparative study. BioNanoScience. 2019;9(3):545–52.
[340] Karunakaran G, Jagathambal M, Kumar GS, Kolesnikov E. Hylotelephium telephium flower extract-mediated biosynthesis of CuO and ZnO nanoparticles with promising antioxidant and antibacterial properties for healthcare applications. JOM. 2020;72(3):1264–72.
[341] Moon SA, Salunke BK, Saha P, Deshmukh AR, Kim BS. Comparison of dye degradation potential of biosynthesized copper oxide, manganese dioxide, and silver nanoparticles using Kalopanax pictus plant extract. Korean J Chem Eng. 2018;35(3):702–8.
[342] Nagaraj E, Karuppannan K, Shanmugam P, Venugopal S. Exploration of bio-synthesized copper oxide nanoparticles using pterolobium hexapetalum leaf extract by photocatalytic activity and biological evaluations. J Clust Sci. 2019;30(4):1157–68.
[343] Bhatnagar A, Sillanpää M, Witek-Krowiak A. Agricultural waste peels as versatile biomass for water purification – a review. Chem Eng J. 2015;270:244–71.
[344] Kyzas GZ, Deliyanni EA. Modified activated carbons from potato peels as green environmental-friendly adsorbents for the treatment of pharmaceutical effluents. Chem Eng Res Des. 2015;97:135–44.
[345] Torres JA, Nogueira FGE, Silva MC, Lopes JH, Tavares TS, Ramalho TC, et al. Novel eco-friendly biocatalyst: soybean peroxidase immobilized onto activated carbon obtained from agricultural waste. RSC Adv. 2017;7(27):16460–6.
[346] Marzec M, Tryba B, Kaleńczuk RJ, Morawski AW. Poly (ethylene terephthalate) as a source for activated carbon. Polym Adv Technol. 1999;10(10):588–95.
[347] Bubanale S, Shivashankar M. History, method of production, structure and applications of activated carbon. Int J Eng Tech Res. 2017;6:495–8.
[348] Kemp K, Griffiths J, Campbell S, Lovell K. An exploration of the follow-up up needs of patients with inflammatory bowel disease. J Crohn's Colitis. 2013;7(9):e386–95.
[349] Tang W, Zhang Y, Zhong Y, Shen T, Wang X, Xia X, et al. Natural biomass-derived carbons for electrochemical energy storage. Mater Res Bull. 2017;88:234–41.
[350] Ganan J, Gonzalez J, Gonzalez-Garcia C, Ramiro A, Sabio E, Roman S. Air-activated carbons from almond tree pruning: preparation and characterization. Appl Surf Sci. 2006;252(17):5988–92.
[351] Ould-Idriss A, Stitou M, Cuerda-Correa E, Fernández-González C, Macías-García A, Alexandre-Franco M, et al. Preparation of activated carbons from olive-tree wood revisited. I. Chemical activation with H_3PO_4. Fuel Process Technol. 2011;92(2):261–5.
[352] Esfandiari A, Kaghazchi T, Soleimani M. Preparation and evaluation of activated carbons obtained by physical activation of polyethyleneterephthalate (PET) wastes. J Taiwan Inst Chem Eng. 2012;43(4):631–7.
[353] Bazargan A, Hui CW, McKay G. Porous carbons from plastic waste. Porous carbons–hyperbranched polymers–polymer solvation; 2013. p. 1–25.
[354] Mazlan MAF, Uemura Y, Yusup S, Elhassan F, Uddin A, Hiwada A, et al. Activated carbon from rubber wood sawdust by carbon dioxide activation. Proc Eng. 2016;148:530–7.
[355] Matos J, Nahas C, Rojas L, Rosales M. Synthesis and characterization of activated carbon from sawdust of Algarroba wood. 1. Physical activation and pyrolysis. J Hazard Mater. 2011;196:360–9.
[356] Li W-H, Yue Q-Y, Gao B-Y, Wang X-J, Qi Y-F, Zhao Y-Q, et al. Preparation of sludge-based activated carbon made from paper mill sewage sludge by steam activation for dye wastewater treatment. Desalination. 2011;278(1–3):179–85.
[357] Panadare D. Applications of waste cooking oil other than biodiesel: a review. Iran J Chem Eng (IJChE). 2015;12(3):55–76.
[358] Yao M, Wang H, Zheng Z, Yue Y. Experimental study of n-butanol additive and multi-injection on HD diesel engine performance and emissions. Fuel. 2010;89(9):2191–201.

[359] Gu KX, Li ZQ, Wang JJ, Zhou Y, Zhang H, Zhao B, et al. The effect of cryogenic treatment on the microstructure and properties of Ti-6Al-4V titanium alloy. Materials science forum. Trans Tech Publication; 2013. p. 899–903.
[360] Pinilla J, De Llobet S, Moliner R, Suelves I. Ni-Co bimetallic catalysts for the simultaneous production of carbon nanofibres and syngas through biogas decomposition. Appl Catal B: Environ. 2017;200:255–64.
[361] Ghosh S, Chynoweth DP, Packer ML, Sedzielarz FS, Roess AC, Van Ryzin EM. Anaerobic processes. J Water Pollut Control Fed. 1978;50(10):2388–410.
[362] Suriani A, Dalila A, Mohamed A, Isa I, Kamari A, Hashim N, et al. Synthesis of carbon nanofibres from waste chicken fat for field electron emission applications. Mater Res Bull. 2015;70:524–9.
[363] Barranco V, Lillo-Rodenas M, Linares-Solano A, Oya A, Pico F, Ibañez J, et al. Amorphous carbon nanofibers and their activated carbon nanofibers as supercapacitor electrodes. J Phys Chem C. 2010;114(22):10302–7.
[364] Alptekin E, Canakci M. Optimization of transesterification for methyl ester production from chicken fat. Fuel. 2011;90(8):2630–8.
[365] Nikolaev A, Peshnev B, Ismail A. Preparation of carbon nanofibers from electrocracking gas on an iron oxide catalyst. Solid Fuel Chem. 2009;43(1):35–7.
[366] Alves JO, Zhuo C, Levendis YA, Tenório JAS. Síntese de nanotubos de carbono a partir do bagaço da cana-de-açúcar. Rem: Rev Esc de Minas. 2012;65(3):313–8.
[367] Qu J, Cong Q, Luo C, Yuan X. Adsorption and photocatalytic degradation of bisphenol A by low-cost carbon nanotubes synthesized using fallen leaves of poplar. Rsc Adv. 2013;3(3):961–5.
[368] Suriani A, Dalila A, Mohamed A, Mamat M, Salina M, Rosmi M, et al. Vertically aligned carbon nanotubes synthesized from waste chicken fat. Mater Lett. 2013;101:61–4.
[369] Lotfy VF, Fathy NA, Basta AH. Novel approach for synthesizing different shapes of carbon nanotubes from rice straw residue. J Environ Chem Eng. 2018;6(5):6263–74.
[370] Singh R, Volli V, Lohani L, Purkait MK. Synthesis of carbon nanotubes from industrial wastes following alkali activation and film casting method. Waste Biomass Valoriz. 2020;11(9):4957–66.
[371] Bernd MGS, Bragança SR, Heck N, da Silva Filho LC. Synthesis of carbon nanostructures by the pyrolysis of wood sawdust in a tubular reactor. J Mater Res Technol. 2017;6(2):171–7.
[372] Zhao J-R, Hu J, Li J-F, Chen P. N-doped carbon nanotubes derived from waste biomass and its electrochemical performance. Mater Lett. 2020;261:127146.
[373] Singh R, Volli V, Lohani L, Purkait MK. Synthesis of carbon nanotubes from industrial wastes following alkali activation and film casting method. Waste Biomass Valoriz. 2019;11(9):4957–66.
[374] Zhang B, Song J, Yang G, Han B. Large-scale production of high-quality graphene using glucose and ferric chloride. Chem Sci. 2014;5(12):4656–60.
[375] Le Van K, Luong Thi TT. Activated carbon derived from rice husk by NaOH activation and its application in supercapacitor. Prog Nat Sci: Mater Int. 2014;24(3):191–8.
[376] Bakar RA, Yahya R, Gan SN. Production of high purity amorphous silica from rice husk. Proc Chem. 2016;19:189–95.
[377] Liu N, Huo K, McDowell MT, Zhao J, Cui Y. Rice husks as a sustainable source of nanostructured silicon for high performance Li-ion battery anodes. Sci Rep. 2013;3(1):1919.
[378] Wang H, Xu Z, Kohandehghan A, Li Z, Cui K, Tan X, et al. Interconnected carbon nanosheets derived from hemp for ultrafast supercapacitors with high energy. ACS Nano. 2013;7(6):5131–41.
[379] Zhao H, Zhao TS. Graphene sheets fabricated from disposable paper cups as a catalyst support material for fuel cells. J Mater Chem A. 2013;1(2):183–7.
[380] Salifairus MJ, Soga T, Alrokayan SAH, Khan HA, Rusop M. The synthesis of graphene at different deposition time from palm oil *via* thermal chemical vapor deposition. AIP Conf Proc. 2018;1963(1):020007.
[381] Strudwick AJ, Weber NE, Schwab MG, Kettner M, Weitz RT, Wünsch JR, et al. Chemical vapor deposition of high quality graphene films from carbon dioxide atmospheres. ACS Nano. 2015;9(1):31–42.
[382] Coleman JN. Liquid exfoliation of defect-free graphene. Acc Chem Res. 2013;46(1):14–22.
[383] Bonaccorso F, Lombardo A, Hasan T, Sun Z, Colombo L, Ferrari AC. Production and processing of graphene and 2d crystals. Mater today. 2012;15(12):564–89.
[384] Mishra N, Boeckl J, Motta N, Iacopi F. Graphene growth on silicon carbide: a review. Phys Status Solidi (a). 2016;213(9):2277–89.
[385] Abdolhosseinzadeh S, Asgharzadeh H, Kim HS. Fast and fully-scalable synthesis of reduced graphene oxide. Sci Rep. 2015;5(1):1–7.
[386] Boland CS, Khan U, Ryan G, Barwich S, Charifou R, Harvey A, et al. Sensitive electromechanical sensors using viscoelastic graphene-polymer nanocomposites. Science. 2016;354(6317):1257–60.
[387] Wu Y, Ye P, Capano MA, Xuan Y, Sui Y, Qi M, et al. Top-gated graphene field-effect-transistors formed by decomposition of SiC. Appl Phys Lett. 2008;92(9):092102.
[388] Li XH, Kurasch S, Kaiser U, Antonietti M. Synthesis of monolayer-patched graphene from glucose. Angew Chem Int Ed. 2012;51(38):9689–92.
[389] Salifairus M, Soga T, Alrokayan SA, Khan HA, Rusop M. The synthesis of graphene at different deposition time from palm oil *via* thermal chemical vapor deposition. AIP Conf Proc. AIP Publishing LLC; 2018. p. 020007.
[390] Janus Ł, Radwan-Pragłowska J, Piątkowski M, Bogdał D. Smart, tunable CQDs with antioxidant properties for biomedical applications – ecofriendly synthesis and characterization. Molecules. 2020;25(3):736.
[391] Zhu L, Shen D, Wu C, Gu S. State-of-the-art on the preparation, modification, and application of biomass-derived carbon quantum dots. Ind Eng Chem Res. 2020;59(51):22017–39.
[392] Atchudan R, Edison TNJI, Shanmugam M, Perumal S, Somanathan T, Lee YR. Sustainable synthesis of carbon quantum dots from banana peel waste using hydrothermal process for *in vivo* bioimaging. Phys E: Low-dimensional Syst Nanostructures. 2020;126:114417.
[393] Sharma N, Das GS, Yun K. Green synthesis of multipurpose carbon quantum dots from red cabbage and estimation of their antioxidant potential and bio-labeling activity. Appl Microbiol Biotechnol. 2020;104(16):7187–200.

[394] Yang H, Zhou B, Zhang Y, Liu H, Liu Y, He Y, et al. Valorization of expired passion fruit shell by hydrothermal conversion into carbon quantum dot: physical and optical properties. Waste Biomass Valoriz. 2020;12(4):1–9.
[395] Luo B, Yang H, Zhou B, Ahmed SM, Zhang Y, Liu H, et al. Facile synthesis of luffa sponge activated carbon fiber based carbon quantum dots with green fluorescence and their application in Cr (VI) determination. ACS Omega. 2020;5(10):5540–7.
[396] Zhang Y, Wang J, Wu W, Li C, Ma H, Green A. Economic "Switch-On" sensor for cefixime analysis based on black soya bean carbon quantum dots. J AOAC Int. 2020;103(5):1230–6.
[397] Tajik S, Dourandish Z, Zhang K, Beitollahi H, Van Le Q, Jang HW, et al. Carbon and graphene quantum dots: a review on syntheses, characterization, biological and sensing applications for neurotransmitter determination. RSC Adv. 2020;10(26):15406–29.
[398] Sun Y-P, Zhou B, Lin Y, Wang W, Fernando KS, Pathak P, et al. Quantum-sized carbon dots for bright and colorful photoluminescence. J Am Chem Soc. 2006;128(24):7756–7.
[399] Başoğlu A, Ocak Ü, Gümrükçüoğlu A. Synthesis of microwave-assisted fluorescence carbon quantum dots using roasted–chickpeas and its applications for sensitive and selective detection of Fe^{3+} ions. J Fluorescence. 2020;30(3):1–12.
[400] Abbas A, Tabish TA, Bull SJ, Lim TM, Phan AN. High yield synthesis of graphene quantum dots from biomass waste as a highly selective probe for Fe^{3+} sensing. Sci Rep. 2020;10(1):1–16.
[401] Haque E, Kim J, Malgras V, Reddy KR, Ward AC, You J, et al. Recent advances in graphene quantum dots: synthesis, properties, and applications. Small Methods. 2018;2(10):1800050.
[402] Bacon M, Bradley SJ, Nann T. Graphene quantum dots. Part Part Syst Charact. 2014;31(4):415–28.
[403] Sundaram PA, Augustine R, Kannan M. Extracellular biosynthesis of iron oxide nanoparticles by Bacillus subtilis strains isolated from rhizosphere soil. Biotechnol Bioprocess Eng. 2012;17(4):835–40.
[404] Khan M, Mangrich A, Schultz J, Grasel F, Mattoso N, Mosca D. Green chemistry preparation of superparamagnetic nanoparticles containing Fe_3O_4 cores in biochar. J Anal Appl Pyrolysis. 2015;116:42–8.
[405] Xie W, Guo Z, Gao F, Gao Q, Wang D, Liaw B-S, et al. Shape-, size-and structure-controlled synthesis and biocompatibility of iron oxide nanoparticles for magnetic theranostics. Theranostics. 2018;8(12):3284.
[406] Groiss S, Selvaraj R, Varadavenkatesan T, Vinayagam R. Structural characterization, antibacterial and catalytic effect of iron oxide nanoparticles synthesised using the leaf extract of Cynometra ramiflora. J Mol Struct. 2017;1128:572–8.
[407] Patra JK, Baek K-H. Green biosynthesis of magnetic iron oxide (Fe_3O_4) nanoparticles using the aqueous extracts of food processing wastes under photo-catalyzed condition and investigation of their antimicrobial and antioxidant activity. J Photochem Photobiol B: Biol. 2017;173:291–300.
[408] Bibi I, Nazar N, Ata S, Sultan M, Ali A, Abbas A, et al. Green synthesis of iron oxide nanoparticles using pomegranate seeds extract and photocatalytic activity evaluation for the degradation of textile dye. J Mater Res Technol. 2019;8(6):6115–24.
[409] Irshad MA, Nawaz R, Ur Rehman MZ, Adrees M, Rizwan M, Ali S, et al. Synthesis, characterization and advanced sustainable applications of titanium dioxide nanoparticles: a review. Ecotoxicol Environ Saf. 2021;212:111978.
[410] Singh R, Kumari P, Chavan PD, Datta S, Dutta S. Synthesis of solvothermal derived TiO_2 nanocrystals supported on ground nano egg shell waste and its utilization for the photocatalytic dye degradation. Optical Mater. 2017;73:377–83.
[411] Nadeem M, Tungmunnithum D, Hano C, Abbasi BH, Hashmi SS, Ahmad W, et al. The current trends in the green syntheses of titanium oxide nanoparticles and their applications. Green Chem Lett Rev. 2018;11(4):492–502.
[412] Ramimoghadam D, Hussein MZB, Taufiq-Yap YH. Synthesis and characterization of ZnO nanostructures using palm olein as biotemplate. Chem Cent J. 2013;7(1):1–10.
[413] Deep A, Kumar K, Kumar P, Kumar P, Sharma AL, Gupta B, et al. Recovery of pure ZnO nanoparticles from spent Zn-MnO_2 alkaline batteries. Env Sci Technol. 2011;45(24):10551–6.
[414] Deep A, Sharma AL, Mohanta GC, Kumar P, Kim K-H. A facile chemical route for recovery of high quality zinc oxide nanoparticles from spent alkaline batteries. Waste Manag. 2016;51:190–5.
[415] Farzana R, Rajarao R, Behera PR, Hassan K, Sahajwalla V. Zinc oxide nanoparticles from waste Zn-C battery *via* thermal route: characterization and properties. Nanomaterials (Basel, Switz). 2018;8(9):717.
[416] Farzana R, Rajarao R, Behera PR, Hassan K, Sahajwalla V. Zinc oxide nanoparticles from waste Zn-C battery *via* thermal route: characterization and properties. Nanomaterials. 2018;8(9):717.
[417] Davaeifar S, Modarresi M-H, Mohammadi M, Hashemi E, Shafiei M, Maleki H, et al. Synthesizing, characterizing, and toxicity evaluating of Phycocyanin-ZnO nanorod composites: a back to nature approaches. Colloids Surf B: Biointerfaces. 2019;175:221–30.
[418] Jain D, Shivani AAB, Singh H, Daima HK, Singh M, Mohanty SR, et al. Microbial fabrication of zinc oxide nanoparticles and evaluation of their antimicrobial and photocatalytic properties. Front Chem. 2020;8:778.
[419] Surendra T, Roopan SM, Al-Dhabi NA, Arasu MV, Sarkar G, Suthindhiran K. Vegetable peel waste for the production of ZnO nanoparticles and its toxicological efficiency, antifungal, hemolytic, and antibacterial activities. Nanoscale Res Lett. 2016;11(1):1–10.
[420] Ravichandran V, Sumitha S, Ning CY, Xian OY, Kiew Yu U, Paliwal N, et al. Durian waste mediated green synthesis of zinc oxide nanoparticles and evaluation of their antibacterial, antioxidant, cytotoxicity and photocatalytic activity. Green Chem Lett Rev. 2020;13(2):102–16.
[421] Dmochowska A, Czajkowska J, Jędrzejewski R, Stawiński W, Migdał P, Fiedot-Toboła M. Pectin based banana peel extract as a stabilizing agent in zinc oxide nanoparticles synthesis. Int J Biol Macromol. 2020;165:1581–92.
[422] Abdullah F, Bakar NA, Bakar MA. Comparative study of chemically synthesized and low temperature bio-inspired Musa acuminata peel extract mediated zinc oxide nanoparticles for enhanced visible-photocatalytic degradation of organic

contaminants in wastewater treatment. J Hazard Mater. 2021;406:124779.
[423] Rambabu K, Bharath G, Banat F, Show PL. Green synthesis of zinc oxide nanoparticles using Phoenix dactylifera waste as bioreductant for effective dye degradation and antibacterial performance in wastewater treatment. J Hazard Mater. 2021;402:123560.
[424] Jayaseelan C, Rahuman AA, Kirthi AV, Marimuthu S, Santhoshkumar T, Bagavan A, et al. Novel microbial route to synthesize ZnO nanoparticles using Aeromonas hydrophila and their activity against pathogenic bacteria and fungi. Spectrochim Acta Part A, Mol Biomole Spectrosc. 2012;90:78–84.
[425] Mohd Yusof H, Mohamad R, Zaidan UH, Rahman NAA. Sustainable microbial cell nanofactory for zinc oxide nanoparticles production by zinc-tolerant probiotic Lactobacillus plantarum strain TA4. Microb Cell Factories. 2020;19(1):10.
[426] Chikkanna MM, Neelagund SE, Rajashekarappa KK. Green synthesis of zinc oxide nanoparticles (ZnO NPs) and their biological activity. SN Appl Sci. 2018;1(1):117.
[427] Doan Thi TU, Nguyen TT, Thi YD, Ta Thi KH, Phan BT, Pham KN. Green synthesis of ZnO nanoparticles using orange fruit peel extract for antibacterial activities. RSC Adv. 2020;10(40):23899–907.
[428] Modi S, Fulekar MH. Green synthesis of zinc oxide nanoparticles using garlic skin extract and its characterization. J Nanostruct. 2020;10(1):20–7.
[429] Abdullah FH, Abu Bakar NHH, Abu Bakar M. Comparative study of chemically synthesized and low temperature bio-inspired Musa acuminata peel extract mediated zinc oxide nanoparticles for enhanced visible-photocatalytic degradation of organic contaminants in wastewater treatment. J Hazard Mater. 2021;406:124779.
[430] Javed M, Shaik AH, Khan TA, Imran M, Aziz A, Ansari AR, et al. Synthesis of stable waste palm oil based CuO nanofluid for heat transfer applications. Heat Mass Transf. 2018;54(12):3739–45.
[431] Tshireletso P, Ateba CN, Fayemi OEJM. Spectroscopic and antibacterial properties of CuONPs from orange, lemon and tangerine peel extracts: potential for combating bacterial resistance. Molecules. 2021;26(3):586.
[432] Chaudhary S, Rohilla D, Umar A, Kaur N, Shanavas AJCI. Synthesis and characterizations of luminescent copper oxide nanoparticles: toxicological profiling and sensing applications. Ceram Int. 2019;45(12):15025–35.
[433] Fuku X, Modibedi M, Mathe MJSAS. Green synthesis of Cu/Cu2O/CuO nanostructures and the analysis of their electrochemical properties. SN Appl Sci. 2020;2(5):1–15.
[434] Mahmoud NM, Mohamed HI, Ahmed SB, Akhtar SJCP. Efficient biosynthesis of CuO nanoparticles with potential cytotoxic activity. Chem Pap. 2020;74(9):1–11.
[435] Alhumaimess MS, Essawy AA, Kamel MM, Alsohaimi IH, Hassan HJN. Biogenic-mediated synthesis of mesoporous Cu_2O/CuO nano-architectures of superior catalytic reductive towards nitroaromatics. Nanomaterials. 2020;10(4):781.
[436] Nwanya AC, Ndipingwi MM, Mayedwa N, Razanamahandry L, Ikpo CO, Waryo T, et al. Maize (Zea mays L.) fresh husk mediated biosynthesis of copper oxides: Potentials for pseudo capacitive energy storage. Electrochim Acta. 2019;301:436–48.
[437] Nwanya AC, Botha S, Ezema FI, Maaza M. Functional metal oxides synthesized using natural extracts from waste maize materials. Curr Res Green SustaChem. 2021;4:100054.
[438] Segovia-Guzmán MO, Román-Aguirre M, Verde-Gomez JY, Collins-Martínez VH, Zaragoza-Galán G, Ramos-Sánchez VH. Green Cu2O/TiO_2 heterojunction for glycerol photoreforming. Catal Today. 2018;349:88–97.
[439] El-Batal AI, El-Sayyad GS, El-Ghamery A, Gobara M. Response surface methodology optimization of melanin production by Streptomyces cyaneus and synthesis of copper oxide nanoparticles using gamma radiation. J Clust Sci. 2017;28(3):1083–112.
[440] Ullah H, Ullah Z, Fazal A, Irfan M. Use of vegetable waste extracts for controlling microstructure of CuO nanoparticles: green synthesis, characterization, and photocatalytic applications. J Chem. 2017;2017:2721798.
[441] Barman K, Dutta P, Chowdhury D, Baruah PK. Green biosynthesis of copper oxide nanoparticles using waste colocasia esculenta leaves extract and their application as recyclable catalyst towards the synthesis of 1, 2, 3-triazoles. BioNanoScience. 2021;11(1):1–11.
[442] Rajkumar S, Elanthamilan E, Balaji TE, Sathiyan A, Jafneel NE, Merlin JP. Compounds, recovery of copper oxide nanoparticles from waste SIM cards for supercapacitor electrode material. J Alloy Compd. 2020;849:156582.
[443] Mdlovu NV, Chiang C-L, Lin K-S, Jeng R-C. Recycling copper nanoparticles from printed circuit board waste etchants *via* a microemulsion process. J Clean Prod. 2018;185:781–96.
[444] Xiu F-R, Zhang F-S. Size-controlled preparation of Cu_2O nanoparticles from waste printed circuit boards by supercritical water combined with electrokinetic process. J Hazard Mater. 2012;233:200–6.
[445] Liu K, Yang J, Hou H, Liang S, Chen Y, Wang J, et al. Facile and cost-effective approach for copper recovery from waste printed circuit boards *via* a sequential mechanochemical/leaching/recrystallization process. Environ Sci Technol. 2019;53(5):2748–57.
[446] Xiu F-R, Zhang F-S. Preparation of nano-Cu_2O/TiO_2 photocatalyst from waste printed circuit boards by electrokinetic process. J Hazard Mater. 2009;172(2–3):1458–63.
[447] Nan J, Han D, Yang M, Cui M, Hou X. Recovery of metal values from a mixture of spent lithium-ion batteries and nickel-metal hydride batteries. Hydrometallurgy. 2006;84(1–2):75–80.
[448] Sun J, Zhou W, Zhang L, Cheng H, Wang Y, Tang R, et al. Bioleaching of copper-containing electroplating sludge. J Environ Manag. 2021;285:112133.
[449] Wu J-Y, Chou W-S, Chen W-S, Chang F-C, Shen Y-H, Chang J-E, et al. Recovery of cupric oxide from copper-containing wastewater sludge by acid leaching and ammonia purification process. Desal Water Treat. 2012;47(1–3):120–9.
[450] Heuss-Aßbichler S, John M, Klapper D, Bläß UW, Kochetov G. Recovery of copper as zero-valent phase and/or copper oxide nanoparticles from wastewater by ferritization. J Environ Manag. 2016;181:1–7.
[451] El-Nasr RS, Abdelbasir S, Kamel AH, Hassan SS. Environmentally friendly synthesis of copper nanoparticles

from waste printed circuit boards. Sep Purif Technol. 2020;230:115860.
[452] Li H, Oraby E, Eksteen J. Recovery of copper and the deportment of other base metals from alkaline glycine leachates derived from waste printed circuit boards (WPCBs). Hydrometallurgy. 2021;199:105540.
[453] Chaudhary K, Prakash K, Mogha NK, Masram DT. Fruit waste (Pulp) decorated CuO NFs as promising platform for enhanced catalytic response and its peroxidase mimics evaluation. Arab J Chem. 2020;13(4):4869–81.
[454] Wang Q, Zhang Y, Xiao J, Jiang H, Hu T, Meng C. Copper oxide/cuprous oxide/hierarchical porous biomass-derived carbon hybrid composites for high-performance supercapacitor electrode. J Alloy Compd. 2019;782:1103–13.
[455] Torres-Arellano S, Reyes-Vallejo O, Enriquez JP, Aleman-Ramirez J, Huerta-Flores A, Moreira J, et al. Biosynthesis of cuprous oxide using banana pulp waste extract as reducing agent. Fuel. 2021;285:119152.
[456] Araya-Castro K, Chao T-C, Durán-Vinet B, Cisternas C, Rubilar O. Green synthesis of copper oxide nanoparticles using protein fractions from an aqueous extract of Brown Algae Macrocystis pyrifera. Processes. 2021;9(1):78.
[457] Borah R, Saikia E, Bora SJ, Chetia B. Banana pulp extract mediated synthesis of Cu2O nanoparticles: an efficient heterogeneous catalyst for the ipso-hydroxylation of arylboronic acids. Tetrahedron Lett. 2017;58(12):1211–5.
[458] Kasture M, Patel P, Prabhune A, Ramana C, Kulkarni A, Prasad B. Synthesis of silver nanoparticles by sophorolipids: effect of temperature and sophorolipid structure on the size of particles. J Chem Sci. 2008;120(6):515–20.
[459] Jain N, Bhargava A, Majumdar S, Tarafdar J, Panwar J. Extracellular biosynthesis and characterization of silver nanoparticles using Aspergillus flavus NJP08: a mechanism perspective. Nanoscale. 2011;3(2):635–41.
[460] Singaravelu G, Arockiamary J, Kumar VG, Govindaraju K. A novel extracellular synthesis of monodisperse gold nanoparticles using marine alga, Sargassum wightii Greville. Colloids Surf B: Biointerfaces. 2007;57(1):97–101.
[461] Moriwaki H, Yamada K, Usami H. Electrochemical extraction of gold from wastes as nanoparticles stabilized by phospholipids. Waste Manag. 2017;60:591–5.
[462] Velmurugan P, Anbalagan K, Manosathyadevan M, Lee K-J, Cho M, Lee S-M, et al. Green synthesis of silver and gold nanoparticles using Zingiber officinale root extract and antibacterial activity of silver nanoparticles against food pathogens. Bioprocess Biosyst Eng. 2014;37(10):1935–43.
[463] Liu Y, Song X, Cao F, Li F, Wang M, Yang Y, et al. Banana peel-derived dendrite-shaped Au nanomaterials with dual inhibition toward tumor growth and migration. Int J Nanomed. 2020;15:2315.
[464] van Ham TJ, Esposito A, Kumita JR, Hsu S-TD, Schierle GSK, Kaminski CF, et al. Towards multiparametric fluorescent imaging of amyloid formation: studies of a YFP model of α-synuclein aggregation. J Mol Biol. 2010;395(3):627–42.
[465] Joo C, Balci H, Ishitsuka Y, Buranachai C, Ha T. Advances in single-molecule fluorescence methods for molecular biology. Annu Rev Biochem. 2008;77:51–76.
[466] Giepmans BN, Adams SR, Ellisman MH, Tsien RY. The fluorescent toolbox for assessing protein location and function. Science. 2006;312(5771):217–24.
[467] Yamamoto N, Tsuchiya H, Hoffman RM. Tumor imaging with multicolor fluorescent protein expression. Int J Clin Oncol. 2011;16(2):84–91.
[468] Los GV, Encell LP, McDougall MG, Hartzell DD, Karassina N, Zimprich C, et al. HaloTag: a novel protein labeling technology for cell imaging and protein analysis. ACS Chem Biol. 2008;3(6):373–82.
[469] Cubeddu R, Comelli D, D'Andrea C, Taroni P, Valentini G. Time-resolved fluorescence imaging in biology and medicine. J Phys D: Appl Phys. 2002;35(9):R61.
[470] Nasir I, Fatih W, Svensson A, Radu D, Linse S, Lago CC, et al. High throughput screening method to explore protein interactions with nanoparticles. PLoS One. 2015;10(8):e0136687.
[471] Behzadi S, Serpooshan V, Tao W, Hamaly MA, Alkawareek MY, Dreaden EC, et al. Cellular uptake of nanoparticles: journey inside the cell. Chem Soc Rev. 2017;46(14):4218–44.
[472] Ni X, Jia S, Duan X, Ding D, Li K. Fluorescent nanoparticles for noninvasive stem cell tracking in regenerative medicine. J Biomed Nanotechnol. 2018;14(2):240–56.
[473] Zhao P, Xu Q, Tao J, Jin Z, Pan Y, Yu C, et al. Near infrared quantum dots in biomedical applications: current status and future perspective. Wiley Interdiscip Rev: Nanomed Nanobiotechnol. 2018;10(3):e1483.
[474] Li C, Li F, Zhang Y, Zhang W, Zhang X-E, Wang Q. Real-time monitoring surface chemistry-dependent *in vivo* behaviors of protein nanocages *via* encapsulating an NIR-II Ag2S quantum dot. ACS Nano. 2015;9(12):12255–63.
[475] Hsiao WW-W, Hui YY, Tsai P-C, Chang H-C. Fluorescent nanodiamond: a versatile tool for long-term cell tracking, super-resolution imaging, and nanoscale temperature sensing. Acc Chem Res. 2016;49(3):400–7.
[476] Cong L, Takeda M, Hamanaka Y, Gonda K, Watanabe M, Kumasaka M, et al. Uniform silica coated fluorescent nanoparticles: synthetic method, improved light stability and application to visualize lymph network tracer. PLoS One. 2010;5(10):e13167.
[477] Xu R, Huang L, Wei W, Chen X, Zhang X, Zhang X. Real-time imaging and tracking of ultrastable organic dye nanoparticles in living cells. Biomaterials. 2016;93:38–47.
[478] Jung DH, Hwang S, Song GW, Ahn CS, Moon DB, Ha TY, et al. Survival benefit of early cancer detection through regular endoscopic screening for de novo gastric and colorectal cancers in korean liver transplant recipients. Transpl Proc. 2016;48(1):145–51.
[479] Ryvolova M, Chomoucka J, Drbohlavova J, Kopel P, Babula P, Hynek D, et al. Modern micro and nanoparticle-based imaging techniques. Sens (Basel). 2012;12(11):14792–820.
[480] Fan Q, Cheng K, Hu X, Ma X, Zhang R, Yang M, et al. Transferring biomarker into molecular probe: melanin nanoparticle as a naturally active platform for multimodality imaging. J Am Chem Soc. 2014;136(43):15185–94.
[481] Montet X, Montet-Abou K, Reynolds F, Weissleder R, Josephson L. Nanoparticle imaging of integrins on tumor cells. Neoplasia. 2006;8(3):214–22.
[482] Jackson P, Periasamy S, Bansal V, Geso M. Evaluation of the effects of gold nanoparticle shape and size on contrast enhancement in radiological imaging. Australas Phys Eng Sci Med. 2011;34(2):243–9.

[483] Han X, Xu K, Taratula O, Farsad K. Applications of nanoparticles in biomedical imaging. Nanoscale. 2019;11(3):799–819.
[484] Cuccurullo V, Di Stasio GD, Mazzarella G, Cascini GL. Microvascular invasion in HCC: the molecular imaging perspective. Contrast Media Mol Imaging. 2018;2018:9487938.
[485] Hwang ES, Cao C, Hong S, Jung HJ, Cha CY, Choi JB, et al. The DNA hybridization assay using single-walled carbon nanotubes as ultrasensitive, long-term optical labels. Nanotechnology. 2006;17(14):3442–5.
[486] Santra S, Malhotra A. Fluorescent nanoparticle probes for imaging of cancer. Wiley Interdiscip Rev-Nanomed Nanobiotechnol. 2011;3(5):501–10.
[487] Markovic S, Belz J, Kumar R, Cormack RA, Sridhar S, Niedre M. Near-infrared fluorescence imaging platform for quantifying *in vivo* nanoparticle diffusion from drug loaded implants. Int J Nanomed. 2016;11:1213–23.
[488] Genovese D, Bonacchi S, Juris R, Montalti M, Prodi L, Rampazzo E, et al. Prevention of self-quenching in fluorescent silica nanoparticles by efficient energy transfer. Angew Chem Int Ed Engl. 2013;52(23):5965–8.
[489] Grebenik EA, Nadort A, Generalova AN, Nechaev AV, Sreenivasan VK, Khaydukov EV, et al. Feasibility study of the optical imaging of a breast cancer lesion labeled with upconversion nanoparticle biocomplexes. J Biomed Opt. 2013;18(7):76004.
[490] Cai Z, Ye Z, Yang X, Chang Y, Wang H, Liu Y, et al. Encapsulated enhanced green fluorescence protein in silica nanoparticle for cellular imaging. Nanoscale. 2011;3(5):1974–6.
[491] Dubreil L, Leroux I, Ledevin M, Schleder C, Lagalice L, Lovo C, et al. Multi-harmonic imaging in the second near-infrared window of nanoparticle-labeled stem cells as a monitoring tool in tissue depth. ACS Nano. 2017;11(7):6672–81.
[492] Lee S, Cha EJ, Park K, Lee SY, Hong JK, Sun IC, et al. A near-infrared-fluorescence-quenched gold-nanoparticle imaging probe for *in vivo* drug screening and protease activity determination. Angew Chem Int Ed Engl. 2008;47(15):2804–7.
[493] Wei Y, Chen Q, Wu B, Zhou A, Xing D. High-sensitivity *in vivo* imaging for tumors using a spectral up-conversion nanoparticle NaYF4:Yb3+, Er3+ in cooperation with a microtubulin inhibitor. Nanoscale. 2012;4(13):3901–9.
[494] Jiang S, Gnanasammandhan MK, Zhang Y. Optical imaging-guided cancer therapy with fluorescent nanoparticles. J R Soc Interface. 2010;7(42):3–18.
[495] Pericleous P, Gazouli M, Lyberopoulou A, Rizos S, Nikiteas N, Efstathopoulos EP. Quantum dots hold promise for early cancer imaging and detection. Int J Cancer. 2012;131(3):519–28.
[496] Pons T, Bouccara S, Loriette V, Lequeux N, Pezet S, Fragola A. *In vivo* imaging of single tumor cells in fast-flowing bloodstream using near-infrared quantum dots and time-gated imaging. ACS Nano. 2019;13(3):3125–31.
[497] Peng C-W, Li Y. Application of quantum dots-based biotechnology in cancer diagnosis: current status and future perspectives. J Nanomaterials. 2010;2010.
[498] Hua X-W, Bao Y-W, Wu F-G. Fluorescent carbon quantum dots with intrinsic nucleolus-targeting capability for nucleolus imaging and enhanced cytosolic and nuclear drug delivery. ACS Appl Mater Interfaces. 2018;10(13):10664–77.
[499] Iannazzo D, Pistone A, Salamò M, Galvagno S, Romeo R, Giofré SV, et al. Graphene quantum dots for cancer targeted drug delivery. Int J Pharma. 2017;518(1–2):185–92.
[500] McHugh KJ, Jing L, Behrens AM, Jayawardena S, Tang W, Gao M, et al. Biocompatible semiconductor quantum dots as cancer imaging agents. Adv Mater. 2018;30(18):1706356.
[501] Shao J, Zhang J, Jiang C, Lin J, Huang P. Biodegradable titanium nitride MXene quantum dots for cancer photothera-nostics in NIR-I/II biowindows. Chem Eng J. 2020;400:126009.
[502] Tao W, Ji X, Xu X, Islam MA, Li Z, Chen S, et al. Antimonene quantum dots: synthesis and application as near-infrared photothermal agents for effective cancer therapy. Angew Chem. 2017;129(39):12058–62.
[503] Chen H, Liu Z, Wei B, Huang J, You X, Zhang J, et al. Redox responsive nanoparticle encapsulating black phosphorus quantum dots for cancer theranostics. Bioact Mater. 2021;6(3):655–65.
[504] Zhang R, Liu Y, Yu L, Li Z, Sun S. Preparation of high-quality biocompatible carbon dots by extraction, with new thoughts on the luminescence mechanisms. Nanotechnology. 2013;24(22):225601.
[505] Cheng C, Xing M, Wu Q. A universal facile synthesis of nitrogen and sulfur co-doped carbon dots from cellulose-based biowaste for fluorescent detection of Fe3 + ions and intracellular bioimaging. Mater Sci Eng C-Mater Biol Appl. 2019;99:611–9.
[506] Dong Y, Pang H, Yang HB, Guo C, Shao J, Chi Y, et al. Carbon-based dots co-doped with nitrogen and sulfur for high quantum yield and excitation-independent emission. Angew Chem Int Ed. 2013;52(30):7800–4.
[507] Xu Y, Wu M, Liu Y, Feng XZ, Yin XB, He XW, et al. Nitrogen-doped carbon dots: a facile and general preparation method, photoluminescence investigation, and imaging applications. Chem–A Eur J. 2013;19(7):2276–83.
[508] Wu ZL, Zhang P, Gao MX, Liu CF, Wang W, Leng F, et al. One-pot hydrothermal synthesis of highly luminescent nitrogen-doped amphoteric carbon dots for bioimaging from Bombyx mori silk–natural proteins. J Mater Chem B. 2013;1(22):2868–73.
[509] Wu X, Tian F, Wang W, Chen J, Wu M, Zhao JX. Fabrication of highly fluorescent graphene quantum dots using L-glutamic acid for *in vitro*/*in vivo* imaging and sensing. J Mater Chem C. 2013;1(31):4676–84.
[510] Shang W, Zhang X, Zhang M, Fan Z, Sun Y, Han M, et al. The uptake mechanism and biocompatibility of graphene quantum dots with human neural stem cells. Nanoscale. 2014;6(11):5799–806.
[511] Zhang M, Bai L, Shang W, Xie W, Ma H, Fu Y, et al. Facile synthesis of water-soluble, highly fluorescent graphene quantum dots as a robust biological label for stem cells. J Mater Chem. 2012;22(15):7461–7.
[512] Yan F, Bai Z, Ma T, Sun X, Zu F, Luo Y, et al. Surface modification of carbon quantum dots by fluorescein derivative for dual-emission ratiometric fluorescent hypochlorite biosensing and *in vivo* bioimaging. Sens Actuators B: Chem. 2019;296:126638.

[513] Hu Y, Yang J, Tian J, Jia L, Yu J. Waste frying oil as a precursor for one-step synthesis of sulfur-doped carbon dots with pH-sensitive photoluminescence. Carbon. 2014;77:775–82.
[514] Park SY, Lee HU, Park ES, Lee SC, Lee JW, Jeong SW, et al. Photoluminescent green carbon nanodots from food-waste-derived sources: large-scale synthesis, properties, and biomedical applications. ACS Appl Mater Interfaces. 2014;6(5):3365–70.
[515] Xue M, Zou M, Zhao J, Zhan Z, Zhao S. Green preparation of fluorescent carbon dots from lychee seeds and their application for the selective detection of methylene blue and imaging in living cells. J Mater Chem B. 2015;3(33):6783–9.
[516] Xue M, Zhan Z, Zou M, Zhang L, Zhao S. Green synthesis of stable and biocompatible fluorescent carbon dots from peanut shells for multicolor living cell imaging. N J Chem. 2016;40(2):1698–703.
[517] Yao Y, Gedda G, Girma W, Yen C, Ling Y, Chang J. Magnetofluorescent carbon dots derived from crab shell for targeted dual-modality bioimaging and drug delivery. Acs Appl Mater Interfaces. 2017;9(16):13887–99.
[518] Bankoti K, Rameshbabu A, Datta S, Das B, Mitra A, Dhara S. Onion derived carbon nanodots for live cell imaging and accelerated skin wound healing. J Mater Chem B. 2017;5(32):6579–92.
[519] Manaf S, Hegde G, Mandal U, Wui W, Roy P. Functionalized carbon nano-scale drug delivery systems from biowaste sago bark for cancer cell imaging. Curr Drug Delivery. 2017;14(8):1071–7.
[520] Cheng C, Shi Y, Li M, Xing M, Wu Q. Carbon quantum dots from carbonized walnut shells: structural evolution, fluorescence characteristics, and intracellular bioimaging. Mater Sci Eng C-Mater Biol Appl. 2017;79:473–80.
[521] Pati P, McGinnis S, Vikesland P. Waste not want not: life cycle implications of gold recovery and recycling from nanowaste. Environ Sci-Nano. 2016;3(5):1133–43.
[522] Oestreicher V, García CS, Soler-Illia GJAA, Angelomé PC. Gold recycling at laboratory scale: from nanowaste to nanospheres. ChemSusChem. 2019;12(21):4882–8.
[523] Hwang C, Kim JM, Kim J. Influence of concentration, nanoparticle size, beam energy, and material on dose enhancement in radiation therapy. J Radiat Res. 2017;58(4):405–11.
[524] Meledandri CJ, Stolarczyk JK, Brougham DF. Hierarchical gold-decorated magnetic nanoparticle clusters with controlled size. ACS Nano. 2011;5(3):1747–55.
[525] Sardar R, Shumaker-Parry J. Spectroscopic and microscopic investigation of gold nanoparticle formation: ligand and temperature effects on rate and particle size. J Am Chem Soc. 2011;133(21):8179–90.
[526] Geng J, Li K, Pu KY, Ding D, Liu B. Conjugated polymer and gold nanoparticle co-loaded PLGA nanocomposites with eccentric internal nanostructure for dual-modal targeted cellular imaging. Small. 2012;8(15):2421–9.
[527] Sarode GS, Maniyar N, Choudhary N, Sarode SC, Patil S. Gold nanoparticles: a novel approach in early detection of oral cancers. J Contemp Dent Pract. 2018;19(4):357–8.
[528] Kumar A, Boruah B, Liang X. Gold nanoparticles: promising nanomaterials for the diagnosis of cancer and HIV/AIDS. J Nanomater. 2011;2011:202187.
[529] He H, Xie C, Ren J. Nonbleaching fluorescence of gold nanoparticles and its applications in cancer cell imaging. Anal Chem. 2008;80(15):5951–7.
[530] Peng C, Gao X, Xu J, Du B, Ning X, Tang S, et al. Targeting orthotopic gliomas with renal-clearable luminescent gold nanoparticles. Nano Res. 2017;10(4):1366–76.
[531] Liu J, Yu M, Zhou C, Yang S, Ning X, Zheng J. Passive tumor targeting of renal-clearable luminescent gold nanoparticles: long tumor retention and fast normal tissue clearance. J Am Chem Soc. 2013;135(13):4978–81.
[532] Fan M, Han Y, Gao S, Yan H, Cao L, Li Z, et al. Ultrasmall gold nanoparticles in cancer diagnosis and therapy. Theranostics. 2020;10(11):4944–57.
[533] Swietach P, Vaughan-Jones R, Harris A, Hulikova A. The chemistry, physiology and pathology of pH in cancer. Philos Trans R Soc B-Biolog Sci. 1638;369:2014.
[534] Yu KK, Li K, Qin HH, Zhou Q, Qian CH, Liu YH, et al. Construction of pH-sensitive "Submarine" based on gold nanoparticles with double insurance for intracellular pH mapping, quantifying of whole cells and *in vivo* applications. ACS Appl Mater Interfaces. 2016;8(35):22839–48.
[535] Yu K, Li K, Lu C, Xie Y, Liu Y, Zhou Q, et al. Multifunctional gold nanoparticles as smart nanovehicles with enhanced tumour-targeting abilities for intracellular pH mapping and *in vivo* MR/fluorescence imaging. Nanoscale. 2020;12(3):2002–10.
[536] Chen J, Than A, Li N, Ananthanarayanan A, Zheng X, Xi F, et al. Sweet graphene quantum dots for imaging carbohydrate receptors in live cells. FlatChem. 2017;5:25–32.
[537] Li N, Than A, Chen J, Xi F, Liu J, Chen P. Graphene quantum dots based fluorescence turn-on nanoprobe for highly sensitive and selective imaging of hydrogen sulfide in living cells. Biomater Sci. 2018;6(4):779–84.
[538] Gao T, Wang X, Yang L-Y, He H, Ba X-X, Zhao J, et al. Red, yellow, and blue luminescence by graphene quantum dots: syntheses, mechanism, and cellular imaging. ACS Appl Mater Interfaces. 2017;9(29):24846–56.
[539] Hong G-L, Zhao H-L, Deng H-H, Yang H-J, Peng H-P, Liu Y-H, et al. Fabrication of ultra-small monolayer graphene quantum dots by pyrolysis of trisodium citrate for fluorescent cell imaging. Int J Nanomed. 2018;13:4807.
[540] Hasan MT, Gonzalez-Rodriguez R, Lin CW, Campbell E, Vasireddy S, Tsedev U, et al. Rare-earth metal ions doped graphene quantum dots for near-ir *in vitro*/*in vivo*/*ex vivo* imaging applications. Adv Optical Mater. 2020;8(21):2000897.
[541] Zhu S, Zhou N, Hao Z, Maharjan S, Zhao X, Song Y, et al. Photoluminescent graphene quantum dots for *in vitro* and *in vivo* bioimaging using long wavelength emission. RSC Adv. 2015;5(49):39399–403.
[542] Badrigilan S, Shaabani B, Gharehaghaji N, Mesbahi A. Iron oxide/bismuth oxide nanocomposites coated by graphene quantum dots:"Three-in-one" theranostic agents for simultaneous CT/MR imaging-guided *in vitro* photothermal therapy. Photodiagnosis Photodynamic Ther. 2019;25:504–14.
[543] Li Z, Wang D, Xu M, Wang J, Hu X, Anwar S, et al. Fluorine-containing graphene quantum dots with a high singlet oxygen generation applied for photodynamic therapy. J Mater Chem B. 2020;8(13):2598–606.

[544] Nurunnabi M, Khatun Z, Huh KM, Park SY, Lee DY, Cho KJ, et al. *In vivo* biodistribution and toxicology of carboxylated graphene quantum dots. ACS Nano. 2013;7(8):6858–67.
[545] Xu A, He P, Ye C, Liu Z, Gu B, Gao B, et al. Polarizing graphene quantum dots toward long-acting intracellular reactive oxygen species evaluation and tumor detection. ACS Appl Mater Interfaces. 2020;12(9):10781–90.
[546] Fan H-y, Yu X-h, Wang K, Yin Y-j, Tang Y-j, Tang Y-l, et al. Graphene quantum dots (GQDs)-based nanomaterials for improving photodynamic therapy in cancer treatment. Eur J Medicinal Chem. 2019;182:111620.
[547] Huang C-L, Huang C-C, Mai F-D, Yen C-L, Tzing S-H, Hsieh H-T, et al. Application of paramagnetic graphene quantum dots as a platform for simultaneous dual-modality bioimaging and tumor-targeted drug delivery. J Mater Chem B. 2015;3(4):651–64.
[548] Yao X, Tian Z, Liu J, Zhu Y, Hanagata N. Mesoporous silica nanoparticles capped with graphene quantum dots for potential chemo–photothermal synergistic cancer therapy. Langmuir. 2017;33(2):591–9.
[549] Joshi PN, Agawane S, Athalye MC, Jadhav V, Sarkar D, Prakash R. Multifunctional inulin tethered silver-graphene quantum dots nanotheranostic module for pancreatic cancer therapy. Mater Sci Eng: C. 2017;78:1203–11.
[550] Atchudan R, Edison TNJI, Shanmugam M, Perumal S, Somanathan T, Lee YR. Sustainable synthesis of carbon quantum dots from banana peel waste using hydrothermal process for *in vivo* bioimaging. Phys E: Low-dimensional Syst Nanostruct. 2021;126:114417.
[551] Anthony AM, Murugan R, Subramanian R, Selvarangan GK, Pandurangan P, Dhanasekaran A, et al. Ultra-radiant photoluminescence of glutathione rigidified reduced carbon quantum dots (r-CQDs) derived from ice-biryani for *in vitro* and *in vivo* bioimaging applications. Colloids Surf A: Physicochem Eng Asp. 2020;586:124266.
[552] Ding Z, Li F, Wen J, Wang X, Sun R. Gram-scale synthesis of single-crystalline graphene quantum dots derived from lignin biomass. Green Chem. 2018;20(6):1383–90.
[553] Zhang Y-P, Ma J-M, Yang Y-S, Ru J-X, Liu X-Y, Ma Y, et al. Synthesis of nitrogen-doped graphene quantum dots (N-GQDs) from marigold for detection of Fe^{3+} ion and bioimaging. Spectrochim Acta Part A: Mol Biomole Spectrosc. 2019;217:60–7.
[554] Liu Y, Miyoshi H, Nakamura M. Nanomedicine for drug delivery and imaging: a promising avenue for cancer therapy and diagnosis using targeted functional nanoparticles. Int J Cancer. 2007;120(12):2527–37.
[555] Liu-Seifert H, Siemers E, Holdridge KC, Andersen SW, Lipkovich I, Carlson C, et al. Delayed-start analysis: mild Alzheimer's disease patients in solanezumab trials, 3.5 years. Alzheimer's Dement (N York, N Y). 2015;1(2):111–21.
[556] Weishaupt D, Kochli VD, Marincek B, Kim EE. How does MRI work? An introduction to the physics and function of magnetic resonance imaging. J Nucl Med. 2007;48(11):1910.
[557] Yao L, Xu S. Detection of magnetic nanomaterials in molecular imaging and diagnosis applications. Nanotechnol Rev. 2014;3(3):247–68.
[558] Trinder D, Macey DJ, Olynyk JK. The new iron age. Int J Mol Med. 2000;6(6):607–19.
[559] Blümich B, Callaghan PT. Principles of nuclear magnetic resonance microscopy. Magnetic Reson Chem. 1995;33(4):322–2.
[560] McGonagle D, Gibbon W, O'Connor P, Green M, Pease C, Emery P. Characteristic magnetic resonance imaging entheseal changes of knee synovitis in spondylarthropathy. Arthritis Rheumatism. 1998;41(4):694–700.
[561] Colombo M, Carregal-Romero S, Casula MF, Gutiérrez L, Morales MP, Böhm IB, et al. Biological applications of magnetic nanoparticles. Chem Soc Rev. 2012;41(11):4306.
[562] Caravan P, Ellison JJ, McMurry TJ, Lauffer RB. Gadolinium(III) chelates as MRI contrast agents: structure, dynamics, and applications. Chem Rev. 1999;99(9):2293–352.
[563] Servant A, Jacobs I, Bussy C, Fabbro C, Pach E, Ballesteros B, et al. Gadolinium-functionalised multi-walled carbon nanotubes as a T 1 contrast agent for MRI cell labelling and tracking. Carbon. 2016;97:126–33.
[564] Tóth É, Helm L, Merbach A. Relaxivity of Gadolinium(III) complexes: theory and mechanism. John Wiley & Sons, Ltd; 2013. p. 25–81.
[565] Ghaghada KB, Starosolski ZA, Bhayana S, Stupin I, Patel CV, Bhavane RC, et al. Pre-clinical evaluation of a nanoparticle-based blood-pool contrast agent for MR imaging of the placenta. Placenta. 2017;57:60–70.
[566] Vargo KB, Zaki AA, Warden-Rothman R, Tsourkas A, Hammer DA. Superparamagnetic iron oxide nanoparticle micelles stabilized by recombinant oleosin for targeted magnetic resonance imaging. Small (Weinh an der Bergstrasse, Ger). 2015;11(12):1409–13.
[567] Kievit FM, Zhang M. Surface engineering of iron oxide nanoparticles for targeted cancer therapy. Acc Chem Res. 2011;44(10):853–62.
[568] Mekuria SL, Debele TA, Tsai H-C. Encapsulation of Gadolinium Oxide Nanoparticle (Gd2O3) contrasting agents in PAMAM dendrimer templates for enhanced magnetic resonance imaging *in vivo*. ACS Appl Mater Interfaces. 2017;9(8):6782–95.
[569] Lin W, Hyeon T, Lanza GM, Zhang M, Meade TJ. Magnetic nanoparticles for early detection of cancer by magnetic resonance imaging. MRS Bull. 2009;34(6):441–8.
[570] Donato H, França M, Candelária I, et al. Liver MRI: from basic protocol to advanced techniques. Eur J Radiol. 2017;93:30–9.
[571] McQueen FM. Magnetic resonance imaging in early inflammatory arthritis: what is its role? Rheumatology. 2000;39(7):700–6.
[572] Tonolli-Serabian I, Poet JL, Dufour M, Carasset S, Mattei JP, Roux H. Magneic resonance imaging of the wrist in rheumatoid arthritis: comparison with other inflammatory joint diseases and control subjects. Clin Rheumatol. 1996;15(2):137–42.
[573] Cormode DP, Skajaa T, van Schooneveld MM, Koole R, Jarzyna P, Lobatto ME, et al. Nanocrystal core high-density lipoproteins: a multimodality contrast agent platform. Nano Lett. 2008;8(11):3715–23.
[574] Bai B, Zuo Z, Cheong SH, Vo B, Harper E, Lovshe D, et al. Novel chromosomal aberration as evidence of clonal evolution in a case of relapsed acute myeloid leukemia. Am Chin J Med Sci. 2012;5(1):48.

[575] Rauscher A, Barth M, Herrmann K-H, Witoszynskyj S, Deistung A, Reichenbach JR. Improved elimination of phase effects from background field inhomogeneities for susceptibility weighted imaging at high magnetic field strengths. Magnetic Reson Imaging. 2008;26(8):1145–51.
[576] Parkes LM, Hodgson R, Lu LT, Tung LD, Robinson I, Fernig DG, et al. Cobalt nanoparticles as a novel magnetic resonance contrast agent-relaxivities at 1.5 and 3 Tesla. Contrast Media Mol Imaging. 2008;3(4):150–6.
[577] Suri SS, Fenniri H, Singh B. Nanotechnology-based drug delivery systems. J Occup Med Toxicol (London, Engl). 2007;2:16–6.
[578] Calero-DdelC VL, Santiago-Quiñonez DI, Rinaldi C. Quantitative nanoscale viscosity measurements using magnetic nanoparticles and SQUID AC susceptibility measurements. Soft Matter. 2011;7(9):4497.
[579] Zborowski M, Chalmers JJ. Volume magnetic susceptibilities of selected substances. Elsevier; 2007. p. 443–4
[580] Barreto JA, O'Malley W, Kubeil M, Graham B, Stephan H, Spiccia L. Cancer research: nanomaterials: applications in cancer imaging and therapy (Adv Mater 12/2011). Adv Mater. 2011;23(12):H2.
[581] Pimpha N, Woramongkolchai N, Sunintaboon P, Saengkrit N. Recyclable iron oxide loaded poly (methyl methacrylate) core/polyethyleneimine shell nanoparticle as antimicrobial nanomaterial for zoonotic pathogen controls. J Clust Sci. 2021;1:1–11.
[582] Mornet S, Vasseur S, Grasset F, Duguet E. Magnetic nanoparticle design for medical diagnosis and therapy. J Mater Chem. 2004;14(14):2161–75.
[583] Wu W, Changzhong Jiang CJ, Roy VAL. Recent progress in magnetic iron oxide–semiconductor composite nanomaterials as promising photocatalysts. Nanoscale. 2015;7(1):38–58.
[584] Alizadeh N, Salimi A. Multienzymes activity of metals and metal oxide nanomaterials: applications from biotechnology to medicine and environmental engineering. J Nanobiotechnol. 2021;19(1):26.
[585] Lai C-W, Wang Y-H, Lai C-H, Yang M-J, Chen C-Y, Chou P-T, et al. Iridium-complex-functionalized Fe_3O_4/SiO2 core/shell nanoparticles: a facile three-in-one system in magnetic resonance imaging, luminescence imaging, and photodynamic therapy. Small. 2008;4(2):218–24.
[586] Zhou Q, Wei Y. For better or worse, iron overload by superparamagnetic iron oxide nanoparticles as a MRI contrast agent for chronic liver diseases. Chem Res Toxicol. 2016;30(1):73–80.
[587] Ahmed M, Douek M. The role of magnetic nanoparticles in the localization and treatment of breast cancer. BioMed Res Int. 2013;2013:281230.
[588] Israel LL, Galstyan A, Holler E, Ljubimova JY. Magnetic iron oxide nanoparticles for imaging, targeting and treatment of primary and metastatic tumors of the brain. J Controlled Release: Off J Controlled Rel Soc. 2020;320:45–62.
[589] Corot C, Robert P, Idee J, Port M. Recent advances in iron oxide nanocrystal technology for medical imaging☆. Adv Drug Delivery Rev. 2006;58(14):1471–504.
[590] McCarthy JR, Weissleder R. Multifunctional magnetic nanoparticles for targeted imaging and therapy. Adv drug delivery Rev. 2008;60(11):1241–51.
[591] Sosnovik DE, Nahrendorf M, Weissleder R. Magnetic nanoparticles for MR imaging: agents, techniques and cardiovascular applications. Basic Res Cardiol. 2008;103(2):122–30.
[592] Carroll MRJ, Huffstetler PP, Miles WC, Goff JD, Davis RM, Riffle JS, et al. The effect of polymer coatings on proton transverse relaxivities of aqueous suspensions of magnetic nanoparticles. Nanotechnology. 2011;22(32):325702.
[593] Lam T, Avti PK, Pouliot P, Maafi F, Tardif J-C, Rhéaume É, et al. Fabricating water dispersible superparamagnetic iron oxide nanoparticles for biomedical applications through ligand exchange and direct conjugation. Nanomater (Basel, Switz). 2016;6(6):100.
[594] Balasubramaniam S, Kayandan S, Lin Y-N, Kelly DF, House MJ, Woodward RC, et al. Toward design of magnetic nanoparticle clusters stabilized by biocompatible diblock copolymers for T2-weighted MRI contrast. Langmuir. 2014;30(6):1580–7.
[595] Bulte JWM, Kraitchman DL. Iron oxide MR contrast agents for molecular and cellular imaging. NMR Biomed. 2004;17(7):484–99.
[596] Zhang F, Huang X, Qian C, Zhu L, Hida N, Niu G, et al. Synergistic enhancement of iron oxide nanoparticle and gadolinium for dual-contrast MRI. Biochem Biophys Res Commun. 2012;425(4):886–91.
[597] Wei Y, Zhao M, Yang F, Mao Y, Xie H, Zhou Q. Iron overload by superparamagnetic iron oxide nanoparticles is a high risk factor in cirrhosis by a systems toxicology assessment. Sci Rep. 2016;6:29110.
[598] Singh N, Jenkins GJS, Asadi R, Doak SH. Potential toxicity of superparamagnetic iron oxide nanoparticles (SPION). Nano Rev. 2010;1:5358. doi: 10.3402/nano.v1i0.5358-10.3402/nano.v1i0.5358.
[599] Wu M, Huang S. Magnetic nanoparticles in cancer diagnosis, drug delivery and treatment. Mol Clin Oncol. 2017;7(5):738–46.
[600] Gupta AK, Gupta M. Synthesis and surface engineering of iron oxide nanoparticles for biomedical applications. Biomaterials. 2005;26(18):3995–4021.
[601] Lindemann A, Lüdtke-Buzug K, Fräderich BM, Gräfe K, Pries R, Wollenberg B. Biological impact of superparamagnetic iron oxide nanoparticles for magnetic particle imaging of head and neck cancer cells. Int J Nanomed. 2014;9:5025–40.
[602] Ferguson RM, Khandhar AP, Kemp SJ, Arami H, Saritas EU, Croft LR, et al. Magnetic particle imaging with tailored iron oxide nanoparticle tracers. IEEE Trans Med Imaging. 2015;34(5):1077–84.
[603] Torkashvand N, Sarlak N. Fabrication of a dual T1 and T2 contrast agent for magnetic resonance imaging using cellulose nanocrystals/Fe_3O_4 nanocomposite. Eur Polym J. 2019;118:128–36.
[604] Roman M. Toxicity of cellulose nanocrystals: a review. Ind Biotechnol. 2015;11(1):25–33.
[605] Lin N, Dufresne A. Nanocellulose in biomedicine: current status and future prospect. Eur Polym J. 2014;59:302–25.
[606] Endes C, Camarero-Espinosa S, Mueller S, Foster E, Petri-Fink A, Rothen-Rutishauser B, et al. A critical review of the current knowledge regarding the biological impact of nanocellulose. J Nanobiotechnol. 2016;14(1):1–14.

[607] Bindschedler S, Vu Bouquet TQT, Job D, Joseph E, Junier P. Fungal biorecovery of gold from E-waste. Elsevier; 2017. p. 53–81.
[608] Jamalipour Soufi G, Iravani S. Eco-friendly and sustainable synthesis of biocompatible nanomaterials for diagnostic imaging: current challenges and future perspectives. Green Chem. 2020;22(9):2662–87.
[609] Gurunathan S, Han J, Park JH, Kim J-H. A green chemistry approach for synthesizing biocompatible gold nanoparticles. Nanoscale Res Lett. 2014;9(1):248.
[610] Narayanan S, Sathy BN, Mony U, Koyakutty M, Nair SV, Menon D. Biocompatible magnetite/gold nanohybrid contrast agents *via* green chemistry for MRI and CT bioimaging. ACS Appl Mater Interfaces. 2011;4(1):251–60.
[611] Eyvazzadeh N, Shakeri-Zadeh A, Fekrazad R, Amini E, Ghaznavi H, Kamrava SK. Gold-coated magnetic nanoparticle as a nanotheranostic agent for magnetic resonance imaging and photothermal therapy of cancer. Lasers Med Sci. 2017;32(7):1469–77.
[612] Kumagai M, Kano MR, Morishita Y, Ota M, Imai Y, Nishiyama N, et al. Enhanced magnetic resonance imaging of experimental pancreatic tumor *in vivo* by block copolymer-coated magnetite nanoparticles with TGF-β inhibitor. J Controlled Rel. 2009;140(3):306–11.
[613] Kumagai M, Sarma TK, Cabral H, Kaida S, Sekino M, Herlambang N, et al. Enhanced *in vivo* magnetic resonance imaging of tumors by PEGylated iron-oxide-gold core–shell nanoparticles with prolonged blood circulation properties. Macromol Rapid Commun. 2010;31(17):1521–8.
[614] Lyon JL, Fleming DA, Stone MB, Schiffer P, Williams ME. Synthesis of Fe oxide core/Au shell nanoparticles by iterative hydroxylamine seeding. Nano Lett. 2004;4(4):719–23.
[615] Wang J, Luo Q, Fan M, Suzuki IS, Suzuki MH, Engelhard Y, et al. Monodispersed core–shell Fe_3O_4@Au nanoparticles. J Phys Chem B. 2005;109(46):21593–601.
[616] Xu Z, Hou Y, Sun S. Magnetic core/shell Fe_3O_4/Au and Fe_3O_4/Au/Ag nanoparticles with tunable plasmonic properties. J Am Chem Soc. 2007;129(28):8698–9.
[617] Kim TK, Seo KS, Kwon SO, Kim HS, Kim JH, Jeong MW, et al. Applying the quality by design to robust optimization and design space define for erythropoietin cell culture process. Bull Korean Chem Soc. 2019;40(10):1002–12.
[618] Kojima H, Mukai Y, Yoshikawa M, Kamei K, Yoshikawa T, Morita M, et al. Simple PEG conjugation of SPIO *via* an Au–S bond improves its tumor targeting potency as a novel MR tumor imaging agent. Bioconjugate Chem. 2010;21(6):1026–31.
[619] Larson TA, Bankson J, Aaron J, Sokolov K. Hybrid plasmonic magnetic nanoparticles as molecular specific agents for MRI/optical imaging and photothermal therapy of cancer cells. Nanotechnology. 2007;18(32):325101.
[620] Modugno G, Ménard-Moyon C, Prato M, Bianco A. Carbon nanomaterials combined with metal nanoparticles for theranostic applications. Br J Pharmacol. 2015;172(4):975–91.
[621] Faria PCBd, Santos LId, Coelho JP, Ribeiro HB, Pimenta MA, Ladeira LO, et al. Oxidized multiwalled carbon nanotubes as antigen delivery system to promote superior CD8+ T cell response and protection against cancer. Nano Lett. 2014;14(9):5458–70.
[622] Chen Z, Zhang A, Wang X, Zhu J, Fan Y, Yu H, et al. The advances of carbon nanotubes in cancer diagnostics and therapeutics. J Nanomater. 2017;2017:1–13.
[623] Cha C, Shin SR, Annabi N, Dokmeci MR, Khademhosseini A. Carbon-based nanomaterials: multifunctional materials for biomedical engineering. Carbon Mater Nanotechnol. 2013;7(4):2891–7.
[624] Krueger A. Paper cutout DIY kit; 2010. p. 475.
[625] Zhang M, Cao Y, Chong Y, Ma Y, Zhang H, Deng Z, et al. Graphene oxide based theranostic platform for T1-weighted magnetic resonance imaging and drug delivery. ACS Appl Mater Interfaces. 2013;5(24):13325–32.
[626] Ma X, Tao H, Yang K, Feng L, Cheng L, Shi X, et al. A functionalized graphene oxide-iron oxide nanocomposite for magnetically targeted drug delivery, photothermal therapy, and magnetic resonance imaging. Nano Res. 2012;5(3):199–212.
[627] Chen W, Yi P, Zhang Y, Zhang L, Deng Z, Zhang Z. Composites of aminodextran-coated Fe_3O_4 nanoparticles and graphene oxide for cellular magnetic resonance imaging. ACS Appl Mater Interfaces. 2011;3(10):4085–91.
[628] Yin M, Wang M, Miao F, Ji Y, Tian Z, Shen H, et al. Water-dispersible multiwalled carbon nanotube/iron oxide hybrids as contrast agents for cellular magnetic resonance imaging. Carbon. 2012;50(6):2162–70.
[629] Al Faraj A, Shaik AS, Al Sayed B. Preferential magnetic targeting of carbon nanotubes to cancer sites: noninvasive tracking using MRI in a murine breast cancer model. Nanomedicine. 2015;10(6):931–48.
[630] Gonzalez-Rodriguez R, Campbell E, Naumov A. Multifunctional graphene oxide/iron oxide nanoparticles for magnetic targeted drug delivery dual magnetic resonance/fluorescence imaging and cancer sensing. PLoS One. 2019;14(6):e0217072.
[631] Mkhoyan KA, Contryman AW, Silcox J, Stewart DA, Eda G, Mattevi C, et al. Atomic and electronic structure of graphene-oxide. Nano Lett. 2009;9(3):1058–63.
[632] Zhu X, Liu Y, Li P, Nie Z, Li J. Applications of graphene and its derivatives in intracellular biosensing and bioimaging. Analyst. 2016;141(15):4541–53.
[633] O'Neal SL, Zheng W. Manganese toxicity upon overexposure: a decade in review. Curr Environ Health Rep. 2015;2(3):315–28.
[634] Hu F, Zhao YS. Inorganic nanoparticle-based T1 and T1/T2 magnetic resonance contrast probes. Nanoscale. 2012;4(20):6235.
[635] Qu D, Wang X, Bao Y, Sun Z. Recent advance of carbon dots in bio-related applications. J Phys: Mater. 2020;3(2):22003.
[636] Tripathi M, Sahu JN, Ganesan P. Effect of process parameters on production of biochar from biomass waste through pyrolysis: a review. Renew Sustain Energy Rev. 2016;55:467–81.
[637] Queiroz LS, de Souza LKC, Thomaz KTC, Leite Lima ET, da Rocha Filho GN, do Nascimento LAS, et al. Activated carbon obtained from amazonian biomass tailings (acai seed): modification, characterization, and use for removal of metal ions from water. J Environ Manag. 2020;270:110868.
[638] Fan H, Zhang M, Bhandari B, Yang C-H. Food waste as a carbon source in carbon quantum dots technology and their

applications in food safety detection. Trends Food Sci Technol. 2020;95:86–96.
[639] Xu Y, Tang C-J, Huang H, Sun C-Q, Zhang Y-K, Ye Q-F, et al. Green synthesis of fluorescent carbon quantum dots for detection of Hg^{2+}. Chin J Anal Chem. 2014;42(9):1252–8.
[640] Mewada A, Pandey S, Shinde S, Mishra N, Oza G, Thakur M, et al. Green synthesis of biocompatible carbon dots using aqueous extract of Trapa bispinosa peel. Mater Sci Eng: C. 2013;33(5):2914–7.
[641] Zhang J, Yuan Y, Gao M, Han Z, Chu C, Li Y, et al. Imaging agents carbon dots as a new class of diamagnetic chemical exchange saturation transfer (diaCEST) MRI contrast agents. Angewandte. 2019;58:9871–5.
[642] Wang H, Shen J, Li Y, Wei Z, Cao G, Gai Z, et al. Magnetic iron oxide–fluorescent carbon dots integrated nanoparticles for dual-modal imaging, near-infrared light-responsive drug carrier and photothermal therapy. Biomater Sci. 2014;2(6):915–23.
[643] Liu X, Jiang H, Ye J, Zhao C, Gao S, Wu C, et al. Nitrogen-doped carbon quantum dot stabilized magnetic iron oxide nanoprobe for fluorescence, magnetic resonance, and computed tomography triple-modal *in vivo* bioimaging. Adv Funct Mater. 2016;26(47):8694–706.
[644] Gulani V, Calamante F, Shellock FG, Kanal E, Reeder SB. Gadolinium deposition in the brain: summary of evidence and recommendations. Lancet Neurol. 2017;16(7):564–70.
[645] Ji Z, Ai P, Shao C, Wang T, Yan C, Ye L, et al. Manganese-doped carbon dots for magnetic resonance/optical dual-modal imaging of tiny brain glioma. ACS Biomater Sci Eng. 2018;4(6):2089–94.
[646] Rub Pakkath SA, Chetty SS, Selvarasu P, Vadivel Murugan A, Kumar Y, Periyasamy L, et al. Transition metal ion (Mn^{2+}, Fe^{2+}, Co^{2+}, and Ni^{2+})-doped carbon dots synthesized *via* microwave-assisted pyrolysis: a potential nanoprobe for magneto-fluorescent dual-modality bioimaging. ACS Biomater Sci Eng. 2018;4(7):2582–96.
[647] Zhao M, Beauregard DA, Loizou L, Davletov B, Brindle KM. Non-invasive detection of apoptosis using magnetic resonance imaging and a targeted contrast agent. Nat Med. 2001;7(11):1241–4.
[648] Hatakeyama S, Sugihara K, Shibata TK, Nakayama J, Akama TO, Tamura N, et al. Targeted drug delivery to tumor vasculature by a carbohydrate mimetic peptide. Proc Natl Acad Sci U S Am. 2011;108(49):19587–92.
[649] Yadollahpour A, Rashidi S. Magnetic nanoparticles: a review of chemical and physical characteristics important in medical applications. Orient J Chem. 2015;31(Special Issue 1):25–30.
[650] Liu Y, Ai K, Yuan Q, Lu L. Fluorescence-enhanced gadolinium-doped zinc oxide quantum dots for magnetic resonance and fluorescence imaging. Biomaterials. 2011;32(4):1185–92.
[651] Zhang Y, Nayak T, Hong H, Cai W. Biomedical applications of zinc oxide nanomaterials. Curr Mol Med. 2013;13(10):1633–45.
[652] Nagraik R, Sharma A, Kumar D, Mukherjee S, Sen F, Kumar AP. Amalgamation of biosensors and nanotechnology in disease diagnosis: mini-review. Sens Int. 2021;2:100089.
[653] Townshend B, Xiang JS, Manzanarez G, Hayden EJ, Smolke CD. A multiplexed, automated evolution pipeline enables scalable discovery and characterization of biosensors. Nat Commun. 2021;12(1):1437.
[654] Sing J, Vyas A, Wang S, Prasad R. Microbial biotechnology: basic research and applications. 1 edn. 2020.
[655] Clark LC, Gollan F, Gupta VB. The oxygenation of blood by gas dispersion. Science. 1950;111(2874):85–7.
[656] Cammann K. Bio-sensors based on ion-selective electrodes. Fresenius' Z für analytische Chem. 1977;287(1):1–9.
[657] Ali J, Najeeb J, Ali MA, Aslam MF, Raza A. Biosensors: their fundamentals, designs, types and most recent impactful applications: a review. J J Biosens Bioelectron. 2017;8:1–9.
[658] Svechtarova MI, Buzzacchera I, Toebes BJ, Lauko J, Anton N, Wilson CJ. Sensor devices inspired by the five senses: a review. Electroanalysis. 2016;28(6):1201–41.
[659] Naresh V, Lee N. A review on biosensors and recent development of nanostructured materials-enabled biosensors. Sens (Switz). 2021;21(4):1–35.
[660] Mishra RK, Hubble LJ, Martín A, Kumar R, Barfidokht A, Kim J, et al. Wearable flexible and stretchable glove biosensor for on-site detection of organophosphorus chemical threats. ACS Sens. 2017;2(4):553–61.
[661] Pundir CS, Narang J. Biosensors an introductory textbook. 1 edn. Jenny Stanford Publishing; 2017.
[662] World Health Organizations. Global report on diabetes. Geneva; 2016.
[663] Bruen D, Delaney C, Florea L, Diamond D. Glucose sensing for diabetes monitoring: recent developments. Sensors (Basel, Switzerland). 2017;17(8):1866.
[664] Pohanka M, Skladal P. Electrochemical biosensors – principles and applications. J Appl Biomed. 2008;6(2):57–64.
[665] Revathi C, Rajendra kumar RT. Chapter 7 – Enzymatic and nonenzymatic electrochemical biosensors, In: M Hywel, CS Rout, DJ Late, editors. Woodhead Publishing; 2019, p. 259–300.
[666] Muthuchamy N, Gopalan A, Lee K-P. Highly selective non-enzymatic electrochemical sensor based on a titanium dioxide nanowire–poly(3-aminophenyl boronic acid)–gold nanoparticle ternary nanocomposite. RSC Adv. 2018;8(4):2138–47.
[667] Mehrabi H, Kazemi-Mireki M. CuO nanoparticles: an efficient and recyclable nanocatalyst for the rapid and green synthesis of 3,4-dihydropyrano[c]chromenes. Chin Chem Lett. 2011;22(12):1419–22.
[668] Zhang Y, Li N, Xiang Y, Wang D, Zhang P, Wang Y, et al. A flexible non-enzymatic glucose sensor based on copper nanoparticles anchored on laser-induced graphene. Carbon. 2020;156:506–13.
[669] Tuerhong M, Xu Y, Yin X-B. Review on carbon dots and their applications. Chin J Anal Chem. 2017;45(1):139–50.
[670] Putzbach W, Ronkainen NJ. Immobilization techniques in the fabrication of nanomaterial-based electrochemical biosensors: a review. Sens (Basel, Switz). 2013;13(4):4811–40.
[671] Ahmad R, Tripathy N, Ahn M-S, Bhat KS, Mahmoudi T, Wang Y, et al. Highly efficient non-enzymatic glucose sensor based on CuO modified vertically-grown ZnO nanorods on electrode. Sci Rep. 2017;7(1):5715.
[672] Markides H, Rotherham M, El Haj AJ. Biocompatibility and toxicity of magnetic nanoparticles in regenerative medicine. J Nanomater. 2012;2012:614094.

[673] Li Z-X, Luo D, Li M-M, Xing X-F, Ma Z-Z, Xu H. Recyclable Fe_3O_4 Nanoparticles catalysts for aza-michael addition of acryl amides by magnetic field. Catalysts. 2017;7(7):219.
[674] Kim H, Lee K, Woo SI, Jung Y. On the mechanism of enhanced oxygen reduction reaction in nitrogen-doped graphene nanoribbons. Phys Chem Chem Phys. 2011;13(39):17505–10.
[675] Liu Y, Wang M, Zhao F, Xu Z, Dong S. The direct electron transfer of glucose oxidase and glucose biosensor based on carbon nanotubes/chitosan matrix. Biosens Bioelectron. 2005;21(6):984–8.
[676] Zhang W, Li X, Zou R, Wu H, Shi H, Yu S, et al. Multifunctional glucose biosensors from Fe_3O_4 nanoparticles modified chitosan/graphene nanocomposites. Sci Rep. 2015(June);5:1–9.
[677] World Health Organization (WHO)-Fact sheets. Cancer; 2021
[678] Etzioni R, Urban N, Ramsey S, McIntosh M, Schwartz S, Reid B, et al. The case for early detection, nature reviews. Cancer. 2003;3(4):243–52.
[679] Cohen JD, Li L, Wang Y, Thoburn C, Afsari B, Danilova L, et al. Detection and localization of surgically resectable cancers with a multi-analyte blood test. Sci (N York, NY). 2018;359(6378):926–30.
[680] Pasinszki T, Krebsz M, Tung TT, Losic D. Carbon nanomaterial based biosensors for non-invasive detection of cancer and disease biomarkers for clinical diagnosis. Sens (Basel, Switz). 2017;17(8):1919.
[681] Sekhon SS, Kaur P, Kim Y-H, Sekhon SS. 2D graphene oxide–aptamer conjugate materials for cancer diagnosis. NPJ 2D Mater Appl. 2021;5(1):21.
[682] Cheng C, Li S, Thomas A, Kotov NA, Haag R. Functional graphene nanomaterials based architectures: biointeractions, fabrications, and emerging biological applications. Chem Rev. 2017;117(3):1826–914.
[683] Liu Z, Robinson JT, Sun X, Dai H. PEGylated nanographene oxide for delivery of water-insoluble cancer drugs. J Am Chem Soc. 2008;130(33):10876–7.
[684] Tan J, Lai Z, Zhong L, Zhang Z, Zheng R, Su J, et al. A graphene oxide-based fluorescent aptasensor for the turn-on detection of CCRF-CEM. Nanoscale Res Lett. 2018;13(1):66.
[685] Berkmans AJ, Jagannatham M, Priyanka S, Haridoss P. Synthesis of branched, nano channeled, ultrafine and nano carbon tubes from PET wastes using the arc discharge method. Waste Manag. 2014;34(11):2139–45.
[686] Singh C, Srivastava S, Ali MA, Gupta TK, Sumana G, Srivastava A, et al. Carboxylated multiwalled carbon nanotubes based biosensor for aflatoxin detection. Sens Actuators B: Chem. 2013;185:258–64.
[687] C. International Agency for Research on. IARC monographs on the evaluations of carcinogenic risks to human; 1993. p. 489–521.
[688] Moss MO. Risk assessment for aflatoxins in foodstuffs. Int Biodeterior Biodegrad. 2002;50(3):137–42.
[689] Parkin DM, Pisani P, Ferlay J. Global cancer statistics. CA: A Cancer J Clinicians. 1999;49(1):33–64.
[690] Hussain S, Amjad M. A review on gold nanoparticles (GNPs) and their advancement in cancer therapy. Int J Nanomater, Nanotechnol Nanomed. 2021;7(1):19–25.
[691] Alam MN, Das S, Batuta S, Roy N, Chatterjee A, Mandal D, et al. Leaf extract: an efficient green multifunctional agent for the controlled synthesis of Au nanoparticles. ACS Sustain Chem Eng. 2014;2(4):652–64.
[692] Ahmed S, Annu A, Ikram S, Yuda S. Biosynthesis of gold nanoparticles: a green approach. J Photochem Photobiol B: Biol. 2016;161:141–53.
[693] Zhang R, Wang S, Huang X, Yang Y, Fan H, Yang F, et al. Gold-nanourchin seeded single-walled carbon nanotube on voltammetry sensor for diagnosing neurogenerative Parkinson's disease. Anal Chim Acta. 2020;1094:142–50.
[694] Surmeier DJ, Obeso JA, Halliday GM. Selective neuronal vulnerability in Parkinson disease, nature reviews. Neuroscience. 2017;18(2):101–13.
[695] Cebrián C, Sulzer D. Neuroinflammation as a potential mechanism underlying parkinsons disease, parkinson's disease. Elsevier; 2017. p. 245–79.
[696] Curulli A, Cesaro SN, Coppe A, Silvestri C, Palleschi G. Functionalization and Dissolution of single-walled carbon nanotubes by chemical-physical and electrochemical treatments. Microchim Acta. 2006;152(3):225–32.
[697] Jain A, Homayoun A, Bannister CW, Yum K. Single-walled carbon nanotubes as near-infrared optical biosensors for life sciences and biomedicine. Biotechnol J. 2015;10(3):447–59.
[698] Letchumanan I, Gopinath SCB, Md Arshad MK, Anbu P, Lakshmipriya T. Gold nano-urchin integrated label-free amperometric aptasensing human blood clotting factor IX: a prognosticative approach for "Royal disease". Biosens Bioelectron. 2019;131:128–35.
[699] Lakshmipriya T, Fujimaki M, Gopinath SCB, Awazu K, Horiguchi Y, Nagasaki Y. A high-performance waveguide-mode biosensor for detection of factor IX using PEG-based blocking agents to suppress non-specific binding and improve sensitivity. Analyst. 2013;138(10):2863–70.
[700] Bohli N, Chammem H, Meilhac O, Mora L, Abdelghani A. Electrochemical impedance spectroscopy on interdigitated gold microelectrodes for glycosylated human serum albumin characterization. IEEE Trans Nanobiosci. 2017;16(8):676–81.
[701] Napi MLM, Sultan SM, Ismail R, How KW, Ahmad MK. Electrochemical-based biosensors on different zinc oxide nanostructures: a review. Materials. 2019;12(18):1–34.
[702] Xu JK, Zhang FF, Sun JJ, Sheng J, Wang F, Sun M. Bio and nanomaterials based on Fe_3O_4. Molecules. 2014;19(12):21506–28.
[703] Khezerlou A, Alizadeh-sani M, Azizi-lalabadi M, Ehsani A. Microbial Pathogenesis Nanoparticles and their antimicrobial properties against pathogens including bacteria, fungi, parasites and viruses. Microb Pthogenesis. 2018;123(August):505–26.
[704] Wang L, Hu C, Shao L. The antimicrobial activity of nanoparticles: present situation and prospects for the future. Int J Nanomed. 2017;12:1227.
[705] Murthy S, Effiong P, Fei CC. Metal oxide nanoparticles in biomedical applications. Metal oxide powder technologies. Elsevier; 2020. p. 233–51.
[706] Dizaj SM, Mennati A, Jafari S, Khezri K, Adibkia K. Antimicrobial activity of carbon-based nanoparticles. Adv Pharm Bull. 2015;5(1):19–23.
[707] Das Purkayastha M, Manhar AK, Mandal M, Mahanta CL. Industrial waste-derived nanoparticles and microspheres can be potent antimicrobial and functional ingredients. J Appl Chem. 2014;2014:1–12.

[708] Salesa B, Martí M, Frígols B, Serrano-Aroca Á. Carbon nanofibers in pure form and in calcium alginate composites films: new cost-effective antibacterial biomaterials against the life-threatening multidrug-resistant staphylococcus epidermidis. Polymers. 2019;11(3):453.
[709] Song K, Wu Q, Zhang Z, Ren S, Lei T, Negulescu II, et al. Porous carbon nanofibers from electrospun biomass tar/polyacrylonitrile/silver hybrids as antimicrobial materials. ACS Appl Mater Interfaces. 2015;7(27):15108–16.
[710] Umar MF, Ahmad F, Saeed H, Usmani SA, Owais M, Rafatullah M. Bio-mediated synthesis of reduced graphene oxide nanoparticles from chenopodium album: their antimicrobial and anticancer activities. Nanomaterials. 2020;10(6):1096.
[711] Thiyagarajulu N, Arumugam S, Narayanan AL, Mathivanan T, Renuka RR. Green synthesis of reduced graphene nanosheets using leaf extract of tridax procumbens and its potential *in vitro* biological activities; 2020.
[712] Chu GM, Jung CK, Kim HY, Ha JH, Kim JH, Jung MS, et al. Effects of bamboo charcoal and bamboo vinegar as antibiotic alternatives on growth performance, immune responses and fecal microflora population in fattening pigs. Anim Sci J. 2013;84(2):113–20.
[713] Varghese S, Kuriakose S, Jose S. Antimicrobial activity of carbon nanoparticles isolated from natural sources against pathogenic gram-negative and gram-positive bacteria. J Nanosci. 2013;2013:1–5.
[714] Azizi-Lalabadi M, Hashemi H, Feng J, Jafari SM. Carbon nanomaterials against pathogens; the antimicrobial activity of carbon nanotubes, graphene/graphene oxide, fullerenes, and their nanocomposites. Adv Colloid Interface Sci. 2020;284:102250.
[715] Noor S, Shah Z, Javed A, Ali A, Hussain SB, Zafar S, et al. A fungal based synthesis method for copper nanoparticles with the determination of anticancer, antidiabetic and antibacterial activities. J Microbiol Methods. 2020;174:105966.
[716] Rajeshkumar S, Menon S, Kumar SV, Tambuwala MM, Bakshi HA, Mehta M, et al. Antibacterial and antioxidant potential of biosynthesized copper nanoparticles mediated through Cissus arnotiana plant extract. J Photochem Photobiol B: Biol. 2019;197:111531.
[717] Jeronsia JE, Joseph LA, Vinosha PA, Mary AJ, Das SJ. Camellia sinensis leaf extract mediated synthesis of copper oxide nanostructures for potential biomedical applications. Mater Today: Proc. 2019;8:214–22.
[718] Sukri SNAM, Shameli K, Wong MM-T, Teow S-Y, Chew J, Ismail NA. Cytotoxicity and antibacterial activities of plant-mediated synthesized zinc oxide (ZnO) nanoparticles using Punica granatum (pomegranate) fruit peels extract. J Mol Struct. 2019;1189:57–65.
[719] Raja A, Ashokkumar S, Marthandam RP, Jayachandiran J, Khatiwada CP, Kaviyarasu K, et al. Eco-friendly preparation of zinc oxide nanoparticles using Tabernaemontana divaricata and its photocatalytic and antimicrobial activity. J Photochem Photobiol B: Biol. 2018;181:53–8.
[720] Jacinto MJ, Silva VC, Valladão DMS, Souto RS. Biosynthesis of magnetic iron oxide nanoparticles: a review. Biotechnol Lett. 2021;43(1):1–12.
[721] Farouk F, Abdelmageed M, Azam Ansari M, Azzazy HME. Synthesis of magnetic iron oxide nanoparticles using pulp and seed aqueous extract of Citrullus colocynth and evaluation of their antimicrobial activity. Biotechnol Lett. 2020;42(2):231–40.
[722] Niraimathee V, Subha V, Ravindran RE, Renganathan S. Green synthesis of iron oxide nanoparticles from Mimosa pudica root extract. Int J Environ Sustain Dev. 2016;15(3):227–40.
[723] Daniel SK, Vinothini G, Subramanian N, Nehru K, Sivakumar M. Biosynthesis of Cu, ZVI, and Ag nanoparticles using Dodonaea viscosa extract for antibacterial activity against human pathogens. J Nanopart Res. 2013;15(1):1–10.
[724] Pattanayak M, Nayak P. Green synthesis and characterization of zero valent iron nanoparticles from the leaf extract of Azadirachta indica (Neem). World J Nano Sci Technol. 2013;2(1):6–9.
[725] Senthil M, Ramesh C. Biogenic synthesis of Fe_3O_4 nanoparticles using tridax procumbens leaf extract and its antibacterial activity on pseudomonas aeruginosa. Dig J Nanomater Biostruct (DJNB). 2012;7(4).
[726] Arularasu M, Devakumar J, Rajendran T. An innovative approach for green synthesis of iron oxide nanoparticles: characterization and its photocatalytic activity. Polyhedron. 2018;156:279–90.
[727] Vitta Y, Figueroa M, Calderon M, Ciangherotti C. Synthesis of iron nanoparticles from aqueous extract of Eucalyptus robusta Sm and evaluation of antioxidant and antimicrobial activity. Mater Sci Energy Technol. 2020;3:97–103.
[728] Sundrarajan M, Bama K, Bhavani M, Jegatheeswaran S, Ambika S, Sangili A, et al. Obtaining titanium dioxide nanoparticles with spherical shape and antimicrobial properties using M. citrifolia leaves extract by hydrothermal method. J Photochem Photobiol B: Biol. 2017;171:117–24.
[729] Gebre SH, Sendeku MG. New frontiers in the biosynthesis of metal oxide nanoparticles and their environmental applications: an overview. SN Appl Sci. 2019;1(8):1–28.
[730] Alavi M, Karimi N. Characterization, antibacterial, total antioxidant, scavenging, reducing power and ion chelating activities of green synthesized silver, copper and titanium dioxide nanoparticles using Artemisia haussknechtii leaf extract, artificial cells. Nanomed, Biotechnol. 2018;46(8):2066–81.
[731] Shahriari M, Hemmati S, Zangeneh A, Zangeneh MM. Biosynthesis of gold nanoparticles using Allium noeanum Reut. ex Regel leaves aqueous extract; characterization and analysis of their cytotoxicity, antioxidant, and antibacterial properties. Appl Organomet Chem. 2019;33(11):e5189–89.
[732] Devi P, Saini S, Kim KH. The advanced role of carbon quantum dots in nanomedical applications. Biosens Bioelectron. 2019;141(March):111158.
[733] Lin F, Li C, Chen Z. Bacteria-derived carbon dots inhibit biofilm formation of Escherichia coli without affecting cell growth. Front Microbiol. 2018;9(Feb):1–9.
[734] Doghish AS, El-Sayyad GS, Sallam AM, Khalil WF, El Rouby WMA. Graphene oxide and its nanocomposites with EDTA or chitosan induce apoptosis in MCF-7 human breast cancer. RSC Advances. 2021;11(46):29052–64.
[735] Mezni A, Saber NB, Alhadhrami A, Gobouri A, Aldalbahi A, Hay S, et al. Highly biocompatible carbon nanocapsules

derived from plastic waste for advanced cancer therapy. J Drug Delivery Sci Technol. 2017;41:351–8.
[736] Negri V, Pacheco-Torres J, Calle D, López-Larrubia P. Carbon nanotubes in biomedicine. Top Curr Chem (Cham). 2020;378(1):15.
[737] Zhou X, Wang Y, Gong C, Liu B, Wei G. Production, structural design, functional control, and broad applications of carbon nanofiber-based nanomaterials: a comprehensive review. Chem Eng J. 2020;126189.
[738] Ashfaq M, Khan S, Verma N. Synthesis of PVA-CAP-based biomaterial in situ dispersed with Cu nanoparticles and carbon micro-nanofibers for antibiotic drug delivery applications. Biochem Eng J. 2014;90:79–89.
[739] Wang C-J, Chen T-C, Lin J-H, Huang P-R, Tsai H-J, Chen C-S. One-step preparation of hydrophilic carbon nanofiber containing magnetic Ni nanoparticles materials and their application in drug delivery. J Colloid Interface Sci. 2015;440:179–88.
[740] Thiyagarajulu N, Arumugam S. Green synthesis of reduced graphene oxide nanosheets using leaf extract of lantana camara and its in-vitro biological activities. J Clust Sci. 2020;32:1–10.
[741] Chu M, Peng J, Zhao J, Liang S, Shao Y, Wu Q. Laser light triggered-activated carbon nanosystem for cancer therapy. Biomaterials. 2013;34(7):1820–32.
[742] Naik GG, Shah J, Balasubramaniam AK, Sahu AN. Applications of natural product-derived carbon dots in cancer biology. Nanomedicine. 2021;16(7):587–608.
[743] Şimşek S, Şüküroğlu AA, Yetkin D, Özbek B, Battal D, Genç R. DNA-damage and cell cycle arrest initiated anti-cancer potency of super tiny carbon dots on MCF7 cell line. Sci Rep. 2020;10(1):1–14.
[744] Jia Q, Zheng X, Ge J, Liu W, Ren H, Chen S, et al. Synthesis of carbon dots from Hypocrella bambusae for bimodel fluorescence/photoacoustic imaging-guided synergistic photodynamic/photothermal therapy of cancer. J Colloid Interface Sci. 2018;526:302–11.
[745] Thakur M, Kumawat MK, Srivastava R. Multifunctional graphene quantum dots for combined photothermal and photodynamic therapy coupled with cancer cell tracking applications. RSC Adv. 2017;7(9):5251–61.
[746] Tade RS, Nangare SN, Patil AG, Pandey A, Deshmukh PK, Patil DR, et al. Recent advancement in bio-precursor derived graphene quantum dots: synthesis, characterization and toxicological perspective. Nanotechnology. 2020;31(29):292001.
[747] Kotcherlakota R, Das S, Patra CR. Therapeutic applications of green-synthesized silver nanoparticles. Elsevier; 2019. p. 389–428
[748] Sunderam V, Thiyagarajan D, Lawrence AV, Mohammed SSS, Selvaraj A. In-vitro antimicrobial and anticancer properties of green synthesized gold nanoparticles using Anacardium occidentale leaves extract. Saudi J Biol Sci. 2019;26(3):455–9.
[749] Noah N. Potential applications of greener synthesized silver and gold nanoparticles in medicine. Springer; 2020. p. 95–126
[750] Yallappa S, Manjanna J, Dhananjaya BL, Vishwanatha U, Ravishankar B, Gururaj H. Phytosynthesis of gold nanoparticles using Mappia foetida leaves extract and their conjugation with folic acid for delivery of doxorubicin to cancer cells. J Mater Sci: Mater Med. 2015;26(9):1–12.
[751] Andreescu S, Ornatska M, Erlichman JS, Estevez A, Leiter J. Biomedical applications of metal oxide nanoparticles, Fine particles in medicine and pharmacy. Springer; 2012. p. 57–100.
[752] Jeevanandam J, Kulabhusan PK, Sabbih G, Akram M, Danquah MK. Phytosynthesized nanoparticles as a potential cancer therapeutic agent. 3 Biotech. 2020;10(12):1–26.
[753] Kalaiarasi A, Sankar R, Anusha C, Saravanan K, Aarthy K, Karthic S, et al. Copper oxide nanoparticles induce anticancer activity in A549 lung cancer cells by inhibition of histone deacetylase. Biotechnol Lett. 2018;40(2):249–56.
[754] Singh RP. Potential of biogenic plant-mediated copper and copper oxide nanostructured nanoparticles and their utility. Springer; 2019. p. 115–76.
[755] Sulaiman GM, Tawfeeq AT, Jaaffer MD. Biogenic synthesis of copper oxide nanoparticles using olea europaea leaf extract and evaluation of their toxicity activities: an *in vivo* and *in vitro* study. Biotechnol Prog. 2018;34(1):218–30.
[756] Xue Y, Yu G, Shan Z, Li Z. Phyto-mediated synthesized multifunctional Zn/CuO NPs hybrid nanoparticles for enhanced activity for kidney cancer therapy: a complete physical and biological analysis. J Photochem Photobiol B: Biol. 2018;186:131–6.
[757] Mirzaei H, Darroudi M. Zinc oxide nanoparticles: biological synthesis and biomedical applications. Ceram Int. 2017;43(1):907–14.
[758] Bisht G, Rayamajhi S. ZnO nanoparticles: a promising anticancer agent. Nanobiomedicine. 2016;3(Godište 2016):3–9.
[759] Vijayakumar S, Vaseeharan B, Malaikozhundan B, Shobiya M. Laurus nobilis leaf extract mediated green synthesis of ZnO nanoparticles: characterization and biomedical applications. Biomed Pharmacotherapy. 2016;84:1213–22.
[760] Chung I-M, Rahuman AA, Marimuthu S, Kirthi AV, Anbarasan K, Rajakumar G. An investigation of the cytotoxicity and caspase-mediated apoptotic effect of green synthesized zinc oxide nanoparticles using Eclipta prostrata on human liver carcinoma cells. Nanomaterials. 2015;5(3):1317–30.
[761] Padalia H, Chanda S. Characterization, antifungal and cytotoxic evaluation of green synthesized zinc oxide nanoparticles using Ziziphus nummularia leaf extract, artificial cells. Nanomed, Biotechnol. 2017;45(8):1751–61.
[762] Bano S, Nazir S, Nazir A, Munir S, Mahmood T, Afzal M, et al. Microwave-assisted green synthesis of superparamagnetic nanoparticles using fruit peel extracts: surface engineering, T2 relaxometry, and photodynamic treatment potential. Int J Nanomed. 2016;11:3833.
[763] Namvar F, Rahman HS, Mohamad R, Baharara J, Mahdavi M, Amini E, et al. Cytotoxic effect of magnetic iron oxide nanoparticles synthesized *via* seaweed aqueous extract. Int J Nanomed. 2014;9:2479.
[764] Waghmode MS, Gunjal AB, Mulla JA, Patil NN, Nawani NN. Studies on the titanium dioxide nanoparticles: biosynthesis, applications and remediation. SN Appl Sci. 2019;1(4):1–9.
[765] Sha B, Gao W, Han Y, Wang S, Wu J, Xu F, et al. Potential application of titanium dioxide nanoparticles in the

prevention of osteosarcoma and chondrosarcoma recurrence. J Nanosci Nanotechnol. 2013;13(2):1208–11.
[766] Ganesan K, Jothi VK, Natarajan A, Rajaram A, Ravichandran S, Ramalingam S. Green synthesis of Copper oxide nanoparticles decorated with graphene oxide for anticancer activity and catalytic applications. Arab J Chem. 2020;13(8):6802–14.
[767] Rao VR. Antioxidant agents. Elsevier; 2016. p. 137–50
[768] Khalil I, Yehye WA, Etxeberria AE, Alhadi AA, Dezfooli SM, Julkapli NBM, et al. Nanoantioxidants: recent trends in antioxidant delivery applications. Antioxidants. 2020;9(1):24.
[769] Murru C, Badía-Laíño R, Díaz-García ME. Synthesis and characterization of green carbon dots for scavenging radical oxygen species in aqueous and oil samples. Antioxidants. 2020;9(11):1147.
[770] Das S, Bag BG, Basu R. Abroma augusta Linn bark extract-mediated green synthesis of gold nanoparticles and its application in catalytic reduction. Appl Nanosci. 2015;5(7):867–73.
[771] Abdullah JAA, Eddine LS, Abderrhmane B, Alonso-González M, Guerrero A, Romero A. Green synthesis and characterization of iron oxide nanoparticles by pheonix dactylifera leaf extract and evaluation of their antioxidant activity. Sustain Chem Pharm. 2020;17:100280.
[772] Gottimukkala K, Harika R, Zamare D. Green synthesis of iron nanoparticles using green tea leaves extract. J Nanomed Biother Discov. 2017;7:151.
[773] Kaur M, Chopra DS. Green synthesis of iron nanoparticles for biomedical applications. Glob J Nanomed. 2018;4:1–10.
[774] Akinola PO, Lateef A, Asafa TB, Beukes LS, Hakeem AS, Irshad HM. Multifunctional titanium dioxide nanoparticles biofabricated *via* phytosynthetic route using extracts of Cola nitida: antimicrobial, dye degradation, antioxidant and anticoagulant activities. Heliyon. 2020;6(8):e04610.
[775] Bobo D, Robinson KJ, Islam J, Thurecht KJ, Corrie SR. Nanoparticle-based medicines: a review of FDA-approved materials and clinical trials to date. Pharm Res. 2016;33(10):2373–87.
[776] Caster JM, Patel AN, Zhang T, Wang A. Investigational nanomedicines in 2016: a review of nanotherapeutics currently undergoing clinical trials. Wiley Interdiscip Rev: Nanomed Nanobiotechnol. 2017;9(1):e1416.
[777] Ventola CL. The nanomedicine revolution: part 1: emerging concepts. Pharm Therapeutics. 2012;37(9):512.
[778] Maier-Hauff K, Ulrich F, Nestler D, Niehoff H, Wust P, Thiesen B, et al. Efficacy and safety of intratumoral thermotherapy using magnetic iron-oxide nanoparticles combined with external beam radiotherapy on patients with recurrent glioblastoma multiforme. J Neuro-oncology. 2011;103(2):317–24.
[779] Hao R, Lan H, Kuang C, Wang H, Guo L. Superior potassium storage in chitin-derived natural nitrogen-doped carbon nanofibers. Carbon. 2018;128:224–30.
[780] Pan Y, Sahoo NG, Li L. The application of graphene oxide in drug delivery. Expert Opin Drug Delivery. 2012;9(11):1365–76.
[781] Priyadarsini S, Mohanty S, Mukherjee S, Basu S, Mishra M. Graphene and graphene oxide as nanomaterials for medicine and biology application. J Nanostruct Chem. 2018;8(2):123–37.
[782] R Ikram, BM Jan, W Ahmad, Advances in synthesis of graphene derivatives using industrial wastes precursors; prospects and challenges. J Mater Res Technol. 2020;9.
[783] Wang F, Wang Y-C, Dou S, Xiong M-H, Sun T-M, Wang J. Doxorubicin-tethered responsive gold nanoparticles facilitate intracellular drug delivery for overcoming multidrug resistance in cancer cells. ACS Nano. 2011;5(5):3679–92.
[784] Patra JK, Kwon Y, Baek K-H. Green biosynthesis of gold nanoparticles by onion peel extract: synthesis, characterization and biological activities. Adv Powder Technol. 2016;27(5):2204–13.
[785] Badıllı U, Myollarasouli F, Bakirhan NK, Ozkan Y, Ozkan SA. Role of quantum dots in pharmaceutical and biomedical analysis, and its application in drug delivery. TrAC Trends Anal Chem. 2020;131:116013.
[786] Fahmi MZ, Haris A, Permana AJ, Wibowo DLN, Purwanto B, Nikmah YL, et al. Bamboo leaf-based carbon dots for efficient tumor imaging and therapy. RSC Adv. 2018;8(67):38376–83.
[787] Chung HK, Wongso V, Sambudi NS. Biowaste-derived carbon dots/hydroxyapatite nanocomposite as drug delivery vehicle for acetaminophen. J Sol–Gel Sci Technol. 2020;93(1):214–23.
[788] Kim CG, Kye Y-C, Yun C-H. The role of nanovaccine in cross-presentation of antigen-presenting cells for the activation of CD^{8+} T cell responses. Pharmaceutics. 2019;11(11):612.
[789] Xu J, Lv J, Zhuang Q, Yang Z, Cao Z, Xu L, et al. A general strategy towards personalized nanovaccines based on fluoropolymers for post-surgical cancer immunotherapy. Nat Nanotechnol. 2020;15(12):1043–52.
[790] Qiao Y, Wan J, Zhou L, Ma W, Yang Y, Luo W, et al. Stimuli-responsive nanotherapeutics for precision drug delivery and cancer therapy. Wiley Interdiscip Rev: Nanomed Nanobiotechnol. 2019;11(1):e1527.
[791] Yin W-m, Li Y-w, Gu Y-q, Luo M. Nanoengineered targeting strategy for cancer immunotherapy. Acta Pharmacol Sin. 2020;41(7):902–10.
[792] Zaman M, Good MF, Toth I. Nanovaccines and their mode of action. Methods. 2013;60(3):226–31.
[793] Lin AY, Lunsford J, Bear AS, Young JK, Eckels P, Luo L, et al. High-density sub-100-nm peptide-gold nanoparticle complexes improve vaccine presentation by dendritic cells *in vitro*. Nanoscale Res Lett. 2013;8(1):1–11.
[794] Gheibi Hayat SM, Darroudi M. Nanovaccine: a novel approach in immunization. J Cell Physiol. 2019;234(8):12530–6.
[795] Shevtsov MA, Nikolaev BP, Yakovleva LY, Parr MA, Marchenko YY, Eliseev I, et al. 70-kDa heat shock protein coated magnetic nanocarriers as a nanovaccine for induction of anti-tumor immune response in experimental glioma. J Controlled Rel. 2015;220:329–40.
[796] Liu F, Sun J, Yu W, Jiang Q, Pan M, Xu Z, et al. Quantum dot-pulsed dendritic cell vaccines plus macrophage polarization for amplified cancer immunotherapy. Biomaterials. 2020;242:119928.
[797] Hu Y, Yang J, Tian J, Jia L, Yu J-S. Green and size-controllable synthesis of photoluminescent carbon nanoparticles from waste plastic bags. RSC Adv. 2014;4(88):47169–76.
[798] Zhang Y, Petibone D, Xu Y, Mahmood M, Karmakar A, Casciano D, et al. Toxicity and efficacy of carbon nanotubes and graphene: the utility of carbon-based nanoparticles in nanomedicine. Drug Metab Rev. 2014;46(2):232–46.
[799] Mu Q, Jiang G, Chen L, Zhou H, Fourches D, Tropsha A, et al. Chemical basis of interactions between engineered

nanoparticles and biological systems. Chem Rev. 2014;114(15):7740–81.
[800] Qi W, Tian L, An W, Wu Q, Liu J, Jiang C, et al. Curing the toxicity of multi-walled carbon nanotubes through native small-molecule drugs. Sci Rep. 2017;7(1):1–14.
[801] Arunkumar T, Karthikeyan R, Ram Subramani R, Viswanathan K, Anish M. Synthesis and characterisation of multi-walled carbon nanotubes (MWCNTs). Int J Ambient Energy. 2020;41(4):452–6.
[802] Raphey V, Henna T, Nivitha K, Mufeedha P, Sabu C, Pramod K. Advanced biomedical applications of carbon nanotube. Mater Sci Eng: C. 2019;100:616–30.
[803] Hirano A, Wada M, Tanaka T, Kataura H. Oxidative stress of carbon nanotubes on proteins is mediated by metals originating from the catalyst remains. ACS Nano. 2019;13(2):1805–16.
[804] de Menezes BRC, Rodrigues KF, da Silva Fonseca BC, Ribas RG, do Amaral Montanheiro TL, Thim GP. Recent advances in the use of carbon nanotubes as smart biomaterials. J Mater Chem B. 2019;7(9):1343–60.
[805] Ali S, Rehman SAU, Luan H-Y, Farid MU, Huang H. Challenges and opportunities in functional carbon nanotubes for membrane-based water treatment and desalination. Sci Total Environ. 2019;646:1126–39.
[806] Francis AP, Devasena T. Toxicity of carbon nanotubes: a review. Toxicol Ind Health. 2018;34(3):200–10.
[807] Darbandi A, Gottardo E, Huff J, Stroscio M, Shokuhfar T. A review of the cell to graphene-based nanomaterial interface. Jom. 2018;70(4):566–74.
[808] An W, Zhang Y, Zhang X, Li K, Kang Y, Akhtar S, et al. Ocular toxicity of reduced graphene oxide or graphene oxide exposure in mouse eyes. Exp Eye Res. 2018;174:59–69.
[809] Leng W, Wu M, Pan H, Lei X, Chen L, Wu Q, et al. The SGLT2 inhibitor dapagliflozin attenuates the activity of ROS-NLRP3 inflammasome axis in steatohepatitis with diabetes mellitus. Ann Transl Med. 2019;7(18):429.
[810] Shi Z, Zhang K, Zhou H, Jiang L, Xie B, Wang R, et al. Increased miR-34c mediates synaptic deficits by targeting synaptotagmin 1 through ROS-JNK-p53 pathway in Alzheimer's disease. Aging Cell. 2020;19(3):e13125.
[811] Zhang Y, Wang Y, Zhou D, Zhang L-S, Deng F-X, Shu S, et al. Angiotensin II deteriorates advanced atherosclerosis by promoting MerTK cleavage and impairing efferocytosis through the AT1R/ROS/p38 MAPK/ADAM17 pathway. Am J Physiol-Cell Physiology. 2019;317(4):C776–87.
[812] Kirtonia A, Sethi G, Garg M. The multifaceted role of reactive oxygen species in tumorigenesis. Cell Mol Life Sci. 2020;77:4459–83.
[813] Makvandi P, Ghomi M, Ashrafizadeh M, Tafazoli A, Agarwal T, Delfi M, et al. A review on advances in graphene-derivative/polysaccharide bionanocomposites: therapeutics, pharmacogenomics and toxicity. Carbohydr Polym. 2020;116952.
[814] Gidwani B, Sahu V, Shukla SS, Pandey R, Joshi V, Jain VK, et al. Quantum dots: prospectives, toxicity, advances and applications. J Drug Delivery Sci Technol. 2021;61:102308.
[815] Zhao M-X, Zhu B-J. The research and applications of quantum dots as nano-carriers for targeted drug delivery and cancer therapy. Nanoscale Res Lett. 2016;11(1):1–9.
[816] Ye L, Yong K-T, Liu L, Roy I, Hu R, Zhu J, et al. A pilot study in non-human primates shows no adverse response to intravenous injection of quantum dots. Nat Nanotechnol. 2012;7(7):453–8.
[817] Sajid M, Ilyas M, Basheer C, Tariq M, Daud M, Baig N, et al. Impact of nanoparticles on human and environment: review of toxicity factors, exposures, control strategies, and future prospects. Environ Sci Pollut Res. 2015;22(6):4122–43.
[818] Choi O, Hu Z. Size dependent and reactive oxygen species related nanosilver toxicity to nitrifying bacteria. Environ Sci Technol. 2008;42(12):4583–8.
[819] Aitken RJ, Chaudhry M, Boxall A, Hull M. Manufacture and use of nanomaterials: current status in the UK and global trends. Occup Med. 2006;56(5):300–6.
[820] Nikzamir M, Akbarzadeh A, Panahi Y. An overview on nanoparticles used in biomedicine and their cytotoxicity. J Drug Delivery Sci Technol. 2020;61:102316.
[821] Liu G, Gao J, Ai H, Chen X. Applications and potential toxicity of magnetic iron oxide nanoparticles. Small. 2013;9(9–10):1533–45.
[822] Mahmoudi M, Simchi A, Imani M, Milani AS, Stroeve P. An *in vitro* study of bare and poly (ethylene glycol)-co-fumarate-coated superparamagnetic iron oxide nanoparticles: a new toxicity identification procedure. Nanotechnology. 2009;20(22):225104.
[823] Song B, Zhou T, Yang W, Liu J, Shao L. Contribution of oxidative stress to TiO_2 nanoparticle-induced toxicity. Environ Toxicol Pharmacol. 2016;48:130–40.
[824] Bahadar H, Maqbool F, Niaz K, Abdollahi M. Toxicity of nanoparticles and an overview of current experimental models. Iran Biomed J. 2016;20(1):1.
[825] Huang C-C, Aronstam RS, Chen D-R, Huang Y-W. Oxidative stress, calcium homeostasis, and altered gene expression in human lung epithelial cells exposed to ZnO nanoparticles. Toxicol Vitro. 2010;24(1):45–55.
[826] Osman IF, Baumgartner A, Cemeli E, Fletcher JN, Anderson D. Genotoxicity and cytotoxicity of zinc oxide and titanium dioxide in HEp-2 cells. Nanomedicine. 2010;5(8):1193–203.
[827] Lei R, Wu C, Yang B, Ma H, Shi C, Wang Q, et al. Integrated metabolomic analysis of the nano-sized copper particle-induced hepatotoxicity and nephrotoxicity in rats: a rapid *in vivo* screening method for nanotoxicity. Toxicol Appl Pharmacol. 2008;232(2):292–301.
[828] Meng H, Chen Z, Xing G, Yuan H, Chen C, Zhao F, et al. Ultrahigh reactivity provokes nanotoxicity: explanation of oral toxicity of nano-copper particles. Toxicol Lett. 2007;175(1–3);102–10.
[829] Sani A, Cao C, Cui D. Toxicity of gold nanoparticles (AuNPs): a review. Biochem Biophys Rep. 2021;26:100991.
[830] Li X, Hu Z, Ma J, Wang X, Zhang Y, Wang W, et al. The systematic evaluation of size-dependent toxicity and multi-time biodistribution of gold nanoparticles. Colloids Surf B: Biointerfaces. 2018;167:260–6.
[831] Pan Y, Neuss S, Leifert A, Fischler M, Wen F, Simon U, et al. Size-dependent cytotoxicity of gold nanoparticles. Small. 2007;3(11):1941–9.
[832] Vales G, Suhonen S, Siivola KM, Savolainen KM, Catalán J, Norppa H. Genotoxicity and cytotoxicity of gold nanoparticles *in vitro*: role of surface functionalization and particle size. Nanomaterials. 2020;10(2):271.
[833] Kempasiddaiah M, Kandathil V, Dateer RB, Sasidhar BS, Patil SA, Patil SA. Immobilizing biogenically synthesized

palladium nanoparticles on cellulose support as a green and sustainable dip catalyst for cross-coupling reaction. Cellulose. 2020;27(6):3335–57.
[834] Afewerki S, Franco A, Balu AM, Tai C-W, Luque R, Córdova A. Sustainable and recyclable heterogenous palladium catalysts from rice husk-derived biosilicates for Suzuki-Miyaura cross-couplings, aerobic oxidations and stereoselective cascade carbocyclizations. Sci Rep. 2020;10(1):6407.
[835] Bloch K, Pardesi K, Satriano C, Ghosh S. Bacteriogenic platinum nanoparticles for application in nanomedicine. Front Chem. 2021;9(32):624344.
[836] Gahlawat G, Choudhury AR. A review on the biosynthesis of metal and metal salt nanoparticles by microbes. RSC Adv. 2019;9(23):12944–67.
[837] Al-Radadi NS. Green synthesis of platinum nanoparticles using Saudi's Dates extract and their usage on the cancer cell treatment. Arab J Chem. 2019;12(3):330–49.
[838] Thakkar KN, Mhatre SS, Parikh RY. Biological synthesis of metallic nanoparticles. Nanomedicine. 2010;6(2):257–62.
[839] Jeyaraj M, Gurunathan S, Qasim M, Kang M-H, Kim J-H, Comprehensive A. Review on the synthesis, characterization, and biomedical application of platinum nanoparticles. Nanomaterials. 2019;9(12):1719.
[840] Haleemkhan A, Naseem B, Vardhini B. Synthesis of nanoparticles from plant extracts. Int J Mod Chem Appl Sci. 2015;2(3):195–203.
[841] Hussain I, Singh NB, Singh A, Singh H, Singh SC. Green synthesis of nanoparticles and its potential application. Biotechnol Lett. 2016;38(4):545–60.
[842] Saratale RG, Saratale GD, Shin HS, Jacob JM, Pugazhendhi A, Bhaisare M, et al. New insights on the green synthesis of metallic nanoparticles using plant and waste biomaterials: current knowledge, their agricultural and environmental applications. Environ Sci Pollut Res. 2018;25(11):10164–83.
[843] Baskaran B, Muthukumarasamy A, Chidambaram S, Sugumaran A, Ramachandran K, Rasu Manimuthu T. Cytotoxic potentials of biologically fabricated platinum nanoparticles from Streptomyces sp. on MCF-7 breast cancer cells. IET Nanobiotechnol. 2017;11(3):241–6.
[844] Eramabadi P, Masoudi M, Makhdoumi A, Mashreghi M. Microbial cell lysate supernatant (CLS) alteration impact on platinum nanoparticles fabrication, characterization, antioxidant and antibacterial activity. Mater Sci Eng C. 2020;117:111292.